UNCLASSIFIED

AD NUMBER

AD482130

NEW LIMITATION CHANGE

TO

Approved for public release, distribution unlimited

FROM

Distribution authorized to U.S. Gov't. agencies and their contractors; Administrative/Operational Use; May 1966. Other requests shall be referred to Command General, Army Electronics Command, Attn: AMSEL-KL-TS, Ft Monmouth, NJ 07703-5601.

AUTHORITY

USAEC ltr, 16 Jun 1971

THIS PAGE IS UNCLASSIFIED

482130

OPTICAL PUMPS FOR LASERS

Final Report

Covering Period From

1 July 1964 - 25 February 1966

Contract DA28-043-AMC-00292(E)

DA Task 1P6-22001-A-055-02

United States Army Electronics Command
Fort Monmouth, New Jersey 07703

Westinghouse Research Laboratories
Westinghouse Electric Corporation
Pittsburgh, Pennsylvania 15235

DISTRIBUTION STATEMENT

This document is subject to special export controls and each transmittal to foreign governments or foreign nationals may be made only with prior approval of CG, U. S. Army Electronics Command, Fort Monmouth, N. J.

Attn: AMSEL-KL-TS

NOTICES

Disclaimers

The findings in this report are not to be construed as an official Department of the Army position, unless so designated by other authorized documents.

The citation of trade names and names of manufacturers in this report is not to be construed as official Government indorsement or approval of commercial products or services referenced herein.

Disposition

Destroy this report when it is no longer needed. Do not return it to the originator.

Qualified requesters may obtain copies of this report from DDC. DDC release to CFSTI is not authorized.

OPTICAL PUMPS FOR LASERS

Final Report

Covering Period From

1 July 1964 - 25 February 1966

Objective: To achieve efficient optical pumps for high-powered lasers, methods of enhancing preferred outputs, minimizing unwanted spectral outputs and minimizing input requirements will be investigated. Specific optical pumps will be developed.

Contract DA28-043-AMC-00292(E)

Technical Guidelines Dated 22 January 1964

DA Task 1P6-22001-A-055-02

Prepared by:

R. Schlecht

C. H. Church

D. A. Larson

L. Gampel

I. Liberman

This document is subject to special export controls and each transmittal to foreign governments or foreign nationals may be made only with prior approval of CG, U. S. Army Electronics Command, Fort Monmouth, N. J.

Attn: AMSEL-KL-TS

Qualified requesters may obtain copies
of this report from DDC. DDC release
to CFSTI is not authorized.

Table of Contents

Table of Contents (Cont'd)

PURPOSE

The purpose of this research program is to achieve efficient optical pumps for lasers. This initial phase may be divided into two tasks: a survey of the literature on laser materials to ascertain the parameters pertaining to pumping, and a study of optical pumps for lasers, both pulsed and continuous. The literature survey and the pulsed lamp studies will be made primarily at the Research Laboratories in Pittsburgh with the investigation of the continuously operating lamps being made at the Lamp Division in Bloomfield.

ABSTRACT

The continuously operating high pressure mercury discharge has been demonstrated as an effective vehicle for the efficient excitation of intense lines from a number of metals whose radiating excited states are < 5 e.v. above the ground state. The metals In, Ga, Tl, Cs and Na introduced into the arc in the form of iodides have been studied in lamps having diameters from 2.6 mm to 22 mm. Spectral distributions and irradiance measurements are given for these lamps at input power densities in the range 20-2000W/cm^3.

OPTICAL PUMPS FOR LASERS

U.S. AEL CONTRACT NO. DA-28-043-AMC-00292(E)

DA TASK NO. 1P6-22001-A-055-02

Final Report Covering Period
July 1, 1964 - February 25, 1966

FACTUAL DATA

A. Continuous Laser Pumps

1) Introduction

The optical pumping of lasers requires relatively large amounts of radiation in discreet spectral regions. The use of broad continuous spectral sources such as xenon flash lamps or incandescent filaments is normally quite inefficient and in some instances where excitation bands are very narrow only an extremely small fraction of the input power can be utilized. One means of obtaining large amounts of energy in narrow spectral regions is to use the radiation of atoms excited in a gas discharge. The high pressure mercury discharge, for example, the standard 400 watt High Pressure Lamp commonly used for street lighting, can supply 10-20W in each of four lines in the near ultraviolet and visible spectral range.

Recently, however, it has been found[1] that this discharge can be used as a vehicle into which many elements can be introduced to produce radiation of the more intense lines of these elements at appreciably higher powers. It thus became possible to generate radiation at fairly high power levels in narrow spectral regions and to determine to some extent the spectral region in which the lamp would radiate. In our studies under this contract we have endeavored to determine which spectral lines can be efficiently excited, how the power levels and geometry affect the efficiency and to broaden the understanding of these discharges to the end of obtaining an efficient match of light sources and laser materials.

The high pressure mercury discharge is contained in a quartz envelope having tungsten electrodes at each end and connected to the external leads by means of a molybdenum ribbon pressed in the quartz to provide the vacuum tight seal. The shape and dimensions of the standard 400 watt arc tube are shown in Figure 1. The arc tube contains a fixed amount of mercury which during operation is completely vaporized and has a pressure of 2 to 3 atmospheres. In addition to the mercury, argon is added at a pressure of 25 torr. This facilitates starting and protects the electrodes from excessive bombardment during the initial low pressure mercury phase as the lamp heats up. When the lamp reaches rated wattage the wall temperature is in excess of 700°C and the coolest points, normally the ends of the lamp, are about 600°C.

The high pressure discharge is considered to be in a state of thermal equilibrium with both the gas and electrons having the same temperature. On the axis of the discharge the temperature has been found to be about 6500°K[1,2,3] and falls in a parabolic manner to about 1000°K at the wall. Since thermal equilibrium exists, the fraction of the atoms in an energy state V_x electron volts above the ground level is given by Boltzmann's law

$$\frac{N_x}{N_o} = \frac{(g_x)}{(g_o)} \exp\text{-}(11{,}600 V_x/T)$$

where T is the temperature in the region being considered; g_x/g_o is the ratio of the statistical weights of the excited state "x" and the ground state "o".

This expression is plotted in Figure 2 for two temperatures (6000°K, 5000°K). It is seen there that the fraction of atoms in a given state decreases rapidly with increasing energy of that state. The decrease is about a factor of ten for each 1 ev increase above ground for a temperature of 5000°K. At higher temperatures this decrease is less and at lower temperatures

it is greater. This condition is important since it means that metals having desired radiation originating from levels which are low relative to those of mercury, even if present in the discharge at much lower concentrations than the mercury, will radiate strongly. For example, the 5350Å thallium line is readily seen at pressures much less than 1 mm in the presence of more than an atmosphere of mercury[4]. In general, however, very intense radiation cannot be obtained with the addition of metals since either the metal vapor pressures are too low or the metals react with the quartz. This problem has been largely overcome by the addition of metal iodides[5] rather than the element. Figure 3 shows the vapor pressure curves for Cs, Tl, TlI, CsI, and Hg. In the case of Tl, the iodide provides a much higher vapor pressure while in the case of Cs, the iodide vapor pressure is considerably lower, however, the problem of chemical reaction with the quartz is greatly reduced. These and a number of other iodides are stable at the temperature of the wall, but are completely dissociated in the high temperature core and recombine again in the cooler regions.

From the two curves in Figure 2, it is also seen that the fraction of atoms in a given level decreases rapidly with temperature. Thus, as the distance from the axis increases the intensity of radiation falls off sharply due to the lowering temperature. Figure 4 shows the manner in which the population of levels at 8 ev and 4 ev vary with temperature. The $V_x = 4$ ev curve has been reduced by a factor of 100 to give the common point at 10,000°K. Using these curves we see that the $V_x = 8$ ev curve decreased by a factor of 5000 in the temperature interval 6500°K-4000°K. In the same interval, the $V_x = 4$ ev curve decreases by a factor of 70. From this we should expect to find that the diameter of arcs containing additives should appear broader and have only the additive lines in the fringes of the discharge. Elenbaas[6]

shows that the yellow mercury lines from the 7.7 ev level at the 4000°K temperature point have fallen to much less than 1% of their intensity at the arc core.

2) Distribution of Power

The input power to the high pressure mercury lamp is dissipated in heating the electrodes, conduction of heat to the arc tube wall, convection losses and radiation. The electrode loss is a function of the current since the voltage drop at the electrode has an essentially constant value of about 15V. In the 400W lamp this loss is about 10% of the input watts.

According to Elenbaas[7] the convection loss is about 1.5W/cm length of arc and the conduction loss is about 11.5W/cm. These two losses represent about 90W of the 400W input. The conduction loss is due to the transfer of heat from the high temperature core of the discharge, across the nonradiating zone of mercury and argon surrounding it, to the wall. The energy loss through an imaginary cylinder in the unexcited zone is $2\pi r \lambda(T) \frac{dT}{dr}$ where r is the radius of the cylinder, $\lambda(T)$ is the coefficient of thermal conductivity of the gas and $\frac{dT}{dr}$ is the temperature gradient. The thermal loss in mercury is essentially constant in the range of arc tube diameters, mercury densities and power loadings of interest to us. The increased thermal conductivity due to the presence of 25 torr of argon increases this loss by $\sim$1.5W/cm length. The total heat dissipation (electrode + gas) with 400W input should therefore be about 130W. The rest of the input should be radiated by the discharge. Measurements of the power radiated as a function of input watts by Elenbaas[8] for the pure mercury discharge show only 72% of the radiation reaching the thermopile detector, and he ascribes this difference to the absorption of the wavelengths 1850Å and shorter, and 4 μ and longer, by the cool gas layer, the tube wall and

the air in the optical path. Thus the discharge watts radiated through the arc tube could be as high as 260W depending upon the transmission of the arc tube material and the wave lengths radiated. When the various metal iodides are added to the discharge the radiation pattern changes reducing the short wavelength mercury radiation and introducing the lines of the additive metals at longer wavelengths, and thus reducing the absorption loss in the tube wall and in the optical path. The additives are such that they do not radiate in the short length region[9]. The loss in the non-radiating zone will be dependent upon the absorption of the molecular iodide vapor and the pressure of the vapor. The single valence iodides, (NaI, TlI, LiI) are transparent to arc radiation while the higher valence iodides are in some cases (SnI_2) strongly absorbing. Appendix A contains a table of the temperatures required for 1 torr and 760 torr of some typical additives and also their energy level diagrams.

3) Instrumentation

A Perkin-Elmer Model 12A Infrared Monochromator has been used to cover the spectral range from about 4100Å to 2 microns. This is a prism instrument with thermopile detector. The spectra were obtained without imaging the arc on the slit. The manual wavelength scanning was replaced by a motor drive which covers the spectrum in about seven minutes. The detector output is fed to a Keithley Model 149 Millimicrovoltmeter, the output of which went to a Texas Instrument Recorder.

The relative response of the complete instrument as a function of wavelength was obtained by scanning the spectrum of a quartz iodine incandescent lamp calibrated by National Bureau of Standards. The lamp output values were given for each 10Å bandwidth from 2500Å-2.6 μ. The recorded

output was divided by the relative dispersion values obtained from the wavelength traverse rate and compared to the output values supplied by N.B.S. The response vs wavelength curve is shown in Figure 5. The absorption dip at 8100Å was checked several times and apparently is real. Since the response is reasonably flat, the spectra run have not been corrected for instrument response. The sensitivity of this instrument required slit widths of approximately 0.5 mm. When greater sensitivity or higher resolution was required a modified Beckman DU was used. This instrument has a quartz prism. A 1P28 and a 7102 Photomultipliers were used as detectors. The 1P28 has its peak sensitivity in the blue and has its cut off at about 6000Å. The 7102 peaks about 8000Å and cuts off about 1.0 μ.

Lumen measurements were obtained with a Weston eye sensitivity corrected barrier layer cell which compared an in line measurement of the unknown lamp with a mercury lamp whose lumen output had been measured using spherical photometry. Lamps were operated on ac with a variable choke as ballast. AC operation results in a power between .7 and .9 since the current voltages are not in phase. The power is also dependent upon the time of ignition during each cycle.

4) Spectral Effects of Additives to High Pressure Mercury Discharge

Visible and infrared spectra of the standard 400 watt high pressure mercury lamp operating at 400 and 600 watts in a glass outer envelope with ~500 torr N_2 is shown in Figure 6. This lamp contains 66 mg of mercury, has a 70 mm electrode spacing and an i.d. of 18 mm. Under these conditions the lamp voltage is approximately 140 volts and the luminous efficiency is about 54 lumens per watt. In Figure 7 the spectrum is shown from 3000Å to 6000Å.

The glass envelope cuts out the radiation below 3000Å. At the higher wattage all lines have increased in intensity almost in proportion to the wattage increase. The yellow 5770-90Å lines and the infrared lines show larger increase than the 5461Å + 4358Å lines. This indicates an increase in gas temperature. There are, however, no pronounced changes and they should not be expected as there are no changes in atom concentration in the arc.

The spectra obtained with the addition of various metal iodides to the high pressure mercury discharge are shown in Figures 8 through Figure 19. The lamps were operated and measured at both 400 watts and 600 watts.

Gallium Iodide + Mercury	8, 9
Lead Iodide + Mercury	10, 11
Indium Iodide + Mercury	12, 13, 14
Thallium Iodide + Mercury	15
Sodium Iodide + Thallium Iodide + Mercury	16
Potassium Iodide + Mercury	17
Mercury Iodide + Mercury	18
Cesium Iodide + Mercury	19

The gallium iodide, lead iodide and indium iodide lamp spectra were obtained using both the thermopile and the 1P28 detector. This was necessary since these additive lamps have strong radiation in the near ultraviolet and violet region which is not covered by the infrared monochromator. The 1P28 relative response was checked at the mercury lines with Osram standard mercury lamp. The response at 3650Å is 80% that at 4358Å.

Some drift of the zero line was encountered during the seven minute spectral span initially used. This was overcome by using a higher speed drive which covers the spectrum in about one minute. The higher speed drive made it necessary to make spectral runs from short to long wavelengths to prevent jamming of gears at the end of a run.

The slit width for all runs with the infrared monochromator is 0.5 mm.

In all the spectral curves for additive containing discharges the mercury lines are identified as such. The other lines are those of the additive metal.

Figures 8 and 9 show the effect of the addition of about 2 mg of gallium iodide to a lamp identical to the mercury lamp of Fig. 6 and 7. At 400 watts the mercury spectrum is replaced to a large extent by the Ga atomic spectrum. The strong lines in the visible region are the 4172Å and 4032Å Ga lines. In the infrared there is a strong line at ~1.2 μ. There is little other than the increase in proportion to the wattage when the lamp is increased to 600 watts indicating that the GaI is already all in the vapor phase at the 400 watt loading.

Figures 10 and 11 show a lamp to which 25 mg of PbI had been added. In the infrared much of the energy is in a group of lines just above 1.0 μ. At 600 watts the contribution of the Pb spectrum has increased greatly while the mercury contribution remains practically constant. In the shorter wavelength region (Figure 11) much of the energy is seen to be radiated in the 4057Å line and in a group of lines around 3650Å. The increase in wattage in this lamp results in an increase in concentration of the Pb in the discharge due to the increased bulb wall temperature and an excess of PbI. The discharge temperature, appears to be lowered since the ratio of yellow to green mercury lines is decreased at the higher wattage which is the opposite of the mercury lamp case.

Figure 12 is a spectrum of a 20 mm 0.9 lamp containing a relatively large but unmeasured quantity of InI_3. In addition to the indium atomic line spectrum there is a pronounced continuum and the operating voltage is much higher than the similar mercury lamp in Figure 6. Figures 13 and 14 show

the spectra obtained with 1 mg of indium was added to a 26 mm o.d. lamp. The continuum is absent and the operating voltage corresponds to that of a mercury lamp without the indium. The indium lines at 4511A and 4105A are very strong. In addition considerable radiation is present in the infrared with a strong peak at ~1.3 μ. In Figure 13 the spectrum was obtained using twice the normal speed on the recorder drive so the lines appear much broader than in Figure 12. In Figure 14 the indium lines are clearly much broader than those of mercury. The breaks in the rising portions of the indium lines result from unresolved reversal of the lines.

Figure 15 shows thallium iodide in a 20 mm o.d. lamp. The thallium iodide added is considerably greater than the amount vaporized at 400 watts. The principal line in this lamp is at 5350Å and it increases strongly with increasing wattage. The 5461Å Hg line is faint by evident in the break on the long wavelength side of the 5350Å Tl line.

Figure 16 shows the combination of sodium iodide and thallium iodide in one lamp having a 24 mm o.d. arc tube and thermal insulating caps at the arc tube ends to obtain higher cool spot temperature. This is necessary, particularly in the case of NaI which has a relatively low vapor pressure. The principal visible lines are the 5350Å Tl and the Na doublet at 5890-96Å. The latter lines become appreciably broadened at high densities. In the infrared the prominent lines are the 1.15 μ Tl and the 1.3 μ and 8183-95Å Na lines. The Na lines increase more strongly with the higher loading.

Figure 17 shows the effect of the addition of potassium iodide to a 28 mm o.d. arc tube. The intense lines are the resonance lines at 7665Å and 7699Å and a group of lines at 1.1 μ and 1.2 μ. Na is weakly present as an impurity.

Figure 18 shows the effect of the addition of mercury iodide. The lines, except for the Na and Li impurity lines, are those of mercury. The unusual feature in this lamp is that the infrared radiation is much greater than the visible and there is a broad HgI band at 4400Å. The instrument resolution does not allow determination of whether these bands have fine structure.

Figure 19 shows the addition of cesium iodide in a 26 mm o.d. arc tube. The radiation is concentrated in the resonance lines at 8943Å and 8521Å and a line at 1.0 μ. The output of these lines increases about three-fold with the increase from 400W to 600W.

The foregoing spectra amply illustrate the degree to which the spectral output of the high pressure mercury lamp can be modified and a number of narrow spectral bands in which energy can be obtained. A number of these additives were selected for further study.

5) Cesium Iodide-Mercury

CsI is extremely hygroscopic and cannot be exposed to air containing moisture. A small sample of CsI was prepared by the direct reaction of Cs + I_2 under vacuum. A capsule containing Cs under vacuum was broken in an evacuated tube containing I_2 crystals and then heated to about 300°C to form the iodide. Three lamps were made using this material. The arc tubes had 1 mm quartz walls and 24 mm, 20 mm, 10 mm o.d. The lamps were made with tungsten electrodes without emission material and an electrode separation of about 2-1/2 inches. The arc tubes had 120, 60 and 15 mg of mercury respectively and all were filled with argon to 20 torr. The amount of CsI added was not weighed because of the problem involved in maintaining the sample moisture free.

The three arc tubes were mounted in glass outer envelopes filled to 500 torr N_2. Figure 20 shows the spectra obtained with the 26 mm o.d. and

20 mm o.d. diameter lamp at 400 watts and the 10 mm diameter lamp at 250 watts. In the 26 mm diameter lamps, the Cs lines at 8521 and 8943Å are the strongest lines in the spectrum, in the 20 mm diameter they are a little lower in intensity than the strongest mercury lines and in the 10 mm lamp they are very weak. These lamps are not operating at the same CsI vapor pressure and since the vapor pressures are not known, it is not possible to separate the effects of diameter and vapor pressure. Figure 21 shows these lamps all operating at 600 watts. The Cs lines are enhanced relative to mercury in all cases, but the 26 mm diameter lamp shows the strongest Cs lines inspite of the fact that the smallest arc tube should have the highest cool spot temperature. Electrical and lumen output measurements on these lamps are listed below:

	Wattage	Voltage	Current	Lumens	L/W
10 mm dia.	250	220	1.4	9,000	36
	400	197	2.3	14,500	36
	600	181	3.6	22,500	37.5
20 mm dia.	400	143	3.18	13,000	32.5
	600	136	4.9	19,200	32
24 mm dia.	400	139	3.0	10,000	25
	600	122	5.0	14,500	24.1

The power input to the lamp was measured with an AC wattmeter as the power factor varied for different lamp conditions.

The 20 mm diameter lamp after operating base down for the above measurements had CsI condensed on the cool lower end of the arc tube. The lamp was inverted while operating to increase the temperature of this point and therefore the CsI vapor pressure. The lumen output dropped from 19,200 to 15,000 and the voltage dropped from 136 to 119 volts. This is the result of increased radiation in the Cs lines at the expense of Hg.

The 10 mm o.d. arc tube was removed from the outer jacket and operated at 300 watts in a small furnace at ambient temperatures up to 850°C. The spectra at various temperatures were obtained using the modified Beckman monochromator with a 7102 photomultiplier as a detector. This detector sensitivity cuts off wavelengths longer than 1.1 micron and peaks at 8000Å. With no oven heating, the Cs line contribution is very small. With increasing ambient temperature, the Cs contribution increases over the entire temperature range. The spectral curves for several temperatures are shown in Figures 22, 23. The smaller slit width in this instrument shows that the 8500 and 8900Å peaks found with the infrared spectrometer are really each two lines. The voltage is seen to decrease with increasing oven temperature as shown below. The gas temperature also decreases as seen from both the reduced mercury contribution and the reduced ratio of the mercury yellow to green line ratio. The CsI vapor pressures correspond to the coolest point on the arc tube which is considerably higher than the oven ambient.

10 mm dia. lamp in oven — 300 watt input to lamp

Ambient Temp.	Lamp Voltage
300°C	213
400	203
500	187
600	181
700	176
800	175

6) Calcium Iodide-Mercury

A sample of CaI_2 was made in a manner similar to that for the CsI. A 22 mm o.d. arc tube and a 10 mm o.d. arc tube were made containing this material. With the 22 mm arc tube mounted in an outer jacket with N_2 fill and operated at 400 watts, there was no contribution to the spectrum from the Ca.

The lamp was then inverted so that the condensed calcium iodide was on the hottest section of the arc tube and the lamp was operated at 600 watts. The spectrum shown in Figure 24 was obtained using the Model 12A infrared monochromator within the lamp operating in this non-equilibrium condition. There is one peak at 6130Å, which should be the 6162 and 6122Å lines, and a broad peak about 6450Å which appears as three lines at higher resolution. The line at 4226Å appears, as well as the group at 1.9 μ, but the intensity of all Ca lines is low compared to the mercury lines.

The spectrum taken with the arc tube operating in the 500°C oven at 400 watts shows only mercury lines. The Ca contribution increases with increasing oven temperature up to the maximum ambient about 950°C. Spectra at several temperatures are shown in Figures 25, 26. The 10 mm arc tube was operated in the oven at 300 watts with similar results, Figures 27, 28. The relative Ca contribution is considerably less in the smaller lamp.

7) Thallium Iodide-Mercury

A 10 mm diameter arc tube was made containing 8 mg TlI and 16 mg Hg. This lamp was operated at 300 watts in the oven at ambient temperatures up to 850°C. The spectral distribution is shown for several temperatures in Figures 29, 30. These runs were made using the 7102 photomultiplier as a detector. No lines other than the 5350Å Tl line and weak lines at 4358, 5461 and 6550 are present at the higher temperatures in the spectral region 4000Å-1.0 μ. The electrical and lumen values are given below:

Ambient	Wattage (Measured)	Voltage	Current	Relative Lumen Output
450°C	300W	211V	1.62a	17.2
550	300	213	1.66	18.5
600	300	211	1.66	20.2
650	300	207	1.68	22.0
700	300	212	1.64	24.6
750	300	227	1.58	27.7
800	300	247	1.50	28.5
850	300	257	1.48	30.0

From Figures 29 and 30, the 5350 Tl line can be seen to broaden and increase in intensity with increasing vapor pressure of TlI while the mercury lines weaken and essentially disappear. The 5461Å line of Hg disappears into the 5350 line of Tl.

In order to obtain some measure of the energy radiated in the different spectral bands various sets of filters were used in conjunction with a thermopile.

8) Calibration of Thermopile

Measurements of the radiant intensity in various spectral regions were made using an Eppley thermopile having a quartz window. This pile is responsive to radiation below 4.2 μ. The sensitivity of the thermopile was determined using a quartz iodine incandescent lamp which had been calibrated by the National Bureau of Standards for the energy in microwatts per cm^2 per nanometer bandwidth at 43 cm. The range covered was from 2500Å to 2.6 μ. The total radiant intensity at 43cm due to all wavelengths was obtained by plotting the radiant intensity values given and measuring the area under the curve with a planimeter. The value obtained was 8044 $\mu w/cm^2$. Since the detector is sensitive to about 4.2 μ, a correction was made to take into account the energy radiated by the lamp in the 2.6 μ to 4.2 μ region. A black body at

3000°K has about 10% additional radiation in the 2.6-4.2 μ range. The tungsten filament emissivity and the quartz transmission in this range will lower the value of this correction. A figure of 5% was taken as a reasonable approximation of this correction. This gave a value of 8450 $\mu w/cm^2$ at 43 cm. At 100 cm distance a value of 1560 $\mu w/cm^2$ is obtained by application of the inverse square law.

An Osram standard mercury arc lamp was also used to check the calibration. This lamp is calibrated for the absolute radiation intensity for the line group 3650-3663Å and for the relative intensity of the other lines from 2640Å to 5770-5790Å. The Corning filter combination 4600 + 4015 passes only the 5461Å + 5770-90Å lines whose combined radiant intensity was determined to be 102 $\mu w/cm^2$ at 100 cm. Of this only 46 $\mu w/cm^2$ passed the filter combination. At 100 cm the two sources produce 34 μv and 1 μv output of the thermopile. This gave a sensitivity of 46 μw/μv for the detector for both sources.

9) Thermopile Radiation Measurements

In conjunction with the spectral distribution runs, measurements were made of the energy in selected spectral regions using filters to isolate the desired regions. The published transmission curves for the filters used are given in Appendix B. The filters were calibrated for transmission at wavelengths of interest. Following are the pertinent characteristics of the filters used.

The 7910 is a quartz filter which cuts out much of the long wavelength infrared radiated by the hot quartz arc tube and the outer glass envelope.

The 0160 filter is similar to the envelope glass used on the other lamps and removes the μv below about 3000Å and also much of the infrared beyond 3.2 μ.

The 4600 cuts out the infrared beyond 9000Å. In combination with the 3060 it serves to pass only the visible region of the spectrum.

The 4600 and 4015 combination gives a rough measure of the luminosity curve.

The 4600 and 5330 isolates the region from 3200Å-5400Å and has a secondary peak at 7500Å.

The 2550 filter cuts out the visible passing radiation between 7500Å and 2.75 μ.

The water filter cuts out infrared beyond 1.2 μ and also has an absorption band at 1.03 μ. In combination with 2403 it isolates the region from 64000Å-1.2 μ.

Water in combination with 2600 isolates the region from 7200Å to 1.0 μ.

Measurements were made with the thermopile at a distance of 100 cm. The output of the thermopile was measured with a Keithley Model 149 millimicrovoltmeter. Filters were placed in a holder in front of the thermopile. Values listed in the following table are the thermopile outputs in microvolts.

	Osram Standard Lamp 250W Quartz Arc Tube-No Outer Bulb	400W Regular Mercury	
		400W	600W
No Filter	16.3 μv	34.0	54.0
7910	10.8	27.5	44.0
0160	8.5	27.5	43.0
4600	4.25	12.5	19.8
4600 + 4015	1.0	3.2	5.2
4600 + 5330	1.82	5.2	7.9
4600 + 3060	2.5	8.5	13.0
2550	2.4	10.8	19.0
Deionized Water	5.6	15.7	25.0
Deionized Water + 2403	0.4	2.1	3.6
Deionized Water + 2600	0.1	0.75	1.3
No Filter	16.5	34.0	55.0

	Gallium Iodide		Lead Iodide		Indium Iodide	
	400W	600W	400W	600W	400W	600W
No Filter	41.0	67.0	36.0	65.0	36.0	65.0
7910	34.0	58.0	30.0	54.0	30.0	54.0
0160	34.0	58.0	30.0	54.0	30.0	54.0
4600	14.5	24.0	12.5	20.5	12.5	20.5
4600 + 4015	1.6	2.5	2.0	2.6	2.0	2.6
4600 + 5330	9.5	15.0	7.1	12.0	7.1	12.0
4600 + 3060	9.1	14.5	6.6	10.0	6.6	10.0
2550	16.5	26.5	13.5	25.0	13.5	25.0
Deionized Water	19.0	29.5	17.0	29.0	17.0	29.0
Deionized Water + 2403	3.3	5.3	3.2	7.5	3.2	7.5
Deionized Water + 2600	1.2	2.0	0.9	2.2	0.9	2.2
No Filter	41.0	68.0	37.0	65.0	37.0	65.0

	Thallium Iodide		Sodium Iodide Thallium Iodide	
	400W	600W	400W	600W
No Filter	38.5	69.0	48.0	82.0
7[illegible]	32.5	59.0	40.5	70.8
0160	32.5	58.0	40.5	70.8
4600	13.5	24.0	18.5	32.0
4600 + 4015	4.6	8.5	7.05	11.4
4600 + 5330	4.9	8.4	4.4	6.9
4600 + 3060	8.4	15.5	14.0	26.5
2550	15.0	25.5	16.8	28.4
Deionized Water	18.0	31.0	23.8	44.0
Deionized Water + 2403	2.55	4.9	4.25	10.0
Deionized Water + 2600	0.8	1.5	2.15	5.0
No Filter	39.0	69.0	49.0	82.0

	Potassium Iodide		Cesium Iodide	
	400W	600W	400W	600W
No Filter	36.0	67.0	34.0	71.0
7910	30.0	59.0	28.5	62.0
0160	30.0	59.0	28.5	62.0
4600	8.0	13.5	7.7	13.5
4600 + 4015	1.9	3.0	2.0	3.2
4600 + 5330	4.4	7.8	3.4	6.3
4600 + 3060	6.8	11.5	5.8	11.0
2550	16.5	31.0	15.7	34.0
Deionized Water	14.5	26.5	15.5	36.0
Deionized Water + 2403	9.4	19.0	8.1	24.0
Deionized Water + 2600	7.0	13.0	5.3	15.2
No Filter	37.0	68.0	35.0	72.0

	Mercury Iodide		Quartz Iodine Incandescent Standard 192W
	400W	600W	
No Filter	36.0	65.0	34.0
7910	30.0	54.0	
0160	30.0	54.0	
4600	12.5	20.5	4.8
4600 + 4015	2.0	2.6	1.35
4600 + 5330	7.1	12.0	1.55
4600 + 3060	6.6	10.0	
2550	13.5	25.0	22.4
Deionized Water	17.0	29.0	11.3
Deionized Water + 2403	3.2	7.5	
Deionized Water + 2600	0.9	2.2	
No Filter	37.0	65.0	

The addition of the metal iodide increases the total radiation seen by the thermopile. At the 600 watt input this increase above the Hg lamp ranges from 20% to 50% in the various lamps. The maximum output is obtained with the NaI-TlI lamp.

10) Filter Transmission

The filter combinations were calibrated at selected wavelengths for the (4500 + 4015), (4600 + 5330), (H_2O + 2600) (H_2O + 2403) filter combinations.

Filters	Wavelengths	Transmission of Filter
(H_2O + 2403)	8521, 8943	52.5%
	1.01 μ	22.0
(H_2O + 2600)	7698, 7644	59.0
(4600 + 4015)	4511	0
	5350	51.5
	5461	52.0
	5780	37.0
	5890	30.0
	6500	8.0
(4600 + 5330)	3300	7.0
	3650	52.5
	4032	66.0
	4100	66.0
	4173	65.0
	4358	60.0
	4511	52.5
	5350	6.0
	5461	5.0

11) Radiant Intensity Determinations

The thermopile measurements through the 4600 + 4015 filter combination which isolates the region from 5000Å-6000Å were used to determine the radiant intensity in the mercury, thallium and sodium-thallium, iodide lamps in this region. The 4600 + 5330 combination transmits from 3400Å-5000Å and was used in the determination of the strong violet Ca radiation. The potassium lines at 7644Å and 7696Å were isolated by the (H_2O + 2600) combination and the cesium lines at 8521Å and 8949Å were isolated by the (H_2O + 2403) combination.

The corrected microvolt output of the thermopile for the lines of interest in the absence of the filter was determined by the following relation:

$$X = \frac{\text{Measured Output}}{a_i T_i + a_j T_j}$$

where a_i is the fraction of the total radiation viewed contributed by line (determined from spectral distribution). T_i is the filter transmission of line i.

Radiant Intensity Values at 100 cm

Hg 400W Lamp	5461Å 2 5770-90Å	at 400W	335 $\mu w/cm^2$
		600W	545
TlI + Hg	5350Å + 5461Å	400W	415
		600W	765
NaI + TlI	5350Å + 5890-96Å	400W	743
		600W	1265

CaI	4172Å, 4032Å, 4358Å	at 400W	600 $\mu w/cm^2$
		600W	1040
Potassium I	7644Å, 7696Å	400W	540
		600W	1000
CsI	8521Å, 8943Å	400W	625
		600W	1850

These values can be used to determine the total watts radiated in these lines by the lamp if the light distribution pattern is known. A rough conversion factor for microwatts/cm^2 at 100 cm to total watts is 1/10.

From the 400W Hg lamp the thermopile measurement yields 153W radiated at 400W and 243W radiated at 600W. There is therefore an increase of 90W in the measured radiation with a 200W increase in the input watts. With increasing wattage the electrode loss increases by 20W. The thermal conduction loss should not increase appreciably since the temperature increases only slightly. Of the added 200W power into the lamp about 180W should be radiated by the arc. The large difference between 180W and 90W arises because much of the mercury radiation lies in regions not transmitted by the envelope materials. The outer envelope absorbs all the μv of wavelengths shorter than 3000Å and a large part of the radiation from 3000Å to 3330Å, all of which are converted to long wavelength IR radiation (heat).

In the NaI TlI + Hg lamp where the μv radiation is greatly reduced the measured outputs are 220W at 400W and 377W at 600W. This measurement shows an increase of 157W with the 200W increase from 400-600W. Of this increase about 25W are increased electrode loss. In these lamps the electrode drop is higher than in the mercury lamp since the oxide emission mix is not used. This leaves less than 10% of the increased wattage unaccounted for.

Some radiation is present in the absorption regions of the glass, and in addition there are possible increased gas losses due to higher iodide vapor pressures at the higher loading. In the CsI + Hg lamp the increased radiation + electrode loss accounts for practically all of the wattage increase.

It appears reasonable that the radiation measured in this 3000Å-3.0 μ region could in some cases increase more than the increase in input watts since radiation not transmitted by the envelope is being reduced at the same time that the input to the arc is being increased.

Separation of Arc and Envelope Radiation

In an effort to determine the contribution of the envelope radiation to the previous measurements the output of the lamp was monitored before and after the arc was extinguished. It was found that the response of the Eppley thermopile was too slow to obtain meaningful results.

A Perkin-Elmer thermopile with a response time < 0.1 sec and a KBr window which passed radiation out to 25 μ was then obtained. With it the envelope radiation could be accurately extrapolated to zero time after arc cut off. Since this instrument is sensitive out to 25 μ it sees much of the thermal radiation from the hot envelope materials. Measurements of the standard 400W mercury lamp using the two thermopiles at the same distance gave 34 μv for the Eppley and 62 μv for the Perkin-Elmer thermopiles. Measurement of the radiation passing the 4600 Corning filter gave values of 12.5 and 12 μv which indicate that both thermopiles have similar sensitivities within 5%.

The total output measurement of 62 μv represents only 265W detected by the thermopile. The factors contributing to this difference have not been

investigated. Two of the important ones are the convection cooling of outer bulb which is operated in air, and of the arc tube which is operating in N_2. The heat loss in this latter case results in heating the outer bulb at the top which is not seen directly by the thermopile. In addition there is an I.R. absorption loss in the 100 cm path to the thermopile. At most, there is 5% or less of the radiation beyond 25μ.

The arc radiation arriving at the detector can be determined fairly accurately. Some loss in the I.R. will occur due to atmospheric absorption--particularly by H_2O vapor and CO_2.

Figures 31, 32, and 33 show the recorder traces of the output of the KBr thermopile looking at various lamps just before and just after the arc is extinguished. The chart paper is traveling 2.5 mm per sec. The pen drop to about 1/2 value occurs in less than 1 mm travel. From Figures 31, 32, and 33 the following values have been obtained for the % of the total output measurement contributed by the discharge in various lamps.

Fig. 31	a) 400W Hg lamp in glass outer	400W input	42%
	b) " " " " " "	600W "	44
	c) " " bare arc tube	600W "	60
	d) Hg + TlI 10 mm arc tube in glass outer	580W "	55
Fig. 32	a) CsI 10 mm arc tube in glass outer	600W input	48
	b) " 26 " " " " " "	600W "	59
	c) " " " " " " " "	400W "	41
	d) NaI 12 " " " " quartz sleeve	600W "	65
	e) NaI + TlI + Hg 24 mm dia. in glass outer	600W "	62
Fig. 33	a) High Pressure Na in Lucalox	500W input	50
	b) 250W Xe short-arc large electrodes	250W "	31
	c) 250W " " " small electrodes and glass outer bulb	250W "	15

In the 400W Hg lamp the arc radiation would be 0.42 x 62 = 26 μv at 400W compared to 34 μv measured with the Eppley quartz window thermopile. At 600W the measured output was 93 μv. The portion due to arc alone is .44 x 93 = 41 μv. These values correspond closely to the values obtained using the 7910 Corning filter and Eppley quartz window thermopile. This is partly fortuitous since the reflection losses at the filter surfaces help to reduce the value obtained. The "no filter" measurement with the Eppley thermopile contains about 20% contribution due to radiation from the quartz arc tube.

In a NaI-TlI lamp at 600W (not the one described on page 21) the arc radiation is 62% of a total output value of 99 μv giving a value of 61 μv for the arc contribution. Measurement with the Eppley thermopile at the same time yielded a "no filter" value of 71 μv and 62 μv with the 7910 filter.

larger in the case of the bare arc tube mercury discharge since considerable ultraviolet radiation from the arc is normally absorbed by the glass outer bulb and converted to bulb radiation. The TlI additive discharge while showing considerably higher % radiation from the discharge is not as high as the bare arc tube mercury case since mercury still contributes some radiation which is absorbed by the glass. This is also the situation for the 10 mm diameter CsI lamp at 600W. The spectra in Figure 34 show the different degrees of mercury contribution in the CsI (10 mm) and NaI (12 mm) lamps. The NaI lamp in quartz shows the highest discharge contribution. In this lamp even though, as seen in Figure 34b the mercury contribution is fairly strong the mercury contribution is much smaller than in the pure mercury discharge and less ultraviolet is lost by absorption.

The high pressure sodium discharge in polycrystalline alumina has practically no ultraviolet radiation but there are absorption losses in the

ceramic. The Xe short-arc has a much larger fraction of energy in the electrodes which accounts for its low value even without the outer bulb. The second Xe lamp in addition looses considerable ultraviolet radiation by absorption in the glass.

12) The Excitation of Additives

In the preceding section it was shown that the radiation transmitted thru the outer bulb can be increased by the addition, in the form of iodides, of metals having low excitation levels. In this section we shall consider the effect of the additive on the discharge and the discharge conditions desired to optimize the additive radiation output.

If Boltzmann's Law is written in the form

$$n_k = n_o \left(\frac{gk}{go}\right) \exp\left(- {}^{ev}R/kT\right)$$

it is apparent that the population of each excited state would be directly proportional to ground state population so long as the gas temperature remains constant. However, if the arc wattage is to remain constant, the total radiation cannot increase so the gas temperature must decrease if the additive density is increased. The drop in gas temperature reduces the radiation originating from the highest energy states most. Since the mercury atoms levels are much higher than those of the additives, (see Appendix A for energy level diagrams) it is the mercury radiation which is lost to provide the increased wattage of the additive radiation.

When the gas temperature has lowered to the point where mercury radiation is only a small part of the total radiation further reduction results in the decrease of radiation from the higher energy states of the additive. In general this results in a preferential reduction of the I.R. radiation of the additive (see diagrams in appendix A) in favor of the lowest lying levels. Where radiation from these levels terminates on the ground state absorption

will occur and reduce the amount which escapes. The use of iodides which do not absorb this resonance radiation eliminates much of this absorption in the relatively cooler sheath surrounding the discharge where the normal state atoms recombine with the halide. At some point with increasing additive density the resonance radiation is essentially lost due to absorption.

Similar Discharges

Two discharges are considered to be similar if the axial temperature are the same and the temperature distribution between the axis and the wall is the same, i.e. the corresponding points $\frac{r_1}{R_1} = \frac{r_2}{R_2}$ have the same temperature.

Elenbaas[10] has shown that this condition of similarity exists in the pure mercury discharge if the amount of mercury vaporized per cm length and the input power per cm is the same in both lamps. This condition holds over a fairly wide range of diameters and power inputs. In the case of additive and mercury discharges the amount of additive vaporized per cm should also be included as a condition.

If the radiative characteristics of the 20 mm diameter 400W Hg lamp been found desirable and a smaller source size is required, e.g. 10 mm diameter, it would be necessary to increase the density of mercury by a factor of 4 which would increase the operating pressure from 2.5 to 10 atmospheres; require that the cool spot temperature of the smaller arc tube be increased sufficiently to provide fourfold increase in vapor pressure. The wattage loading of the wall in W/cm^2 would double, the pressure quadruple and the voltage nearly treble (actually the 8 times)[10]. The first two conditions do not lend themselves to safe operation of the lamp from a structural standpoint. The third condition reduces the electrode loss which is favorable.

In the mercury discharge if the amount of mercury per cm is reduced the gas temperature would increase to compensate for the reduced number of

radiating atoms and the radiation would remain essentially constant. In an additive discharge where the radiation is predominately that of the additive a reduction in the amount of mercury would produce a much smaller increase in gas temperature because of the smaller contribution to the radiation of mercury atoms. It should however be necessary to maintain the number of additive atoms in the discharge, which means that in the smaller diameter tubes the additive vapor pressure must be increased to maintain the low gas temperature. In the additive lamp the role of mercury becomes partly like that of the argon in the straight Hg-Argon discharge. It acts as a buffer gas which heats the wall and inhibits diffusion. It has another role in addition even when its own atomic radiation is reduced to a level adding essentially nothing to the discharge output. The mercury serves to aid in the broadening of the additive radiation which increases the escape rate (or reduces the inprisonment). This aspect of the discharge has not yet enjoyed much probing but some experiments were done in which the mercury density was varied in TlI-Hg lamps which resulted in increased radiation of the 5350Å line and apparently a broadening of the line since the gas temperature showed a concurrent reduction.

Lamp Tests

In an effort to check some of the above concepts a number of lamps were made containing Ge and In iodides as additives to the mercury. The two iodides were choosen since it was desired that all the additive be vaporized and these two iodides have high vapor pressures. (See table in appendix). In addition controlled amounts were desired and a technique was known which permitted the introduction of the metal and sufficient iodine in the form of HgI_2, both of which are easy to handle, and which react in the discharge to yield the additive metal iodide.

L-105	18 x 20 mm dia.	1.1 mg In + 6 mg HgI_2 + 66 mg Hg
L-106	10 x 12 mm dia.	.3 mg In + 2 mg HgI_2 + 15.5 mg Hg

The electrode spacing was the same in both lamps. The spectra of the lamps are shown at 400W Figure 35 and 600W Figure 36. Examination of the spectra show that the smaller diameter lamp which was expected to have a higher gas temperature and a reduced ratio of In to Hg radiation actually has a lower gas temperature as evidenced by a reduced ratio of Hg 5780 to 5461A radiation and the 4511A and 4105A In lines are stronger relative to the Hg 5461A line. Both conditions are contrary to expectations. However, an examination of the In lines 4511A and 4105A which originate from the same level and whose relative intensities are not affected by gas temperature, shows that the 4105A line which terminates on the ground state has increased relative to the 4511A line which terminates on a state 0.27 ev above the ground state. This indicates that absorption of these two lines is reduced with the shorter optical path in the smaller diameter, lower density lamp.

Reduced absorption for the two indium lines from the lowest excited state would result in an intensity increase of these lines relative to the mercury lines whose absorption should be negligible. Since a large part of the radiation from the arc is in these lines, the higher escape rate helps to keep the gas temperature from increasing. The reduction in arc volume along with the apparently lower gas temperature results in a reduction in the energy radiated which is seen in the thermopile measurements below. It is particularly evident in the case of the 4600 filter which passes only arc radiation.

The thermopile measurements were made on these lamps using the Eppley quartz window thermopile at 100 cm distance.

	L-105 (18x20)		L-106 (10x12)	
	400W	600W	400W	600W
No filter	40	66	38	61
4600	13.5	21.5	10.6	17.6

Four gallium iodide additive lamps were made as follows:

L-109	18 x 20 mm diameter arc tube	72 mg Hg	1.2 mg Ga
L-110	8 x 10 mm	17.5	.3
L-111	8 x 10 mm	15.5	1.4
L-112	8 x 10 mm	14.5	1.2

The spectra of these lamps are shown in Figures 37, 38, 30, and 40. L-109 shows strong broadened Ga lines and relatively weak Hg. L-110 has less Ga and Hg and exhibits a much higher gas temperature. The Hg lines are relatively stronger. The Ga lines are not so broadened as in L-109. L-111 and L-112--the two lamps are similar in spectra. The increase in Ga has resulted in a broadening of the violet lines and a reduction of the Hg contribution.

The Ga lamp L-109 shows a low gas temperature with strong Ga radiation. In L-110 the reduction in the amounts of Hg and Ga result in an increase in gas temperature as would be expected. The Hg lines increase relative to the Ga and the Ga violet lines are considerably reduced in width. In L-111 and L-112 the gas temperature is reduced due to the increased quantity of Ga and the Ga lines are strongly broadened.

The case of Ga follows the pattern of changes as expected from the previously discussed concepts while the In case did not. The principal difference in the large diameter lamps from which we started is one of line width of the additive radiation from the lowest excitation level. In the In lamp the lines were relatively narrow so that absorption of this radiation by the highly populated terminal states would be a strong effect. This would not be the situation with the strongly broadened lines of Ga. The

increased line width is probably due to the increased density of Ge since even though similar weights of each were used the atomic weight of Ge is only about half that of In resulting in double the density for the same weight.

While these tests are suggestive of the correctness of the concepts of the role of the additive a more definitive test would be desirable. The current test is complicated by the presence of HgI which is seen in the spectra and by the fact that the compounds with their high iodine content are not completely transparent.

13) NaI + Hg Lamps

A set of four NaI + Hg arc tubes were made. The first (L-124) had 55 mm electrode spacing and a 10 x 12 mm diameter. It contained 40 mg Hg which gives the same mg/cm loading as in the standard 400W Hg lamp and 20 mg NaI in addition to the argon starting gas. The operating voltage with the mercury completely vaporized was 230 volts. The mercury pressure in the operating arc tube in this lamp is about four times that in the standard lamp.

Figure 41 (a and b) shows the spectrum of this arc tube operating at 600 watts in air inside a quartz cylinder with the ends packed to restrict the air circulation. Figure 41a was obtained using a 1P28 photomultiplier as a detector in the Beckman monochromator which permits smaller slits and better resolution than that used in Figure 41b in which the detector is a thermocouple. The Na doublet at 5890-5896Å is the strongest line seen but the mercury contributes strongly in this spectrum. The Li 6707Å line is plainly seen even though it is there only as an impurity. The luminous output of the arc tube was 49,000 lumens or ~80 lumens per watt which is 50% greater than the standard mercury.

The arc tube was then mounted in 1-1/2" diameter Pyrex outer bulb which was then exhausted and baked at 450°C for one hour before tipping off under vacuum. The spectrum was then obtained at 400 watts using the I.R. monochromator with the thermocouple detector. This spectrum is shown in Figure 42. The Na lines are seen to be increased in intensity relative to the mercury lines due to the higher NaI vapor pressure attained at the higher operating temperature of the quartz arc tube. This lamp was operated for several minutes at 600 watts but the arc tube bulged.

The next arc tube (L-125) was an 8 mm I.D. 1 mm wall having a 25 mm electrode spacing. The mercury was reduced to 20 mg still maintaining the approximate mg/cm used in the first lamp and 25 mg NaI was added. Argon was also present as the starting gas.

The spectrum with the arc tube operating in an evacuated outer bulb at 200 watts 1.7 amps 136 volts is shown in Figure 43a. Again the principal radiation is seen to be the Na 5890-5896Å lines with the mercury spectrum relatively weak and Li evident as an impurity.

A second identical arc tube (L-127) was made and mounted in a 1" diameter outer. This arc tube operated at 140 volts 1.6 amps 200 watts with the spectrum shown in Figure 43b. There is very little difference from the preceding lamp. The mercury lines appear slightly stronger.

Measurements of the radiation were made using a Perkin-Elmer thermopile with a KBr window at a distance of 100 cm. The following values were obtained with 200 watts input to the lamp:

No filter	44 μv
7910	30 "
4600	13 "

The 7910 filter includes the radiation seen in the spectral curve plus the radiation down to about 3000Å. The 4600 filter covers the 3200 to 8000 range. The standard Hg lamp values at 400 watts input are 70, 34 and 14 μv.

With the 7910 filter in place the output was recorded and then followed as the arc was suddenly extinguished. Seventy-eight percent of the energy passing the 7910 filter is seen to be arc radiation. After these measurements the lamp was sent to John Creedon, Contracting Officer's Representative at Fort Monmouth.

A third (L-133) 8 x 10 mm diameter arc tube was made having 23 mm electrode spacing and 20 mg Hg. The NaI quantity was increased to 50 mg in an effort to increase the Na contribution by providing a reservoir of NaI in which the surface temperature might be higher. The arc tube was sealed in an evacuated outer 1-3/8" in diameter.

The spectrum seen in Figure 44b obtained with the I.R. monochromator is essentially the same as that of the preceding lamp. Figure 44a was obtained using a 7102 photomultiplier detector and shows the 5780Å Hg and 5688Å Na lines resolved from the 5890-5896Å Na lines. On the long wavelength side of this line the 6103A Li and 6154-61Å Na lines are indicated by breaks in the slope of the line. The lamp was operated at 230 watts 1.9 amps 135 volts. The lumen output was 19,000 lumens or 83 lumens per watt.

Measurements made with the Perkin-Elmer KBr window thermopile were close to those of the preceding lamp. The arc tube operated at 185 watts.

No Filter	44 μv
7910	28 "
7910 + 4600	11 "

Eighty-two percent of the radiation detected through the 7910 filter is contributed by the arc in the Na lamp. From both the lumen output and thermopile measurements it is obvious that these 8 mm i.d. lamps are far more efficient at producing radiation in the 3000-8000Å range than the standard mercury lamps. This lamp was sent to R. Schlecht at the Pittsburgh Laboratories for additional spectroscopic study.

14) Heavy Wall Capillary Lamps

With the high efficiency of producing visible radiation and the strong radiation from the additive metal found in the lamps just discussed the effort was directed toward lamps having high loading and very small bore. The emphasis was put on NaI additive in lamps having geometry similar to the presently available Nd:YAG laser rod which have a strong absorption band near the Na "D" lines at 5890-96Å.

All previous lamps were made with standard automatic machine pressing for the electrical lead in seal. This was no longer possible with the capillary lamps in the following work and all the seals were hand fabricated in the following manner.

A 20 mm length of thin feather edged molybdenum ribbon was cut to fit the inner diameter. The electrode was welded to one end and a molybdenum wire to the other. These parts were baked in H_2 to remove any oxides and then inserted in the capillary which previously had had an exhaust tube joined to it at the center. The ends of the capillary were closed off under an argon flow. The capillary was then exhausted and the quartz tubing heated to collapse around the molybdenum ribbon to effect the vacuum seal (structure is shown in Figure 45). The seals were leak checked by adding approximately 100 mm of Neon to the arc tube and checking with a high frequency coil for Neon in the closed chamber initially and again after several hours. The arc tubes were then baked and filled in the normal manner. This technique precluded any serious leaks but some of the lamps were found to leak slowly and eventually became inoperable.

The first heavy wall capillary lamp (L-134) had 3.6 mm I.D. 10 mm O.D. The electrode spacing was 37 mm 50 mg NaI and 10 mg Hg were added. The amount of Hg per cm length was reduced by a factor of three compared to

preceding lamps to bring the operating voltage and pressure into reasonable range. Even with this reduction the Hg density is about ten times that of the standard Hg lamp and the operating voltage was > 360 volts.

The arc tube was operated in air in a quartz sleeve at 300 watts .9 amp > 360 volts and its spectrum is shown in Figure 46a. The arc tube was then sealed in an evaucated outer 1-3/8" diameter Pyrex. The spectrum then obtained is shown in Figure 46b. The Na "D" lines are broadened and the mercury lines are reduced at the higher Na concentrations obtained and the lower gas temperature. The 300W in this lamp is about the same w/cm loading in the 8 mm I.D. lamps at 200W. The spectrum in 46b when compared to the spectra of the 8 mm I.D. lamps show even greater intensity of Na "D" lines compared to Hg lines, and have considerably greater broadening of the Na "D" lines.

Thermopile measurements at 350 watts input to the arc tube were as follows:

No Filter	80 μv
7910	63 "
4600 + 7910	29 "

The percentage of radiation detected passing through the 7910 filter due to the arc was found to be greater than 90%.

A second arc tube (L-135) was made with the 3.6 x 10 mm tubing and had an electrode spacing of 33 mm. This arc tube was filled with 48 mg NaI, 10 mg Hg, and 2.6 mg TlI and mounted in a vacuum outer bulb. The spectrum is shown in Figure 47a. The Tl 5350Å line is plainly seen but is less intense than the Na 5890Å line. This lamp had been operated for two hours at 300 watts before the spectrum was run. Adjacent to the 4358Å Hg line is a band at 4450Å which is due to HgI. This band very often appears in lamps containing NaI after they have been operated for some time. The luminous efficiency was approximately 120 lumens per watt.

Measurements with the thermopile and filters at 300 watts, 1.16 amps were

No Filter	62 μv
7910	40 "
7910 + 4600	19 "

By this time the outer bulb contained some gas and was opened to be re-exhausted. The lamp was lost when the outer bulb collapsed during baking.

Another NaI + TlI + Hg arc tube (L-136) was made with the same 3.6 x 10 mm tubing. In this the electrode spacing was 37 mm. The quantity of NaI and mercury remained the same but the TlI was increased to 16 mg. The arc tube was mounted in a vacuum outer and operated at 300 watts 1.1 amps ~360 volts. The spectrum is shown in Figure 47b. In this lamp the Tl 5350Å line is stronger than the Na 5890Å lines. The luminous efficiency is again about 120 lumens per watt.

Thermopile measurements were made at 400 and 600 watts:

	400W	600W
No Filter	85 μv	133 μv
7910	53 "	94 "
7910 + 4600	20 "	40 "

The lamp was then operated at 300 watts for five hours. During this period the lumen output dropped 40% and the voltage dropped to 312 volts..The spectrum at the end of five hours is shown in Figure 48. The Na 5890-96Å lines have been reduced and the Hg lines increased in intensity. The HgI band at 4450Å appears strongly and relatively strong continuum is present, particularly in the infrared region.

A third NaI TlI arc tube (L-137) with 3.6 x 10 mm tubing was made with an electrode spacing of 33 mm. The TlI was increased to 28 mg and the Hg reduced to 5.5 mg to lower the operating voltage. The arc tube was sealed in an evacuated Pyrex outer.

The spectral distribution for this lamp operating at 400 watts 265 volts 1.9 amps is shown in Figure 49a. The luminous efficiency was 90 lumens per watt. When the lamp was inverted to bring the deposited iodides to the hottest part of the arc tube the efficiency increased to 105 lumens per watt and the voltage rose to 340 volts. At 600 watts the efficiency was still 105 lumens per watt and the voltage rose to 365 volts.

Thermopile measurements at 600 watts gave these values:

No Filter	136 μv
7910	90 "
7910 + 4600	33 "

The first two values are close to those found for L-136 at 600 watts. The third is almost 20% lower which agrees fairly well with the lowered lumens per watt value obtained with this lamp.

This lamp was then operated at 400 watts for six hours during which time the lumen value dropped less than 10% but the space between the outer bulb and the arc tube showed gas had developed there during operation.

L-138 was made with 2.6 I.D. 7.5 O.D. tubing and had an electrode spacing of 34 mm. The arc tube was filled with 29 mg NaI and 7.5 mg Hg. When mounted in an evacuated outer bulb the operating characteristics were 200 watts . 75 amps 440 volts 100 lumens per watt. The spectral distribution is shown in Figure 49b.

Thermopile readings at 200 watts were

No Filter	51 μv
7910	32 "
7910 + 4600	14.5 μv

The lamp was operated for two hours at 200 watts with essentially no change in the lumen reading but gas had developed in the outer bulb.

L-139 was made with 3.0 x 10 mm tubing and had a 34 mm spacing. The arc tube was filled with 27 mg NaI and 1.5 mg Hg. Mounted in an evacuated outer bulb, the operating characteristics were 330 watts 3.16 amps 131 volts 74 lumens per watt; 400 watts 3.75 amps 130 volts 85 lumens per watt.

The spectrum at 400 watts is given in Figure 50. The 5688Å Na line is seen to be much stronger in this lamp than any other. The infrared lines are also more intense which indicate higher gas temperature since they come from the higher energy states.

Thermopile measurements were made at both 330 watts and 400 watts as follows:

	330W	400W
No Filter	71 μv	92 μv
7910	40 "	56 "
4600 + 7910	14 "	19 "

From this group of lamps we have found that it is possible to operate additive lamps with diameters as small as 2.6 mm I.D. 7.5 mm O.D. at loading ~100w/cm (400W/cm^3) in an evacuated envelope and obtain visible radiation efficiency much higher than the standard 400W Hg lamp with most of the radiation associated with the additive metal. It appears that higher efficiency is associated with highest mercury density. Operation for a number of hours at these loadings in quartz presents the problem of conversion of NaI to HgI probably due to reactions with the wall.

15) Operation of Arc Tubes in Air

The elimination of the outer jacket on these lamps is desirable to obtain improved proximity of source and laser rod for efficiency of optical coupling. A group of lamps were made using the 3.5 x 10 mm tubing with gas fills of NaI + Hg or TlI + Hg and operated without the jackets.

L-140 30 mm electrode spacing 30 mg NaI - 2 mg Hg. Operating at 400W 3.62 amps 130V the luminous efficiency was measured as approximately 80 lumens per watt. The spectrum as obtained using the RCA 7102 photomultiplier which peaks at 8000Å as a detector is shown in Figure 51. The instrument slit width is 0.1 mm. The two strongest lines are the Na lines at 5890-96 and 8183-95Å. The Na "D" lines are seen to be considerably broadened. A more detailed spectrum of this region is shown in Figures 52, 53, and 54 as the NaI vapor pressure and the loading is increased. In this case the slit width was reduced to .01 mm and the scanning rate was reduced by a factor of 3. Figure 52a,b shows the lamp at 300 watts with and without a fan cooling the lamp. The yellow mercury lines are resolved--the Na "D" lines are not. The 5461Å mercury line illustrates the instrumental width of a line < 1Å wide. With the fan removed the Na lines increase relative to the Hg and begin to broaden. The broadening increases at 360 watts and the 5688Å doublet enters more strongly. As the wattage is increased to 400, 450 and 500 watts the reversal slowly becomes evident and the lines to be as broad as the Hg yellow doublet which has 20Å separation. After operation at 500 watts the arc tube was found to have bulged slightly.

This arc tube (L-140) and another (L-142) having the same quantities in the lamp but only 26 mm electrode spacing were sent to the Westinghouse Research Laboratories group for their studies.

L-144 3.5 x 10 mm diameter 32 mg NaI 1.8 mg Hg 20 mm electrode spacing.

The spectra at 200W, 120V, 2.1a and 300W, 114V, 3.2a are shown in Figures 55, 56. These were run on the P-E IR monochromator. The Na lines are seen to be the dominant ones and the Na "D" lines increase in intensity and broaden with increasing wattage. The 5688Å Na line also shows marked increase. In the IR two groups of strong lines are seen at 8183, 8195Å, and 1.14, 1.13 μ. A third line at 1.84 μ is quite pronounced at the higher wattage. The mercury spectrum is evident but weak. The luminous output increased from an arbitrary value of 84 at 200W to 178 at 300W which is about 40% increase in luminous efficiency.

To obtain a more detailed picture of the Na "D" line region the lamp was operated at 250 and 300 watts and examined using the monochromator with the 7102 PM at a slit width of .01 mm and a slow scan. The spectra are shown in Figure 56a,b. At 250 watts the Na "D" line region is seen to consist of two peaks clearly resolved and widely separated. They are more clearly resolved than the mercury yellow doublet which is separated by 20Å. At 300 watts the radiation is more strongly broadened and the peak separation is increased to about 50Å with the minimum occuring at 5890Å. The stronger peak is at ~5920 and the other at ~5870Å. The radiation is asymmetrically broadened and extends well into the 6154Å Na line.

Since this is a shorter lamp than L-140 the w/cm loading would be comparable to the 457W operation in L-140. It is quite obvious, however, that the Na density in L-144 is much higher from the greater broadening and pronounced reversal present. The gas temperature as indicated by the reduced 5770-90 to 5461Å line ratio appears to be slightly higher at the higher wattage.

L-148 3.5 x 10 mm diameter 31 mg Na 1.9 mg Hg 30 mm electrode spacing.

The spectra as shown in Figure 57a,b at 300W input to lamp are essentially identical to those for L-144. The lamp voltage was 170V which is about 50% higher than L-144 and it is 50% longer. This is really not to be expected since the total mercury weight was the same in both cases. It is possible that with the small quantities of Hg used in these lamps some may have been lost. There is also some difference in the distance from the electrode top to the quartz seal which at this stage is difficult to control. This would affect the lamp volume and cool spot temperature.

Measurements of the luminous output were made at 200 and 300 watts giving values of 8500 and 20,000 lumens. The pronounced increase in lumens indicates the strong dependence of bulb wall temperature on the sodium radiation contribution.

Output measurements were also made using a thermopile and filters at a distance of one meter.

	300W	400W
No Filter	51 μv	70 μv
7910	30 "	49 "
7910 + 4600	11 "	19 "

The total radiation increase is just about proportional to the increase in watts. The total arc radiation which is represented by the 7910 transmission increases considerably more as is also true of the visible as measured with the 7910 + 4600 filter combination. With the lamp operating at 400 watts the output with no filter was followed as the arc was extinguished. This gave a value of 62% of the total radiation as arc radiation. The total radiation values are about 25% lower than those obtained for a similar lamp mounted in an evacuated outer bulb. Losses to the surrounding air by conduction and convection could account for this.

L-152 48 mm electrode spacing 3.5 mm Hg + NaI.

The NaI used in this lamp had been distilled under vacuum and kept in an evacuated capsule. The capsule was opened in an inert atmosphere and inserted into the exhaust tubulation. The lamp was immediately sealed to the vacuum system and evacuated.

Measurements were made at 500, 600, and 700W with the lamp operating horizontally in a 2" diameter Pyrex sleeve. The exhaust tubulation tip off faced downward and the NaI was condensed in the tip off.

The operating characteristics of this lamp are given below:

500W	2.6a	220V	80 LPW
600W	3.25a	210V	94 LPW
700W	3.8 a	210V	103 LPW

The spectrum obtained at 500W with the 7102 detector is shown in Figure 58a. The radiation is principally the Na lines at 8195-8183Å and the broadened "D" lines at 5890-5896Å. The spectral region from 5400Å to 6400Å is shown at higher resolution in Figures 58b and 59a,b at wattage input of 600, 700W. With increasing wattage the Na "D" line radiation peaks increase in intensity and the line width increases considerably. The reversal becomes increasingly more pronounced due to the greater absorption with the increasing Na concentration. This results in a shift in wavelength of the short wavelength peak of the reversal toward shorter wavelength. This shift becomes very critical if it is desired to match the strong absorption of Nd^{+3}:YAG at 5885 ± 3Å. Initially with increasing NaI vapor pressure the radiation in this band will increase. However, if the NaI vapor pressure and therefore the reversal increases too much this absorption peak of Nd^{+3}:YAG will fall within the reversal region and the radiation available for excitation will decrease with increased loading of the lamp. The lamp therefore must be designed for operation at a particular wattage in a particular excitation environment such that the broadening and the reversal combine to yield the

short wavelength peak at the desired wavelength. For higher wattage operation some means of cooling must be provided. It would be possible to operate these lamps with a small appendage in which the NaI was contained at a temperature which gave NaI vapor below the desired value and the optimum conditions could be obtained by adjusting the heating. Since the high reflectance of laser cavity is a strong contributing factor to the lamp temperature and in effect limits the wattage at which the lamp can be operated, the laser head should be transparent to all but the desired exciting radiation and highly reflecting only at this wavelength. This may be accomplished by use of multilayer dichroic coatings designed for optimum reflectance at the desired wavelength.

L-153 1.8 mg Hg 5 mg NaI 20 mm spacing.

Figures 60a,b show the spectra at high resolution of this lamp operating at 250W 124V 2.35a

400W 104V 4.25a

The amplifier gain is decreased by factor of $\frac{50}{85}$ in the 400W spectrum to keep the Hg yellow lines on scale.

The yellow sodium lines are much weaker than in any of the other lamps and show no reversal even at 400W. The mercury yellow lines increase by 35% from 250-400W while the Na yellow line peak increases 70% and broadens to an apparent width of about 20Å at 1/3 of peak. The Li 6707Å line is present and has appreciable intensity. The gas temperature change is not detectable from the relative intensities of the mercury 5461Å and 5770Å lines, but their increased intensity much result from some temperature increase. Since the Na lines increase much more in intensity with the increasing wattage the Na content in the arc must be increasing indicating that an excess of NaI exists but that it is occupying a much lower temperature point on the arc tube. The lamp was operated for one and one-half hours at 300W and showed no detectable changes at that time.

L-143 3.5 x 10 mm diameter 29 mg TlI 1.7 mg Hg 23 mm electrode spacing.

This lamp was operated for about 15 minutes when the voltage was found to be falling and a deposit of TlI was seen on the upper end of the lamp. During the first few minutes of operation the spectrum was obtained with the lamp operating at 200W, 130V, 2.43a, Figure 61. The dominant lines are those of thallium. There is also a faint trace of sodium present. When the wattage was increased to 300 watts the voltage dropped to 90 volts due to the loss of mercury and TlI through a crack in the tipped off exhaust tube.

L-145 3.5 x 10 mm diameter 30 mg TlI 2.3 Mg Hg 26 mm electrode spacing.

Spectra of L-145 are shown in Figure 62a,b. Figure 62a was taken with a small slit (.01 mm) and the 7102 photomultiplier detector. Figure 62b was obtained at .3 mm slit and a thermocouple detector. In both spectra the thallium lines are predominant with Naagain showing as a contamination. In this lamp, however, there is a relatively strong continuum seen in the spectra which is not evident in the earlier work on larger diameter lamps.

This continuum is attributed to the higher TlI pressures obtained in this lamp. The 5350Å line is seen to be strongly reversed. A closer look at this reversal is shown in Figure 63 where this region is scanned more slowly with a small slit. The wavelength marks are given on these figures. At 200 watts the continuum is not evident. The 5350Å "line" is about 70Å wide at the points having intensity values of 1/2 the major peak (the longer wavelength peak has the higher value as was also true in the Na lamps). At 320 watts the background is pronounced and the 5350Å line extends well into the 5461Å Hg line. The Tl line is about 100Å wide.

The light output as measured by an eye sensitivity corrected response cell gave the following values.

250W	198V	1.84a	170	L.O.
300W	204V	2.1a	198	L.O.

A standard 400 watt Hg lamp operating at 400 watts in the same setup had a light output value of 153. This yields a luminous efficiency of 88 lumens per watt at 300 watts. A capillary lamp having the same geometry but only mercury had an output of 84 operating at 300W, 208V, 2.0a.

L-149 3.5 x 10 mm diameter 12 mg TlI 1 mg Hg 28 mm electrode spacing.

The mercury dose and TlI quantities were reduced in an effort to lower the voltage and reduce the amount of continuum. Neither effect was attained to any extent. The spectra of this lamp as shown in Figures 64 and 65a,b were obtained with the lamp operating at 300 watts at a voltage which varied from 172 to 186 volts. They are quite similar to those of L-145 at the same wattage. The infrared continuum appears to be stronger. The luminous efficiency is only 55 lumens per watt.

Measurements were made at 300 watts using thermopile and filters at 100 cm as follows:

	300W
No Filter	48 μv
7910	27 "
7910 + 4600	7.0 "

The total radiation is only ~5% less than that measured for L-144. With the 7910 filter it is 10% less and the visible is ~35% less. The fraction of total energy in the arc was only 43%. The reason for these differences is not yet known. It is believed that the high vapor pressure of TlI in these lamps results in appreciable absorption of arc radiation in the visible.

L-151 2.4 x 8 mm diameter 1.5 mg TlI 1.1 mg Hg 28 mm electrode spacing.

The sharp reduction in the amount of TlI in this lamp was effective in eliminating the continuum as can be seen in Figures 66, 67, and 68 in which the lamp was operated at 300W, 191V, 2.1a and 400W, 181V, 3.7a. The radiation is essentially the thallium spectrum with 5350Å the strongest line. In Figure 68a,b this line is looked at in greater detail. The half width appears to be about 70Å being slightly broader at 400 watts than at 300 watts. The 300 watt shape and width appears to match very closely the 200 watt operation of L-145. The slit in this case is .02 mm rather than .01 and the reversal does not show up as pronounced.

The light output at 400 watts was only 22,000 lumens--about the same as the standard 400 watt Hg lamp.

Measurements were made at 400 watts using thermopile and filters at 100 cm.

	400W
No Filter	71 μv
7910	41 μv
7910 + 4600	10 μv

On a μv/w basis these values are about 10% higher than L-149.

Separation of arc and envelope radiation yielded 42% of total as arc radiation. Quite similar to L-149.

L-146 3.5 x 10 mm diameter 2.2 mg Hg 28 mm electrode spacing.

L-146 was made to compare the luminous and electrical characteristics with other lamps and see if any pronounced differences existed between it and standard lamps. This lamp operated at 300W, 208V, 2.0a (Figure 69). The luminous efficiency was about 75% that of the standard lamp.

16) In Iodide + Hg

A 3.5 mm I.D. capillary lamp was made containing 1 mg InI + 6 mg Hg and having 27 mm electrode spacing. The exhaust tubulation for this lamp was tipped off about 1/2" from the body to provide a cooler temperature for the condensed iodide. This was found to be necessary because the lamp would extinguish during the warm-up period due to the rapid increase in the iodide vapor pressure. The spectra of this lamp taken with a 7102 photomultiplier (L-156) are shown in Fig. 70a, b; the lamp was 5a, 350 watts, 510 watts, operating at 350W (80V, 3.7A) and 625W (122V, 5A) detector. At the lower wattage the lines are narrow and no reversal is evident. At 625W the lines are broad and strongly reversed at 4511 and 4102A and there is a strong continuum throughout the spectrum. The spectrum was also obtained using a 1P28 detector with the lamp at 625 watts and 750 watts. These are shown in Fig. 71a, b. The luminous efficiencies measured were as follows:

500W	40 LPW
625W	48 LPW
750W	56 LPW

17) Ga Iodide + Hg

Another 3.5 x 10 mm capillary lamp (L-158) was made with 35 mm spacing containing 1 mg Ga + 6 mg HgI_2. This was also tipped off long as in the preceding lamp. The spectrum is shown in Figure 72a,b operating at 345W 64V 6a. Figure 72a is with 7102 and b with 1P28 detector. The radiation is principally in the two violet lines originating from the level at 3.07 ev. Higher wattage values were not obtained because the lamp extinguished at higher loading.

18) Square Wave Pulse Operation

Temporary operation at levels much in excess of those which are possible with continuous operation may be obtained by using low duty cycle square wave pulses superimposed upon a D.C. level.

Measurements were made with 100 watt mercury lamps using the circuit shown in Figure 73. The light output was viewed through a monochromator so the lines could be individually monitored. The detector output was coupled directly to a scope so that the output during the pulse could be compared to the D.C. level. The 1 ms current pulse rose from a D.C. level of .75 amp to 5.5 amp during the pulse. The intensity of the 5461Å line rose to 7X and the 5780Å line rose to 12.8X. Since the change in voltage during the pulse is estimated at not more than 5% from the scope trace of the voltage, the efficiency of generation of the mercury yellow lines almost doubles at the high current level while the green line efficiency is about the same. At the higher temperature of the arc during the pulse the yellow lines which originate from a higher level should be expected to increase more than the green line.

A NaI capillary lamp was made and mounted in a evacuated outer bulb. The lamp was operated at 200 watts and pulsed from this level in single pulses of 1 ms duration. The current during the pulse rose from 2.2 to 10 amps. The 5461Å merucry line and the 5890Å sodium line were monitored during the pulse. The 5461Å mercury rose 4.6X and the 5890 Na rose 3.6X. In the D. C. operation the response of the 1P28 to the 5890 Na was $\sim 1/5$ that of the 5461Å mercury line. This indicates that the Na line is not nearly as intense in this lamp at the loading used as would be desirable. The power supply used was not capable of operating the lamp at much higher loading and then pulsing above it.

B. Rapid Scan Monochromator

1) Introduction

The spectral emission from low energy pulsed arc discharges must be measured in order to determine the efficiency of emission into various spectral regions that may be used to selectively pump lasers. We wish to examine the change in the spectral distribution due to line broadening, self-reversal, and increase in the continuum as a function of increasing current and energy density. The usual techniques of measuring the spectral emission using photographic film are not very satisfactory when relatively accurate radiometric data is required, particularly for wavelengths longer than 6500Å. A large part of this difficulty lies in calibrating the absolute spectral sensitivity of the film using a tungsten strip filament lamp. The approach originally planned for this study was to use a multiple channel monochromator similar to that used in our previous work[11]. In this, a number of photodetectors, each connected to a separate oscilloscope channel, measured the time variation of a selected wavelength interval over the spectral range of interest. For complete spectral coverage which is necessary when relatively narrow emission bands are excited, this involves a very large number of data channels (140) for a spectral width of 50Å over the 4000 to 11000Å interval to be examined. For primarily continuum emitting discharges such as those found in high energy xenon flashlamps, one sample every 250Å may suffice. For the additive arc discharges that are primarily in line emission such as would be desired for the low energy selective pumping, a better technique was required.

2) Description of the Wide Spectral Range Rapid Scan Spectrometer

It was necessary in this study to be able to scan rapidly at moderate resolution over a fairly large spectral range. In a recent paper, Hill and Beckner[12] discussed a spectrometer which could scan over a limited

spectral range (~200Å) at rates varying between 10 and 200Å/μsec. W. Niesel et al.[13] described a spectrometer system that includes a monochromator that is capable of scanning over a wider spectral range (typically 3500Å - 7000Å), but at rates of the order of .3Å/μsec.

In the instrument to be described, we have taken the approach of Niesel et al., but have used a rotating mirror which is capable of much higher speed together with a modified Czerny-Turner monochromator layout rather than the Pfund mounting of Niesel et al. The optical system used is much simpler to construct than the Pfund, and allows the use of longer slits for a significant gain in the light intensity (i.e. radiance) passing through the instrument.

The optical arrangement of the basic rapid scan monochromator is shown in Figure 74.

The rotating mirror reflects the collimated beam onto the grating varying the angle of incidence (α). The geometrical relationship between the exit slit, the focusing mirror, and the grating, define an angle of diffraction (β) which is approximately the same for all of these angles of incidence. The projected width of the rotating plane mirror which is the width of the collimating mirror times the cosine of the angle determines the effective width of the grating and thus the aperture and the theoretical resolving power of the instrument. The actual width of the ruled portion of the grating subtending the rotating mirror, together with the distance of the grating from this mirror determines the spectral range of the instrument for a particular grating. These parameters, in the instrument under discussion have been designed to give a spectral range which will require only one separation of overlapping orders.

Figure 75 illustrates the above principles.

In order for rays I and II to be brought to the same focal point at the exit slit:

$$\beta = \beta_1 \cong \beta_2$$

The grating equation is then written for the two cases as

$$m\lambda_1 = d\,(\sin\alpha_1 + \sin\beta) \qquad 1a$$

$$m\lambda_2 = d\,(\sin\alpha_2 + \sin\beta) \qquad 1b$$

Subtracting equation 1b from equation 1a we obtain

$$m\,\lambda = m\,(\lambda_2 - \lambda_1) = d\,(\sin\alpha_2 - \sin\alpha_1) \qquad 2a$$

$$= 2\,d\cos\left(\frac{\alpha_2+\alpha_1}{2}\right)\sin\left(\frac{\alpha_2-\alpha_1}{2}\right) \qquad 2b$$

Equation 2a indicates the factors which govern the spectral range of the instrument (i.e.: λ_1 to λ_2).

It can also be shown from simple geometrical considerations that

$$2(\theta_2 - \theta_1) = 2\Delta\theta = (\alpha_2 - \alpha_1) = \Delta\alpha$$

Now for the maximum light intensity to be diffracted into the first order ($m = 1$), the grating should be used at angles near to the blaze angle.

A possible choice, though not necessarily optimum, is to have α_1 and α_2 on either side of the blaze angle (θ_B) such that $\frac{\alpha_2 + \alpha_1}{2} = \theta_B$

Combining 2 and 3 with θ_β, we obtain for 1st order

$$\Delta\lambda = 2d\cos\theta_B \sin\Delta\theta$$

and for small angular displacements $\Delta\theta \ll 1$ in a short time interval $\Delta t \ll 1$, we can write $\frac{\Delta\lambda}{\Delta t} = 2d\cos\theta_B \frac{\Delta\theta}{\Delta t} = 2d\,\omega\cos\theta_B$

where ω is the angular speed of the mirror in radians/sec.

The actual arrangement of the monochromator consists of two .5 m focal length spherical mirrors arranged as shown in Figure 74. The aperture of the collimating mirror is restricted so as to just fill one of the faces

of the rotating plane mirror; the focusing mirror is wide enough to receive the diffracted beam from both ends of the width of the grating.

The rotating plane mirror presently being used in the six-sided turbine driven mirror of a AVOC-MC300-2 streak camera, mounted with the mirror axis vertical.* The diffraction grating has a 102 mm x 102 mm ruled area, rules with 600 lines/mm, and with a blaze angle of 8°. The width of the mirror face is about 1-2 cm which gives an approximate theoretical resolving power in the first order of 7200 for θ 0°.

If we refer to Figure 74, it can be seen that the angle at which the beam is incident upon the exit slit varies with the illumination of the grating by the rotating mirror. The detector optics and the area of the radiation detector must be designed to include this range of angles. Effectively, this usually results in the detector optics being designed as though the entire focusing mirror were being illuminated as would occur in the more usual monochromator with this size grating. This variation in exit angle, which corresponds to the variation in wavelength, permits filters to be positioned so as to remove the second and higher orders occurring in the same spatial portion of the sweep but still allow the shorter first order wavelengths which are in a different spatial region to be incident upon the detector.

In the instrument being described which is intended to sweep from 4000Å to 1100Å in first order, a Corning CS2-63 filter, which passes wavelengths longer than ~6000Å, is inserted in the longer wavelength position of the exit

*The manufacturers recommend limiting the speed of the mirror to about 1500 cps when the camera is mounted vertically; and a 3/8" thick steel housing was built to contain the mirror fragments in the advent of a mirror exploding at the high rotational speeds possible.

beam just beyond the exit slit thereby removing the shorter wavelength second order from the longer wavelength first order. A partial insertion of the filter permits the first order at the shorter wavelength region (~4000A) to be detected by the same photodetector. Other filters entirely in the entrance optics removes wavelength S shorter than ~4000Å in this instrument.

3) The Detection System

In the present instrument, an S-1 response photomultiplier together with a Tektronix 555 oscilloscope is used to detect and record the radiation. Varying the sweep rate of the oscilloscope changes the effective spectral resolution of the spectral range displayed and a variable time delay generator on the oscilloscope allows different portions of the spectrum to be displayed.

The oscilloscope used for the information display was triggered by an RCA 931A photomultiplier mounted at one side of the grating. The photomultiplier detected the sweeping light beam from the rotating mirror before the light was incident on the grating causing a pulse which could be used as a trigger. The time delay on the oscilloscope allowed various portions of the sweep and thus the spectrum to be displayed. For the pulsed lamp studies, a trigger from the magnetic pickup on the rotating mirror, suit[illegible]yed, is used to trigger the lamp for proper synchronization.

The paper discussing the basic princip[illegible]s of the spe[illegible]gether with spectra of continuous lamps (taken at [illegible]peed of ~90[illegible] sec, [illegible]eting its capabilities resulting from this work [illegible]endix [illegible].

4) Calibration

The ultra-rapid scanning monochromato[illegible] has been use[illegible] obtain the spectrum of a xenon shortarc lamp. This was also done with the h[illegible]gh resolution monochromator setup to be described later. This afforded a calibration [illegible] the resolution and spectral range of the rapid scan spectrometer.

Attempts were made to exploit the spatial resolution property of the instrument by using appropriately placed filters after the exit slit and masks in front of the grating in an attempt to obtain a reasonably flat spectral response. This has proven more difficult than expected due to the precision necessary, and further work must be done in this area.

Photomultipliers having the S-1 and S-11 spectral sensitivities were suitably arranged after the exit slit to detect and measure the spectral range corresponding to their respective optimum sensitivities. This procedure proved satisfactory and was used in obtaining the spectra of the flashlamp radiation to be presented.

The spectral radiance of the tungsten standard lamp (see Table I) was used to calibrate the spectral sensitivity of the instrument, including the photomultipliers. However, the signal from the tungsten lamp was not measurable at the same spectrometer slit widths, photomultiplier voltages, oscilloscope gains, and photomultiplier load resistance values used for the flashlamp observations; therefore, calibration of these parameters was necessary and is tabulated below.

Figure 76 is the recording of the spectral radiance of the calibrated standard tungsten lamp from which the calibrations were made. The mirror was maintained at the same speed of rotation (375 r.p.s.) at which the flashlamp data was recorded for greater ease in wavelength graduation. The slits were opened to a width of 70 divisions, and further information not given on Figure 76 which must be used to compute the calibration factor is:

Upper Trace: S1 response photomultiplier $B^- = 1300$ Volts $R_L = 50\ \Omega$

Lower Trace: S11 response photomultiplier

$B^- = 743$ Volts $R_L = 200\ \Omega$

Table I

Spectral Radiance of Calibrated Tungsten Lamp

Wavelength (λ Angstroms)	Wave Number cm^{-1}	Radiance	
		Micro Watts/ster cm^2 mm^2	Micro Watts/ster cm^{-1} cm^2
3,500	28,571	1.42	1.74
3,700	27,027	2.57	3.52
4,000	25,000	5.24	8.39
4,500	22,222	12.8	25.9
5,000	20,000	25.9	64.8
5,500	18,182	43.0	130.0
6,000	16,667	61.6	211.0
6,500	15,385	82.8	350.0
7,000	14,286	98.7	483.0
7,500	13,333	116	651.0
8,000	12,500	129	827.0
8,500	11,765	138	1000
9,000	11,111	144	1170
9,300	10,753	145	1250
9,500	10,526	146	1320
9,600	10,417	146	1340
10,000	10,000	146	1460
10,500	9,524	145	1600
11,000	9,091	142	1720
12,000	8,333	133	1920

Ratios determined from Tables II, III, IV, V, and VI together with the recording of the tungsten standard lamp of Figure 76 afford a calibration factor (CF) which can be applied to the recording of the flashlamp data so that absolute spectral radiance can be determined. The calibration factor is then

$$C.F.(\upsilon) = \frac{S_s}{S_F} \times \frac{B^-_s}{B^-_F} \times \frac{R_s}{R_F} \times \frac{N}{-} \times \frac{I_\upsilon}{V_\upsilon}$$

where the subscripts S and F refer to the standard lamp and flashlamp respectively, and:

S = voltage from Table II corresponding to slit width used.

B^- = voltage from Table III corresponding to photomultiplier voltage used.

R = voltage from Table IV or V corresponding to value of photomultiplier load resistor used.

N = Attenuation factor of Bausch and Lomb neutral density filter used.

I_υ = radiance at the pertinent wavelength from Table I.

V_υ = voltage read from Figure 76 at the pertinent wavelength.

Table II

Slit Width Calibration

Slit Width (divisions)	20	30	40	50	60	70	80
Oscilloscope Voltage	.22 ± .02	.42 ± .02	.80 ± .04	1.4 ± .1	1.8 ± .1	2.4 ± .1	3.1 ± .2

Table III

Photomultiplier Gain Calibration

	S-1 Response		S-11 Response	
B^- (Volts)	1200	1300	740	780
Oscilloscope Voltage	.42	.75	.0045	.008

Table IV

Calibration of S1 Response Photomultiplier Load Resistors

P.M. Load Resistor (Ω)	50	100	400	
Oscilloscope Volts	.42	.75	2.8	

Table V

Calibration of S11 Response Photomultiplier Load Resistors

P.M. Load Resistor	50	100	200	400	
Oscilloscope Volts	.048	.085	.135	.19	

Table VI

Oscilloscope Gain Calibration

Scale	.005	.05	.1	.1	.5	1.0	2.0	
Reading	.005	.05	.1	.1	.5	1.0	2.0	

C. Pulsed Lamp Spectra

1) Rapid Scan Spectra

The time resolved spectrometric measurements of the pulsed lamps are to ascertain the ratios of line emission to continuum emission over a range of input energies and powers.

The rapid scanning spectrometer was arranged as shown in Figure 77 to observe the arc radiation from an EG & G Type FX-42 linear xenon flashtube.

The geometrical arrangement of the 600 line/mm grating with respect to the other components within the rapid scan spectrometer was set to scan the spectrum from about 4,000Å, to about 11,000Å. To cover this spectral range, the beam was split into two paths after the exit slit as shown in Figure 77 by a 30-30 transmission-reflectivity chrome mirror and detected by

(a) an RCA CS 70007A photomultiplier with an S1 response and

(b) a Dumont 6292 photomultiplier with an S11 response.

The S1 response photomultiplier had a Corning CS3-66 filter in front of the photocathode and covered the spectral range 7500Å-10,500Å. The S-11 response photomultiplier covered the spectral range 4,000Å-6,000Å.

In order to synchronize the firing of the lamp with the scan, the signal from the magnetic pickup of the rotating mirror was used to trigger the flashlamp discharge; a signal from the photomultiplier placed before the grating was then used to trigger the oscilloscope sweep. A Polaroid oscilloscope camera recorded the data. The data was the output voltages of the S1 response photomultiplier and the S11 response photomultiplier used as detectors; the reduction of the voltages to spectral radiances is described in the section on calibration.

In the present arrangement the magnetic pickup is mechanically fixed with respect to the orientation of a given mirror face. There are two pulses per mirror rotation from the magnetic pickup; and there are six pulses per mirror rotation from the light incident on the photomultiplier before the grating. The time interval (τ) between a pulse from the magnetic pickup and the first, second and third pulses from the photomultiplier before the grating is thus a function of the frequency of rotation of the mirror. The time intervals were measured to be $\tau_1 = \frac{.06}{f}$; $\tau_2 = \frac{.06}{f} + \frac{1}{6f}$; $\tau_3 = \frac{.06}{f} + \frac{2}{6f}$; where f is the frequency of rotation of the mirror.

The geometrical arrangement of the 10 cm wide grating with respect to the six sided mirror is such that the grating is illuminated for approximately 25% of the angle through which each mirror face sweeps the light beam. The time for a single spectral scan (single grating illumination) is then $t = \frac{1}{24f}$.

The data is presented as Figures 78 through 87 which was all taken with the mirror rotating at f = 375 r.p.s. This frequency gives $\tau_1 = 160$ μsecs; $\tau_2 = 600$ μsecs; $\tau_3 = 1.04$ millisecs; and a spectral scanning time of about 90 μsecs. A time delay generator was used to delay the time between the signal from the magnetic pickup and the pulse discharge trigger thus synchronizing the arc radiation and the oscilloscope traces of the spectrum as shown below.

In Figures 78 through 87. The oscilloscope photograph (a) was triggered by the same signal that triggered the lamp discharge. The oscilloscope photograph (b) was triggered by the signal from the photomultiplier placed before the spectrometer grating, whereas the (grating) signal itself is displayed in the upper trace of (a). The discharge current through the lamp goes through a calibrated one milli-ohm resistor, and the voltage across this resistor

is displayed in the lower trace of (a). Thus in the photograph (a), the position of the grating signal with respect to the current trace denotes the starting point of the time interval of the arc discharge during which the spectral displays of (b) were made. This starting point can be varied (as the data shows) by varying the time delay discussed above. The spectral lines are observed in the low current portions of the discharge so that the spectral radiance, temperature, and opacity relations can be determined. Information not shown on Figures 78 through 87 and common to this data is given below:

Slit Width: 30 divisions

(a) Upper trace: signal form RCA931A photomultiplier

$B^- = 530$ Volts $R_L = 500$ ohms

(b) Upper trace: S1 response photomultiplier

$B^- = 1200$ Volts $R_L = 50$ ohms.

Lower Trace: S11 response photomultiplier

$B^- = 780$ Volts $R_L = 50$ ohms.

In Table VII the spectral radiance emitted by the flashlamp at three different 80 μsec time intervals of the 600 μsec pulse are tabulated for comparison. (The time intervals are indicated.)

In Table VIII the spectral radiances emitted by the flashlamp at four different energy inputs are tabulated for comparison. In each case the data was taken during an 80 μsec time interval beginning about 330 μsecs after the initiation of the discharge. In Figure 88 the data of Tables VII and VIII has been plotted together with the Planck functions for several temperatures.

Table VII

FLASHLAMP SPECTRAL RADIANCE AS A FUNCTION OF TIME INTERVAL IN PULSE

	Wavelength λ (Angstrom Units)	Wave Number ν (cm^{-1})	Calibration Factor	μsecs to μsecs Flashlamp (Signal Volts)	μsecs to μsecs I_ν (Watts/Ster cm)	μsecs to μsecs Flashlamp (Signal Volts)	μsecs to μsecs I_ν (Watts/Ster cm)	μsecs to μsecs Flashlamp (Signal Volts)	μsecs to μsecs I_ν Watts/Ster cm)
				Figure 78		Figure 79		Figure 80	
S-11 Response Photomultiplier	4500	22,222	1.38	.06	8.3×10^{-2}	.27	3.72×10^{-1}	.12	1.66×10^{-1}
	5000	20,000	1.26	.08	10.5	.31	3.91	.19	2.40
	5500	18,182	1.79	.08	14.3	.31	5.57	.19	3.41
	6000	16,667	1.19	.05	5.95	.19	2.26	.10	1.19
S-1 Response Photomultiplier	6000	16,667	1.40	.025	3.5	.17	2.37	.075	1.05
	6500	15,385	1.03	.04	4.10	.21	2.16	.105	1.04
	7000	14,286	.82	.05	4.10	.26	2.13	.135	1.10
	7500	13,333	.79	.075	5.95	.28	2.21	.16	1.27
	8000	12,500	1.00	.06	6.00	.25	2.50	.14	1.40
	8570	11,669	1.37	.03	4.11	.18	2.47	.10	1.37

Table VIII

FLASHLAMP SPECTRAL RADIANCE AS A FUNCTION OF ENERGY INPUT

	Wavelength λ (Angstrom Units)	Wave Number ν (cm^{-1})	Calibration Factor	Energy Input = 200 Joules		Energy Input = 400 Joules		Energy Input = 600 Joules		Energy Input = 800 Joules	
				Flashlamp (Signal Volts)	I_ν (Watts Ster cm)	Flashlamp (Signal Volts)	I_ν (Watts/Ster cm)	Flashlamp (Signal Volts)	I_ν (Watts/Ster cm)	Flashlamp (Signal Volts)	I_ν
				Figure 79		Figure 81		Figure 82		Figure 84	
S-11 Response Photomultiplier	4500	22,222	1.38	.27	3.72×10^{-1}	.25	3.45×10^{-1}	.27	3.72×10^{-1}	.25	3.45×10^{-1}
	5000	20,000	1.26	.31	3.91	.28	3.52	.30	3.78	.29	3.76
	5500	18,182	1.79	.31	5.57	.28	5.01	.31	5.57	.31	5.57
	6000	16,667	1.19	.19	2.26	.22	2.62	.22	2.62	.25	2.98
	6000	16,667	1.40	.17	2.37	.23	3.22	.35	4.79	.42	5.85
	6500	15,385	1.03	.21	2.16	.25	2.67	.42	6.33	.48	4.94
	7000	14,286	.82	.26	2.13	.26	2.13	.52	4.26	.58	4.76
	7500	13,333	.79	.28	2.21	.26	2.06	.56	4.43	.60	4.75
	8000	12,500	1.00	.25	2.50	.28	2.80	.50	5.00	.52	5.20
	8570	11,669	1.37	.18	2.47	.26	3.56	.40	5.50	.44	6.02
	9000	11,111	1.49			.31	4.61	.42	6.27	.42	6.27
S-1 Response Photomultiplier	9500	10,526	3.05	.16	4.86	.21	6.40	.24	7.30	.26	7.91
	10,000	10,000	18.6	.05	9.3	.09	16.7	.12	22.3	.12	22.3

D. High Resolution Spectroscopy

1) Xenon Short-Arc Spectra

Spectra of a high pressure xenon short-arc lamp (a 1600 watt Osram XBO-1600) were taken with the .5 meter vacuum Jarrell-Ash Ebert Scanning Monochromator in the arrangement of Figure 89. The purpose of this investigation was to measure the spectral radiance of the continuum and the lines, to locate accurately the spectral lines, and also to determine line widths of the self-absorption in any of the lines.

The 1180 line/mm grating in the instrument covered the spectral range from about 3000 Angstroms to 1.6 microns. With this grating the wavelength readout of the instrument corresponded to the true wavelength with an error of 1Å as calibrated by the Jarrell-Ash Company.

The slit width and slit height of the instrument were calibrated using a magnified image, for constant irradiance of a tungsten ribbon filament lamp on the entrance slit and monitoring the transmission through the instrument. The calibrations are tabulated in Table IX and Table X below.

Table IX

Slit Width Calibration

Slit Width (microns)	50	75	100	200	300	400
Recorder Reading	7.5	18.5	34.5	145	336	599

Table X

Slit Height Calibration

Slit Height (mm)	2	5	10	15	20
Recorder Reading	1.2	3.2	6.8	10.0	11.2

A back-biased silicon photodiode and a Dumont 7664 photomultiplier having an S-13 response were used to detect the light output of the monochromator. The spectral response of these detectors was calibrated against the black body radiation emitted by a GE Type 30/T24/17 tungsten ribbon-

filament lamp. This lamp was calibrated by the Eppley Laboratories, Inc., Newport, R.I. for spectral radiance over the range 2500 Angstroms to 2.6 microns when operated at a current of 35 amps. This calibration (in the spectral range of interest) is shown in Table I together with the conversions used for direct reading of the tables of black body radiation functions used[14].

Ratios determined from Tables IX, X, and I and the recording of the standard tungsten lamp in Figures 90, 91, and 92 were used to calculate the calibration factor used in Table XI. This calculation is similar to the calculation done in detail for the Rapid Scan Spectrometer calibration.

Figures 93, 94, and 95 are representative data. Figure 95 consists of observations of a slightly different region of the arc than those of Figures 93 and 94. The wavelengths of the self-absorbed lines were determined from Figure 95. The radiance measurements were made from Figures 93 and 94.

We can estimate the temperature, T(°K), of the arc by considering the radiation as coming from a plane parallel slab of homogeneous temperature. The spectral radiance I_υ is given as

$$I_\upsilon = B_\upsilon \left[1 - e^{-\kappa'_\upsilon d} \right]$$

Where:

I_υ is the spectral radiance of the slab in watts/cm ster.

B_υ is the Planck blackbody spectral radiance in watts/cm ster.

κ'_υ is the spectral absorption coefficient including stimulated emission

$$= \kappa_\upsilon (1 - e^{h\upsilon/kT}) \text{ in } cm^{-1}.$$

κ_υ is the spectral absorption coefficient for the medium in cm^{-1}.

d is the thickness traversed by the radiation perpendicular to the arc in cm.

υ is the frequency in cm^{-1}.

Table II. Temperature of Arc from Spectral Radiance of "Cusps" of Self-Absorbed Lines of Xenon Short-Arc

Wavelength (Angstrom Units)	Wave Number (cm^{-1})	Lamp Current	Recorder Reading	Calibration Factor	Radiance $W/ster/cm^{-1}/cm^2$	Temperature (° K)
8240	12, 136		4.4	6.37×10^4	2.35×10^{-1}	8, 200
8829	11, 325	60 amps	4.0	7.64×10^4	3.06	8, 600
9809	10, 194		2.3	11.8×10^4	2.71	8, 600
8240	12, 136		11.3	2.56×10^4	2.90	8, 200
8829	11, 325	50 amps	10.0	3.06×10^4	3.06	8, 600
9809	10, 194		5.5	4.72×10^4	2.60	8, 600

Table XII Effective Spectral Absorbtivities of Xenon Short-Arc

T = 8, 600° K

Wavelength (Angstrom Units)	Wave Number (cm^{-1})	B_ν	Recorder Reading	Calibration Factor	f_ν	$\frac{I_\nu}{B} = 1 - e^{-\kappa'_\nu d}$	$e^{-\kappa'_\nu d}$	$\kappa'_\nu d$	κ'_ν (Penner & Thomas) T = 8, 703 P = 23.8 atoms
4500	22, 222	3. 26	1. 1	58, 200	6.04×10^{-2}	. 185	. 815	. 205	. 21
5000	20, 000	3. 49	2. 6	25, 800	6.71×10^{-2}	. 192	. 808	. 21	. 197
5500	18, 182	3. 60	3. 15	22, 900	7.20×10^{-2}	. 200	. 800	. 22	. 197
6000	16, 667	3. 62	3. 3	21, 700	7.13×10^{-2}	. 197	. 803	. 21	. 197
6500	15, 385	3. 58	2. 9	26, 300	7.62×10^{-2}	. 213	. 787	24	. 210
7000	14, 286	3. 51	2. 5	31, 000	7.73×10^{-2}	220	780	. 245	. 22
7500	13, 333	3. 40	2. 1	41, 50.	8.73×10^{-2}	257	. 743	. 295	. 23
8000	12, 500	3. 28	1. 5	58, 000	8.72×10^{-2}	. 266	. 734	31	24
8570	11, 669	3. 14	1. 35	76, 500	1.03×10^{-1}	327	. 673	. 395	26
10000	10, 000	2. 75	1. 1	150, 000	1.85×10^{-1}	. 600	. 400	90	32

h and k are Planck's and Boltzmann's constants respectively in units consistent with υ and T.

At the lines 8240Å, 8829Å, and 9809Å, which temperature on the lowest excited state, of Figure 95 in which self absorption is evident, we can consider that the spectral absorption coefficient κ'_{υ} approaches the value one, and that the maximum spectral absorption at the top of the cusps on either side of the line corresponds to the radiance of a blackbody at that wavelength[15].

The values of the radiances of the arc at the wavelengths of the self absorbed lines were obtained from comparisons of the data for Figures 93 and 94 with the radiance of a standard tungsten lamp, after suitable calibration corrections.

The results of these determinations together with approximate arc temperatures ascertained from tables of Planck functions are tabulated below.

Using the temperature T = 8600°K from the maximum of the cusp: (1) the blackbody radiance (B_{υ}) is obtained from the same tables of Planck functions and compared in Table XI with the continuum spectral radiance (I_{υ}) obtained from Figures 93 and 94 after suitable calibration; (2) the continuum spectral absorbtibity $\kappa'_{\upsilon}(T)$ is obtained from the calculations of Penner and Thomas[16] as applied to xenon. These calculations have been programmed on the Burroughs B5500 computer at Westinghouse R&D and the results are incluced in Table XII. The ionization potentials for the calculation were obtained from Allen[17]. The thickness d for the structure was taken to be 1 mm. The agreement between the theory and experiment is probably fortuitous since the theory at such low temperatures is not expected to be so good.

2) Metallic Iodide Lamps

High resolution spectra were taken with the arrangement shown in Figure 96 of a standard 400 watt EHI mercury lamp and TlI, CsI, CaI, InI and NaI additive lamps from 3000Å to 9000Å. The specially selected RCA CS 70007A

photomultiplier tube was used as a detector. The output from the photomultiplier was fed into a 90 cps narrow band amplifier and then into a synchronous detector. The spectrum was recorded on an Esterline Angus strip-chart recorder having a one half second full scale response.

a) Standard Mercury Lamp

The spectrum of the standard EH1 mercury lamp is shown in Figure 97. No lines were observed between 6000Å and 9000Å. This spectrum has not been corrected for detector sensitivity. The lamp has a 20 mm O.D. arc tube and was operated at 145 volts and 3.2 amps (464 watts). High resolution scans of the most intense lines are given in Figures 98 to 102. The slit width used was 50 microns at which width the monochromator has a resolution of approximately .8Å. Under these operating conditions the most intense lines are of the order of one to two angstroms wide. It should also be noted that none of the lines are self-reversed.

b) Thallium Iodide Additive Lamp

The spectrum of the thallium iodide additive lamp is shown in Figure 103. Again no lines were observed between 6000Å and 9000Å. This lamp has a [illegible] mm O.D. arc tube and contains 25 mg of thallium iodide and 66 mg of mercury. It was operated at 127 volts and 3.35 amps (425 watts). Again the spectrum is not corrected for detector sensitivity. When this spectrum is compared to the spectrum of the standard mercury lamp one sees the addition of three broad lines due to the TlI additive. The amplitude attenuation for the mercury lamp scan was 30 whereas the attenuation for the thallium iodide lamp scan was 20. Otherwise the two spectra were taken under identical conditions. From this one sees that the mercury 3650Å and the 4358Å lines are down by a factor of 3.8. The mercury 4047Å line is down by a factor of 4.2 and the 5461Å line by a factor of 3.5. The mercury doublet at 5570Å and 5791Å is down by a

factor of 12.5. High resolution scans of the three Tl lines were taken with a slit width of 50 microns. These are shown in Figures 104 to 106. A high resolution scan of the mercury 5461Å line was also taken with a slit width of 5 microns at which the monochromator resolution is better than .2Å. The line width of this line is seen to be about .8Å. This scan is shown in Figure 107. The Tl lines are much broader than the mercury lines by about a factor of from 15 to 30. All of the Tl lines are self-reversed except for the weakest overlapping lines on the long wavelength side of the main line. These overlapping lines extend for almost 50Å from the center of the main line.

c) CsI Additive Lamp

The spectra of the CsI additive lamp number L79A is shown in Figure 108. The lamp was operated at 600 watts input. The spectrum between 3000Å and 6000Å shows no intense cesium lines. Two strong Cs lines are seen at 8521Å and 8944Å. These are shown in Figures 109 and 110. The peak intensity vs. power input for the two Cs lines and for the Hg line at 10,139Å is shown in Figure 111. The intensity of the Hg line actually decreases with increasing power indicating that the cesium vapor pressure is increasing causing the temperature to drop in the core of the tube. Radial scans were made by the Cs 8521Å line and the Hg 5770Å line across the tube. These are shown in Figure 112. The Hg line is seen to be optically thin whereas the Cs line is much more opaque. This has been discussed by Rautenberg and Johnson[18].

d) GaI Additive Lamp

The GaI additive lamp L110 was operated at 400 watts and a spectrum was recorded. This spectrum is shown in Figure 113. The strongest gallium lines were observed at 4033Å and 4172Å. These lines are shown in Figures 114 and 115. Radial scans were taken of the gallium 4033Å line and the mercury

4047Å line. This is shown in Figure 116. It is seen that this resonance line follows very closely the same profile as the Hg.

e) InI Additive Lamp

The InI additive lamp L106 was operated at 450 watts and a spectrum was recorded. This spectrum is shown in Figure 117. The most intense indium lines are the 3256Å, 4102Å and the 4511Å lines. High resolution scans of these lines taken at 450 watts are shown in Figures 118, 119, and 120.

f) NaI Additive Lamp

The NaI additive lamp number 133 was operated at 290 watts and the spectrum of the lamp was recorded. This is shown in Figure 121. A high resolution scan of the 8183Å and the 8195Å lines of sodium are shown in Figure 122. A high resolution scan at 300 watts was taken from 5650Å to 6000Å. This trace was then overlaid with a high resolution trace of the absorbance spectrum of Yttrium Aluminum Garnet doped with Nd^{3+}. The results are shown in Figure 123. A very close coincidence of the sodium emission lines is observed with several of the absorption bands of Nd^{3+} in YAG. The absorbtion peak at 5886Å has an absorbance value of about 2 as seen from the second decade of the absorbance-trace. The light intensity would be down by i/e in a distance of .7 mm or about 1/2 the radius of the usual YAG laser rods. Therefore the pumping would not be too uniform at the peak of the absorption line. The peak intensity of the sodium emission lines at 5690Å and the doublet at 5890-5896Å is plotted vs. the input power as is the peak intensity of the Hg line at 5770Å in Figure 124. The intensity of the Hg line again saturates due to no further increase in temperature due to increasing power input. The sodium doublet also saturates in peak intensity due to the large density of ground state atoms to reabsorb the doublet line. Therefore, the self absorbed hole becomes larger and larger whereas the wings increase in intensity until the "apparent" half-width of the line is over 50Å wide.

We will now attempt to make some estimates of the half-width to be expected for the Hg lines. In order to determine the electron density one must have some knowledge of the temperature of the inner quartz wall of the tube. Since this tube began to bulge somewhere above 300 watts, we will assume that we were operating at an inner wall temperature of about 1150°C which is about 300 degrees cooler than the melting point of quartz. At this temperature approximately 10% of the sodium iodide is vaporized. We will assume that all of the sodium iodide which is vaporized is dissociated and we therefore have a sodium atom density of about 10^{18} cm^{-3}.

We will determine the temperature of the core of the arc by the ratio of the intensities of the 5460.7Å and the 5769.6Å lines of mercury. We have for the temperature the expression:

$$T = \frac{E_{5770} - E_{5461}}{k} \ln\left[\left\{\left(\frac{I\lambda}{gA}\right)_{5461}\left(\frac{gA}{I\lambda}\right)_{5770}\right\}\right]^{-1}$$

where h = Planck's constant (erg sec-1), c = velocity of light (cm/sec)

k = Boltzmann's constant (erg degree-1), I = intensity of the line

E = excitation energy of the upper state of the line

λ = wavelength of the line, A = transition probability of the line

g = degeneracy of the upper state of the line = 2J+1

From the Atomic Energy Level tables[19] we have

E_{5461} = 62350 cm^{-1} = 1.249 x 10^{-11} ergs

E_{5770} = 71396 cm^{-1} = 1.418 x 10^{-11} ergs

g_{5461} = 3, g_{5770} = 5

Therefore $E_{5770} - E_{5461}$ = 9046 cm^{-1}.

High resolution traces of the lines at 5461Å and 5770Å as shown in Figures 125 and 126. Calibration of the intensities of these lines indicated that

$$\frac{I_{5461}}{I_{5770}} = 14.3$$

We have used the transition probability date of Schouten and Smit[20] to obtain the ratio of the transition probabilities. Although the absolute values of the transition probabilities could be in error by as much as a factor of ten it is likely that the ratio is much better than this. From their data we have

$$\frac{A_{5461}}{A_{5770}} = \frac{37 \times 10^7}{14.1 \times 10^7} = 2.62$$

Putting these values in the above formula we obtain the value

$$T = 6000^{\circ}K$$

Using this temperature in the Saha equation (considering only first ionization)

$$\frac{N_e^2}{N_o - N_e} = \left(\frac{2\pi\, mkT}{h^2}\right)^{3/2} \frac{2Q_1}{Q_o} e^{-V/kT}$$

where

N_e = electron density

N_o = total heavy particle density which for sodium we estimated to be 10^{18}

m = mass of the electron

h = Planck's constant

Q_o = atom partition function $\cong g_o$-degeneracy of the ground state of the atom

Q_1 = ion partition function $\cong g_o$-degeneracy of the ground state of the ion

V = ionization potential of the atom

Substituting in the values for sodium we obtain for the electron density due to sodium

$$N_e^{Na} = 2 \times 10^{17} \text{ cm-3}$$

This value should be increased due to the electrons contributed to the plasma by the mercury and argon. However this contribution is ever so slight due to the high ionization potentials of mercury and argon relative to sodium. We should emphasize that the confidence one can place on this value of the electron density is rather limited. In the first place the sodium atom density is very dependent on the quartz wall temperature and, we as yet, have no good experimental data. Further, as pointed out earlier, the calculation is dependent on the ratio of the transition probabilities. We feel the electron density obtained should be within a factor of ten of the true density.

Continuing blithely on, we calculate the Stark broadening of the mercury lines which one would expect with such an electron density. From Griem[15] we have for the (half) half-width of a Stark-broadened line the expression

$$w_{tot} \quad [1 + 1.75 \alpha (1 - 0.75 r)]w$$

where α and w are the non-broadening parameter and the electron-impact (half) half-width respectively. The parameters have been calculated by Griem[21] for many of the lighter elements but not for mercury. However, calcium has an electronic structure which is very similar to that of mercury. For the mercury transition $7s\ ^3S_1 \rightarrow 6_p\ ^3I_2$ at 5461Å we will use the parameters calculated by Griem for the calcium transition $5s\ ^3S_1 \rightarrow 4p\ ^3P_2$ at 6162Å. From Reference 6 we have at 6000°K

$$\alpha = .055 \times (20)^{1/4} = .116$$

$$w = 5.76 \times 10^{-2} \times 20 = 1.16$$

For r we have the expression

$$r = \frac{\rho_m}{\rho_o} = 6^{1/3}(\pi N)^{1/6} \left(\frac{e^2}{2\pi\epsilon_o kT}\right)^{1/2}$$

where

ρ_m = inter-ionic distance

ρ_o = Debye length

N = total ion density

Inserting the appropriate values in the expression for the width, we obtain a value of

$$w_{tot} = 1.16\text{Å}$$

for the Stark broadened width of the mercury 5461Å line whereas the observed (half) half-width is 1.2Å. It is quite remarkable and fortuitous that the observed and the calculated widths are as close as they are. Neglecting the previous remark we can explain the discrepancy as follows. The instrument resolution is one factor which could easily add to the observed line. Also an increase in the electron density would add to the calculated width since w is linearly dependent on the electron density. Resonance broadening[15] also contributes to the broadening of spectral lines in a dense plasma. Resonance broadening of the 5461Å line is linearly dependent of the density of mercury atoms and the transition probability of this line. Due to the poor quality of the transition probability data one can only say that the resonance broadened width of the 5461Å line is of the same order of magnitude as the Stark broadened width. This would also explain the asymmetric shape of this line.

3. Continuous Laser Pumping Using a NaI Lamp

The NaI additive lamp has been used to pump a YAG ($Y_3Al_5O_{12}$) laser rod double doped with Nd^{3+} and Cr^{3+}. Although the optical quality and therefore the coupling of the lamp to the laser rod was poor, the NaI additive lamp had a lower threshold and greater efficiency than when pumped with a tungsten iodine lamp having very good coupling efficiency. These experiments are discussed in Appendix D (which was presented at the 4th International Conference on Quantum Electronics, April 1965.

Discussion of Metallic Additives in Mercury Vapour Discharges

The high pressure mercury discharge containing additives is considered to be in local thermodynamic equilibrium i.e. the population of the various energy levels are represented by Boltzmann's Law

$$\frac{n_x}{} = n_o \frac{g_x}{g_o} e^{\frac{-eV_x}{KT}}$$

The power radiation at a particular wavelength is determined by the population of the level from which it originates, the photon energy, the transition probability of the excited state, and the statistical weights of the radiating and terminating states.

$$P_\lambda = n_o A_\lambda \frac{g_\lambda}{g_o} \left(\frac{h c}{\lambda}\right) e^{-eV_\lambda/KT}$$

The transition probability is that associated with the effective lifetime of the excited state in the particular discharge as it is affected by imprisonment rather than the natural lifetime of the state in the atom. This value may differ from the natural lifetime by many orders of magnitude.

In the 400 watt high pressure mercury arc the mercury density in the core of the arc is of the order of 10^{18} atom/cm^3. The yellow doublet originating from a level at 8.85 e.v. above the ground level radiates ~15 watts at a gas temperature about 6000°K. The fraction of mercury atoms in this state is only 3.5×10^{-8}. If a metal having an excited state at 3 e.v. were present in the discharge the fraction of its atoms in the 3 e.v. state would be 3×10^{-3}. Assuming the same effective lifetimes in both cases and about the same energy per photon, the density of this additive need only be 10^{-5} that of mercury to yield the same

radiated watts. If the density of the additive can be made a reasonable fraction of the mercury density very intense radiation would be obtained at this wavelength if the temperature could be maintained. This however does not occur as the temperature is found to decrease when additives are introduced into the high pressure mercury vapor arc and the wattage is kept constant.

The power dissipated by the arc has two components; the radiated loss and the thermal losses (conductive and convective).

$$P_i = Pr + Pc$$

If this is rewritten

$$Pr = Pi - Pc$$

it is readily seen that if the input power is not changed and the thermal losses are constant the power radiated by the arc should not change. The thermal losses in the standard 400 watt geometry represent approximately 20% of the power input to the arc. Since this thermal loss consists principally of the conduction of heat from the hot core through the essentially dark sheath of mercury vapor surrounding the arc there will be no radical change with the introduction of a few percent of iodide added. The decrease in effective temperature of the arc with the presence of additives would tend to reduce the dT/dr, reducing the rate of loss but this is compensated for by the increased diameter of the current carrying core and by an increase in thermal conductivity due to the presence of iodine. Thus we should not expect to find any appreciable differences in the total amount of radiation generated in the straight

mercury and additive mercury arcs. The principal differences will be the wavelengths generated, their escape from the arc tube, and the fraction of the total arc radiation which can be obtained in a given line.

Let us examine the conditions in a standard 400 watt high pressure mercury vapor arc tube containing 66 mg of Hg and 25 mg of TlI. The arc tube wall has a minimum temperature region which determines the vapor pressure of the constituents at that point. If this point is 550°C the mercury will be completely vaporized and the TlI pressure will be about 14 torr. The 25 mg is sufficient to provide 50 torr when completely vaporized. The amount of thallium iodide in the vapor phase will depend upon the temperature of the cool region and would increase with increased wattage of the discharge which normally increases the temperature of the arc tube wall. Within the arc at temperatures above 4000°K the TlI is essentially completely dissociated. The principal ion will be Tl in spite of the disparity in the vapor densities since its ionization potential is only 6.1 e.v. compared to 10.38 e.v. for mercury. In the region off the arc center where the temperature drops below 3000°K the Tl atom density decreases rapidly as recombination with iodine takes place. At 2000°K and several mm from the wall recombination is almost complete. There is a pronounced difference between the Hg arc and the Hg-additive arc resulting from the recombination. In the mercury arc the mercury density increases from the core to the wall in accordance with $\frac{I}{T}$ and the radiation must pass through its own vapor to reach the wall. In the additive lamp the metal additive radiation passes through a rapidly decreasing density of its own vapor as recombination occurs. This results in a much reduced absorption of radiation passing through the outer sheath.

If the temperature of the coolest spot on the arc tube wall is increased the vapor pressure of the iodide will increase. This results in increasing radiation from the additive and a reduction in the mercury radiation. The reduction of the mercury radiation is the result of a lower gas temperature brought about by increased role of the additive in radiation and ionization.

The reduction of gas temperature is evidenced by the greater reduction of the Hg yellow lines relative to the green as well as the overall reduction of mercury raditation. If the gas temperature decreases from 6000°K to 5000°K the yellow Hg lines reduce a factor

$$e^{-\ 11{,}600 \times 8.8 \left(\frac{1}{6000}\right) - \left(\frac{1}{5000}\right)} = \sim 30$$

The green Hg line is reduced by

$$e^{-\ 11{,}600 \times 7.7 \left(\frac{1}{6000}\right) - \left(\frac{1}{5000}\right)} = \sim 20$$

The 5350Å and 3776Å Tl lines, if the density were unchanged would decrease by a factor of only 3.3. With the increasing density of Tl the $7^2S\frac{1}{2}$ level increases in population. The 3776Å resonance line suffers increasing imprisonment and this radiation shifts almost completely to the 5350Å line which is absorbed much less (its terminal state (.96 e.v.) at 6000°K has about 1/10 the population of the ground state). The absorption of 3776Å radiation by Tl atoms results in the $7^2S\frac{1}{2}$ excited state which may emit either 5350Å or 3776Å. In such a case it is readily apparent that the resonance lines will rapidly reduce in intensity with increasing density. This condition exists for a number of other atoms, i.e. Ga and In but to a considerably lesser extent since the lower levels are much closer together.

Those elements having the lowest lying radiating states will require the lowest normal atom densities to provide the same population of the lowest excited states. For this reason elements such as Cs, Rb, K, and Na are of special interest. These elements are too reactive to use in quartz and much of the advantage of the low excited state is offset by the low vapor pressure of their iodides. The temperatures required are high but obtainable in quartz arc tubes. For NaI about 700°C is required for 0.1 torr of NaI. At this wall temperature the Na radiation is quite strong in the mercury arc. The lower normal atom densities required means that much less resonance imprisonment will occur and the lifetimes will be kept relatively short resulting in increased radiation of these lines. With increasing Na atom density the line width will broaden and the core of each of the "D" lines will be absorbed. This results in a shifting of the wavelength of maximum intensity to a wavelength shorter than the "D" lines and one longer. The amount of displacement is primarily a function of the vapor density of Na. This has been put to use by shifting the shorter peak into coincidence with the strong absorption peak of Nd^{+3} YAG at 5885Å.

The increase in the line width of radiation from the lowest excited levels and the reversal at the center wavelength has been found in all the additives studied under this contract.

A number of different elements may be added in one lamp and the power radiated at each wavelength will be described by the formula at the beginning of this section

$$P_\lambda = n_o A_\lambda \frac{g_\lambda}{g_o} \left(\frac{h_c}{\gamma}\right) e^{\frac{-eV_\lambda}{KT}}$$

The gas temperature however will decrease in accordance with the effects on ionization and radiation of the total amount of introduced additives. The mixing of additives in a single lamp appears to be a useful tool for increasing radiation in desired regions in those cases where increasing the vapor pressure of the single component is undesirable from the standpoint of temperature limitations or because imprisonment of the desired radiation is shifting the radiation to other spectral regions. It is of course necessary that the "added" additives have their radiation in the desired spectral regions and that their vapor pressures and energy levels are compatible so that both can be effectively excited.

The diameter and the length of the lamps have not been found to play a dominant role so long as sufficient vapor density of the additive is attainable. The smaller diameter lamps require higher vapor density to achieve the same number of excited atoms at a given temperature.

The electrical characteristics of these lamps are essentially those of pure mercury lamps modified to only a small extent by the additive. When the additive vapor pressure is low there is no effect--at somewhat higher additive densities the voltage lowers 10-20% and at very high density of additive it increases.

While it is believed that the mercury density must have a role in the broadening of the additive radiation, and therefore the effective lifetime of the excited state, no clearcut role has been found since the control of Hg and additive densities at the same time was not attempted. It would appear to be a worthwhile area of investigation.

The use of quartz as an envelope material has facilitated the study we have made. It has however some limitations such as limited operating temperature and some chemical reactivity with the materials used, i.e. NaI or with metals we may have desired to use (alkali earths), which limit the loading life and maintenance of these lamps.

Other materials such as polycrystalline alumina or sapphire may offer considerable relief from these problems. They do however add some of their own for they require special sealing techniques which expose metal surfaces to the arc and special protection from the atmosphere to prevent oxidation of the metal end cap.

SUMMARY

The addition of the iodide of Tl, Na, Ga, In, K, and Cs to a high pressure wall stabilized mercury arc has been shown to result in strong radiation from the additive metal and suppression of the mercury radiation due to lower gas temperature.

Spectral distribution curves of the 4000Å - 2.0μ region are presented for these discharges at 400 and 600 watts in quartz arc tubes having approximately 20 mm diameter and 70 mm electrode separation and mounted in an evacuated outer glass envelope. Spectral distribution curves are also presented for Cs, Ca, and Tl iodide additive discharges operating at different ambient temperatures in an oven. These measurements show increasing contribution from the additive metal with increasing temperature.

By means of a thermopile irradiance measurements were made of the radiation passing through the glass envelope. At 600 watts the increase in radiation in the region passed by the glass (.3-3μ) was as much as 60% (in the NaI TlI lamp) when compared to the straight mercury lamp.

The regions of the strongest lines in the different discharges were isolated by means of filters and the light intensity was determined at 100 cm from the lamp. The following is a summary of values at 600 watts input to the lamp:

Hg	5461Å - 5790Å	545 uw/cm^2
Hg + TlI	5350Å - 5461Å	765
Hg + TlI + NaI	5350Å - 5896Å	1265
Hg + GaI_3	4032Å - 4358Å	1040
Hg + KI	7644Å - 7969Å	1000
Hg + CsI	8521Å - 8943Å	1850

Examination of the line profiles show that all the intense additive lines are strongly broadened and reversed at the center.

NaI and TlI have been used as additives in lamps with diameters as small as 2.6 mm and the high intensity and efficiency of radiation found in the larger diameter lamps was maintained. Using heavy wall capillary lamps (3.5 x 10 mm) strong sodium "D" line radiation has been obtained at loadings up to 200W/cm with the arc tube operating in air.

The output and line shape is strongly dependent upon vapor pressure of NaI. With increasing vapor pressure the intensity of Na radiation increases and the lines broaden. The broadening and reversal permits the shifting of the short wavelength side of the reversed line into coincidence with the strong absorption band of the Nd^{+3} YAG laser material. The ability to do this in small diameter lamps results in good optical coupling as well as good spectral match.

References

1. Larson, D.A., Fraser, H.D., Cushing, W.V., Unglert, M.C., "Higher Efficiency Light Source Through Use of Additives to Mercury Discharges", Illum. Engg., 434, June 1963.

2. Kenty, C. and Karash, W.J., "X-Ray Determination of Mercury Arc Temperature", Phys. Rev. 78, 625 (1950).

3. Elenbaas, W., The High Pressure Mercury Vapor Discharge, North-Holland Publishing Company, Amsterdam, pp. 17, 34 (1951).

4. Schnetzler, K. G., U.S. Patent 2,240,353 (1941).

5. Larson, D.A., Fraser, H.D., Cushing, W.V., Unglert, M.C., loc. cit.

6. Elenbaas, W., loc. cit., p. 12.

7. Elenbaas, W., loc. cit., p. 20.

8. Elenbaas, W., loc. cit., p. 21.

9. Larson, D.A., Fraser, H.D., Edris, C.R., Unglert, M.C., "Effect of Metal Iodide Additives on High Pressure Mercury Lamps". Paper presented at National Technical Conference of the Illuminating Engineering Society, Aug. 30 - Sept. 3, 1964, Miami, Florida.

10. Elenbaas, W., loc. cit., p. 55.

11. Church, C.H., Ryan, D., and Lesnick, J.P., "Spectrophotometry and the Use of High Energy Laser Pumps", ONR Laser Flashlamp Conference, Stanford Research Institute, 20 Feb., 1964.

12. Hill, R.A., and Beckner, E.H., "A Rapid Scan Spectrograph for Plasma Spectroscopy", Appl. Optics 3, 929 (1964).

13. Niesel, W., Lubbers, D.W., Schneewolf, D., Richter, J., and Botticher, W., "Double Beam Spectrometer with 10-msec Recording Time," Rev. Sci. Inst. 35, 578 (1964).

14. W. Elenbaas, "The High Pressure Mercury Vapour Discharge", North-Holland Publishing Company, Amsterdam (1951).

15. H.R. Griem, "Plasma Spectroscopy" McGraw-Hill, Inc. (1964).

16. S.S. Penner and M. Thomas, A.I.A.A. Journal, Vol. 2, No. 9 pp. 1572-1575, (Sept. 1964).

17. C.W. Allen, "Astrophysical Quantities", Athlone Press, London, 2nd Ed. (1963).

18. T. H. Rautenberg and P. D. Johnson, Applied Optics 3, 487 (1964).

19. C. E. Moore, Atomic Energy Levels, National Bureau of Standards Circular No. 467, Vol. III (1958).

20. J. W. Schouten and J. A. Smit, Physica 10, 661 (1943).

21. H. R. Griem, Stark Broadening of Isolated Spectral Lines in a Plasma, Naval Research Laboratory Report 6084, June 16, 1964. AD443762

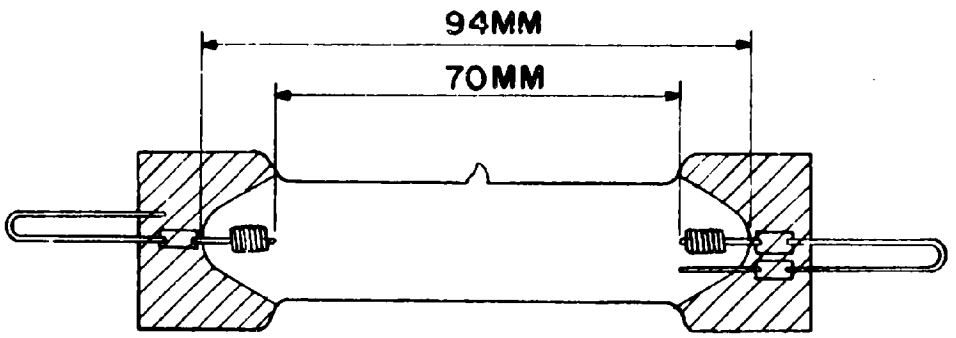

QUARTZ, 18MM I.D., 20MM O.D.

400 WATT ARC TUBE

Figure 1

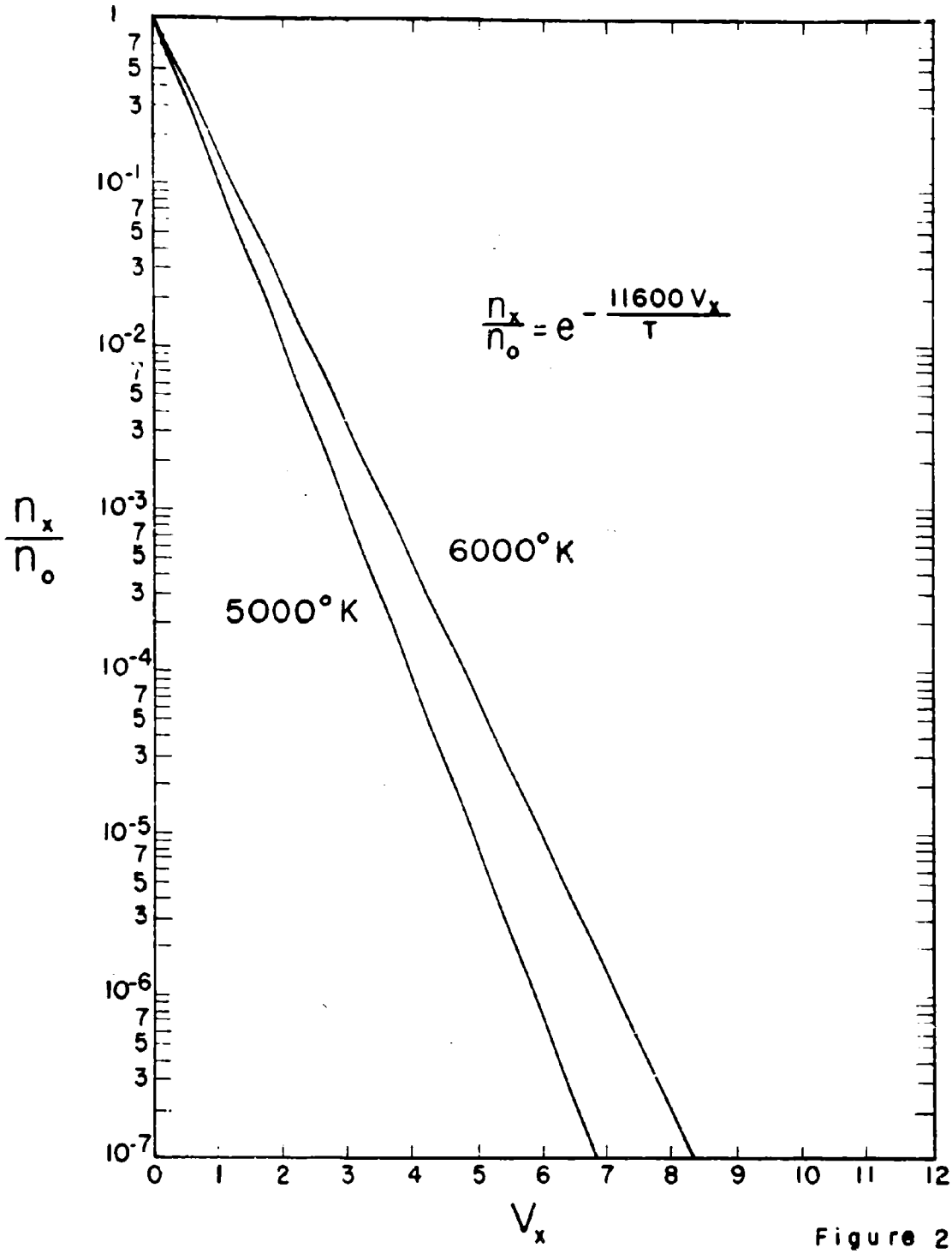
$\frac{n_x}{n_o} = e^{-\frac{11600\,V_x}{T}}$
6000° K
5000° K
$\frac{n_x}{n_o}$
V_x
1
7
5
3
10^{-1}
10^{-2}
10^{-3}
10^{-4}
10^{-5}
10^{-6}
10^{-7}
0 1 2 3 4 5 6 7 8 9 10 11 12

Figure 2

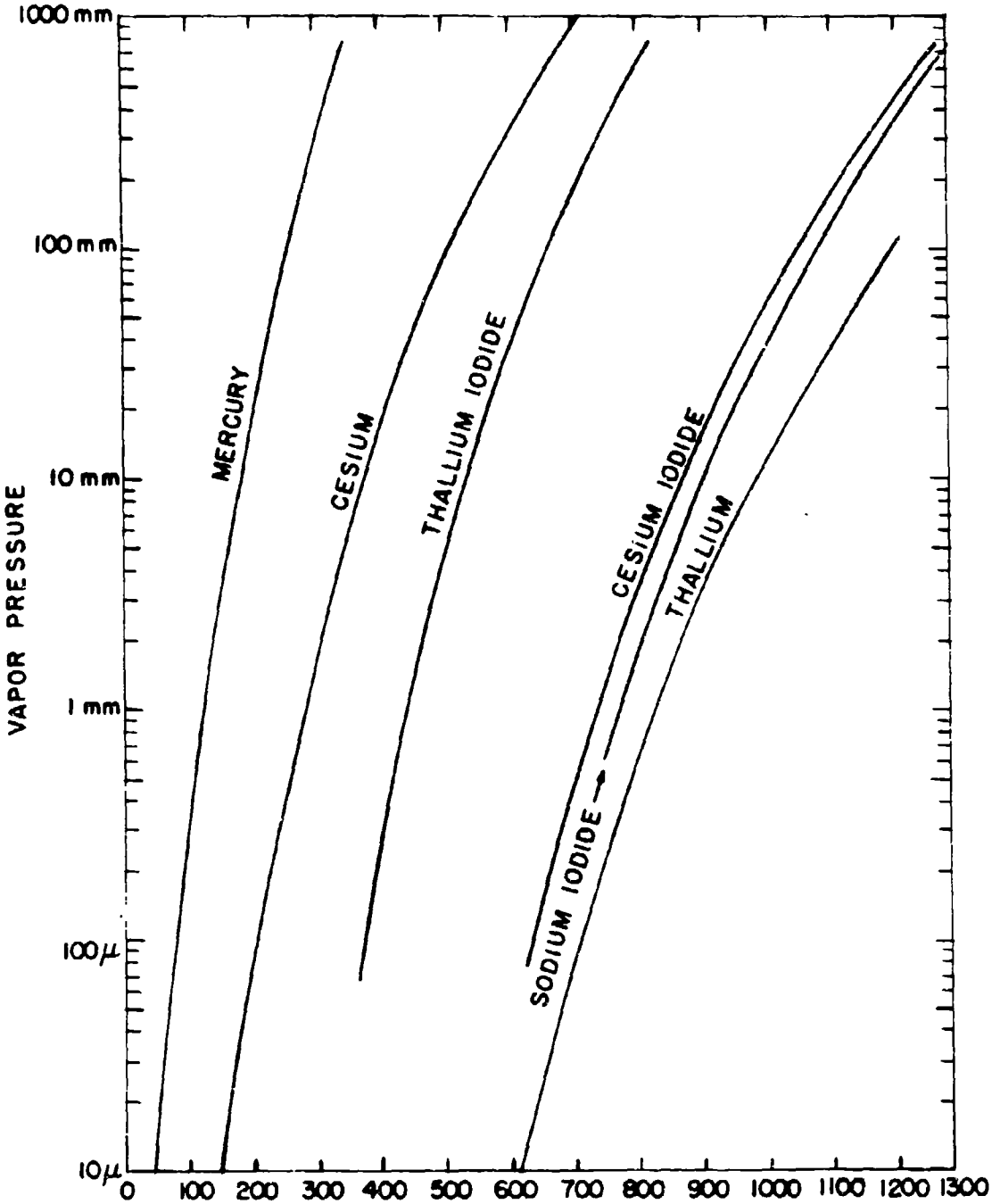
1000 mm
100 mm
10 mm
1 mm
100μ
10μ
VAPOR PRESSURE
MERCURY
CESIUM
THALLIUM IODIDE
CESIUM IODIDE
THALLIUM
SODIUM IODIDE
0
100
200
300
400
500
600
700
800
900
1000
1100
1200
1300
TEMPERATURE- Degrees Centigrade

Figure 3

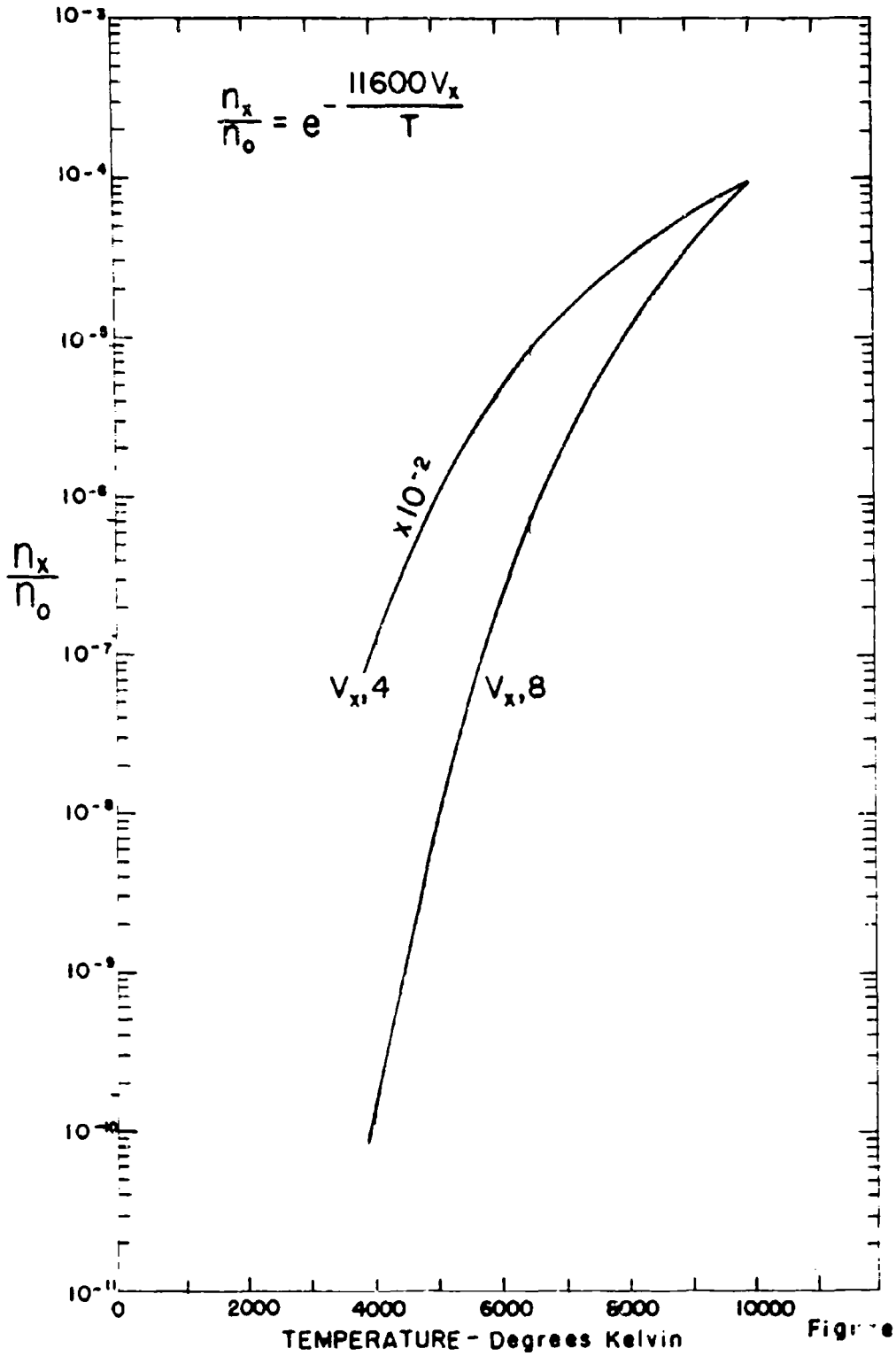
$\frac{n_x}{n_o} = e^{-\frac{11600 V_x}{T}}$
$\frac{n_x}{n_o}$
10^{-3}
10^{-4}
10^{-5}
10^{-6}
10^{-7}
10^{-8}
10^{-9}
10^{-10}
10^{-11}
x10-2
V_x,4
V_x,8
0
2000
4000
6000
8000
10000
TEMPERATURE - Degrees Kelvin

Figure 4

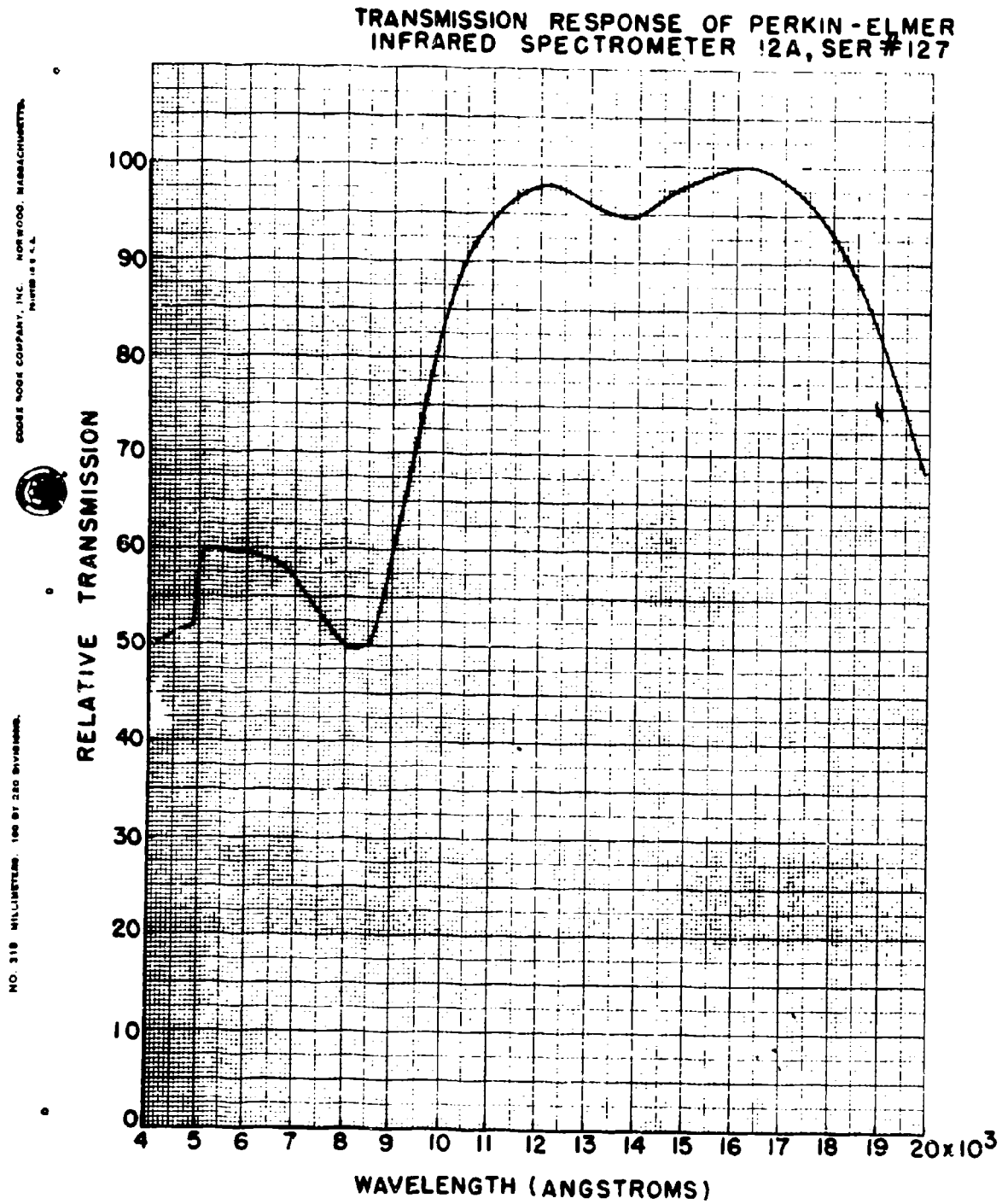
TRANSMISSION RESPONSE OF PERKIN-ELMER
INFRARED SPECTROMETER 12A, SER #127
RELATIVE TRANSMISSION
100
90
80
70
60
50
40
30
20
10
0
4
5
6
7
8
9
10
11
12
13
14
15
16
17
18
19
20x10³
WAVELENGTH (ANGSTROMS)

Figure 5

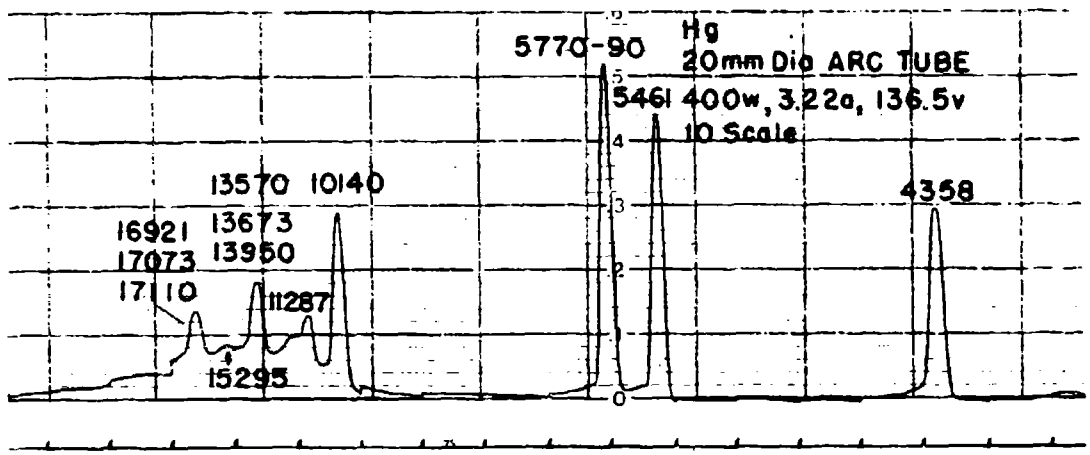
5770-90
Hg
20mm Dia ARC TUBE
5461 400w, 3.22a, 136.5v
10 Scale
13570 10140
16921
13673
17073
13950
17110
11287
15295
4358
0
1
2
3
4
5

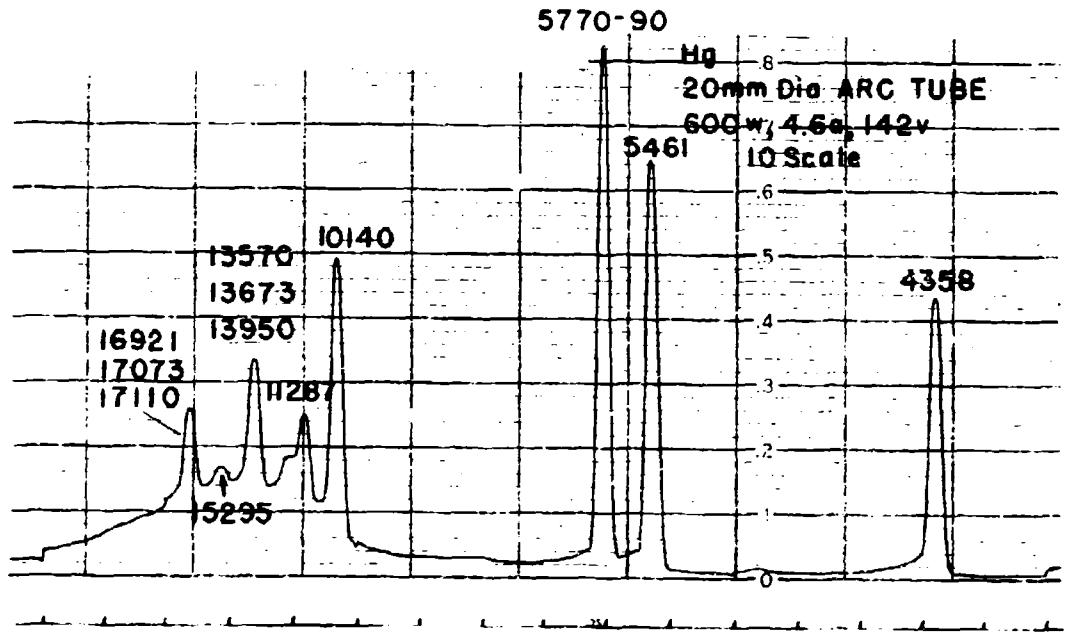
5770-90
Hg
20mm Dia ARC TUBE
600w, 4.6a, 142v
5461
10 Scale
10140
13570
13673
13950
16921
17073
17110
11287
15295
4358
0
1
2
3
4
5
6
8

Figure 6

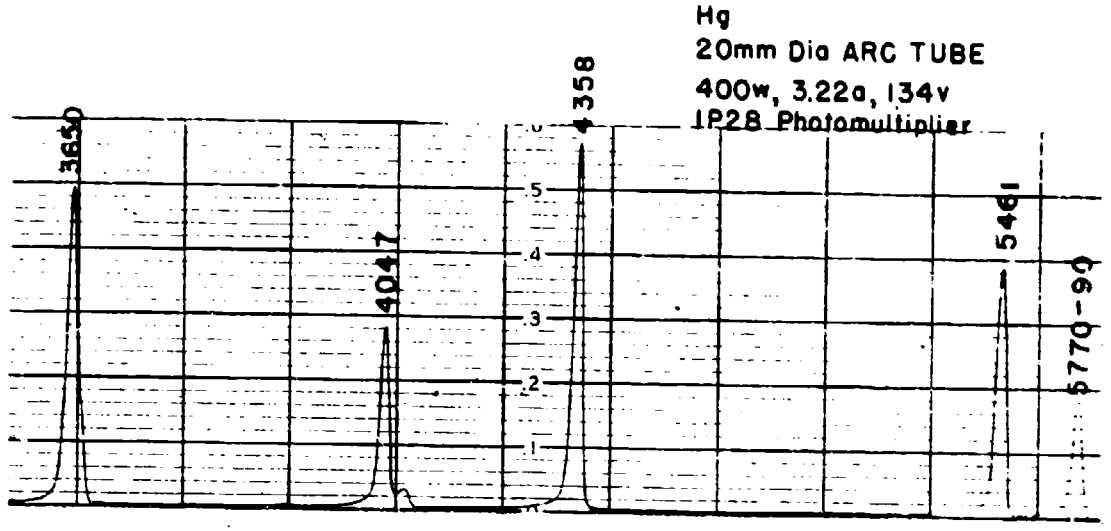
Hg
20mm Dia ARC TUBE
400w, 3.22a, 134v
1P28 Photomultiplier
4358
4047
5461
5770-90
5
4
3
2
1

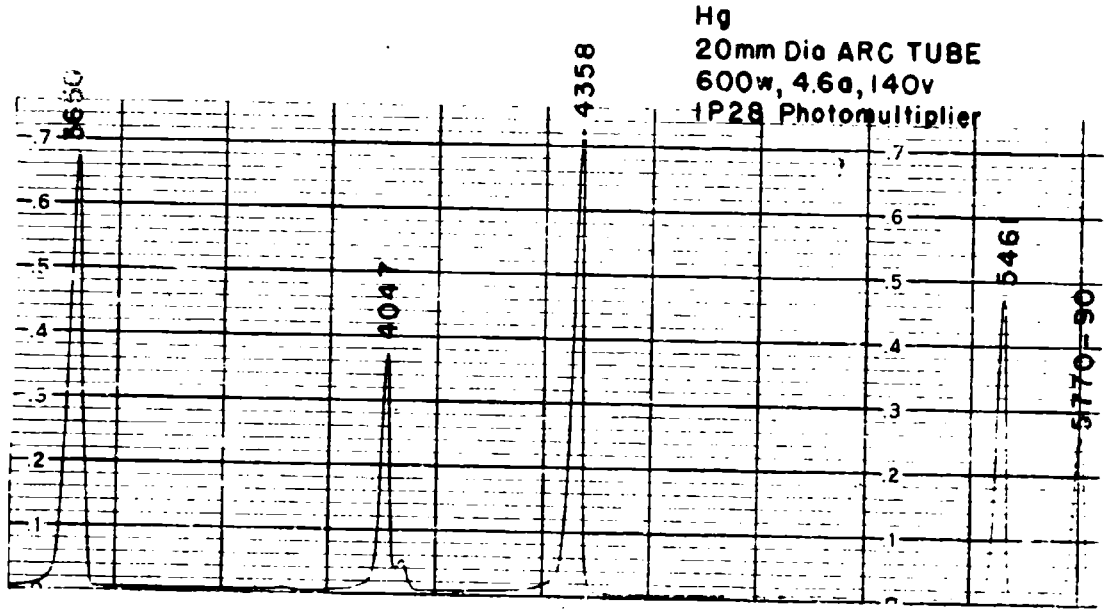
Hg
20mm Dia ARC TUBE
600w, 4.6a, 140v
1P28 Photomultiplier
4358
4047
5461
5770-90
7
6
5
4
3
2
1

Figure 7

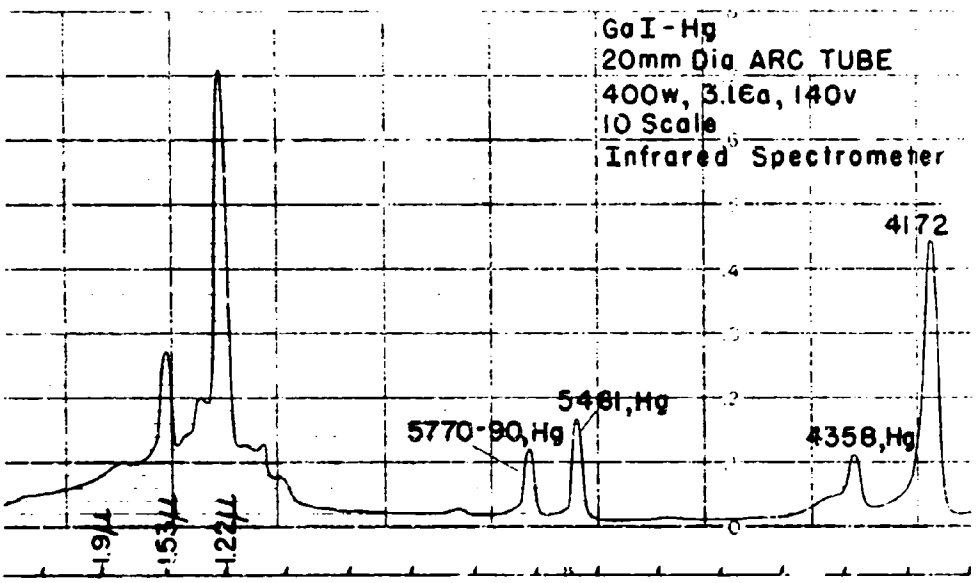
GaI-Hg
20mm Dia. ARC TUBE
400w, 3.16a, 140v
10 Scale
Infrared Spectrometer
4172
5461,Hg
5770-90,Hg
4358,Hg
1.69μ
1.53μ
1.22μ

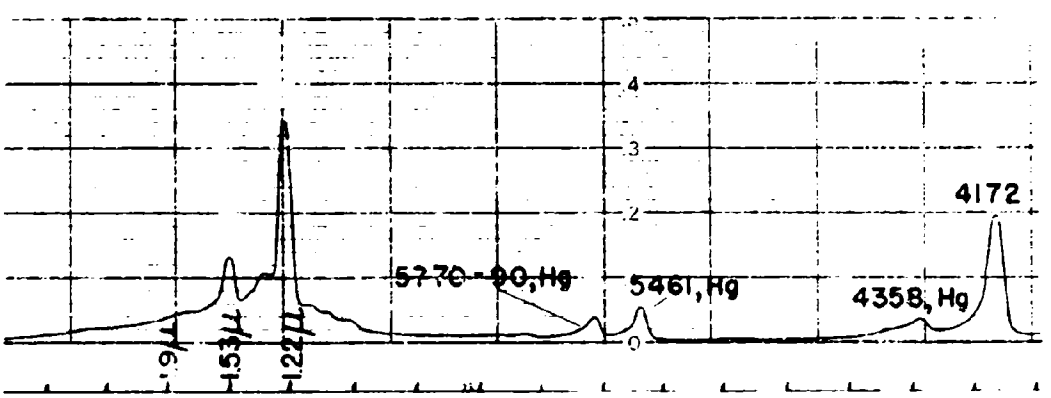
aI-Hg
20mm Dia. ARC TUBE
600w, 4.50a, 144v
30 Scale
4172
5770-90,Hg
5461,Hg
4358,Hg
1.69μ
1.53μ
1.22μ

Figure 8

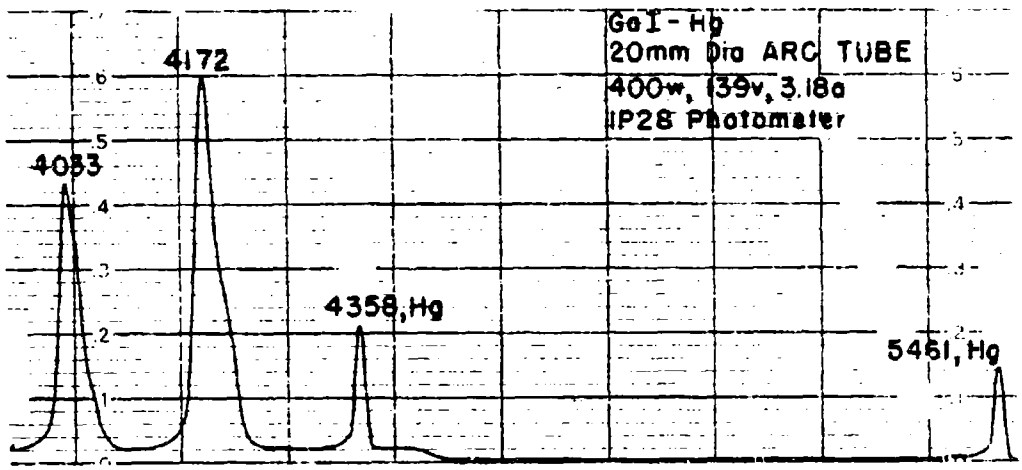
Ga I - Hg
20mm Dia ARC TUBE
400w, 139v, 3.18a
IP28 Photometer
4172
4033
4358, Hg
5461, Hg

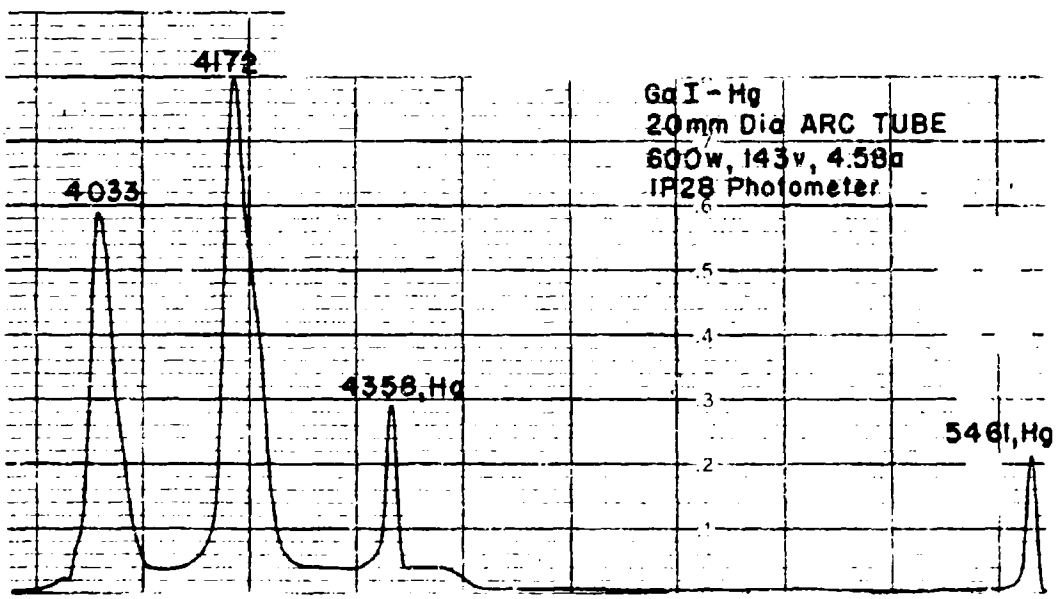
Ga I - Hg
20mm Dia ARC TUBE
600w, 143v, 4.58a
IP28 Photometer
4172
4033
4358, Hg
5461, Hg

Figure 9

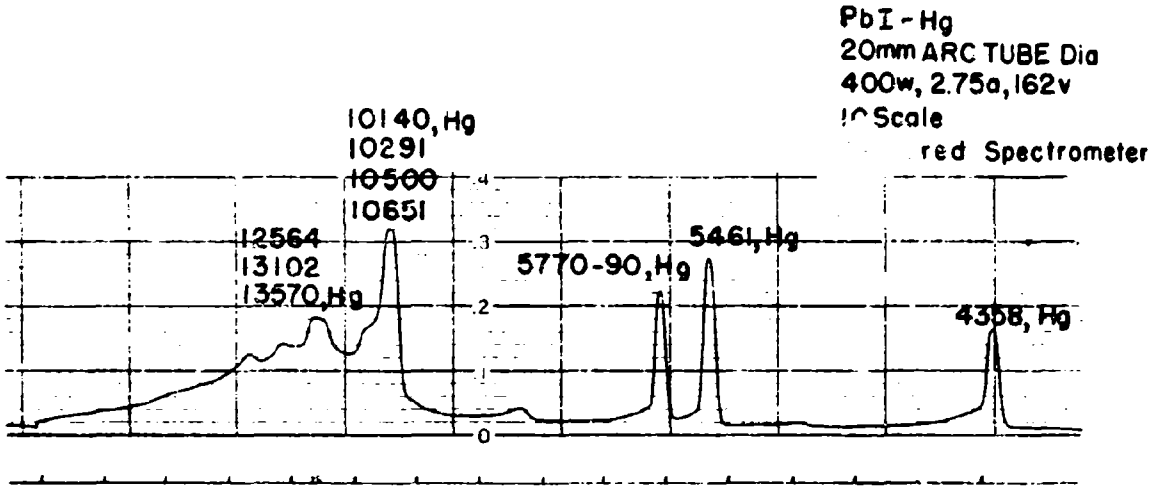
PbI - Hg
20mm ARC TUBE Dia
400w, 2.75a, 162v
10 Scale
red Spectrometer
10140, Hg
10291
10500
10651
12564
13102
13570, Hg
5770-90, Hg
5461, Hg
4358, Hg
4
3
2
1
0

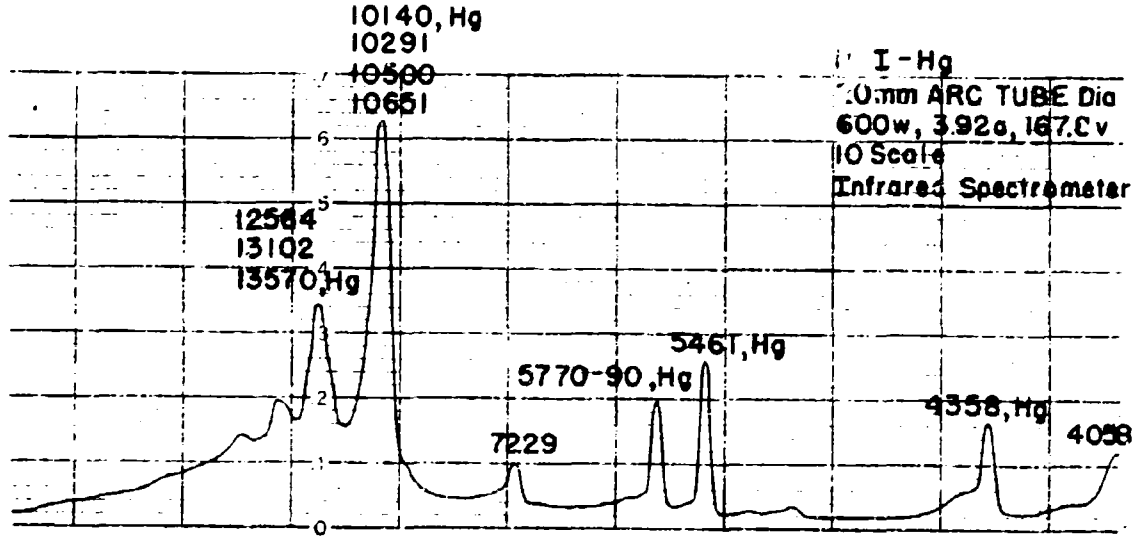
10140, Hg
10291
10500
10651
I - Hg
20mm ARC TUBE Dia
600w, 3.92a, 167.5v
10 Scale
Infrared Spectrometer
12564
13102
13570, Hg
5461, Hg
5770-90, Hg
4358, Hg
7229
4058
6
5
4
3
2
1
0

Figure 10

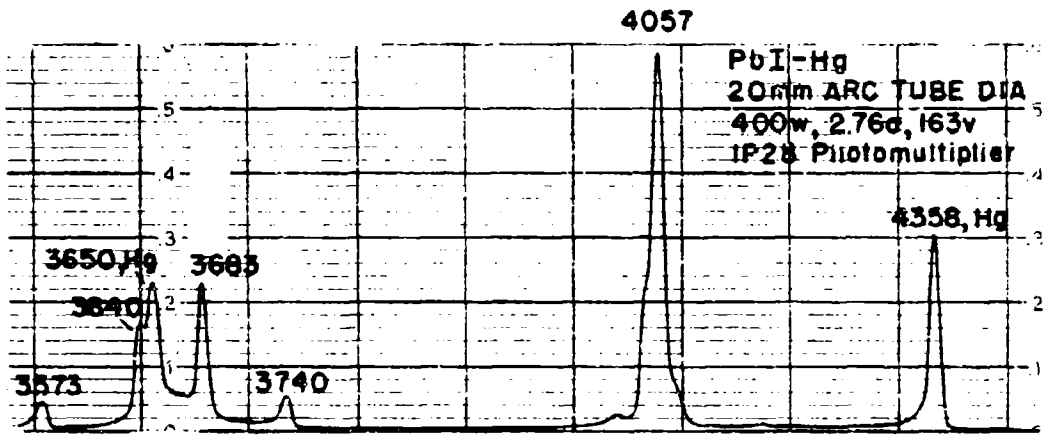
4057
PbI-Hg
20mm ARC TUBE DIA
400w, 2.76a, 163v
1P28 Photomultiplier
4358, Hg
3650, Hg
3683
3640
3573
3740

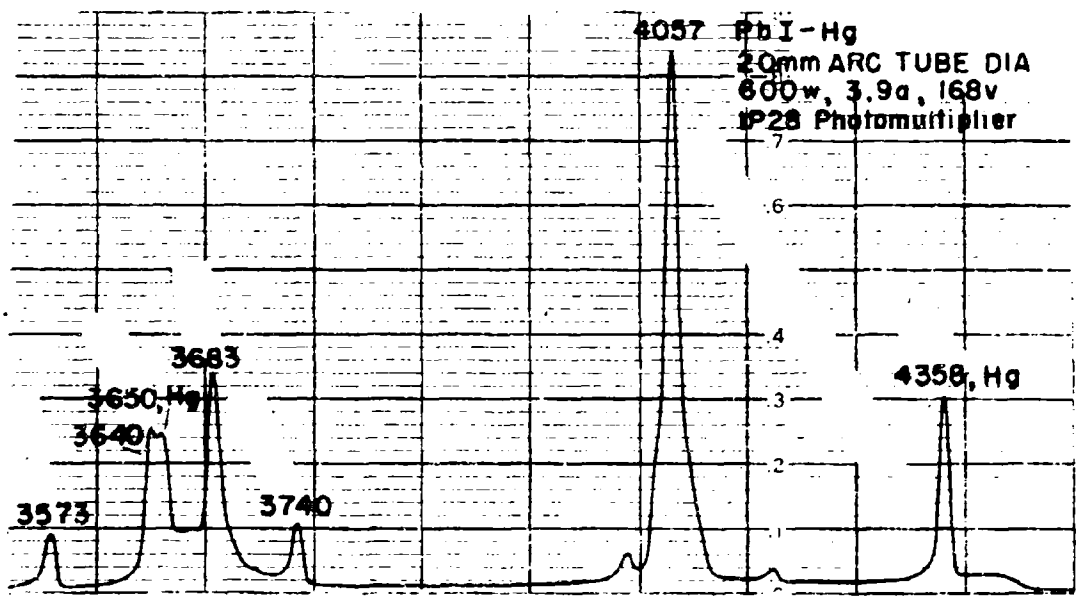
4057
PbI-Hg
20mm ARC TUBE DIA
600w, 3.9a, 168v
1P28 Photomultiplier
4358, Hg
3683
3650, Hg
3640
3573
3740

Figure 11

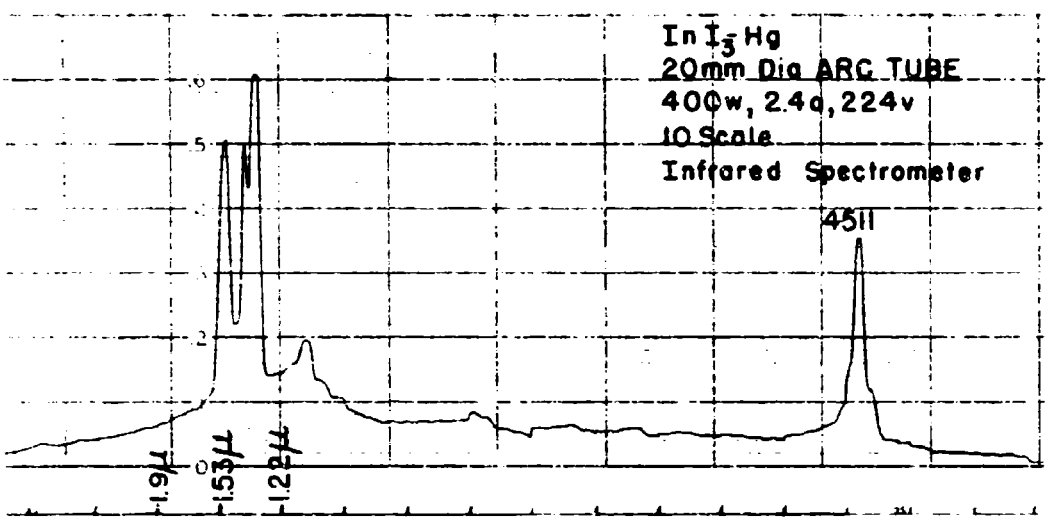
In I_3 Hg
20mm Dia ARC TUBE
400w, 2.4a, 224v
10 Scale
Infrared Spectrometer
4511
1.91μ
1.53μ
1.22μ

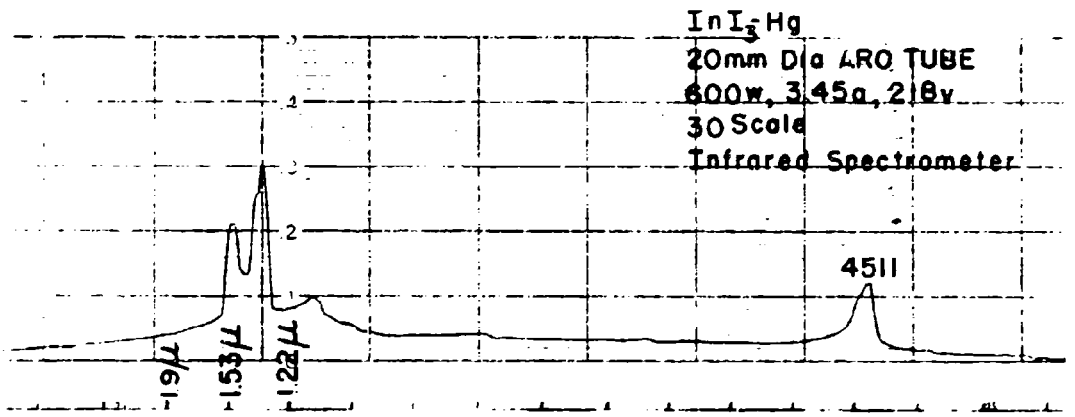
In I_3 Hg
20mm Dia ARC TUBE
600w, 3.45a, 218v
30 Scale
Infrared Spectrometer
4511
1.91μ
1.53μ
1.22μ

Figure 12

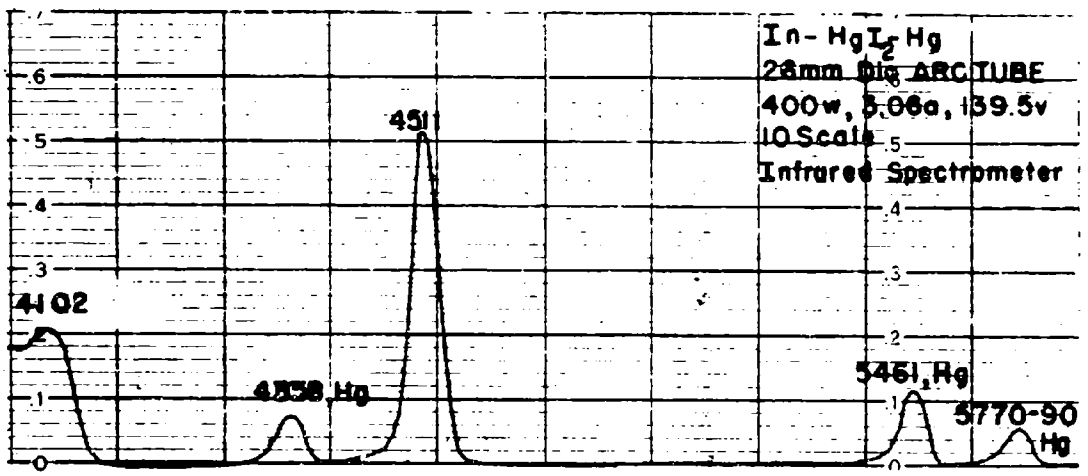
In-HgI2-Hg
26mm Dia ARC TUBE
400w, 3.06a, 139.5v
10 Scale
Infrared Spectrometer
4511
4102
4358 Hg
5461, Hg
5770-90
Hg

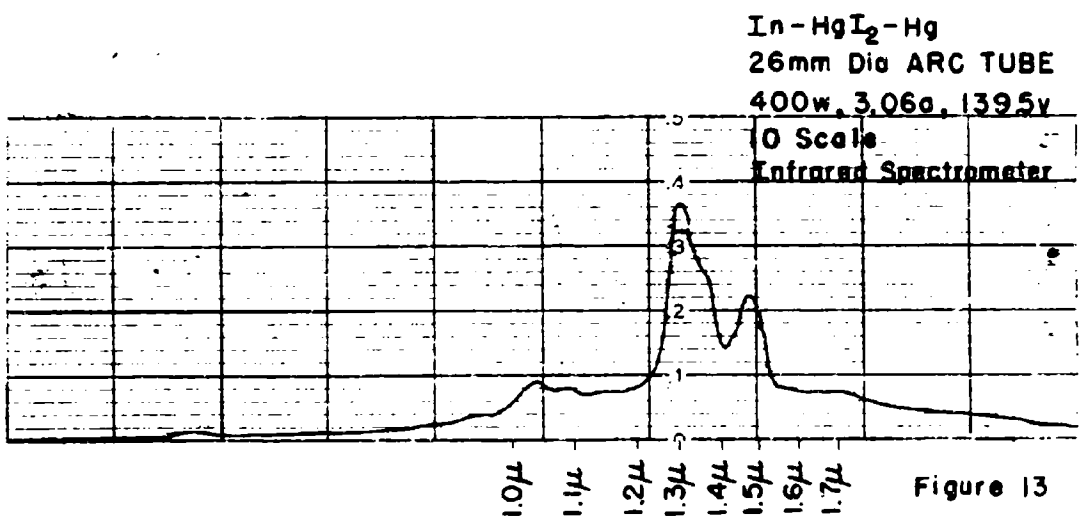
In-HgI2-Hg
26mm Dia ARC TUBE
400w, 3.06a, 139.5v
10 Scale
Infrared Spectrometer
1.0μ
1.1μ
1.2μ
1.3μ
1.4μ
1.5μ
1.6μ
1.7μ

Figure 13

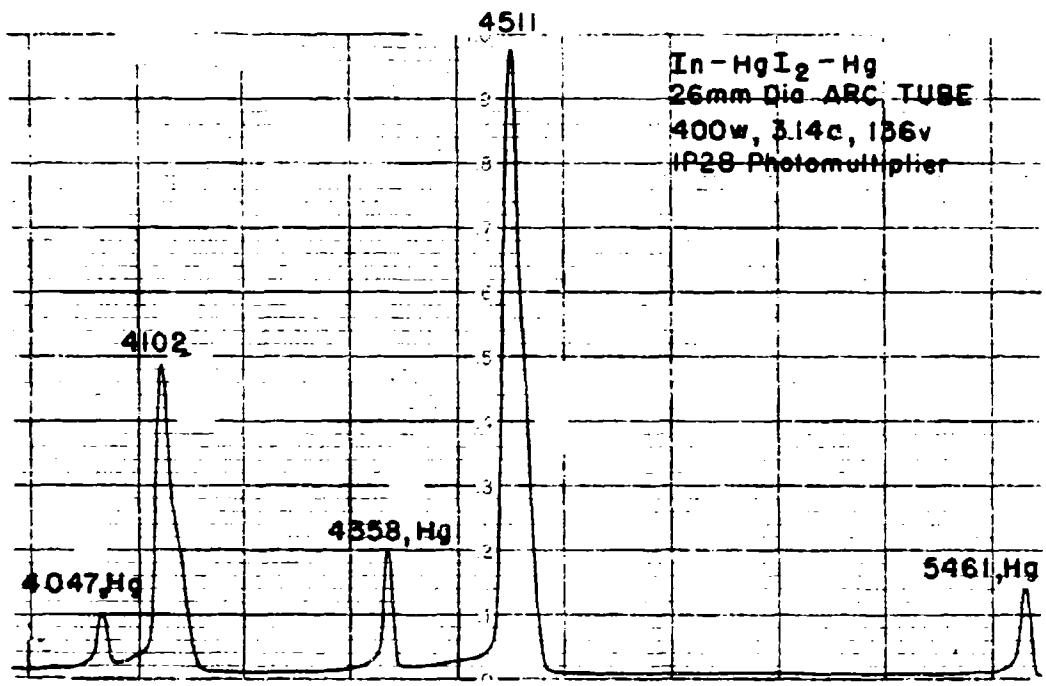
4511
In-HgI2-Hg
26mm Dia ARC TUBE
400w, 3.14c, 136v
IP28 Photomultiplier
4102
4358, Hg
4047, Hg
5461, Hg

Figure 14

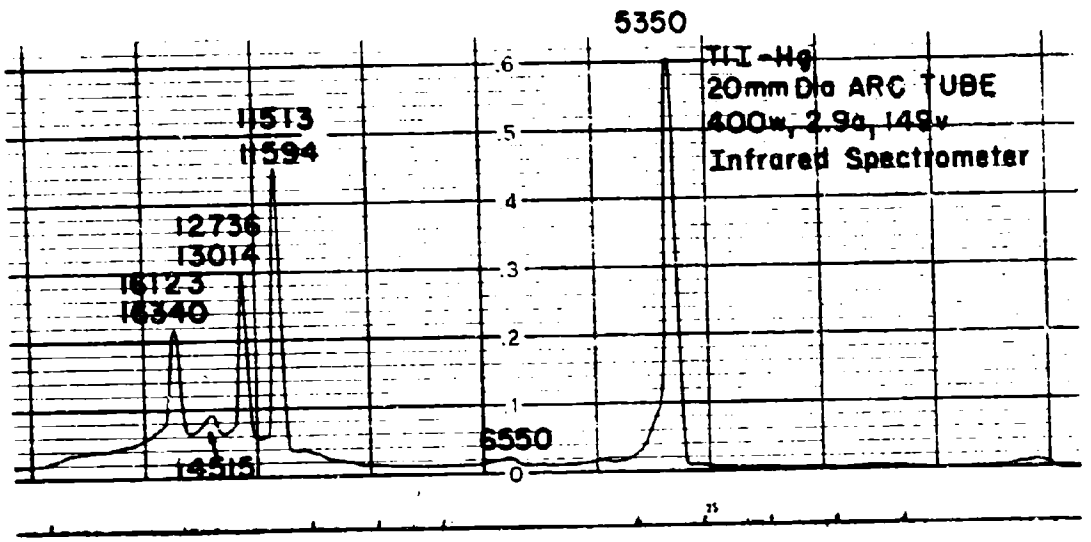
5350
TII-Hg
20mm Dia ARC TUBE
400w, 2.9a, 148v
Infrared Spectrometer
11513
11594
12736
13014
16123
16340
14515
6550
6
5
4
3
2
1
0

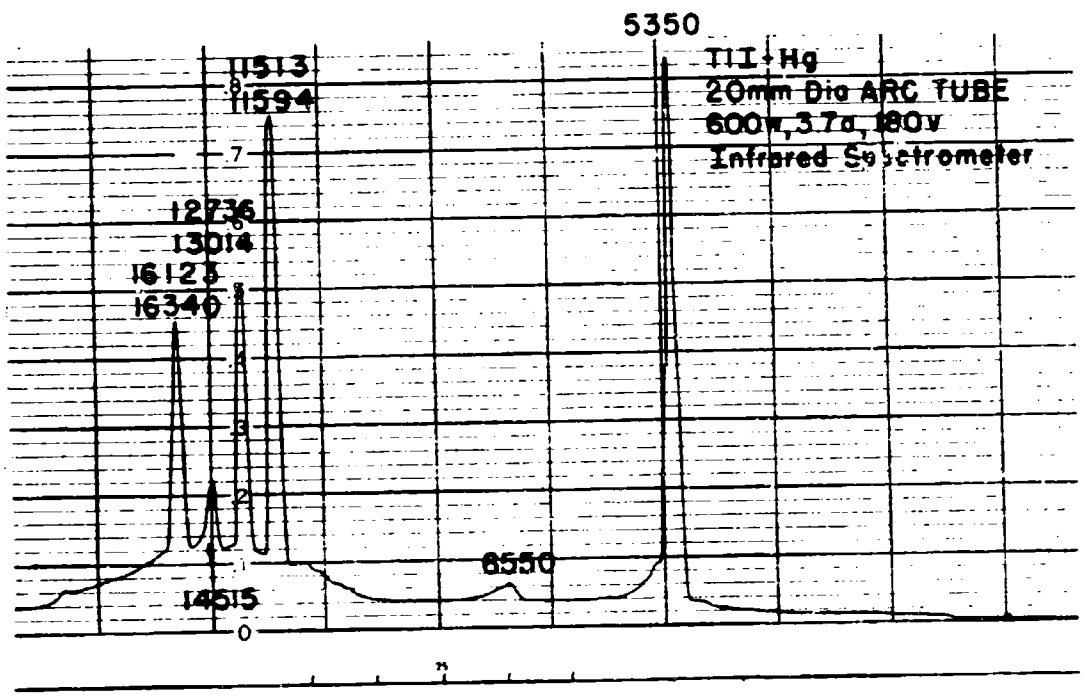
5350
TII-Hg
20mm Dia ARC TUBE
600w, 3.7a, 180v
Infrared Spectrometer
11513
11594
12736
13014
16123
16340
14515
6550
8
7
6
5
4
3
2
1
0

Figure 15

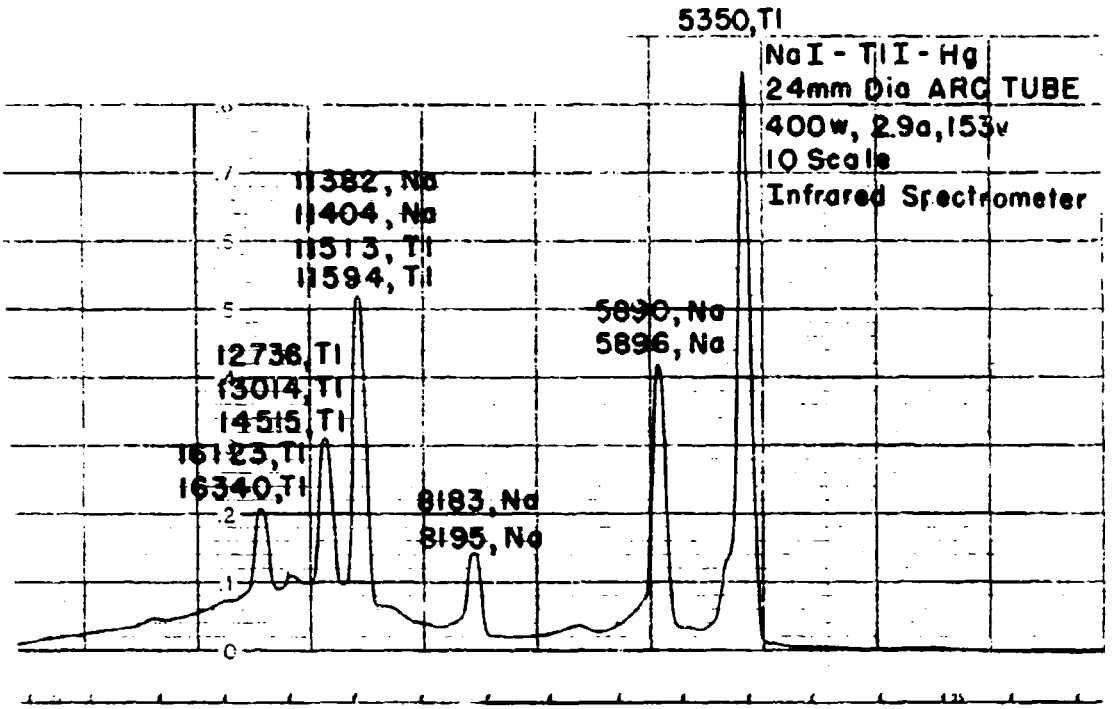
5350,TI
NaI - TlI - Hg
24mm Dia ARC TUBE
400w, 2.9a, 153v
10 Scale
Infrared Spectrometer
11382, Na
11404, Na
11513, TI
11594, TI
12736, TI
13014, TI
14515, TI
16123, TI
16340, TI
8183, Na
8195, Na
5890, Na
5896, Na

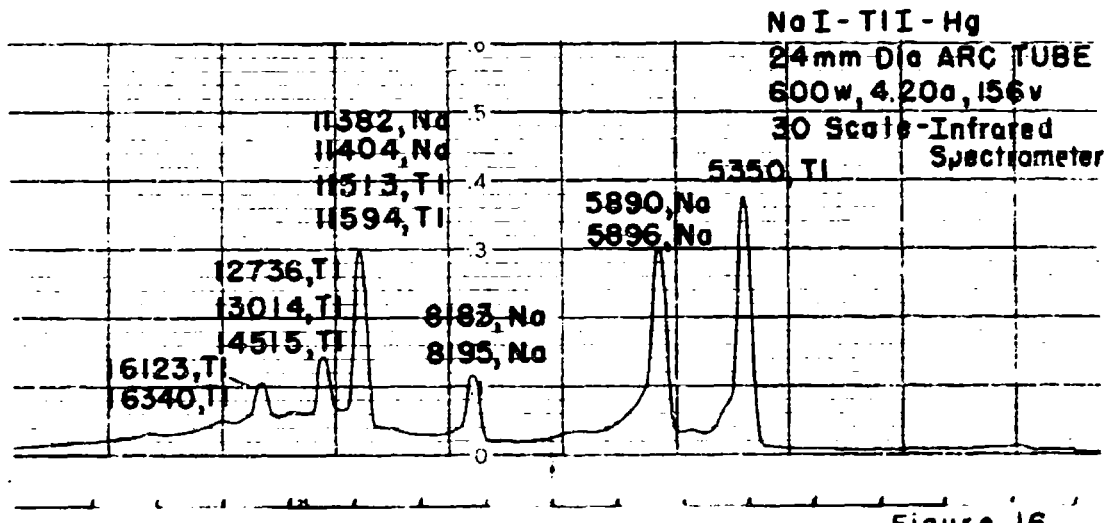
NaI - TlI - Hg
24mm Dia ARC TUBE
600w, 4.20a, 156v
30 Scale - Infrared
Spectrometer
11382, Na
11404, Na
11513, TI
11594, TI
12736, TI
13014, TI
14515, TI
6123, TI
6340, TI
8183, Na
8195, Na
5890, Na
5896, Na
5350, TI

Figure 16

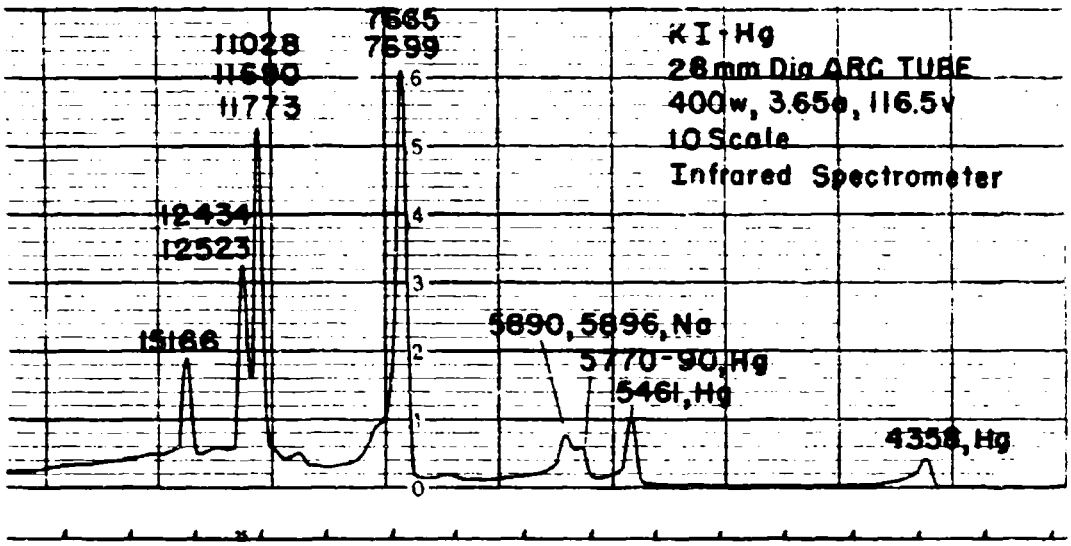
11028
11690
11773
7665
7699
12434
12523
15166
5890, 5896, Na
5770-90, Hg
5461, Hg
4358, Hg
KI + Hg
28mm Dia ARC TUBE
400w, 3.65ϕ, 116.5v
10 Scale
Infrared Spectrometer

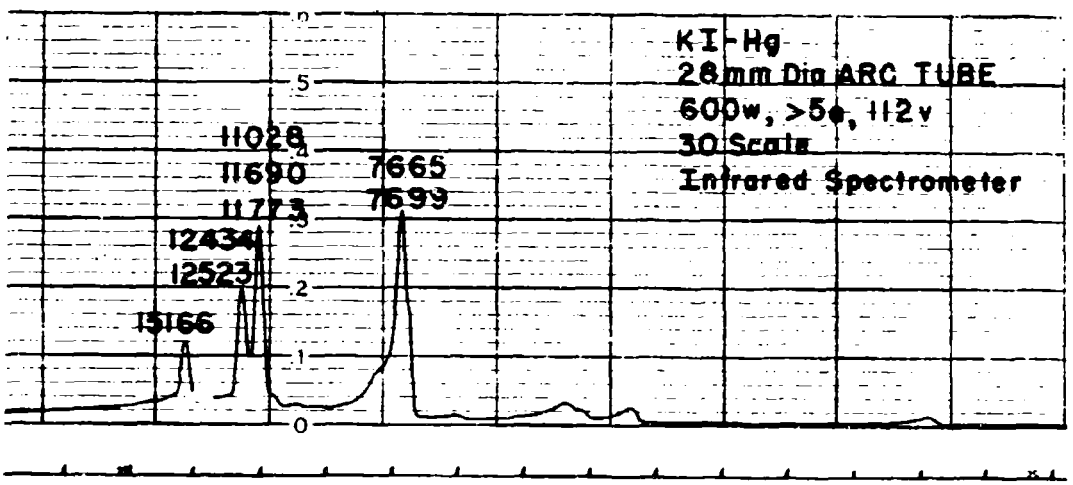
11028
11690
11773
12434
12523
15166
7665
7699
KI-Hg
28mm Dia ARC TUBE
600w, >5ϕ, 112v
30 Scale
Infrared Spectrometer

Figure 17

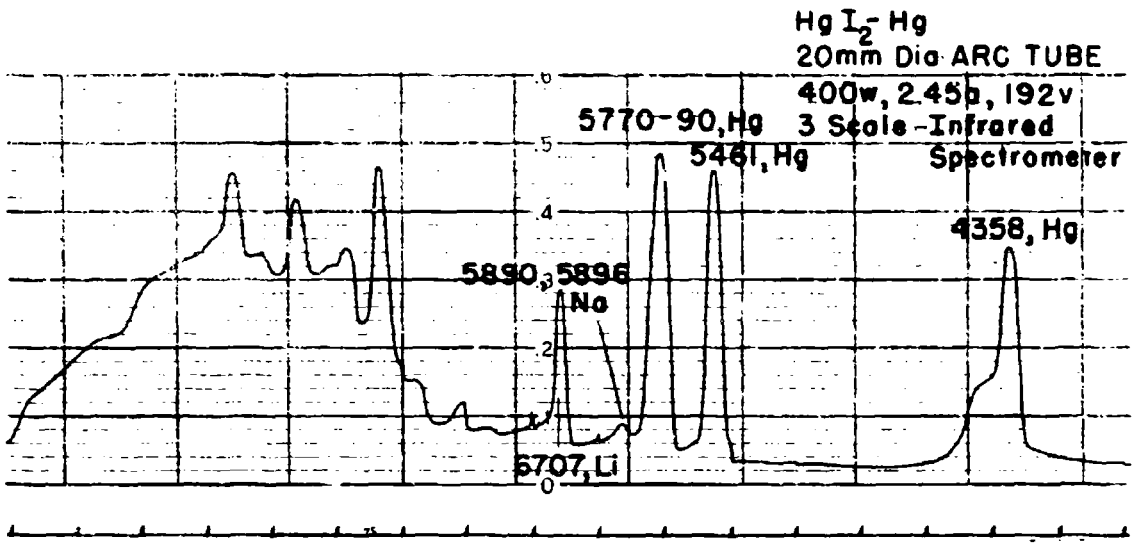
Hg I_2- Hg
20mm Dia ARC TUBE
400w, 2.45a, 192v
3 Scale - Infrared
Spectrometer
5770-90, Hg
5461, Hg
4358, Hg
5890, 5896
Na
6707, Li

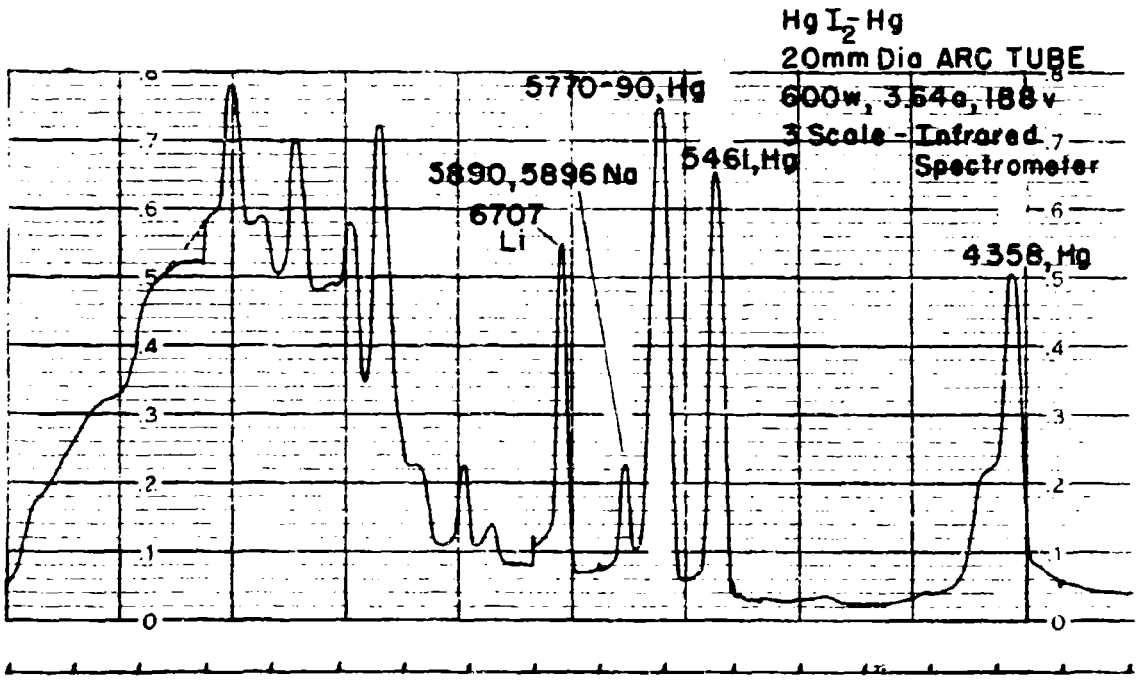
Hg I_2- Hg
20mm Dia ARC TUBE
600w, 3.54a, 188v
3 Scale - Infrared
Spectrometer
5770-90, Hg
5461, Hg
5890, 5896 Na
6707
Li
4358, Hg

Figure 18

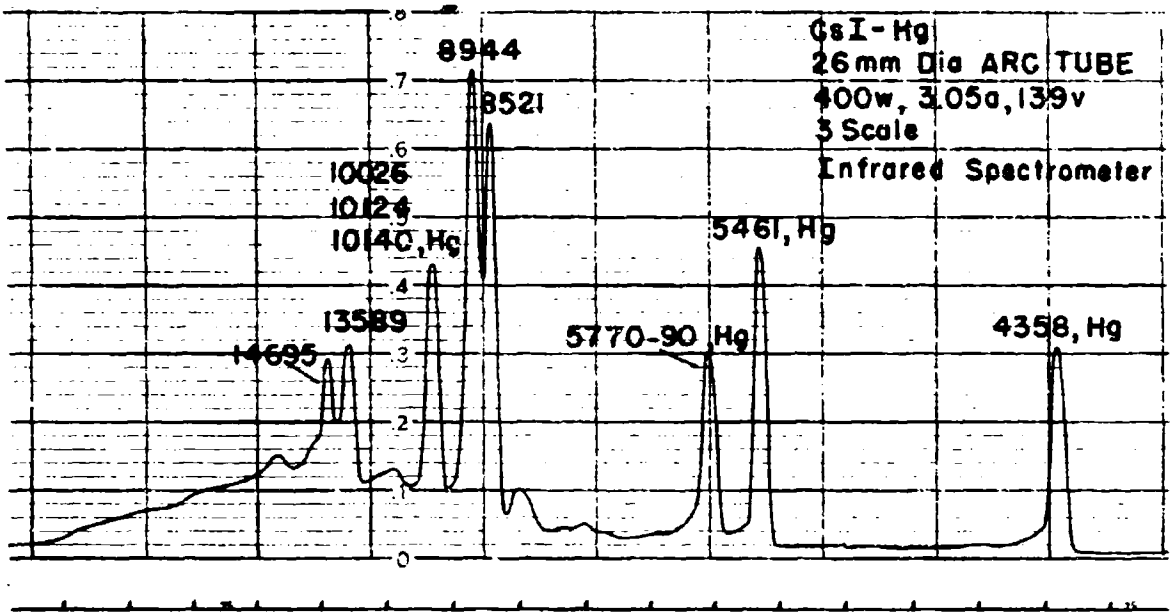
CsI-Hg
26mm Dia ARC TUBE
400w, 3.05a, 139v
3 Scale
Infrared Spectrometer
8944
8521
10026
10124
10140, Hg
13589
14695
5770-90 Hg
5461, Hg
4358, Hg
.8
.7
.6
.4
.3
.2
.1
0

a

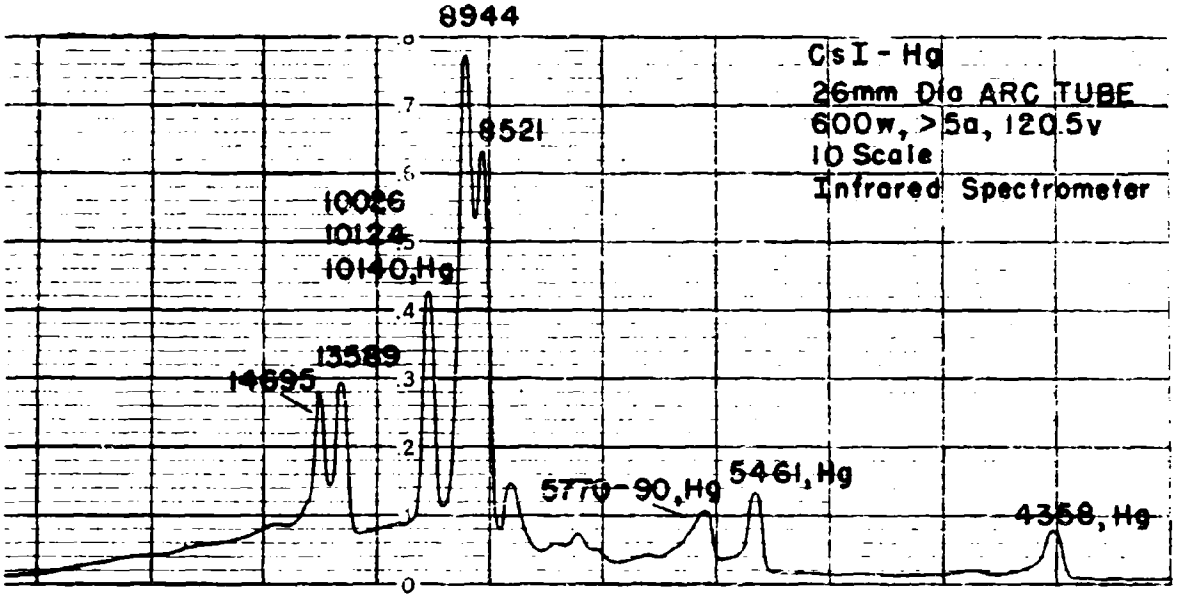
8944
CsI-Hg
26mm Dia ARC TUBE
600w, >5a, 120.5v
10 Scale
Infrared Spectrometer
8521
10026
10124
10140, Hg
13589
14695
5770-90, Hg
5461, Hg
4358, Hg
.8
.7
.6
.5
.4
.3
.2
0

b

Figure 19

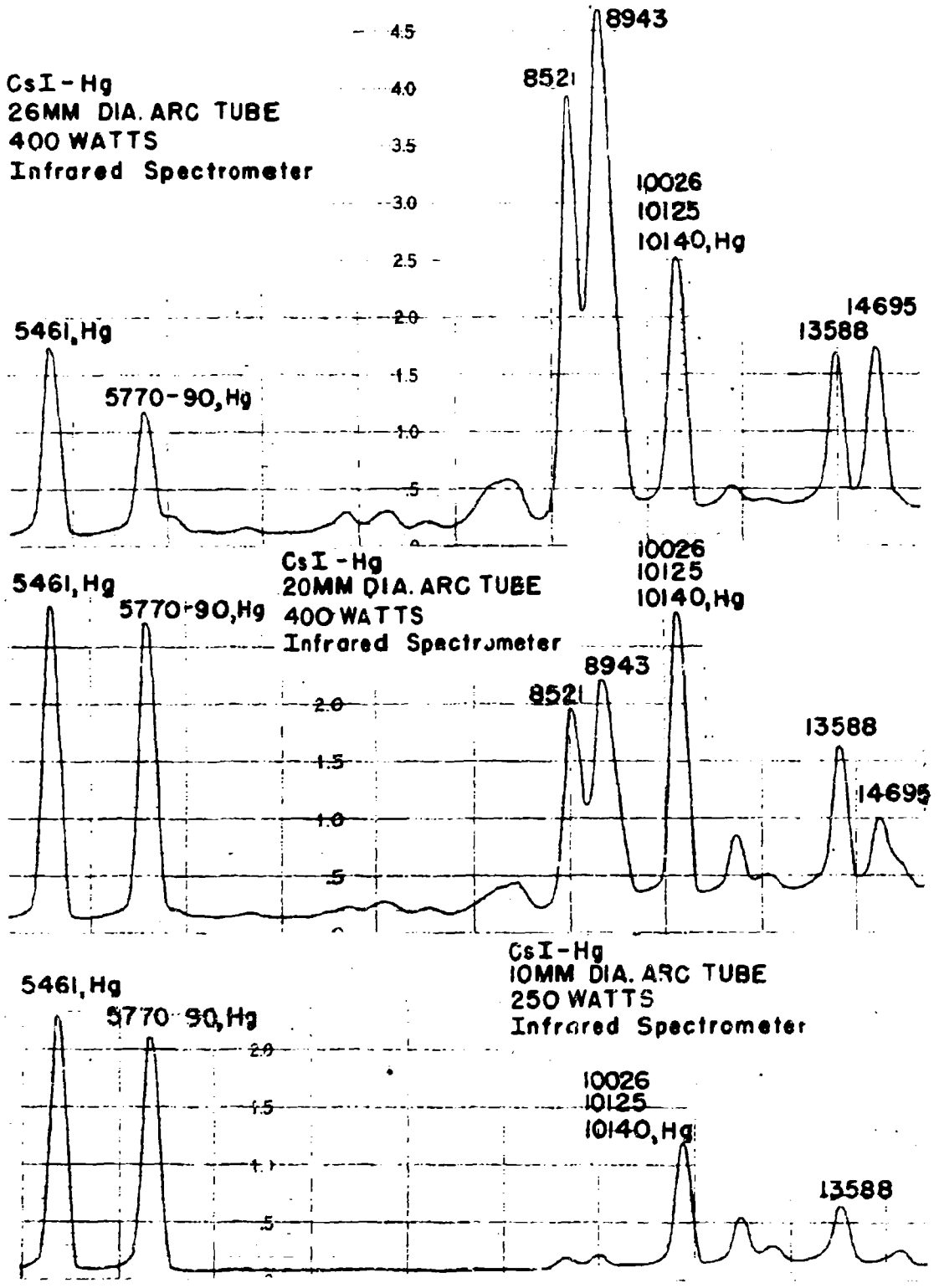
CsI-Hg
26MM DIA. ARC TUBE
400 WATTS
Infrared Spectrometer
4.5
4.0
3.5
3.0
2.5
2.0
1.5
1.0
.5
0
8521
8943
10026
10125
10140, Hg
14695
13588
5461, Hg
5770-90, Hg
CsI-Hg
20MM DIA. ARC TUBE
400 WATTS
Infrared Spectrometer
5461, Hg
5770-90, Hg
10026
10125
10140, Hg
8943
8521
13588
14695
2.0
1.5
1.0
.5
0
CsI-Hg
10MM DIA. ARC TUBE
250 WATTS
Infrared Spectrometer
5461, Hg
5770-90, Hg
2.0
1.5
1.0
.5
0
10026
10125
10140, Hg
13588

Figure 20

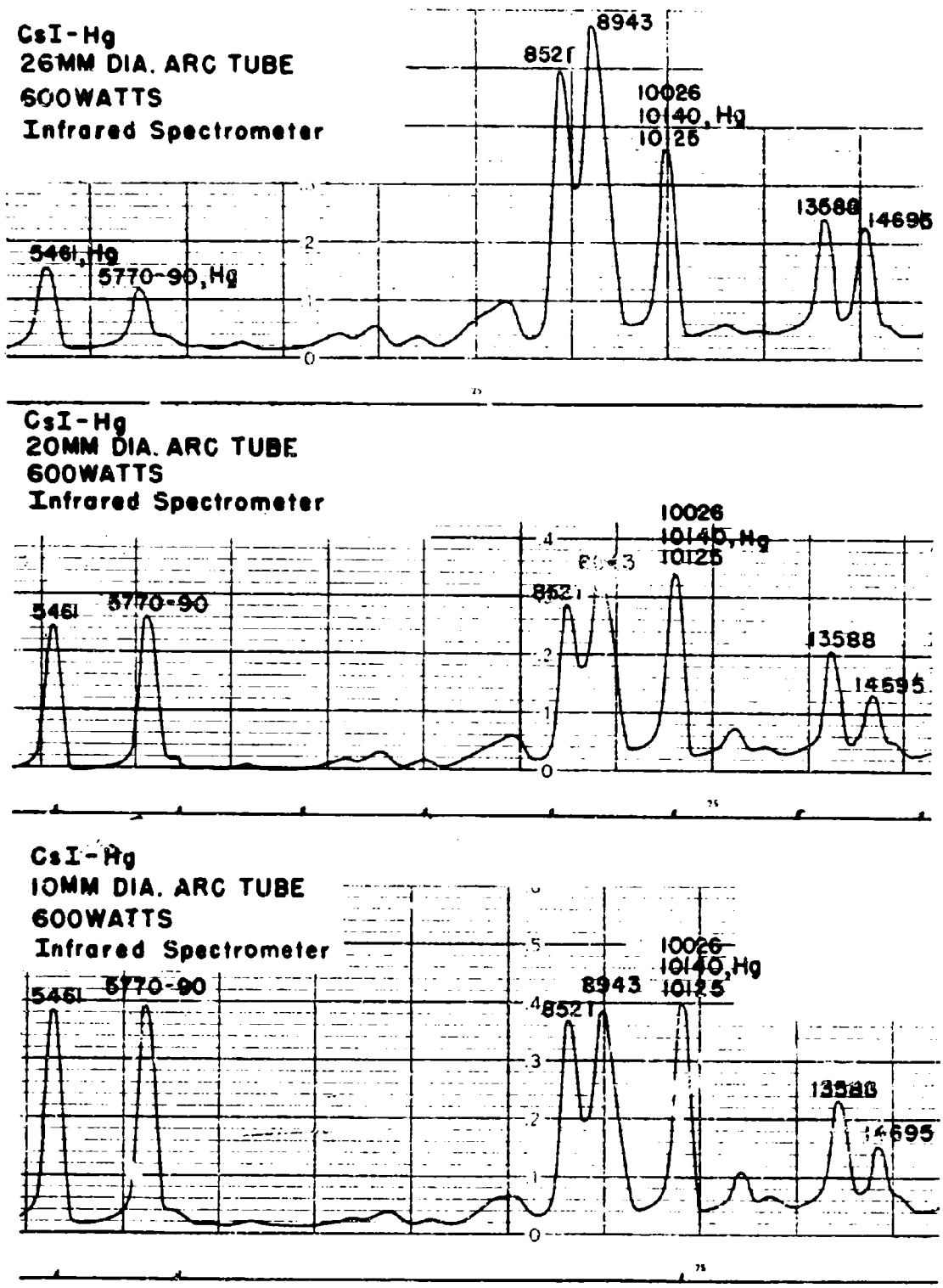
CsI-Hg
26MM DIA. ARC TUBE
600WATTS
Infrared Spectrometer
5461, Hg
5770-90, Hg
8521
8943
10026
10140, Hg
10125
13588
14695
CsI-Hg
20MM DIA. ARC TUBE
600WATTS
Infrared Spectrometer
5461
5770-90
8521
10026
10140, Hg
10125
13588
14695
CsI-Hg
10MM DIA. ARC TUBE
600WATTS
Infrared Spectrometer
5461
5770-90
8521
8943
10026
10140, Hg
10125
13588
14695

Figure 21

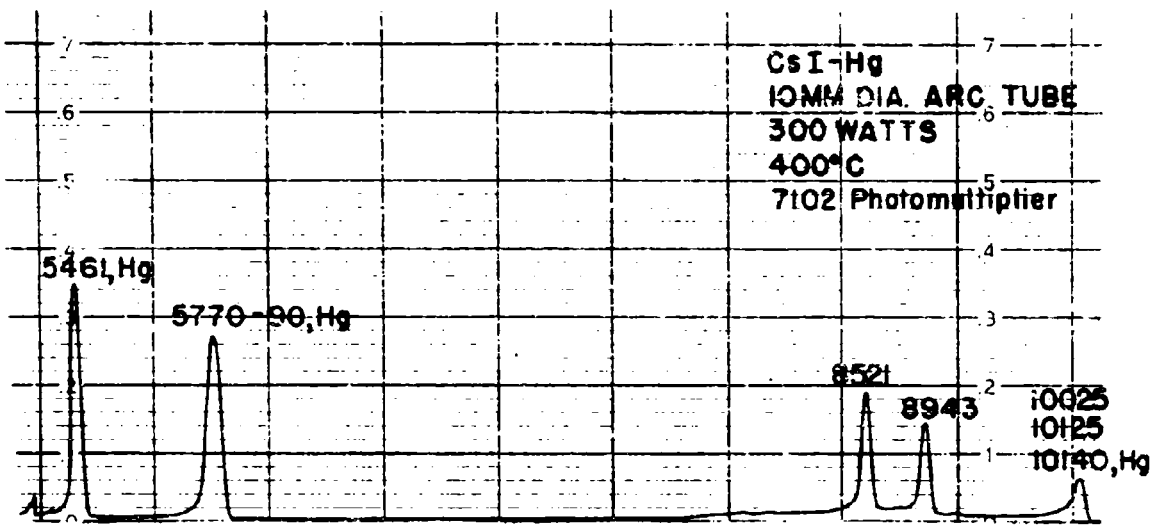
CsI-Hg
10MM DIA. ARC TUBE
300 WATTS
400°C
7102 Photomultiplier
5461, Hg
5770-90, Hg
8521
8943
10025
10125
10140, Hg

a

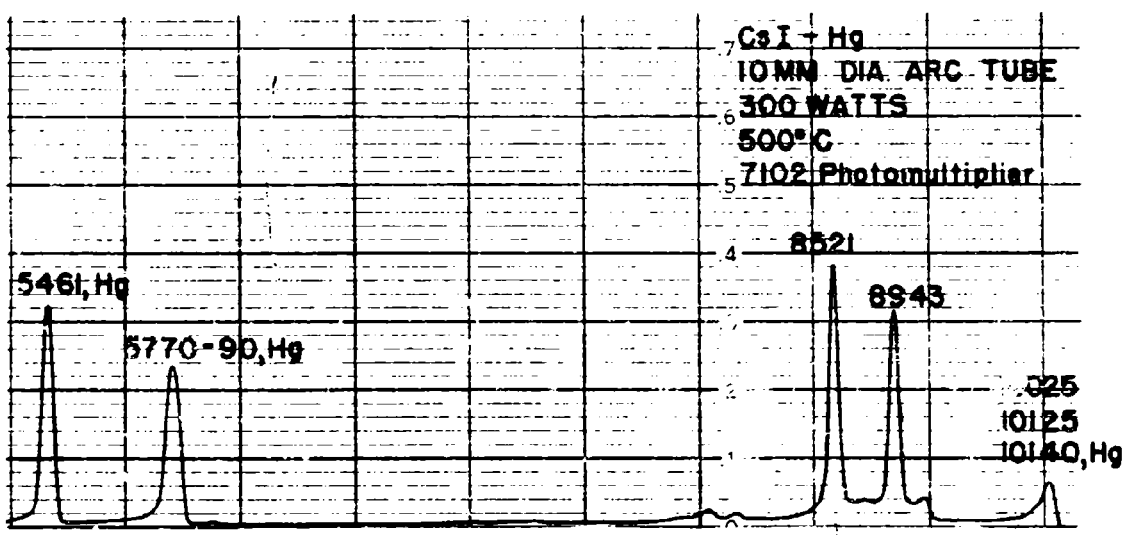
CsI-Hg
10MM DIA. ARC TUBE
300 WATTS
500°C
7102 Photomultiplier
5461, Hg
5770-90, Hg
8521
8943
10125
10140, Hg

b

Figure 22

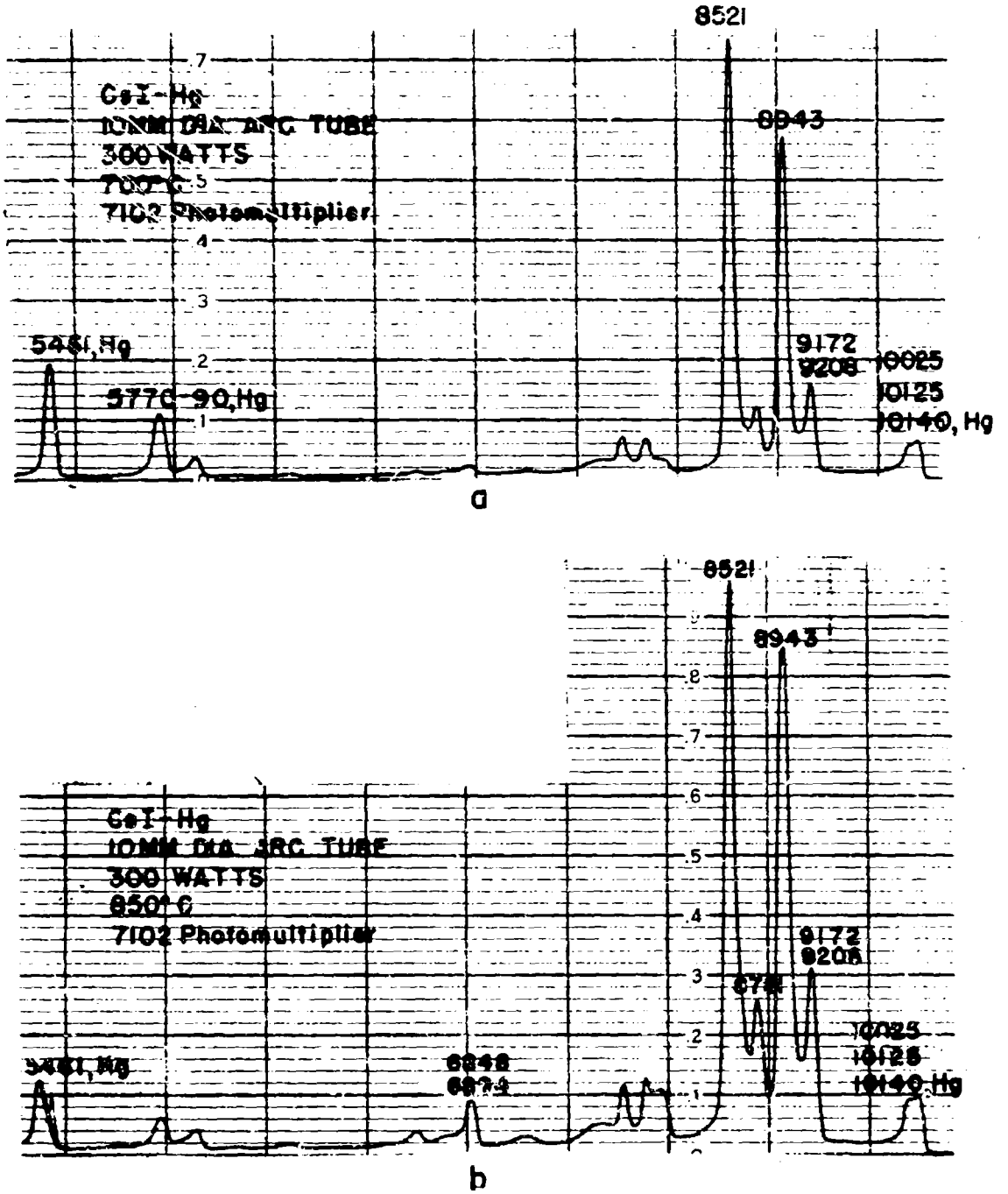
8521
8943
CsI-Hg
300 WATTS
7102 Photomultiplier
5461, Hg
9172
9208
10025
10125
10140, Hg
a
8521
8943
CsI-Hg
300 WATTS
7102 Photomultiplier
9172
9208
10025
10125
10140 Hg
b

Figure 23

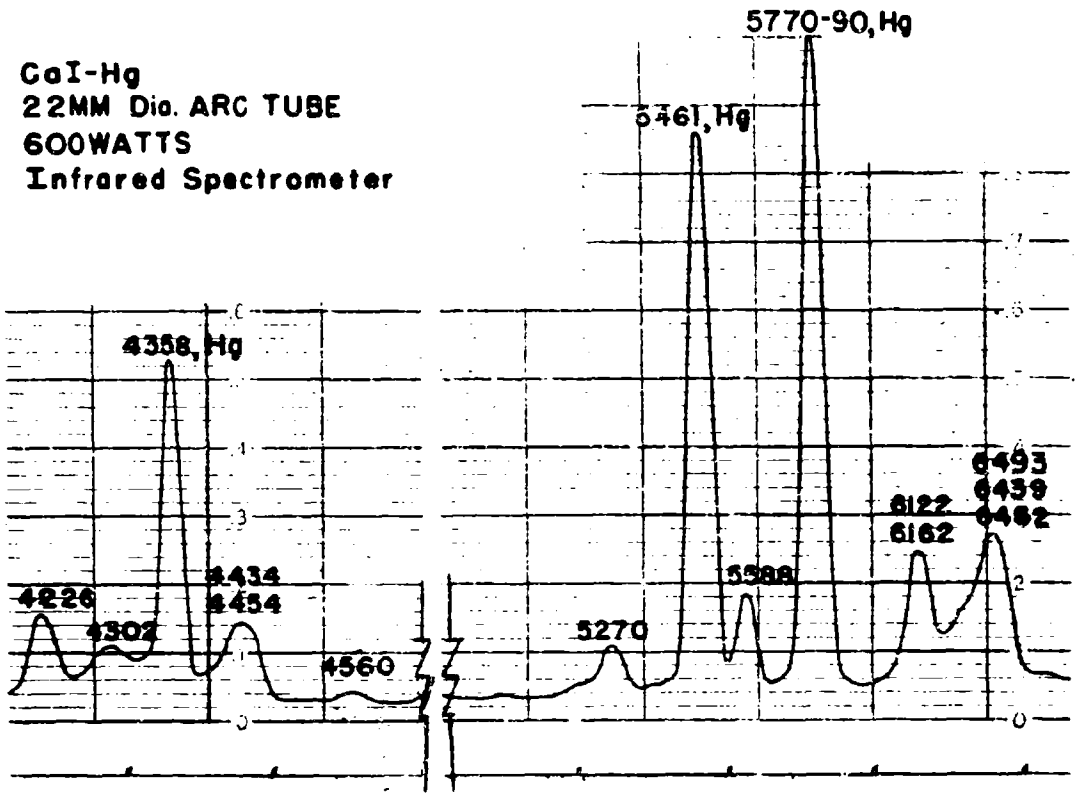
CaI-Hg
22MM Dia. ARC TUBE
600WATTS
Infrared Spectrometer
5770-90, Hg
5461, Hg
4358, Hg
6493
6439
6482
6122
6162
5588
4226
4302
4434
4454
4560
5270

a

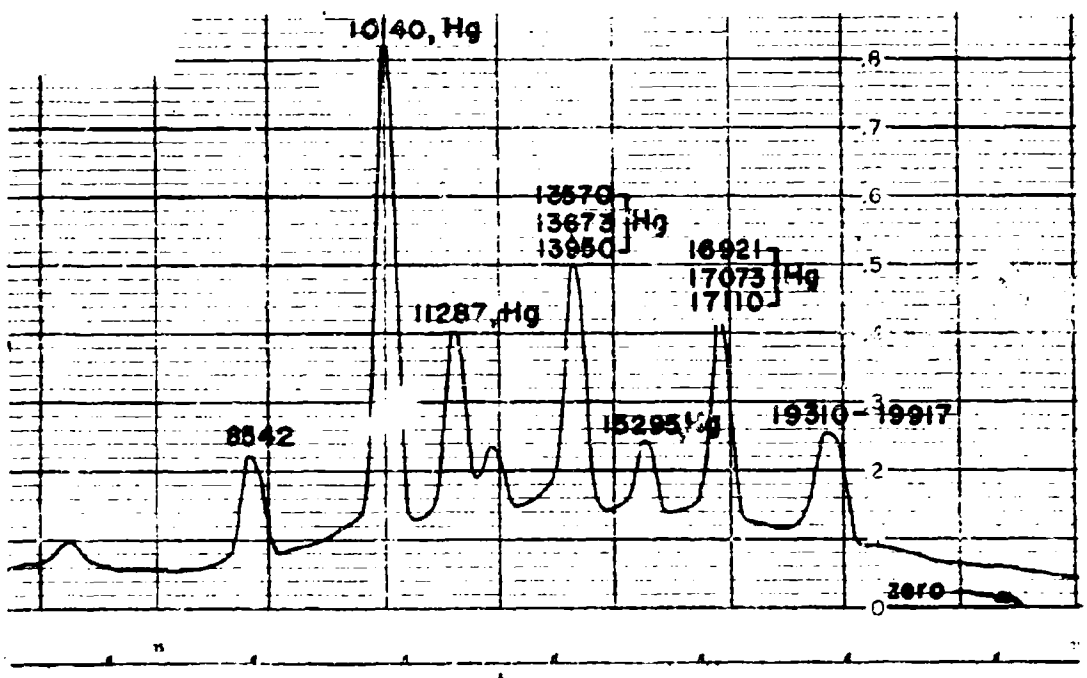
10140, Hg
12570
13673 Hg
13950
16921
17073 Hg
17110
11287, Hg
8842
15295 Hg
19310-19917
zero

b

Figure 24

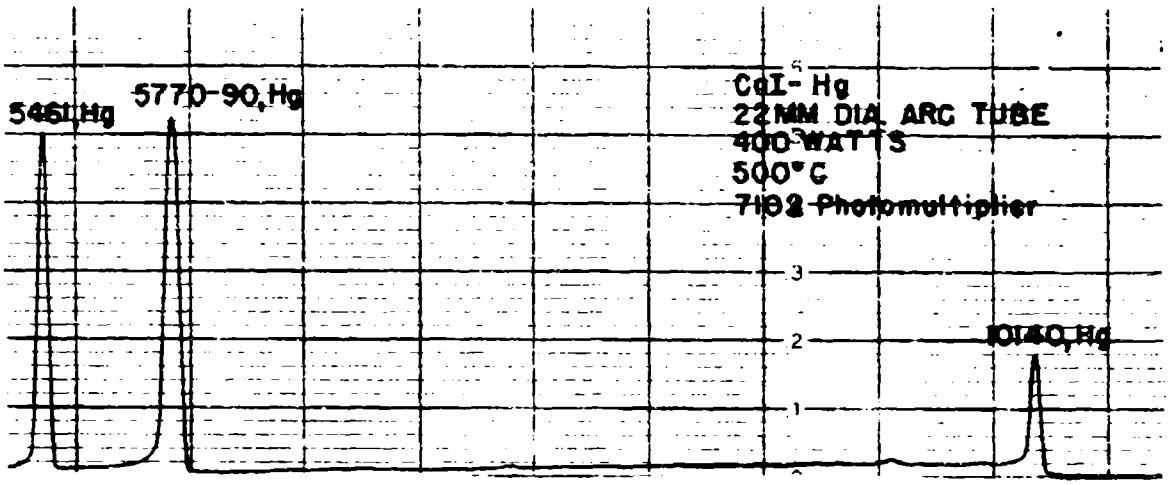
5461,Hg
5770-90,Hg
CdI-Hg
22MM DIA. ARC TUBE
400 WATTS
500°C
7102 Photomultiplier
3
2
10140,Hg
1

a

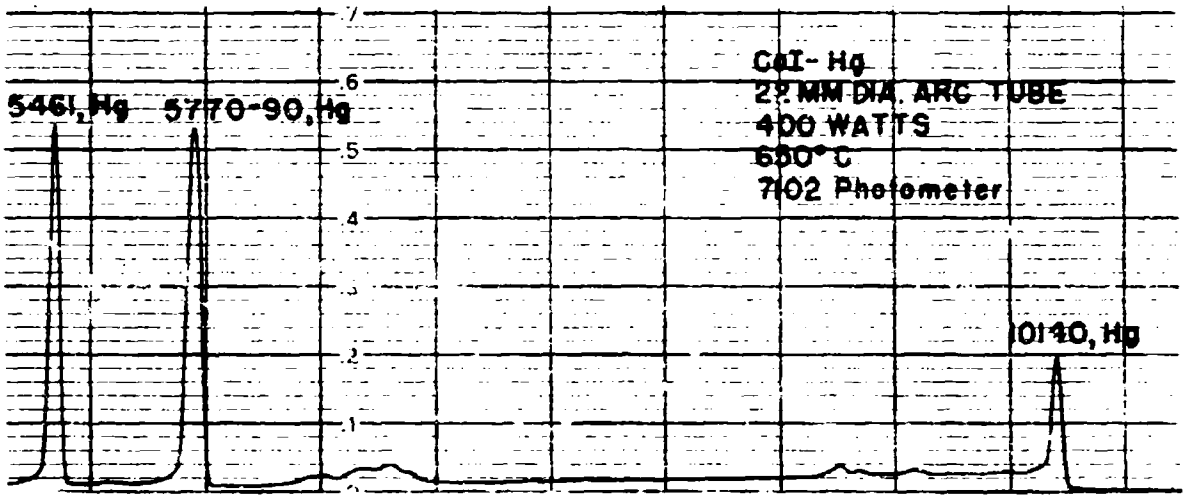
5461,Hg
5770-90,Hg
CdI-Hg
22 MM DIA. ARC TUBE
400 WATTS
650°C
7102 Photometer
.7
.6
.5
.4
.3
.2
.1
10140,Hg

b

Figure 25

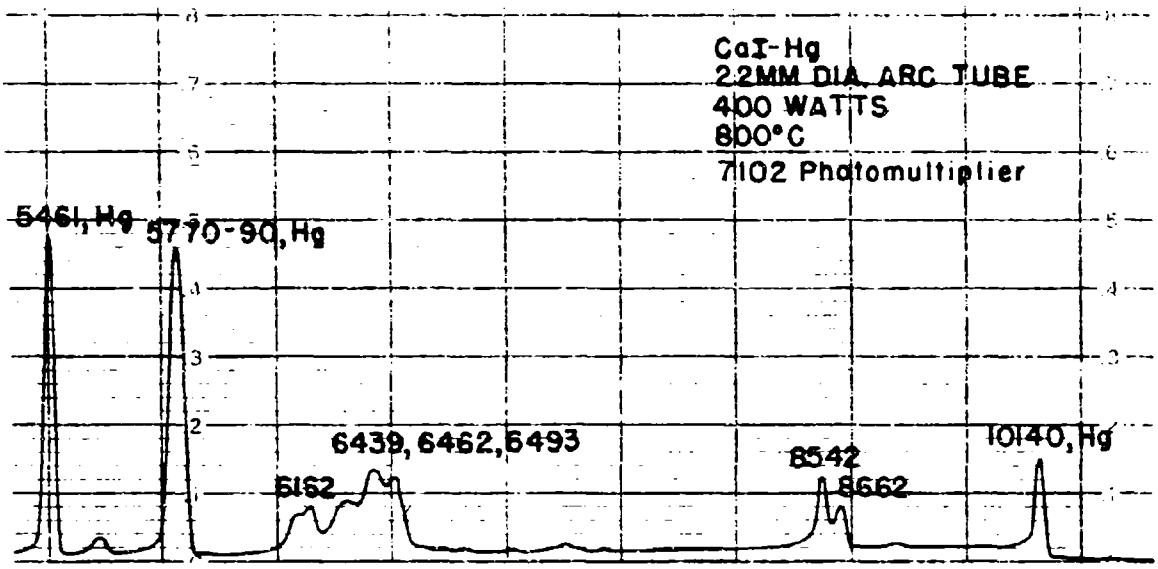
CaI-Hg
22MM DIA. ARC TUBE
400 WATTS
800°C
7102 Photomultiplier
5461, Hg
5770-90, Hg
6162
6439, 6462, 6493
8542
8662
10140, Hg

a

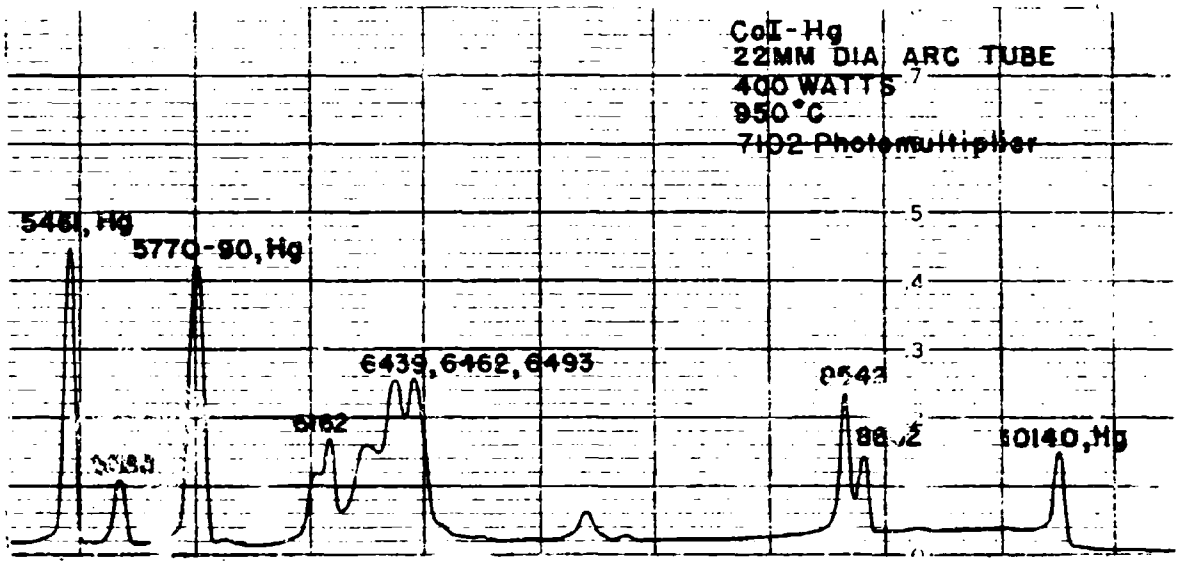
CaI-Hg
22MM DIA. ARC TUBE
400 WATTS
950°C
7102 Photomultiplier
5461, Hg
5770-90, Hg
6162
6439, 6462, 6493
8542
8662
10140, Hg

b

Figure 26

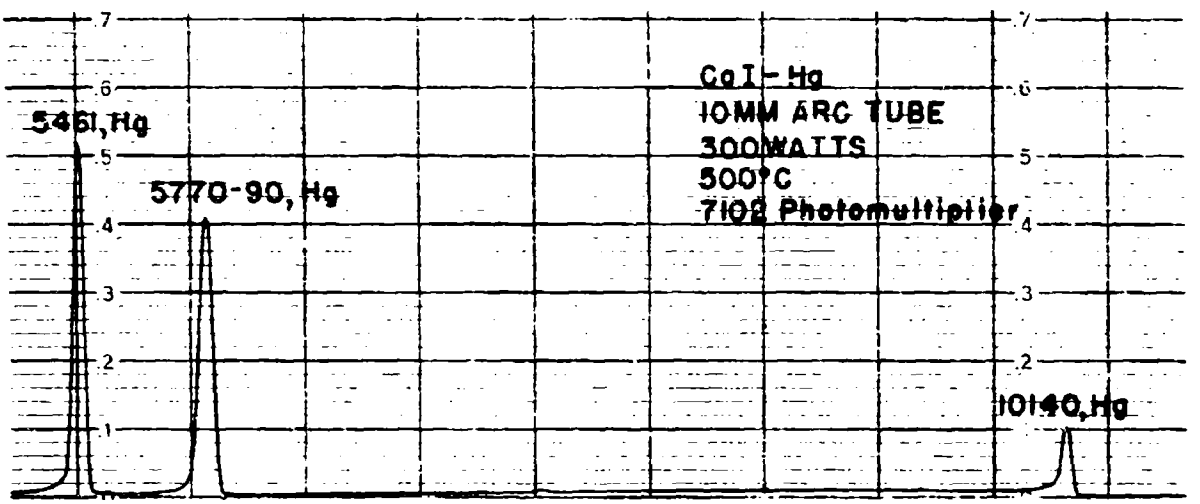
CaI-Hg
10MM ARC TUBE
300WATTS
500°C
7102 Photomultiplier
5461,Hg
5770-90,Hg
10140,Hg

a

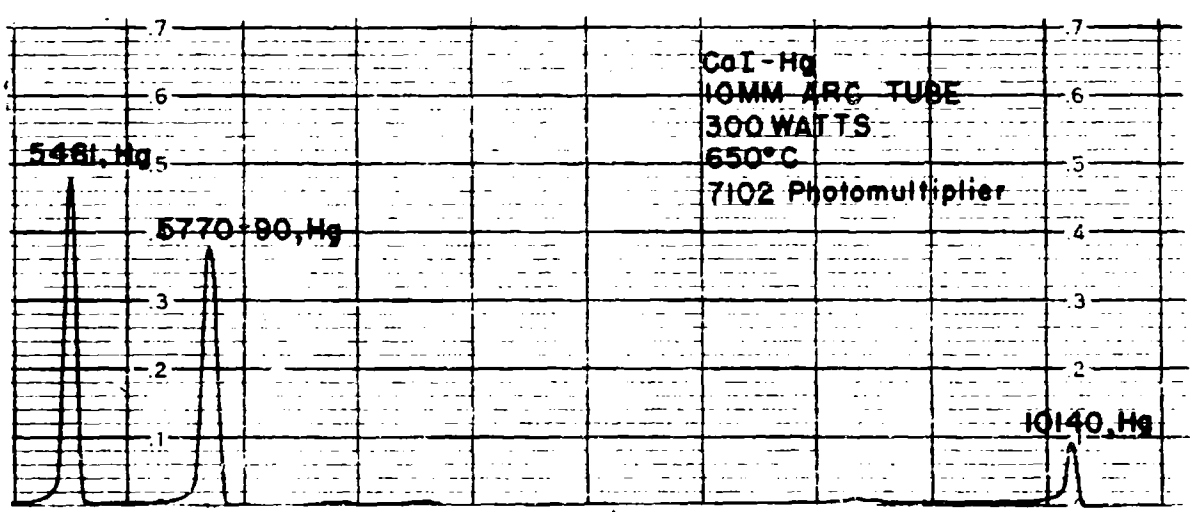
CaI-Hg
10MM ARC TUBE
300WATTS
650°C
7102 Photomultiplier
5461,Hg
5770-90,Hg
10140,Hg

b

Figure 27

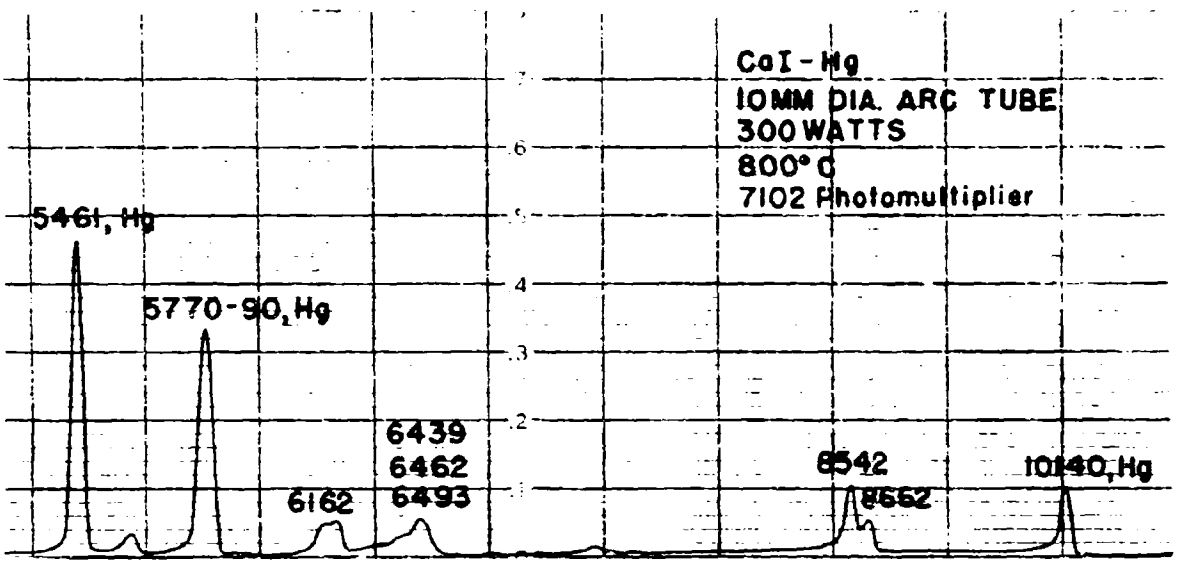
CaI - Hg
10MM DIA. ARC TUBE
300 WATTS
800°C
7102 Photomultiplier
5461, Hg
5770-90, Hg
6162
6439
6462
6493
8542
8662
10140, Hg

a

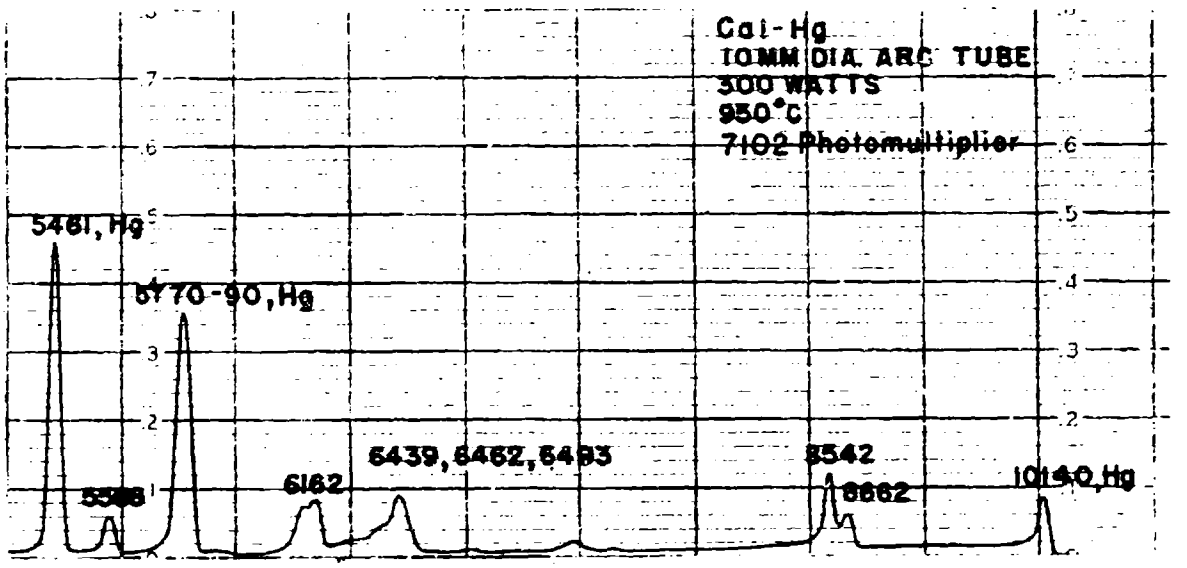
CaI - Hg
10MM DIA. ARC TUBE
300 WATTS
950°C
7102 Photomultiplier
5461, Hg
5770-90, Hg
6162
6439, 6462, 6493
8542
8662
10140, Hg

b

Figure 28

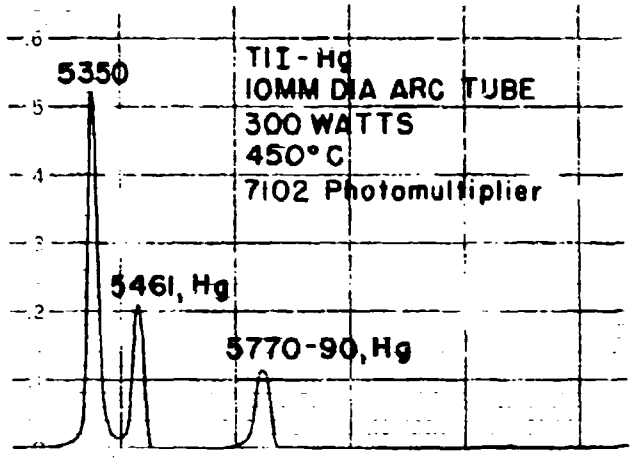
.6
.5
.4
.3
.2
5350
TII-Hg
10MM DIA ARC TUBE
300 WATTS
450° C
7102 Photomultiplier
5461, Hg
5770-90, Hg

a

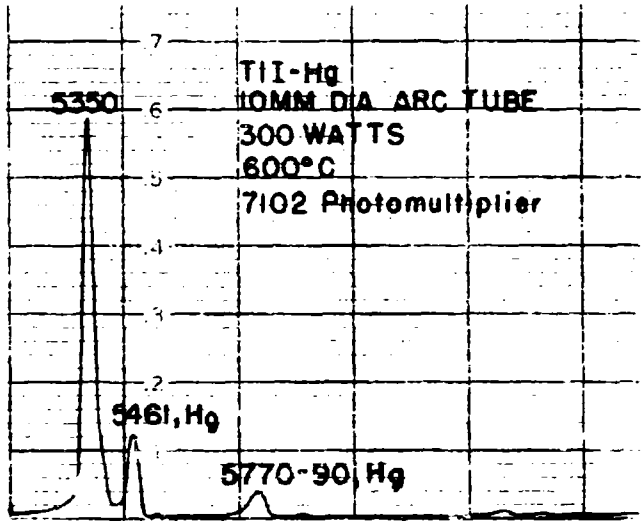
.7
.6
.5
.4
.3
.2
.1
5350
TII-Hg
10MM DIA ARC TUBE
300 WATTS
600° C
7102 Photomultiplier
5461, Hg
5770-90, Hg

b

Figure 29

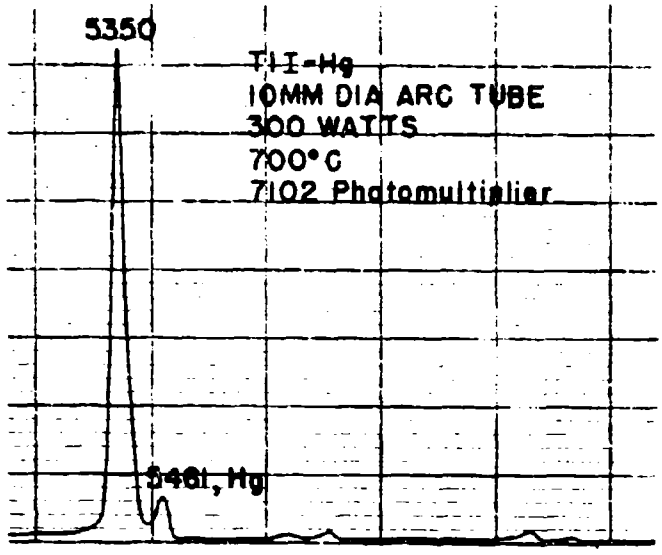
5350
TlI-Hg
10MM DIA ARC TUBE
300 WATTS
700° C
7102 Photomultiplier
5461, Hg

a

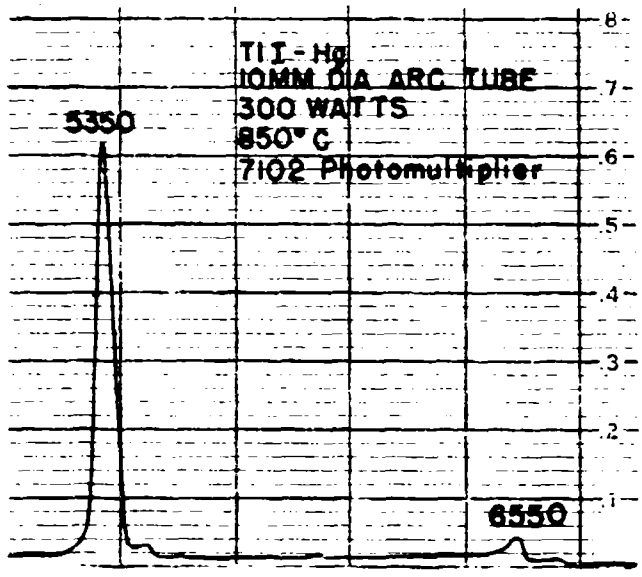
TlI-Hg
10MM DIA ARC TUBE
300 WATTS
850° C
7102 Photomultiplier
5350
6550
.8
.7
.6
.5
.4
.3
.2
.1

b

Figure 30

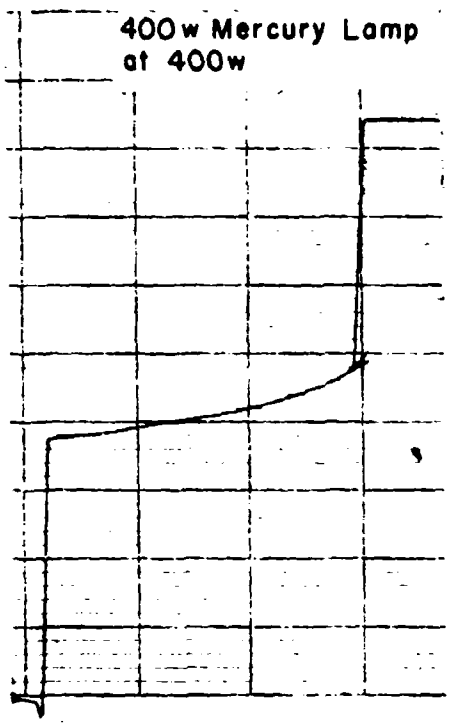

a

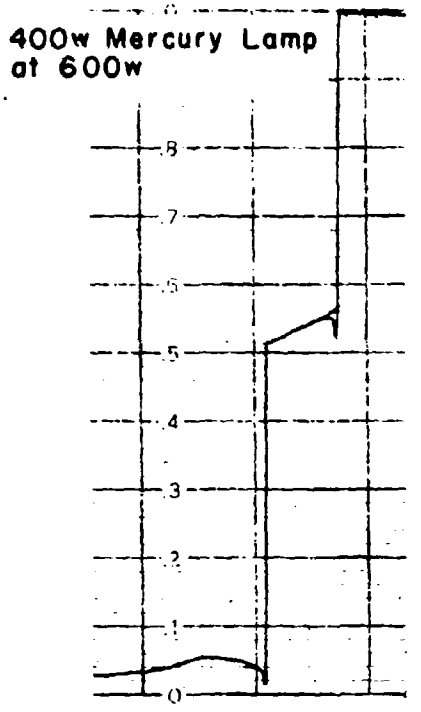

b

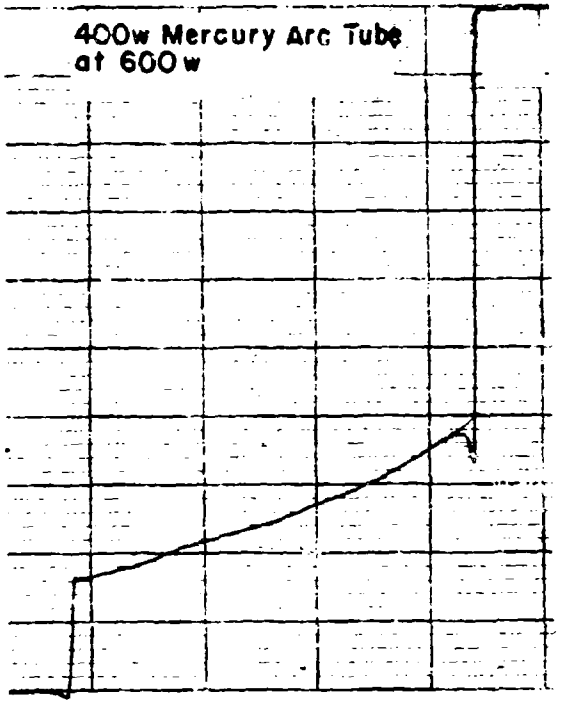

c

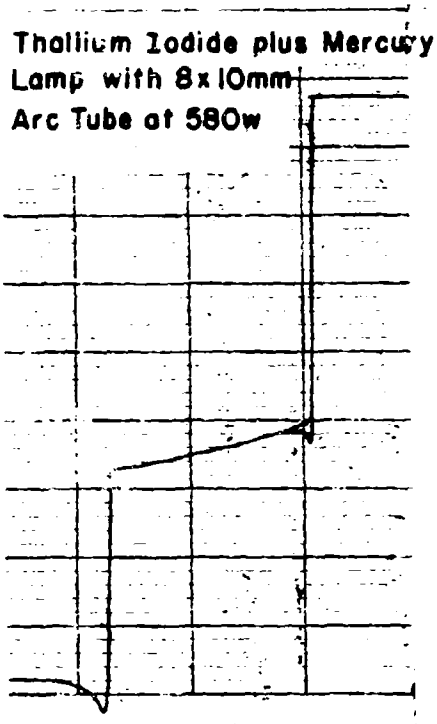

d

Figure 31

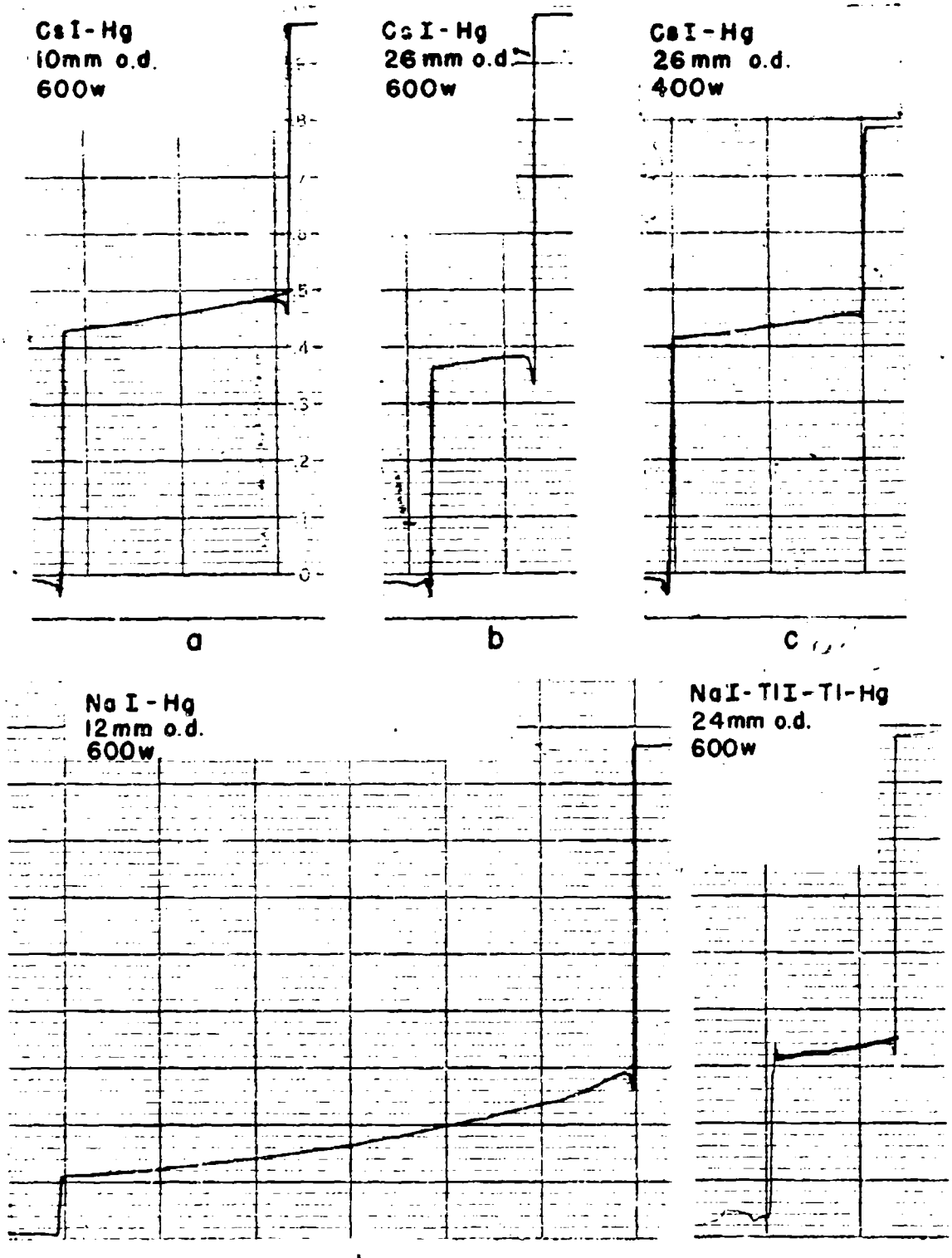
CsI-Hg
10mm o.d.
600w
CsI-Hg
26mm o.d.
600w
CsI-Hg
26mm o.d.
400w
a
b
c
NaI-Hg
12mm o.d.
600w
NaI-TlI-Tl-Hg
24mm o.d.
600w
d
e

Figure 32

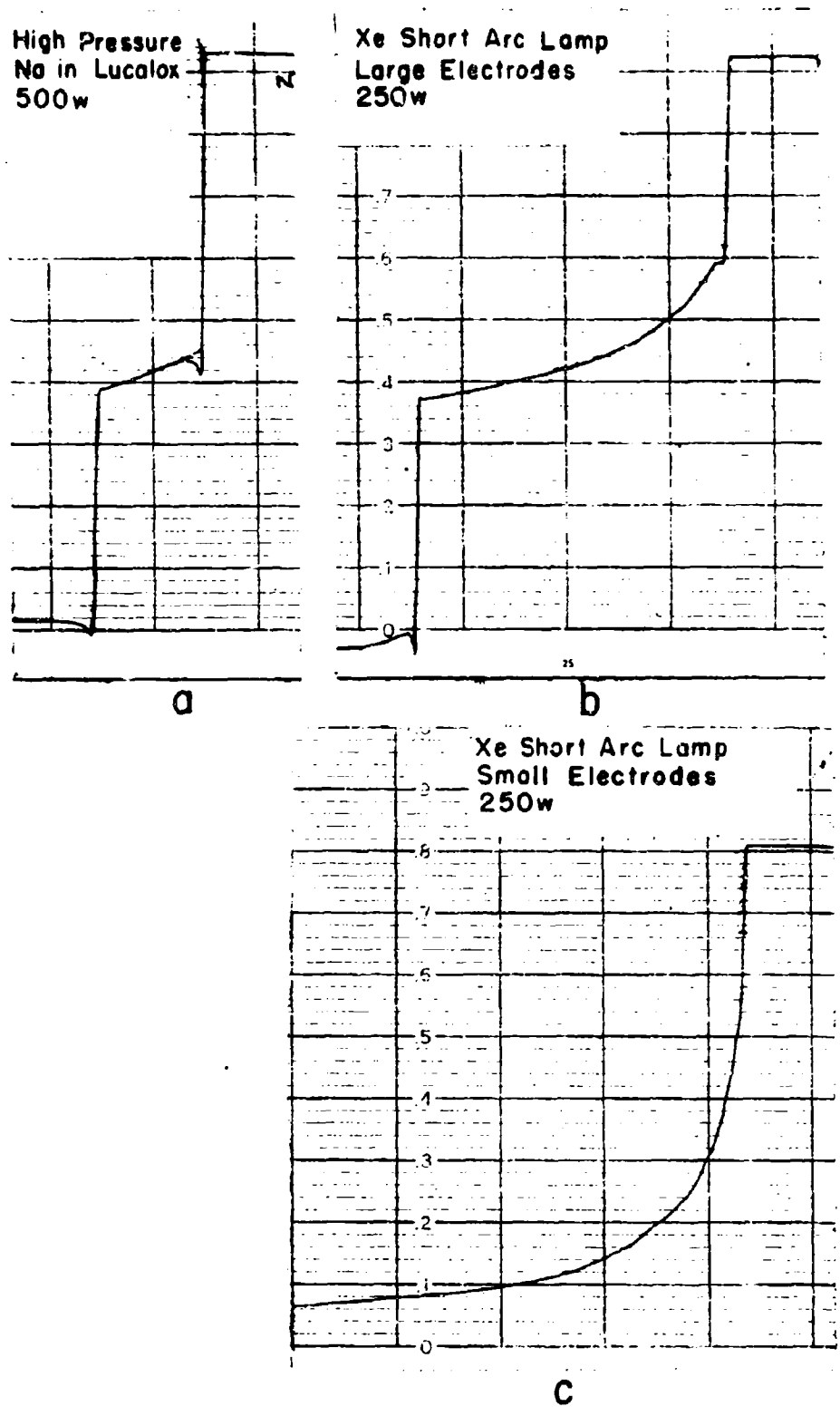
High Pressure
Na in Lucalox
500w
Xe Short Arc Lamp
Large Electrodes
250w
Xe Short Arc Lamp
Small Electrodes
250w
a
b
c

Figure 33

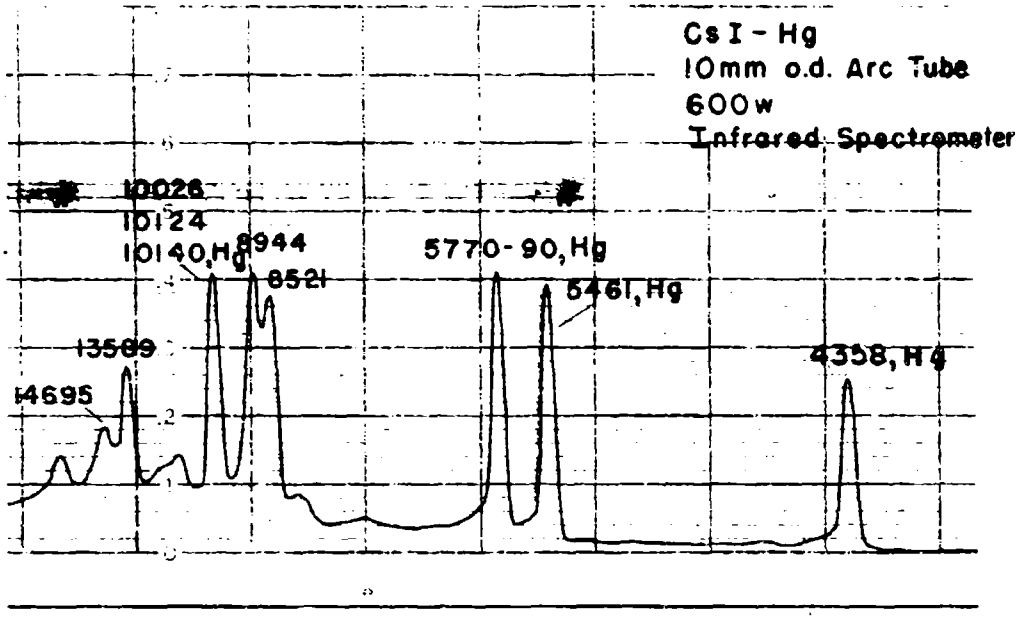
Cs I - Hg
10mm o.d. Arc Tube
600w
Infrared Spectrometer
10026
10124
10140, Hg
8944
8521
13589
14695
5770-90, Hg
5461, Hg
4358, Hg

a

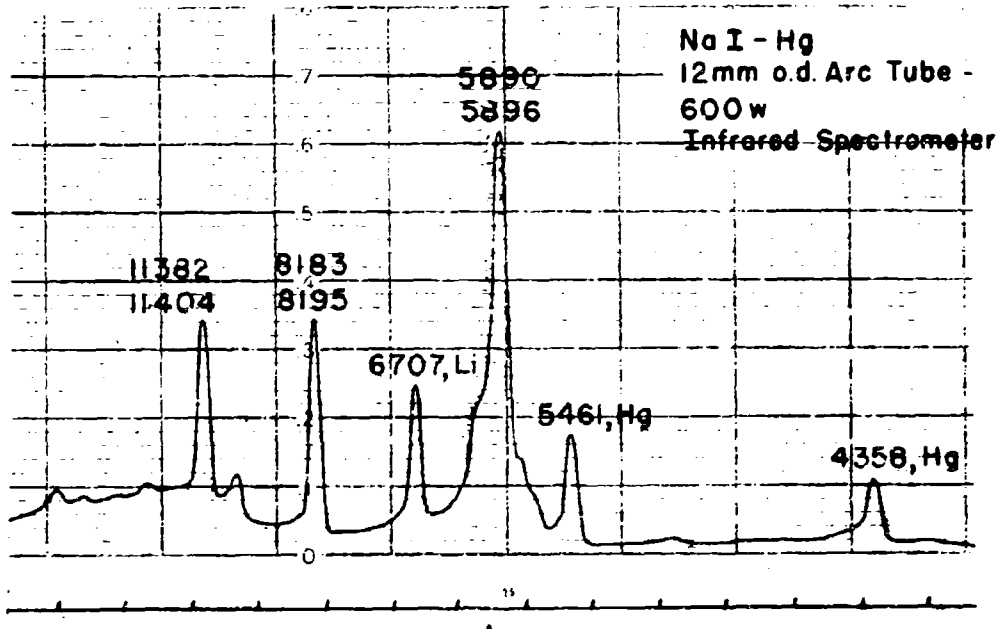
Na I - Hg
12mm o.d. Arc Tube -
600w
Infrared Spectrometer
5890
5896
11382
11404
8183
8195
6707, Li
5461, Hg
4358, Hg

b

Figure 34

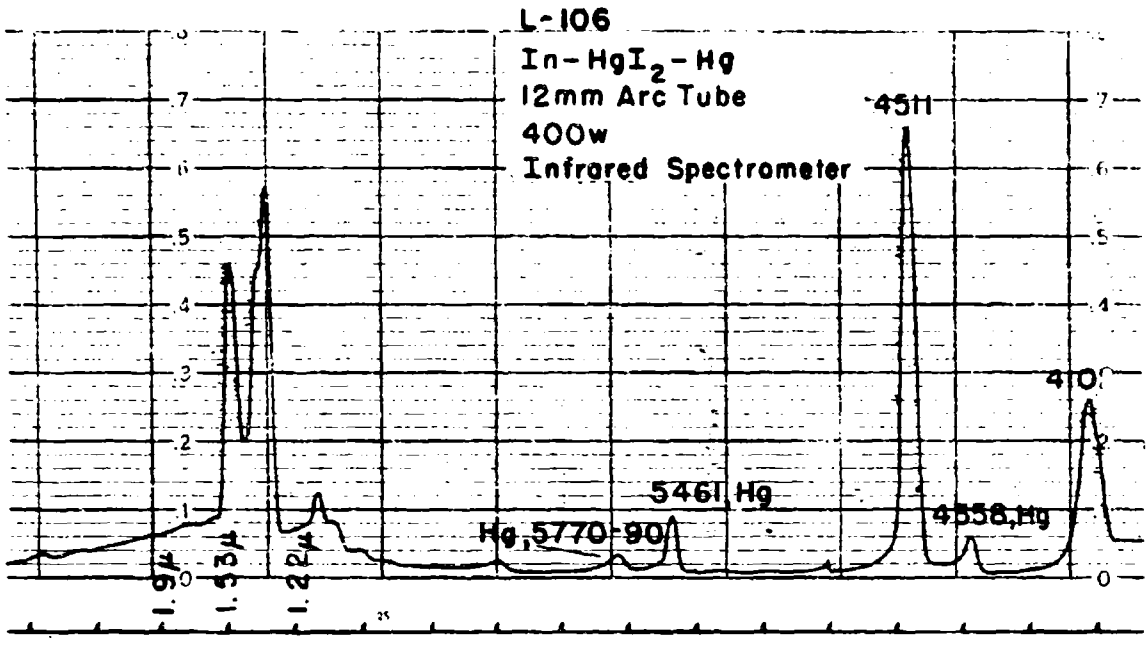
L-106
In-HgI2-Hg
12mm Arc Tube
400w
Infrared Spectrometer
4511
4102
5461, Hg
4358, Hg
Hg, 5770-90
.9μ
5.3μ
2.2μ

a

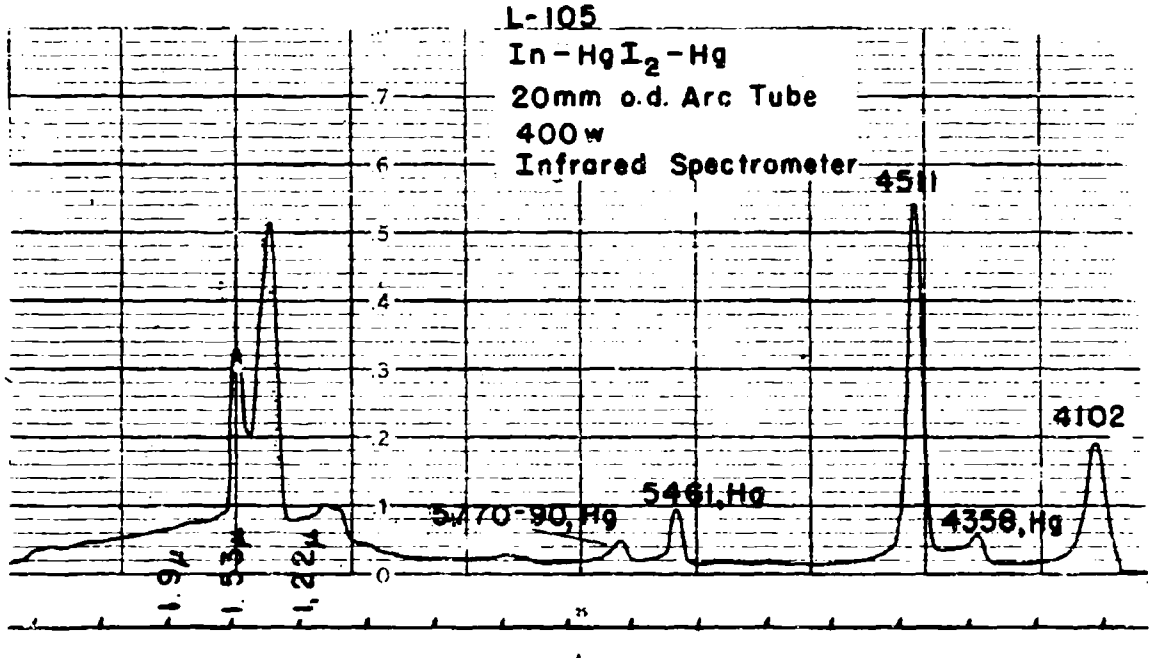
L-105
In-HgI2-Hg
20mm o.d. Arc Tube
400w
Infrared Spectrometer
4511
4102
5461, Hg
5470-90, Hg
4358, Hg
.9μ
5.3μ
2.2μ

b

Figure 35

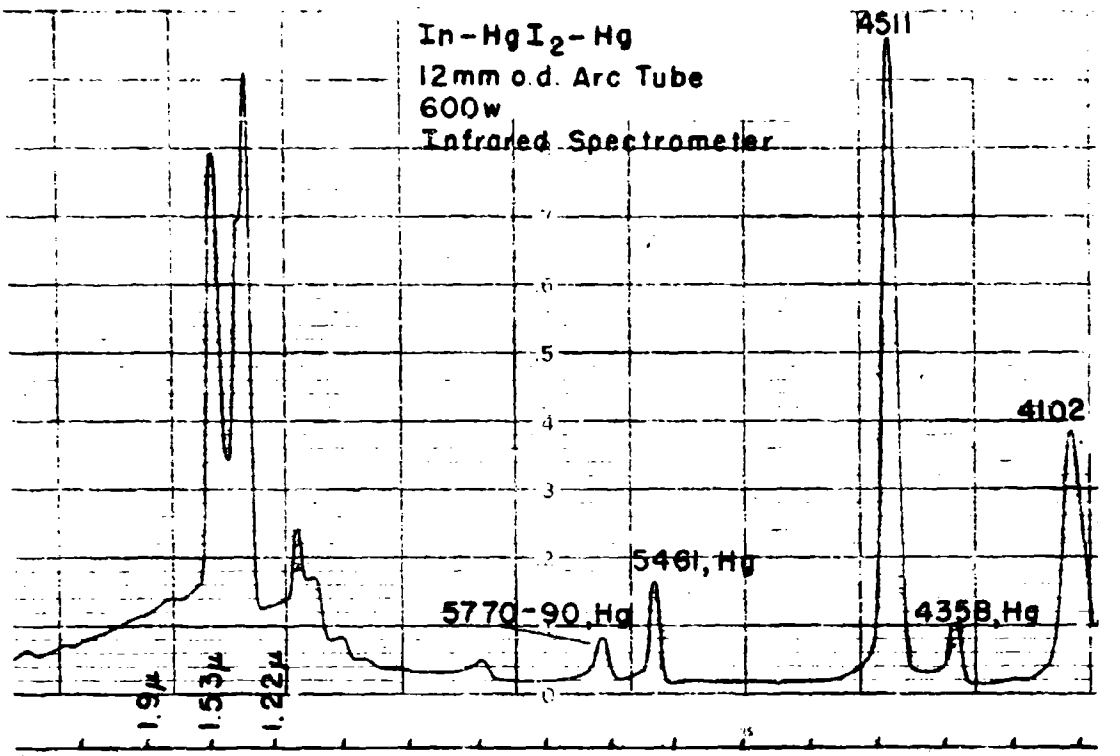
In-HgI2-Hg
12mm o.d. Arc Tube
600w
Infrared Spectrometer
4511
4102
5461, Hg
5770-90, Hg
4358, Hg
1.9μ
1.53μ
1.22μ
.6
.5
.4
.3
.2
0

a

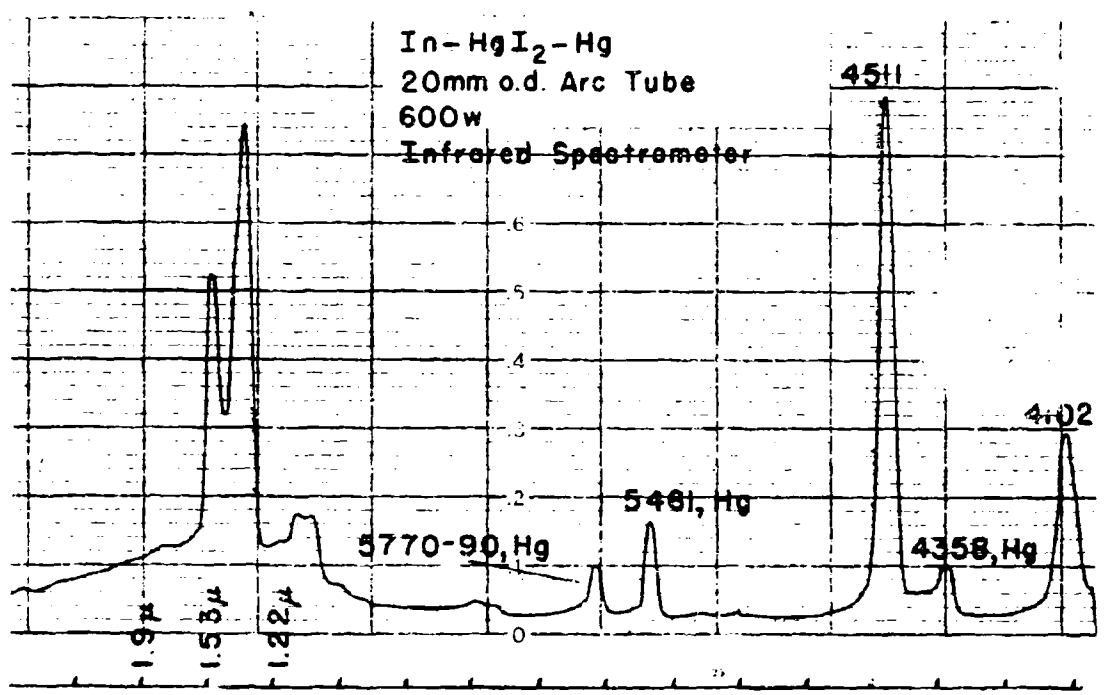
In-HgI2-Hg
20mm o.d. Arc Tube
600w
Infrared Spectrometer
4511
4102
5461, Hg
5770-90, Hg
4358, Hg
1.9μ
1.53μ
1.22μ
.6
.5
.4
.3
.2
0

b

Figure 36

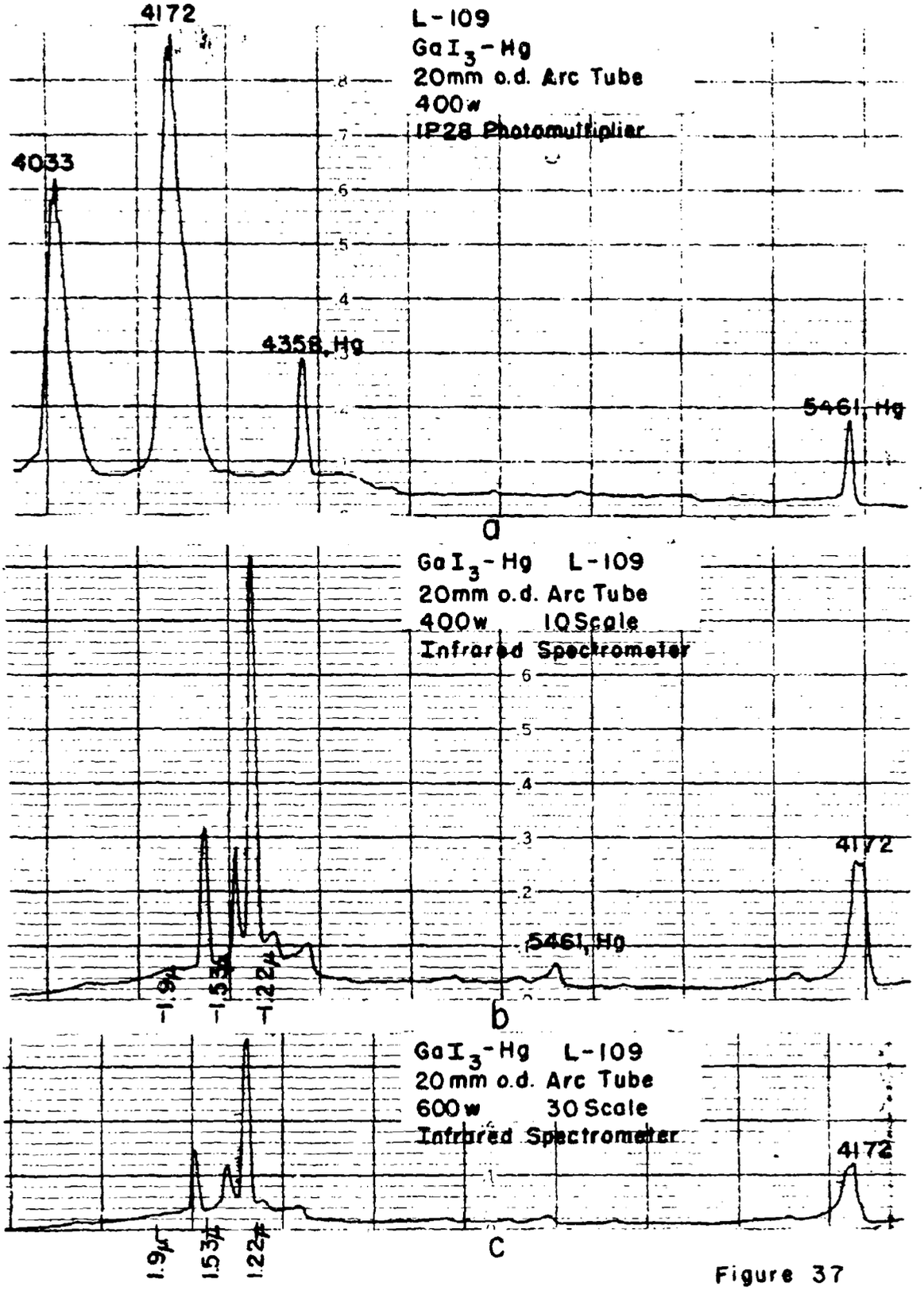
4172
4033
4358, Hg
5461, Hg
L-109
GaI3-Hg
20mm o.d. Arc Tube
400w
IP28 Photomultiplier
a
GaI3-Hg L-109
20mm o.d. Arc Tube
400w 10 Scale
Infrared Spectrometer
4172
5461, Hg
1.9μ
1.53μ
1.22μ
b
GaI3-Hg L-109
20mm o.d. Arc Tube
600w 30 Scale
Infrared Spectrometer
4172
1.9μ
1.53μ
1.22μ
c

Figure 37

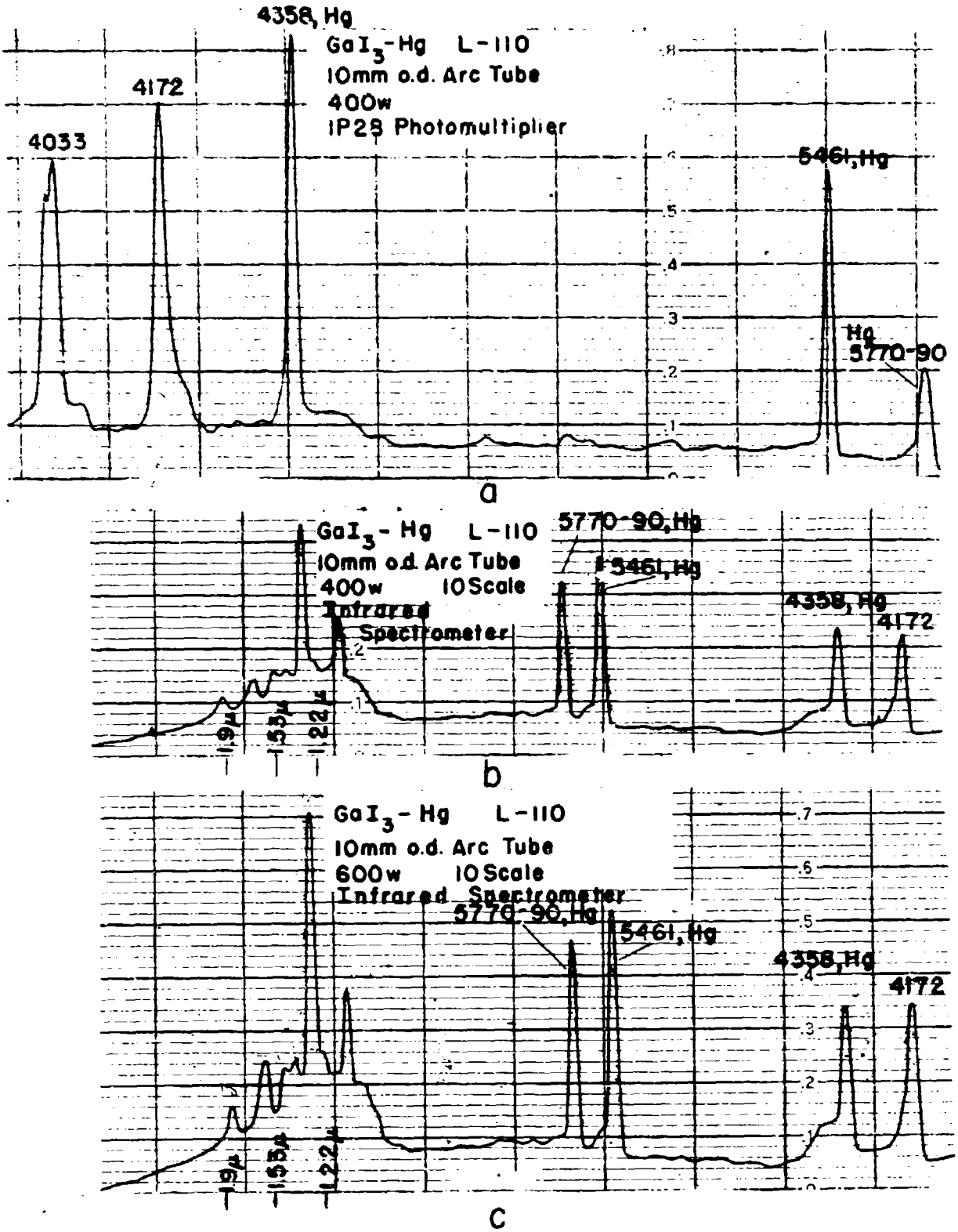
4358, Hg
GaI3 - Hg L-110
10mm o.d. Arc Tube
400w
IP28 Photomultiplier
4172
4033
5461, Hg
Hg
5770-90
a
GaI3 - Hg L-110
10mm o.d. Arc Tube
400w 10 Scale
Infrared
Spectrometer
5770-90, Hg
5461, Hg
4358, Hg
4172
1.9μ
1.53μ
1.22μ
b
GaI3 - Hg L-110
10mm o.d. Arc Tube
600w 10 Scale
Infrared Spectrometer
5770-90, Hg
5461, Hg
4358, Hg
4172
1.9μ
1.53μ
1.22μ
c

Figure 38

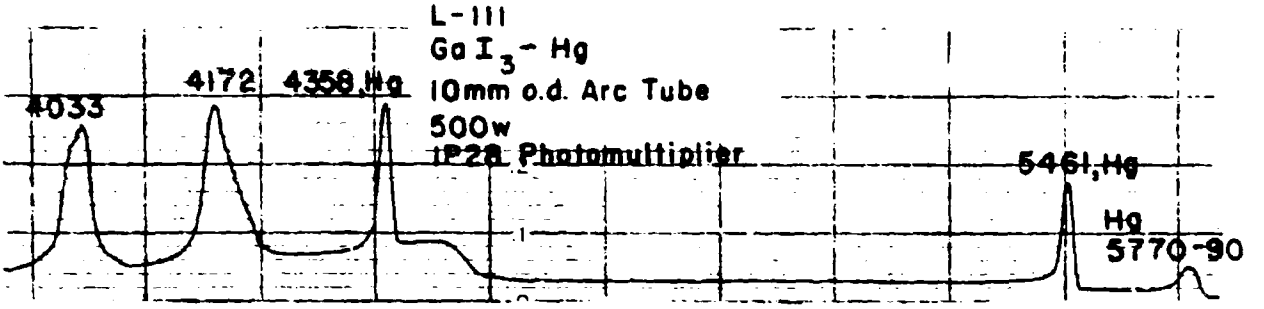
L-111
GaI3 - Hg
10mm o.d. Arc Tube
500w
IP28 Photomultiplier
4033
4172
4358,Hg
5461,Hg
Hg
5770-90

a

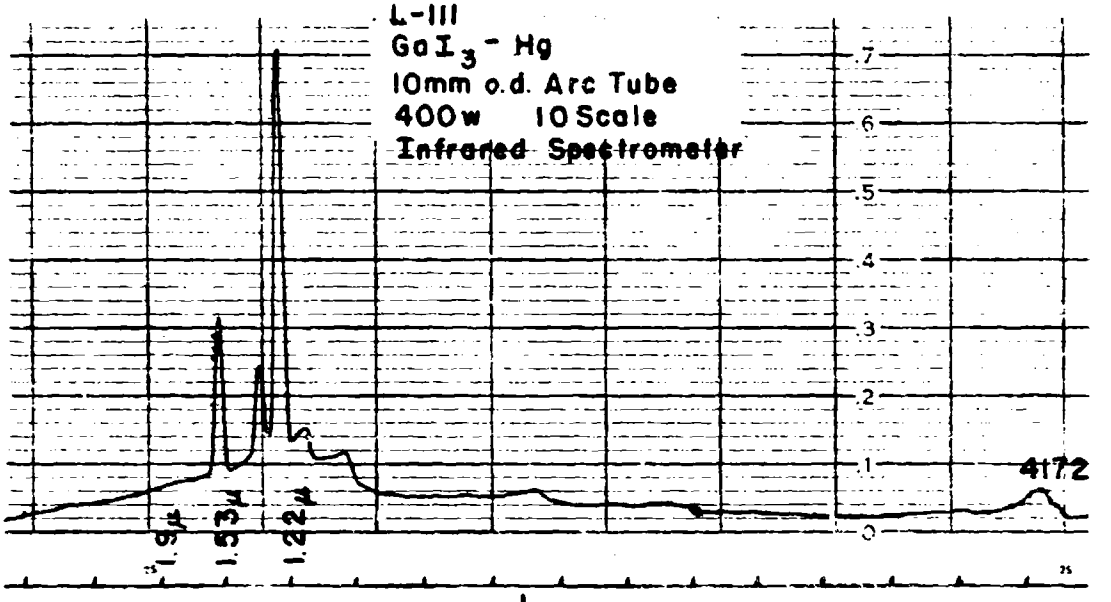
L-111
GaI3 - Hg
10mm o.d. Arc Tube
400w 10 Scale
Infrared Spectrometer
.7
.6
.5
.4
.3
.2
.1
0
4172
1.9μ
1.53μ
1.22μ

b

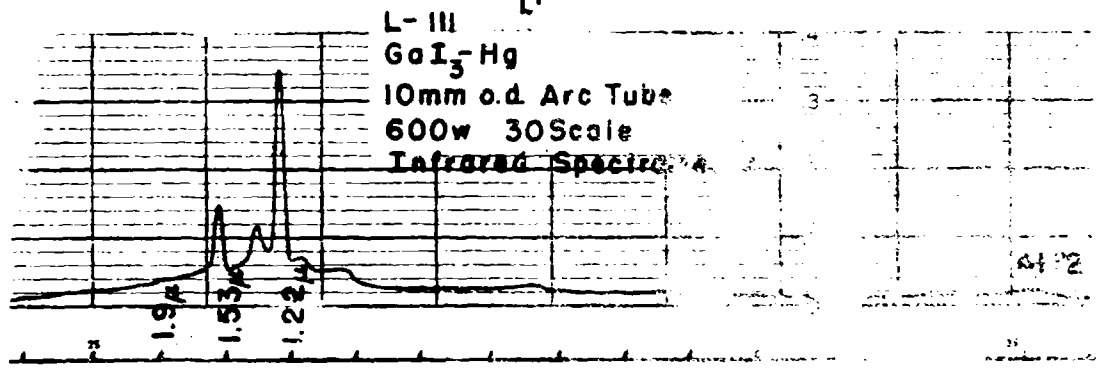
L-111
GaI3-Hg
10mm o.d. Arc Tube
600w 30 Scale
Infrared Spectro
3
4172
1.9μ
1.53μ
1.22μ

.C

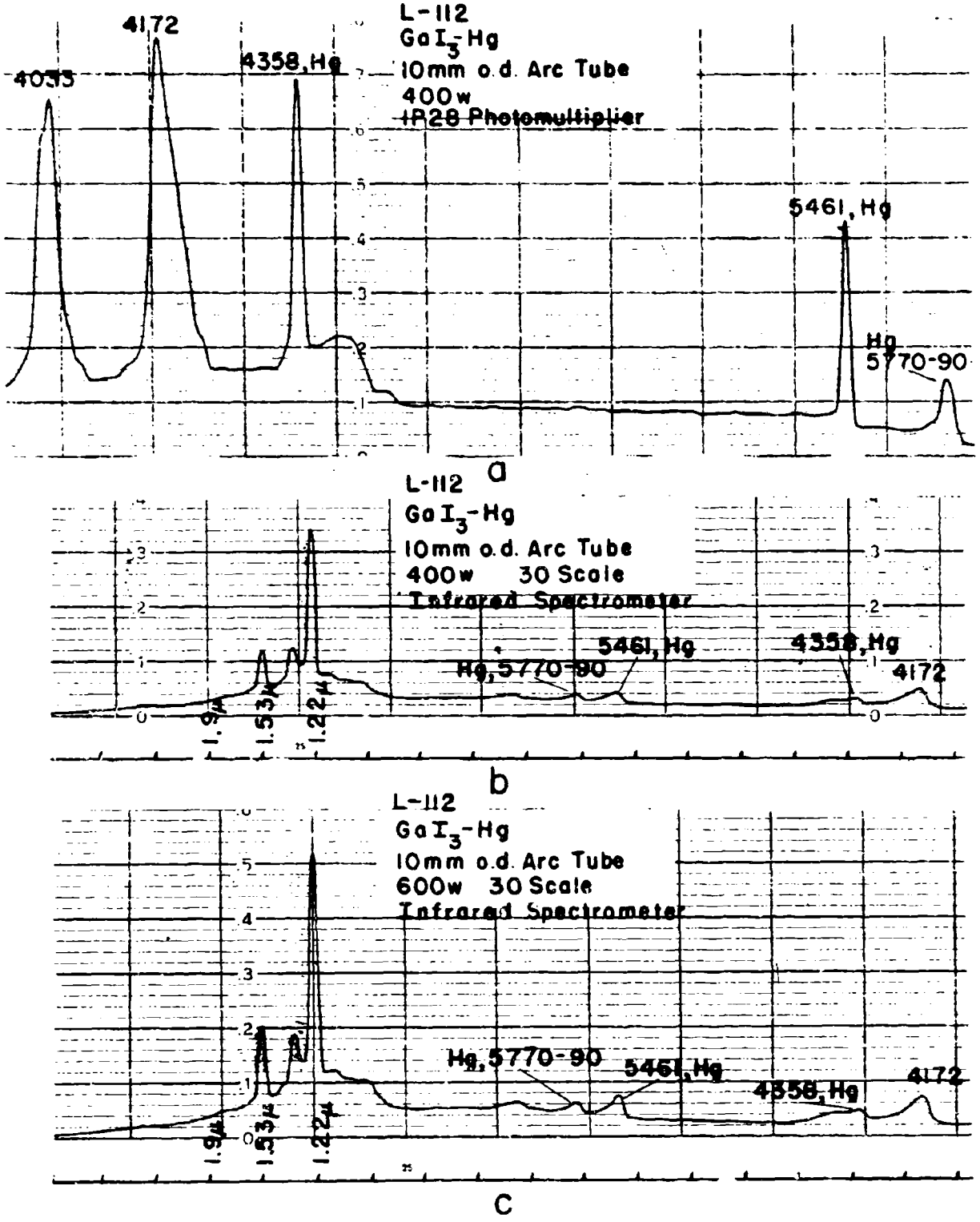
4033
4172
4358, Hg
L-112
GaI3-Hg
10mm o.d. Arc Tube
400w
IP28 Photomultiplier
5461, Hg
Hg
5770-90
a
L-112
GaI3-Hg
10mm o.d. Arc Tube
400w 30 Scale
Infrared Spectrometer
5461, Hg
4358, Hg
Hg, 5770-90
4172
1.9μ
1.53μ
1.22μ
b
L-112
GaI3-Hg
10mm o.d. Arc Tube
600w 30 Scale
Infrared Spectrometer
Hg, 5770-90
5461, Hg
4358, Hg
4172
1.9μ
1.53μ
1.22μ
c

Figure 40

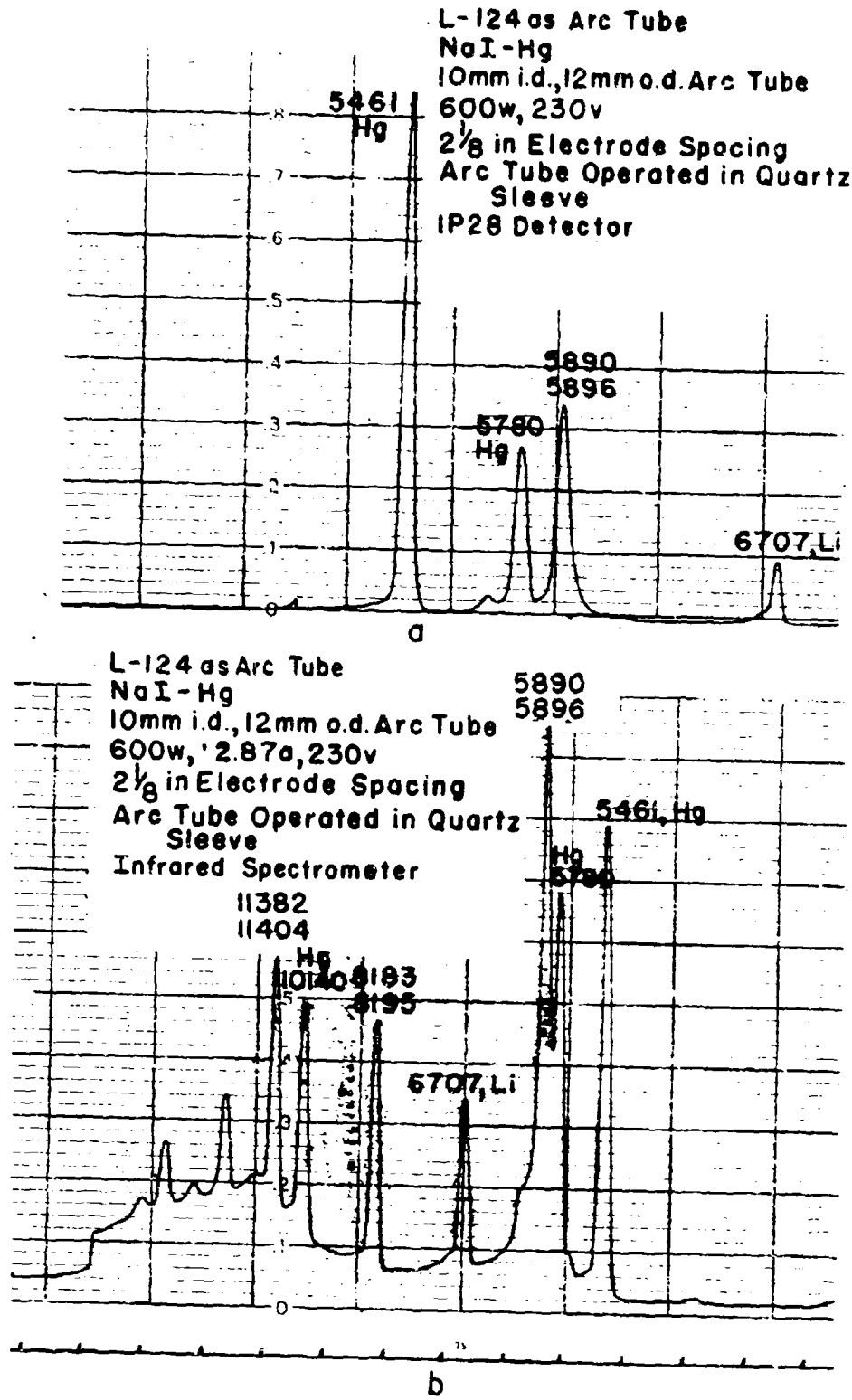
L-124 as Arc Tube
NaI-Hg
10mm i.d., 12mm o.d. Arc Tube
600w, 230v
2⅛ in Electrode Spacing
Arc Tube Operated in Quartz Sleeve
IP28 Detector
5461 Hg
5890
5896
5780 Hg
6707, Li
a
L-124 as Arc Tube
NaI-Hg
10mm i.d., 12mm o.d. Arc Tube
600w, 2.87a, 230v
2⅛ in Electrode Spacing
Arc Tube Operated in Quartz Sleeve
Infrared Spectrometer
11382
11404
Hg
11404
8183
8195
6707, Li
5890
5896
5461, Hg
Hg
5780
b

Figure 41

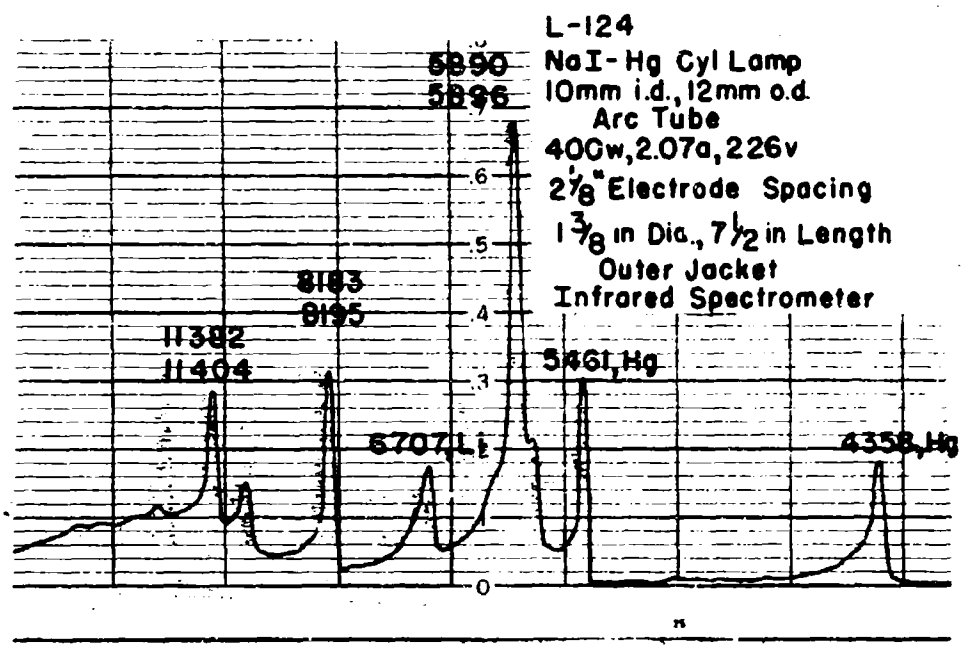
L-124
NaI-Hg Cyl Lamp
10mm i.d., 12mm o.d.
Arc Tube
400w, 2.07a, 226v
2 1/8" Electrode Spacing
1 3/8 in Dia., 7 1/2 in Length
Outer Jacket
Infrared Spectrometer
5890
5896
8183
8195
11382
11404
6707 Li
5461 Hg
4358 Hg
.6
.5
.4
.3
0

Figure 42

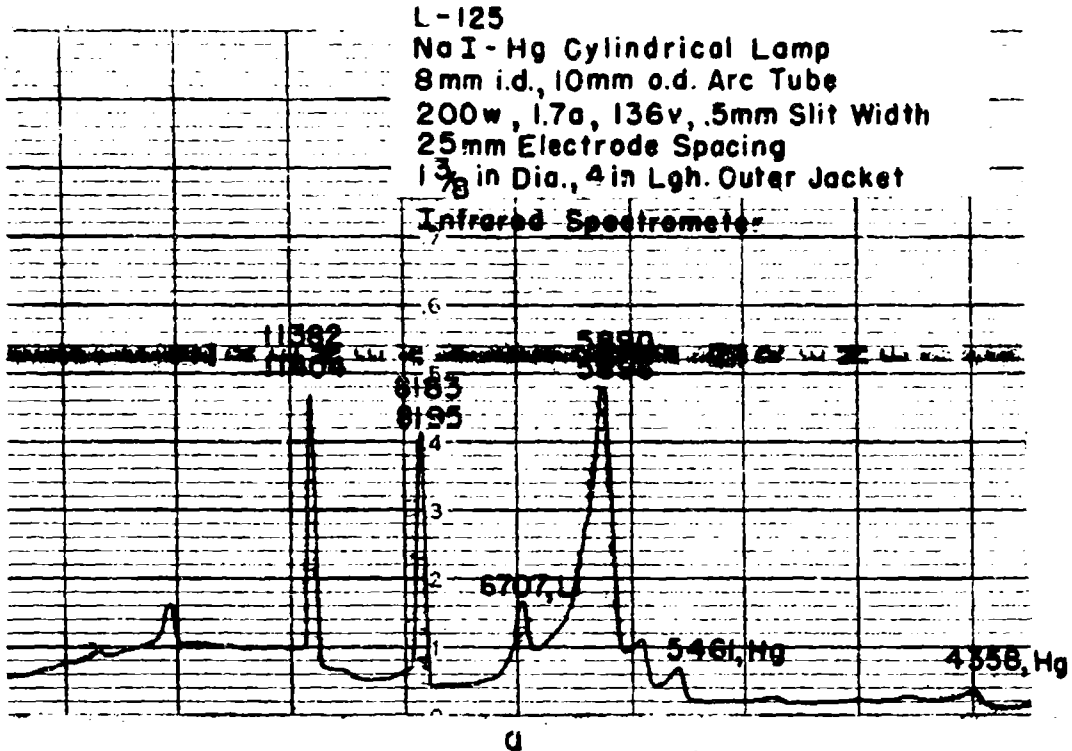
L-125
NaI - Hg Cylindrical Lamp
8mm i.d., 10mm o.d. Arc Tube
200w, 1.7a, 136v, .5mm Slit Width
25mm Electrode Spacing
1 3/8 in Dia., 4 in Lgh. Outer Jacket
Infrared Spectrometer
11382
11404
8183
8195
6707, Li
5461, Hg
4358, Hg

a

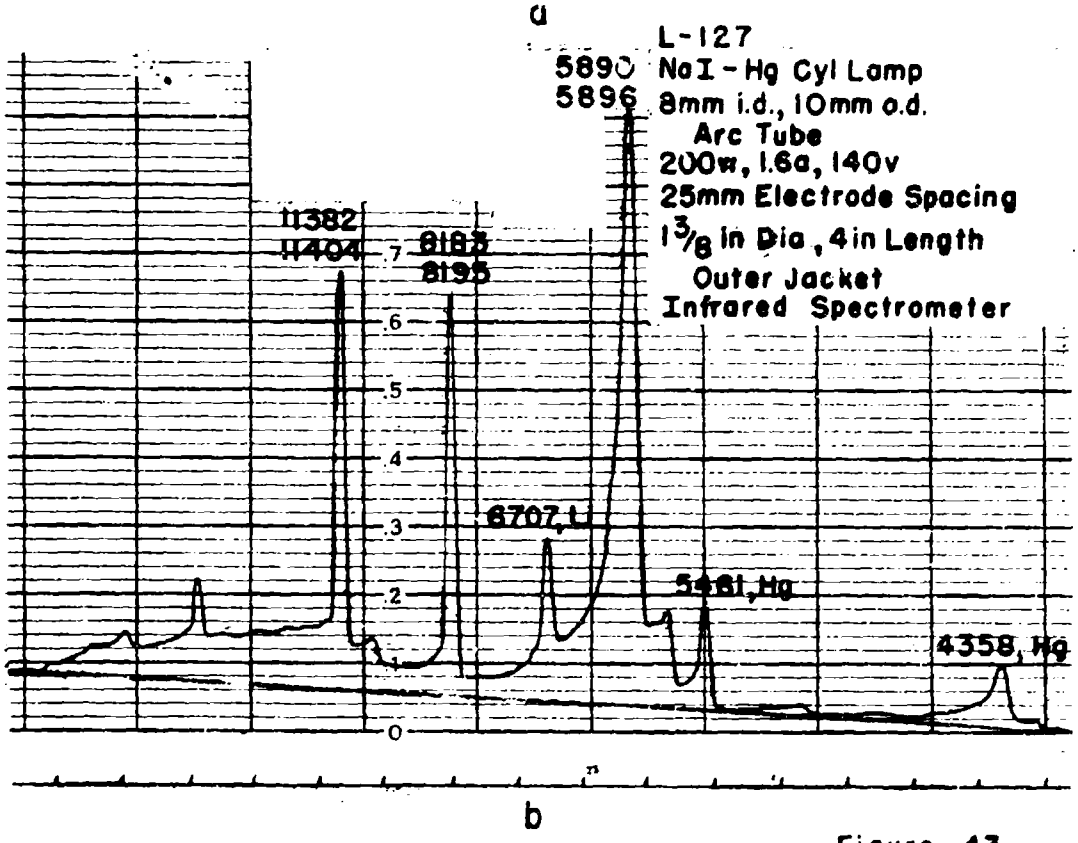
L-127
5890
5896
NaI - Hg Cyl Lamp
8mm i.d., 10mm o.d.
Arc Tube
200w, 1.6a, 140v
25mm Electrode Spacing
1 3/8 in Dia, 4 in Length
Outer Jacket
Infrared Spectrometer
11382
11404
8183
8195
6707, Li
5461, Hg
4358, Hg

b

Figure 43

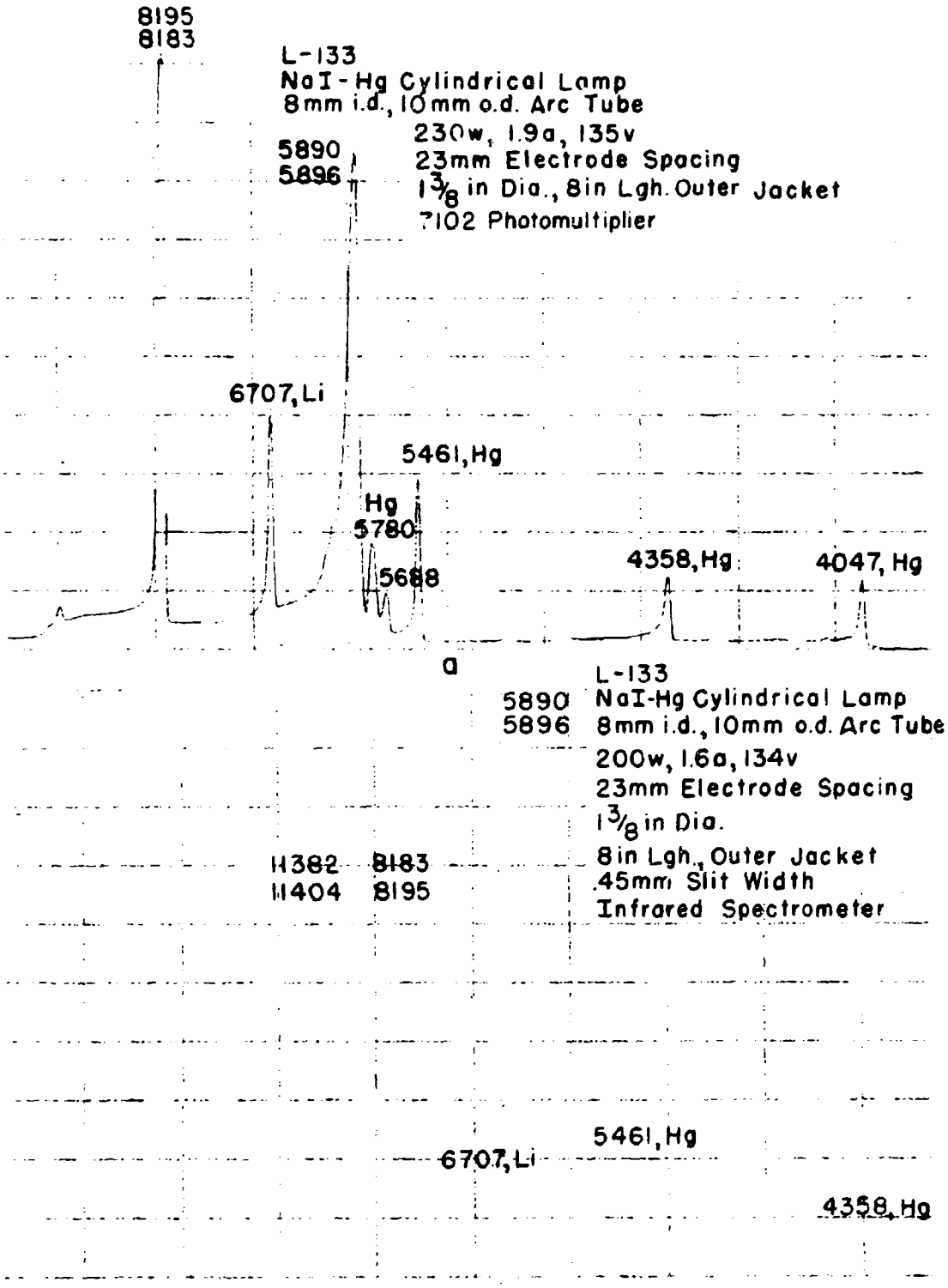
8195
8183
L-133
NaI-Hg Cylindrical Lamp
8mm i.d., 10mm o.d. Arc Tube
230w, 1.9a, 135v
5890
5896
23mm Electrode Spacing
1 3/8 in Dia., 8in Lgh. Outer Jacket
7102 Photomultiplier
6707, Li
5461, Hg
Hg
5780
5688
4358, Hg
4047, Hg
a
L-133
5890
NaI-Hg Cylindrical Lamp
5896
8mm i.d., 10mm o.d. Arc Tube
200w, 1.6a, 134v
23mm Electrode Spacing
1 3/8 in Dia.
8in Lgh., Outer Jacket
11382
8183
.45mm Slit Width
11404
8195
Infrared Spectrometer
5461, Hg
6707, Li
4358, Hg
b

Figure 44

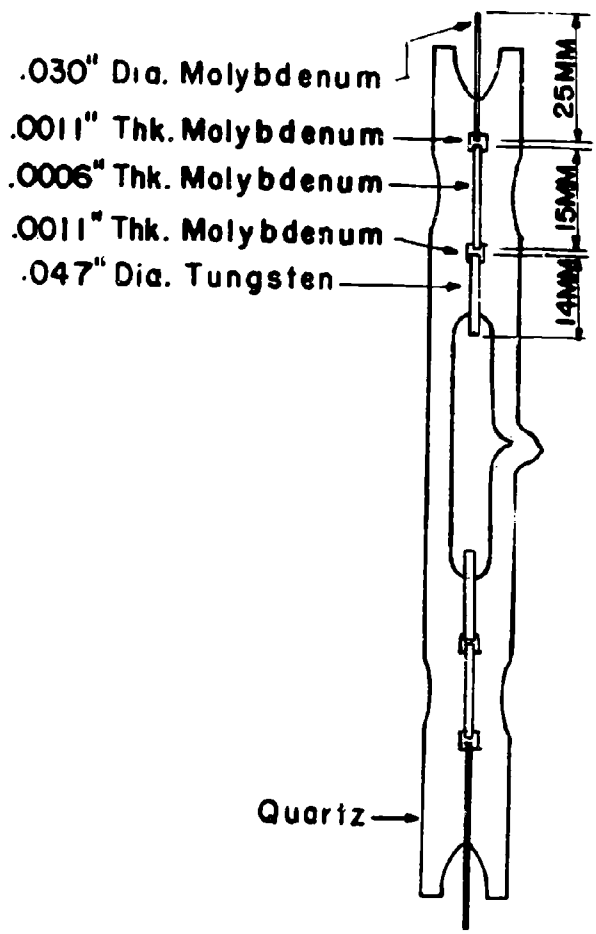

CAPILLARY ARC TUBE

Figure 45

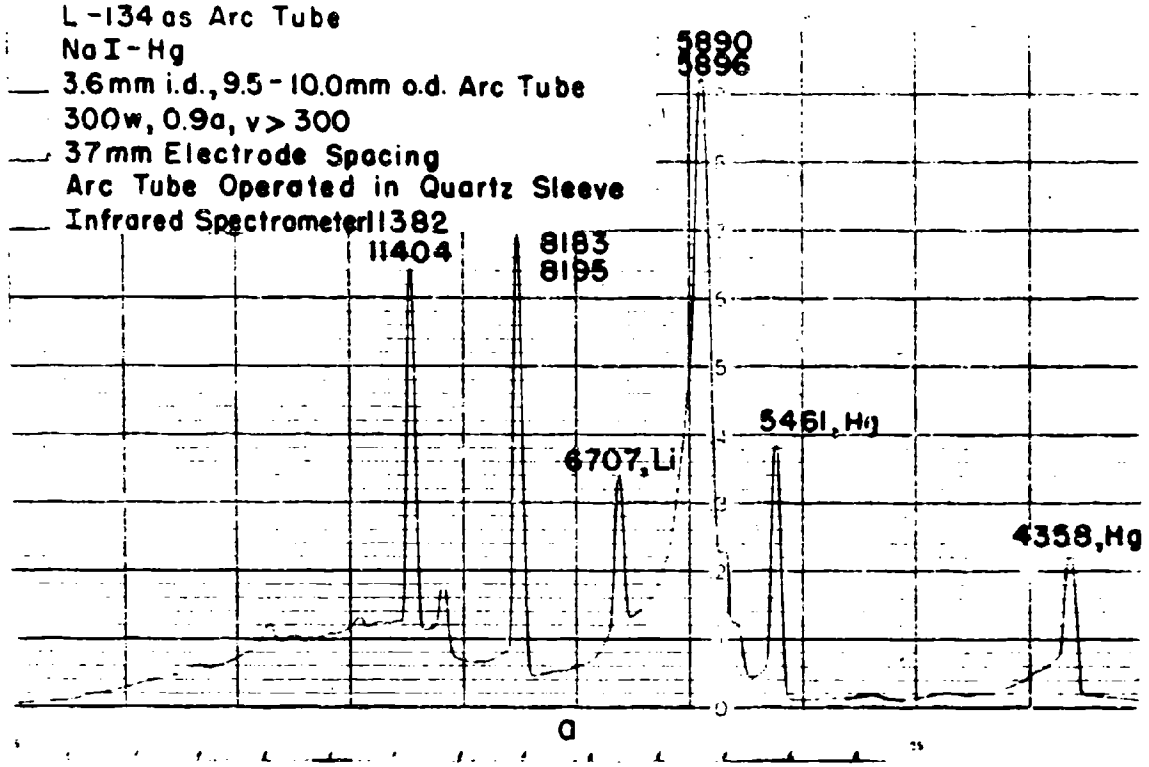
L-134 as Arc Tube
NaI-Hg
3.6mm i.d., 9.5-10.0mm o.d. Arc Tube
300w, 0.9a, v>300
37mm Electrode Spacing
Arc Tube Operated in Quartz Sleeve
Infrared Spectrometer
11382
11404
8183
8195
5890
5896
5461, Hg
6707, Li
4358, Hg

a

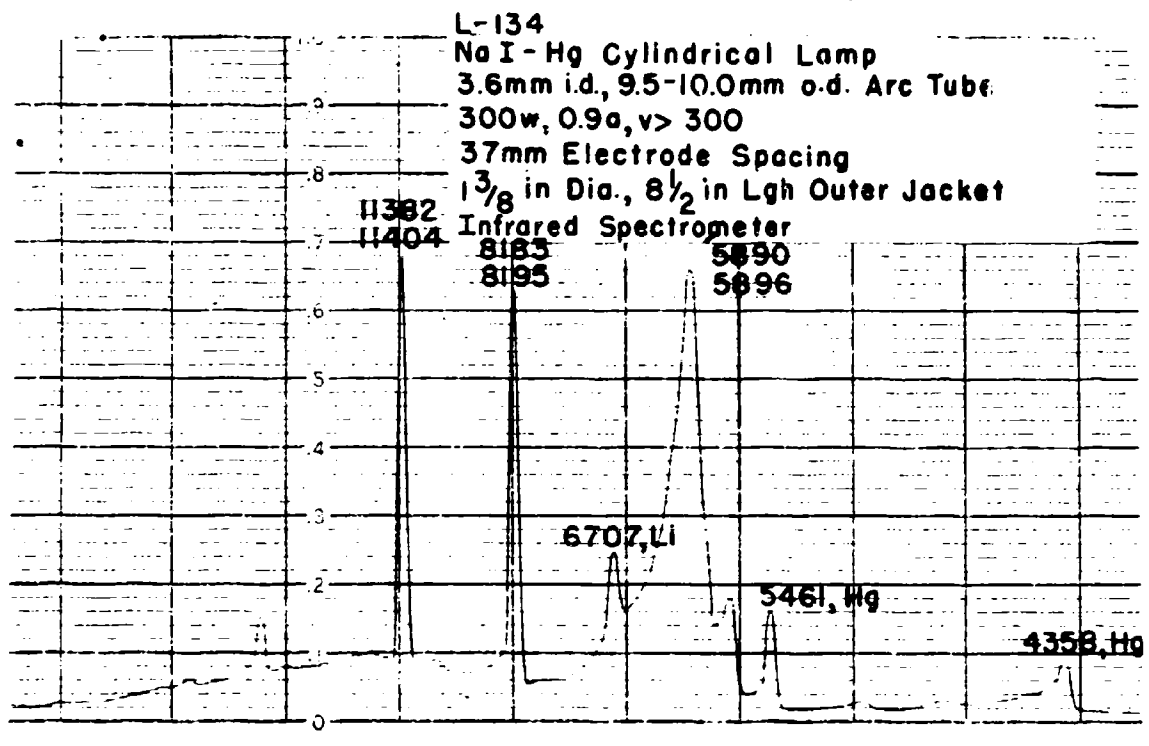
L-134
NaI-Hg Cylindrical Lamp
3.6mm i.d., 9.5-10.0mm o.d. Arc Tube
300w, 0.9a, v>300
37mm Electrode Spacing
1 3/8 in Dia., 8 1/2 in Lgh Outer Jacket
Infrared Spectrometer
11382
11404
8183
8195
5890
5896
6707, Li
5461, Hg
4358, Hg

b

Figure 46

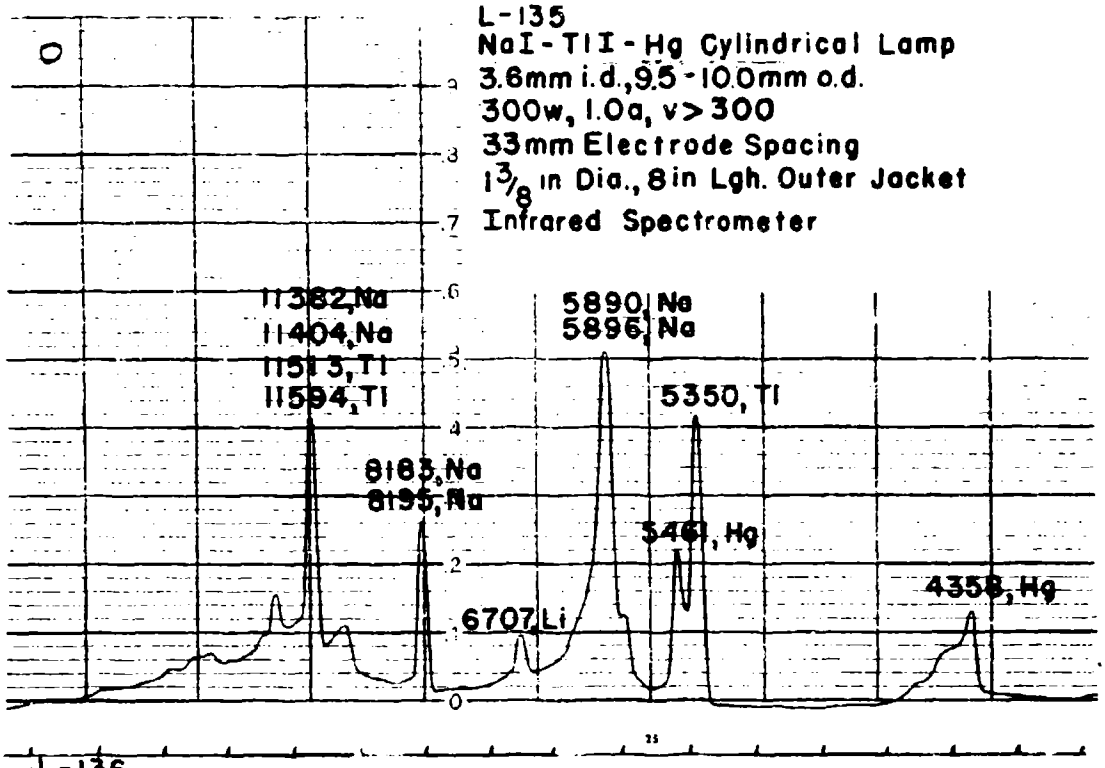
L-135
NaI-TlI-Hg Cylindrical Lamp
3.6mm i.d., 9.5-10.0mm o.d.
300w, 1.0a, v>300
33mm Electrode Spacing
1 3/8 in Dia., 8in Lgh. Outer Jacket
Infrared Spectrometer
11382,Na
11404,Na
11513,Tl
11594,Tl
8183,Na
8195,Na
6707,Li
5890,Na
5896,Na
5461,Hg
5350,Tl
4358,Hg
a

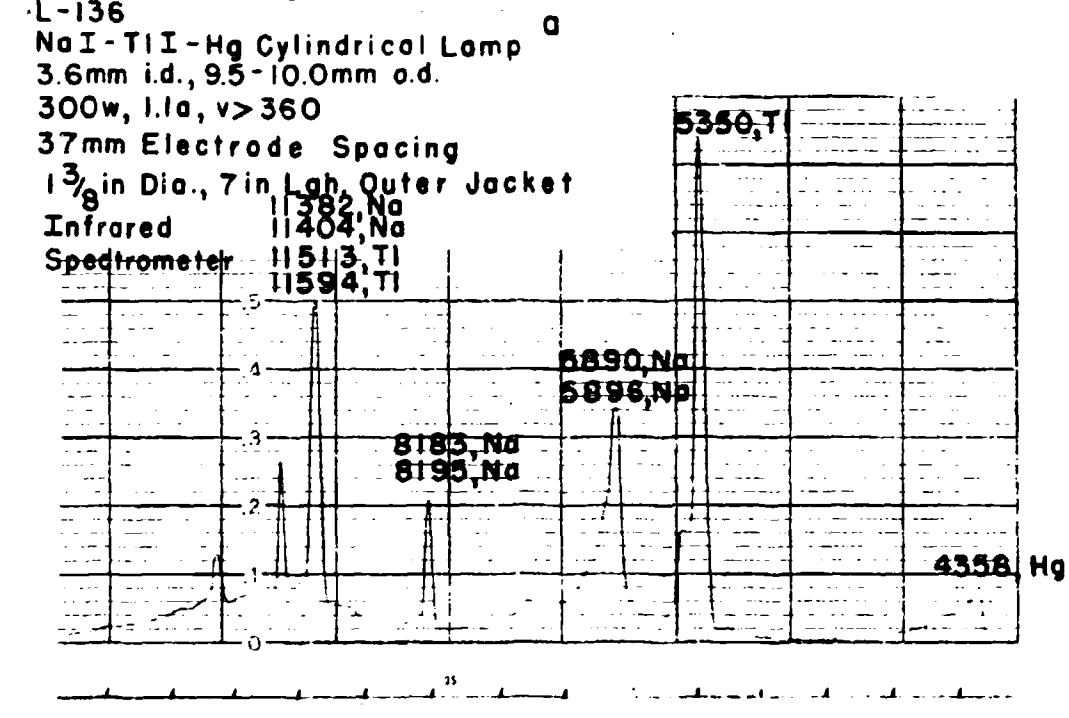
L-136
NaI-TlI-Hg Cylindrical Lamp
3.6mm i.d., 9.5-10.0mm o.d.
300w, 1.1a, v>360
37mm Electrode Spacing
1 3/8 in Dia., 7in Lgh. Outer Jacket
Infrared Spectrometer
11382,Na
11404,Na
11513,Tl
11594,Tl
8183,Na
8195,Na
5890,Na
5896,Na
5350,Tl
4358,Hg
b

Figure 47

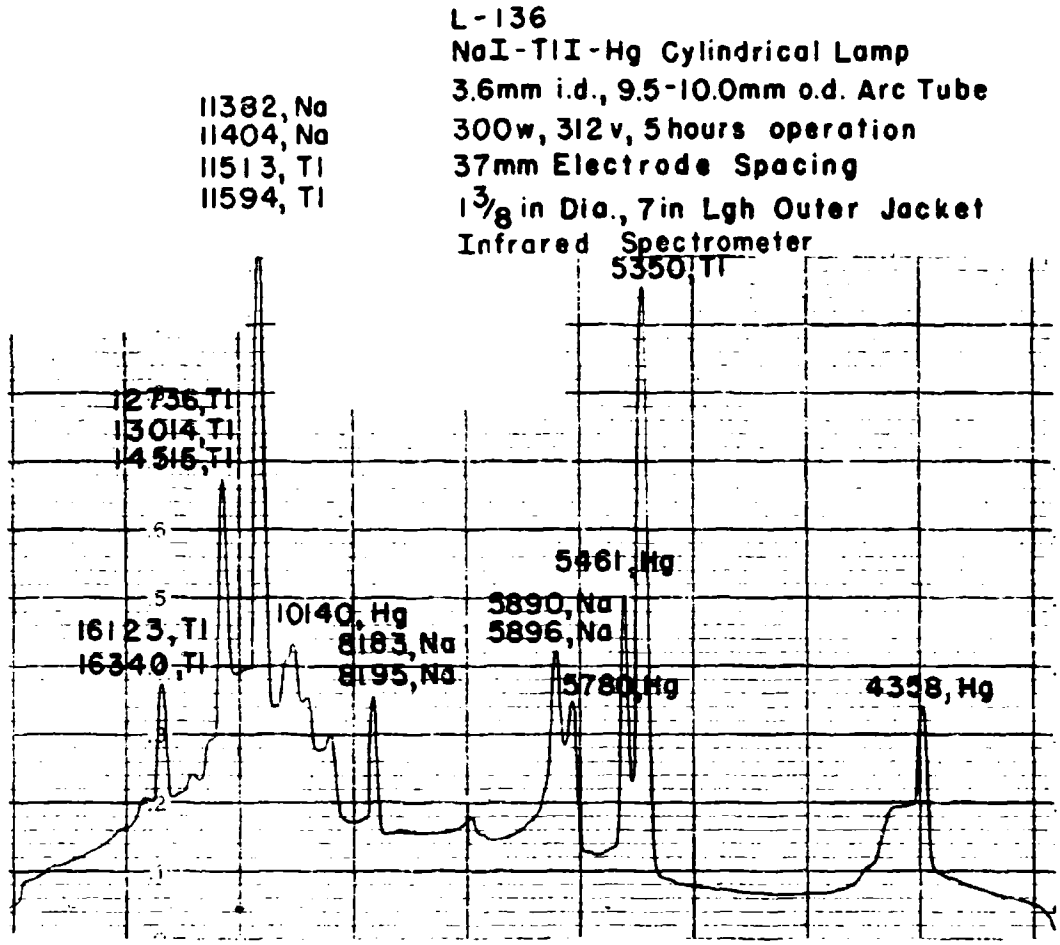
L-136
NaI-TlI-Hg Cylindrical Lamp
3.6mm i.d., 9.5-10.0mm o.d. Arc Tube
300w, 312v, 5 hours operation
37mm Electrode Spacing
1 3/8 in Dia., 7in Lgh Outer Jacket
Infrared Spectrometer
11382, Na
11404, Na
11513, Tl
11594, Tl
5350, Tl
12736, Tl
13014, Tl
14516, Tl
5461, Hg
10140, Hg
8183, Na
8195, Na
3890, Na
5896, Na
16123, Tl
16340, Tl
5780, Hg
4358, Hg
6
5
2
1

Figure 48

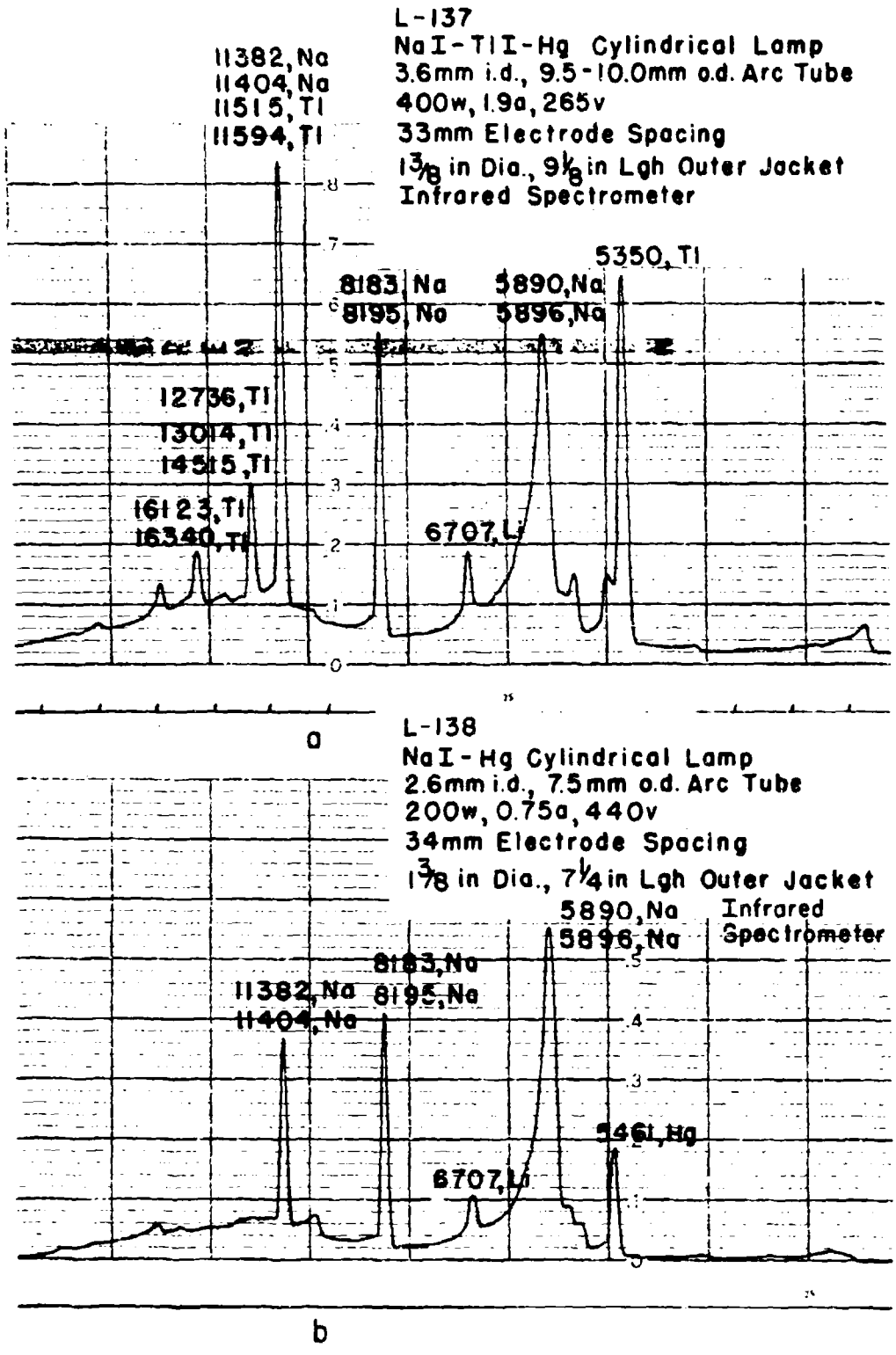
L-137
NaI-TlI-Hg Cylindrical Lamp
3.6mm i.d., 9.5-10.0mm o.d. Arc Tube
400w, 1.9a, 265v
33mm Electrode Spacing
13/8 in Dia., 9 1/8 in Lgh Outer Jacket
Infrared Spectrometer
11382, Na
11404, Na
11515, Tl
11594, Tl
8183, Na
8195, Na
5890, Na
5896, Na
5350, Tl
12736, Tl
13014, Tl
14515, Tl
16123, Tl
16340, Tl
6707, Li
a
L-138
NaI-Hg Cylindrical Lamp
2.6mm i.d., 7.5mm o.d. Arc Tube
200w, 0.75a, 440v
34mm Electrode Spacing
1 3/8 in Dia., 7 1/4 in Lgh Outer Jacket
Infrared Spectrometer
5890, Na
5896, Na
8183, Na
8195, Na
11382, Na
11404, Na
5461, Hg
6707, Li
b

Figure 49

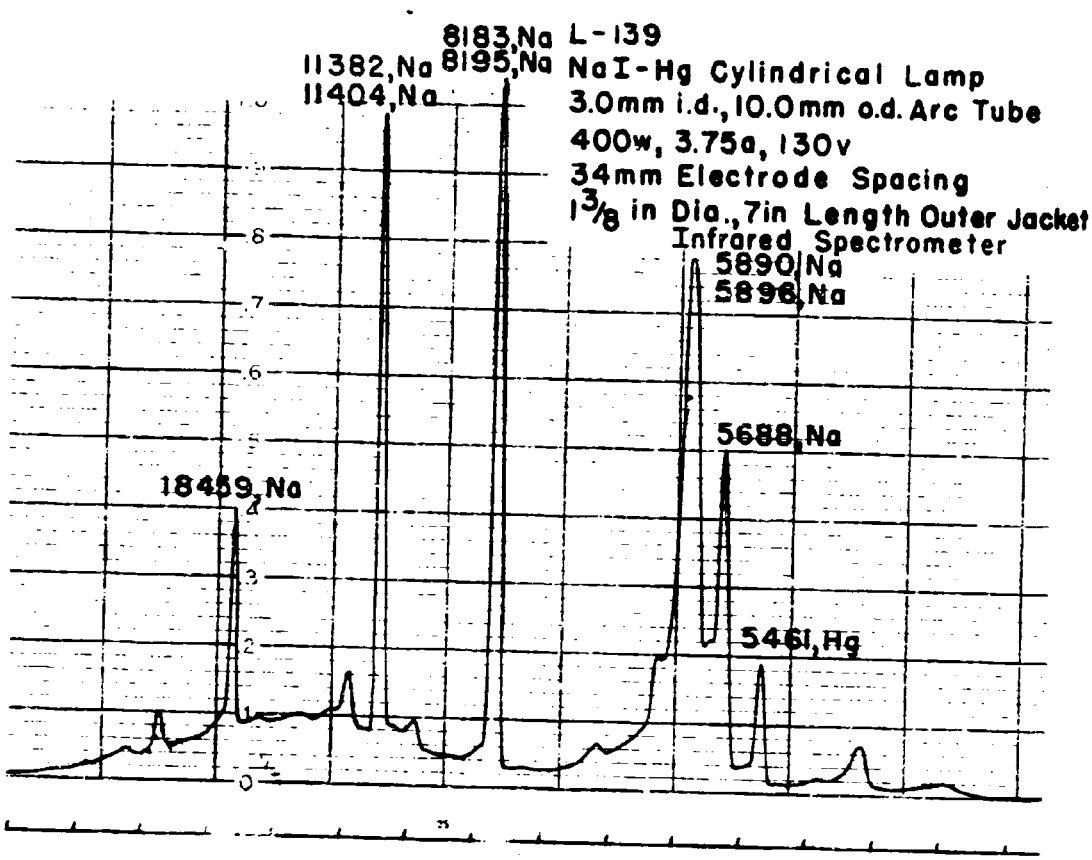
8183,Na
11382,Na
8195,Na
11404,Na
L-139
NaI-Hg Cylindrical Lamp
3.0mm i.d., 10.0mm o.d. Arc Tube
400w, 3.75a, 130v
34mm Electrode Spacing
1 3/8 in Dia., 7in Length Outer Jacket
Infrared Spectrometer
5890,Na
5896,Na
5688,Na
18459,Na
5461,Hg

Figure 50

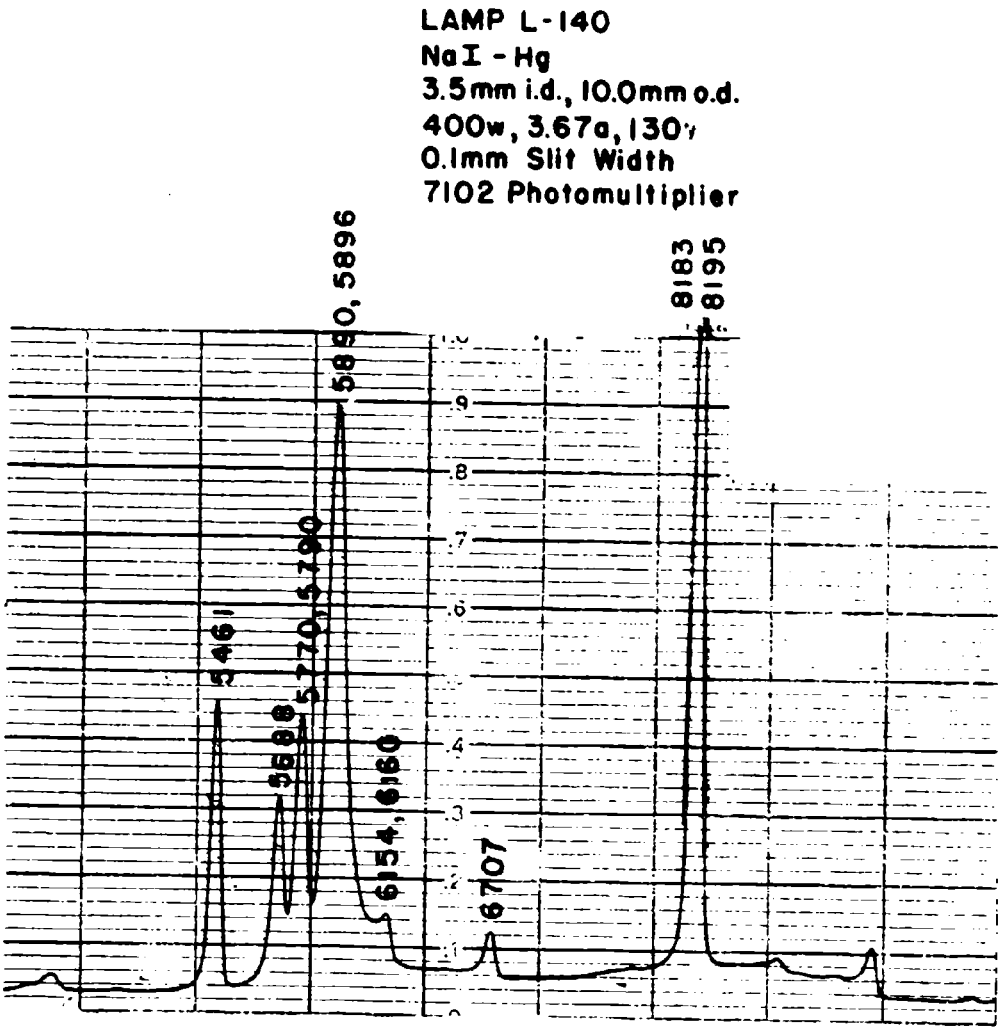
LAMP L-140
NaI - Hg
3.5mm i.d., 10.0mm o.d.
400w, 3.67a, 130v
0.1mm Slit Width
7102 Photomultiplier
5890, 5896
8183
8195
5461
5688
5770, 5790
6154, 6180
6707
.9
.8
.7
.6
.4
.3
.2
.1

Figure 51

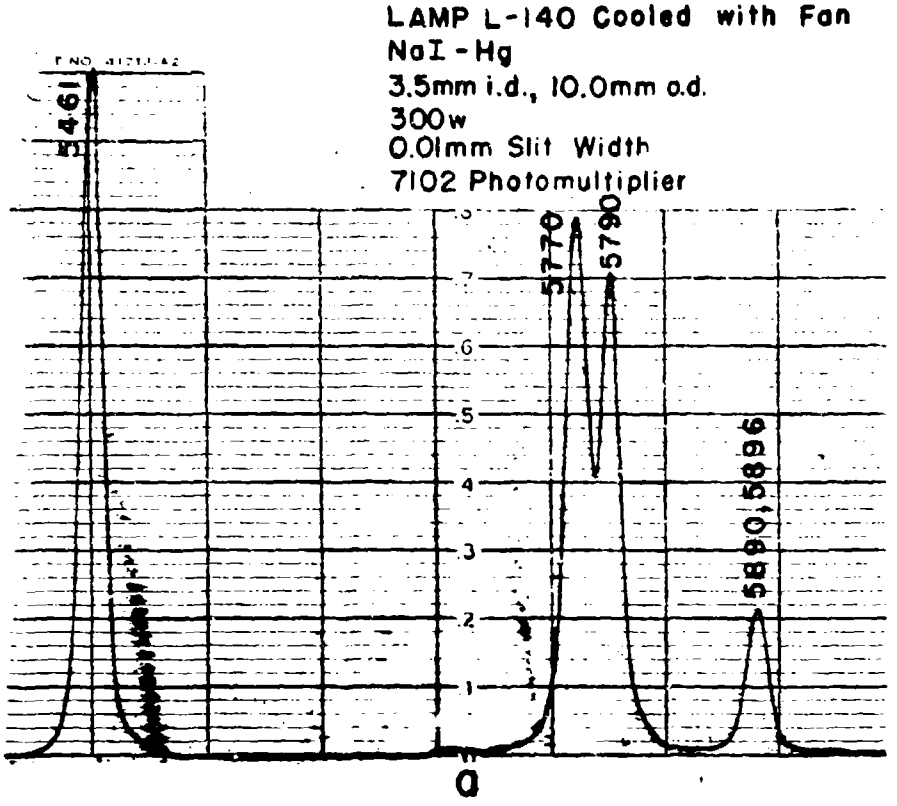
LAMP L-140 Cooled with Fan
NaI - Hg
3.5mm i.d., 10.0mm o.d.
300w
0.01mm Slit Width
7102 Photomultiplier
5461
5770
5790
5890, 5896
a

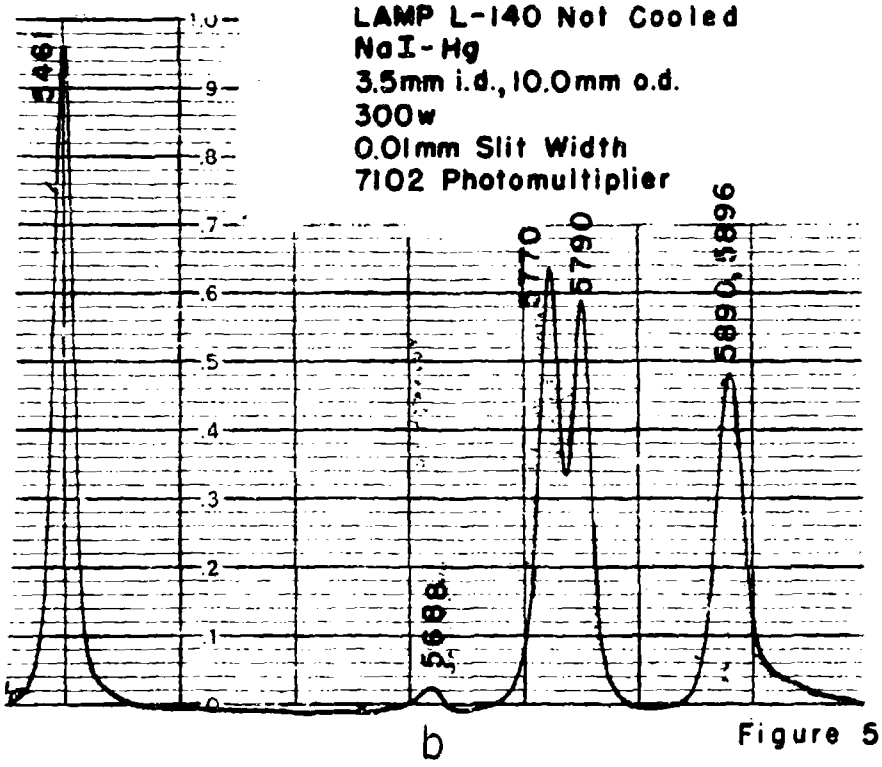
LAMP L-140 Not Cooled
NaI - Hg
3.5mm i.d., 10.0mm o.d.
300w
0.01mm Slit Width
7102 Photomultiplier
5461
5770
5790
5890, 5896
5688
b

Figure 52

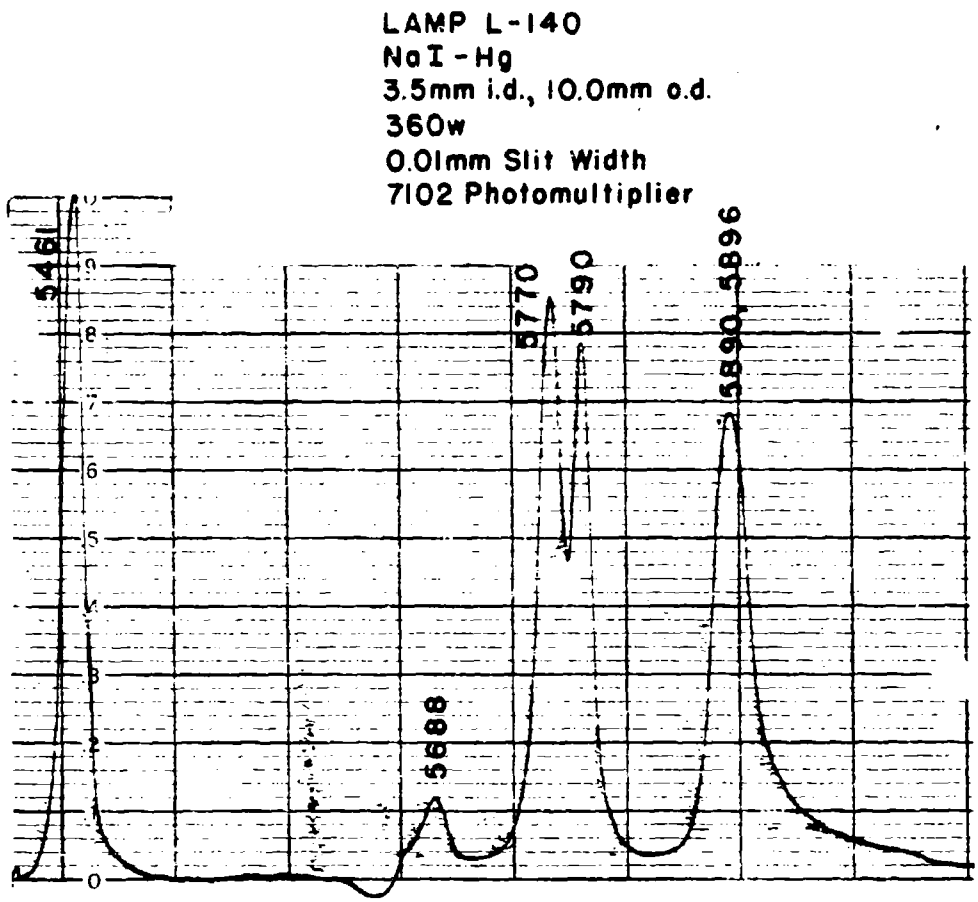
LAMP L-140
NaI - Hg
3.5mm i.d., 10.0mm o.d.
360w
0.01mm Slit Width
7102 Photomultiplier
5461
5770
5790
5890, 5896
5688
9
8
7
6
5
4
3
2
1
0

Figure 53

LAMP L-140
NaI - Hg
3.5mm i.d., 10mm o.d.
0.01mm Slit Width
7102 Photomultiplier

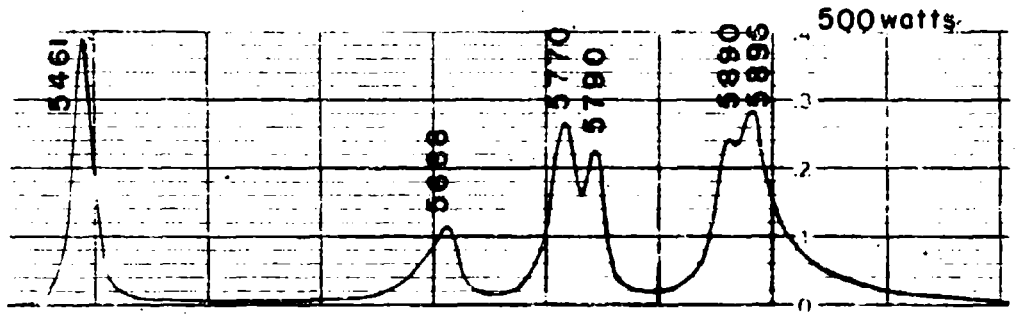

a

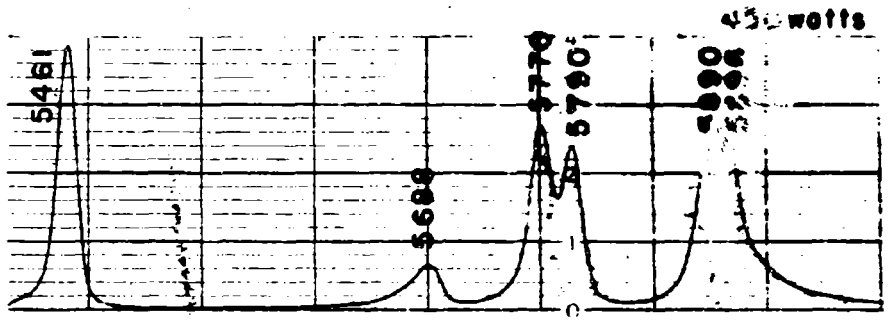

b

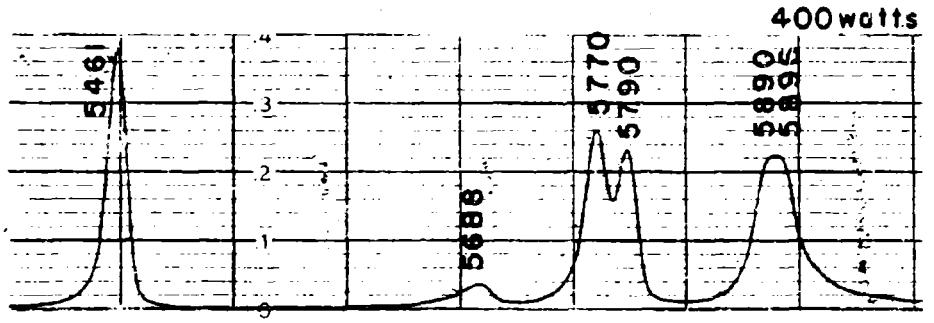

c

Figure 54

LAMP L-144
NaI-Hg
3.5mm i.d., 10.0mm o.d.
0.4mm Slit Width
Infrared Spectrometer

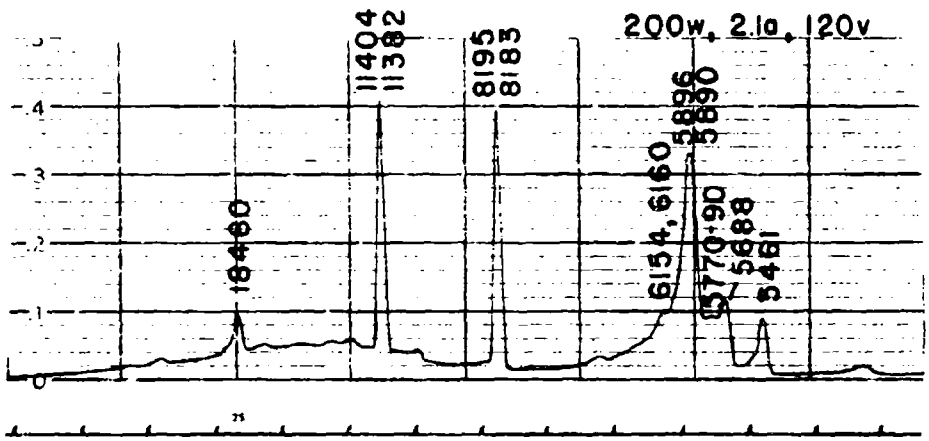

a

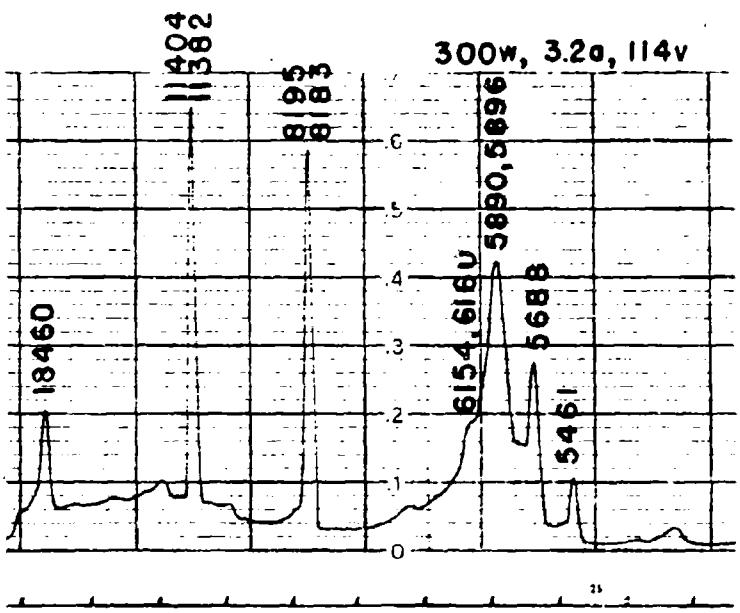

b

Figure 55

LAMP L-144
NaI-Hg
3.5mm i.d., 10.0mm o.d.
0.01mm Slit Width
7102 Photomultiplier

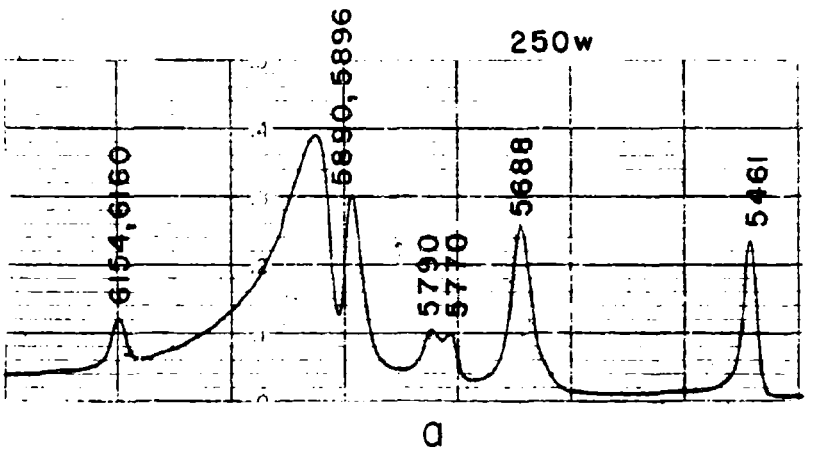

a

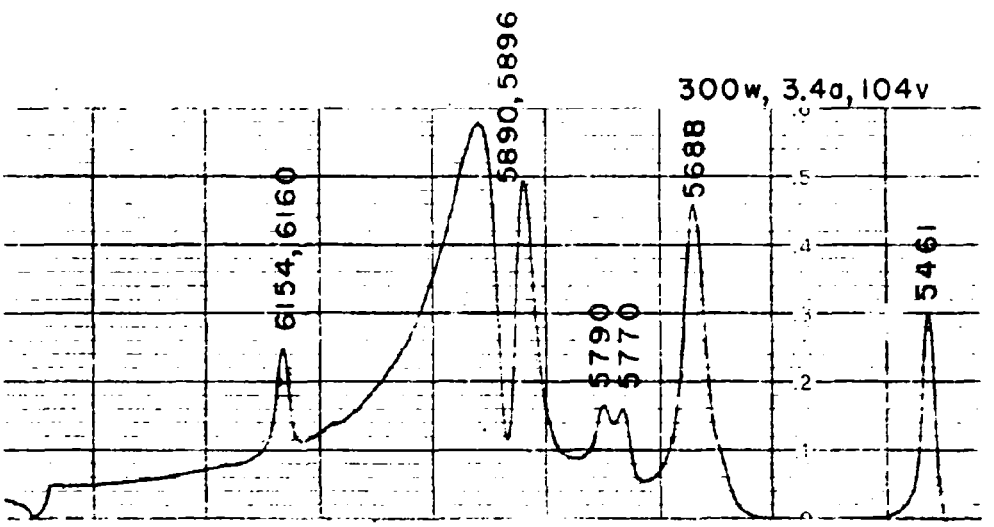

b

Figure 56

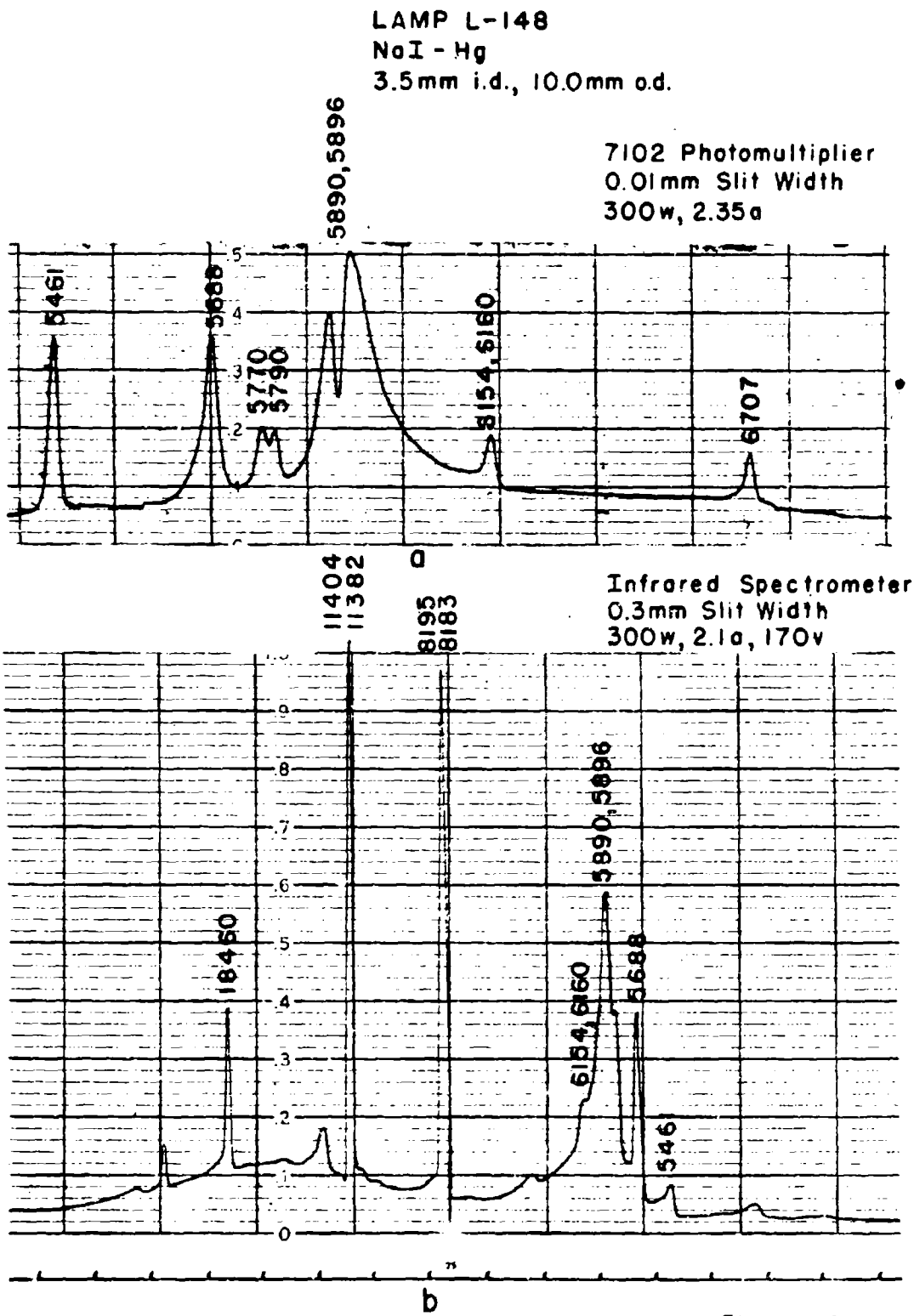
LAMP L-148
NaI - Hg
3.5mm i.d., 10.0mm o.d.
7102 Photomultiplier
0.01mm Slit Width
300w, 2.35a
5890,5896
5461
5688
5770
5790
6154,6160
6707
a
Infrared Spectrometer
0.3mm Slit Width
300w, 2.1a, 170v
11404
11382
8195
8183
18460
5890,5896
6154,6160
5688
5461
b

Figure 57

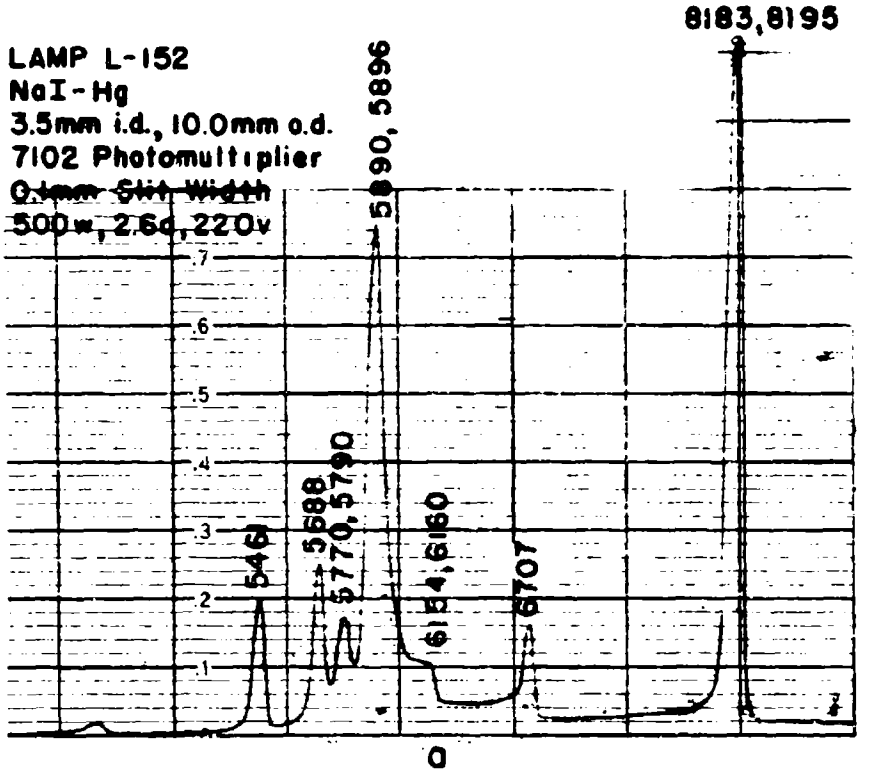
LAMP L-152
NaI - Hg
3.5mm i.d., 10.0mm o.d.
7102 Photomultiplier
0.1mm Slit Width
500w, 2.6a, 220v
8183, 8195
5890, 5896
5770, 5790
5688
5461
6154, 6180
6707
.7
.6
.5
.4
.3
.2
.1

a

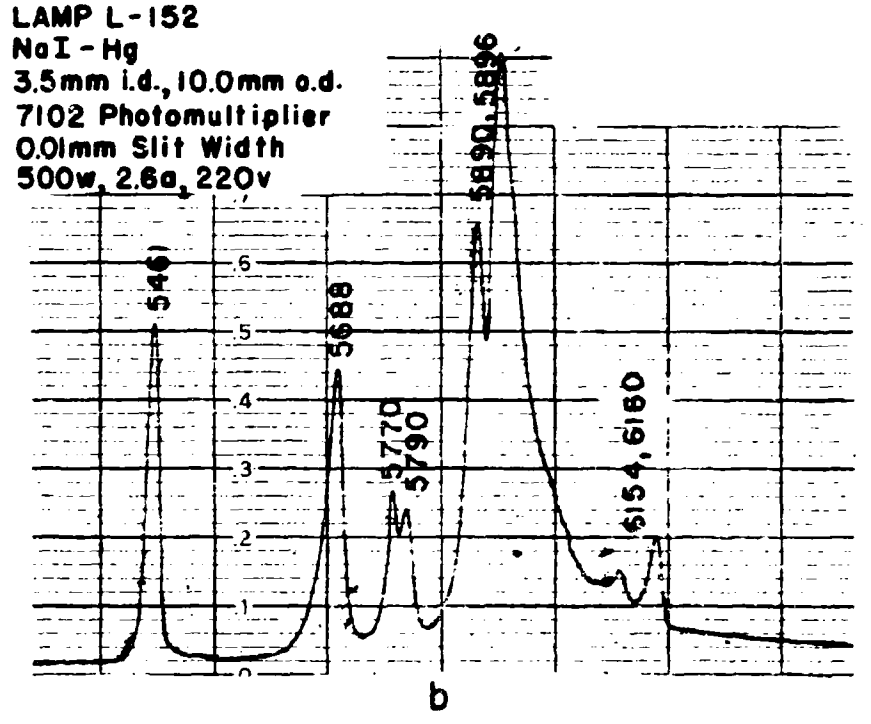
LAMP L-152
NaI - Hg
3.5mm i.d., 10.0mm o.d.
7102 Photomultiplier
0.01mm Slit Width
500w, 2.6a, 220v
5890, 5896
5461
5688
5770
5790
6154, 6180
.6
.5
.4
.3
.2
.1

b

Figure 58

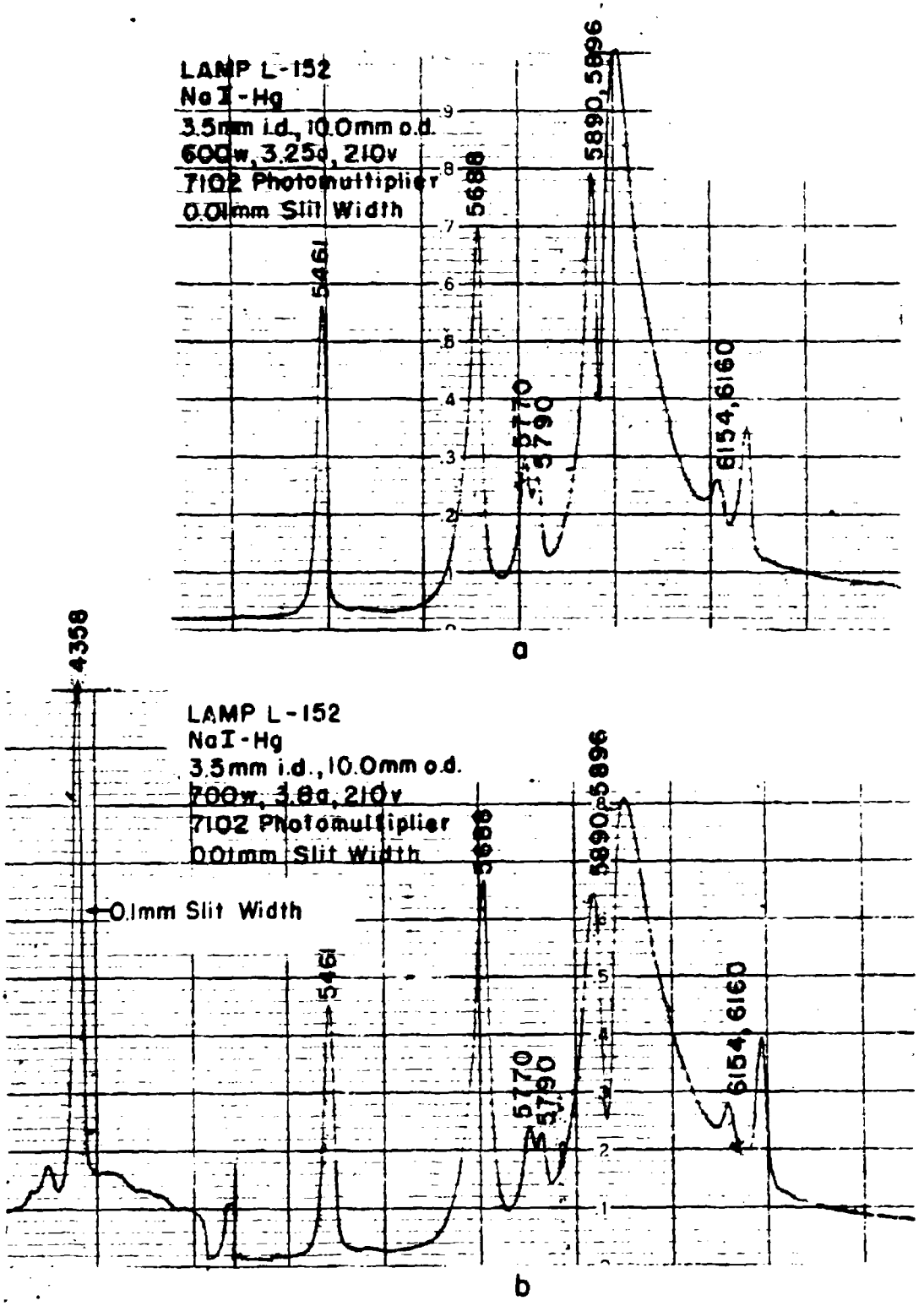
LAMP L-152
NaI-Hg
3.5mm i.d., 10.0mm o.d.
600w, 3.25a, 210v
7102 Photomultiplier
0.01mm Slit Width
5461
5688
5770
5790
5890, 5896
6154, 6160
a
4358
LAMP L-152
NaI-Hg
3.5mm i.d., 10.0mm o.d.
600w, 3.8a, 210v
7102 Photomultiplier
0.01mm Slit Width
0.1mm Slit Width
5461
5688
5770
5790
5890, 5896
6154, 6160
b

Figure 59

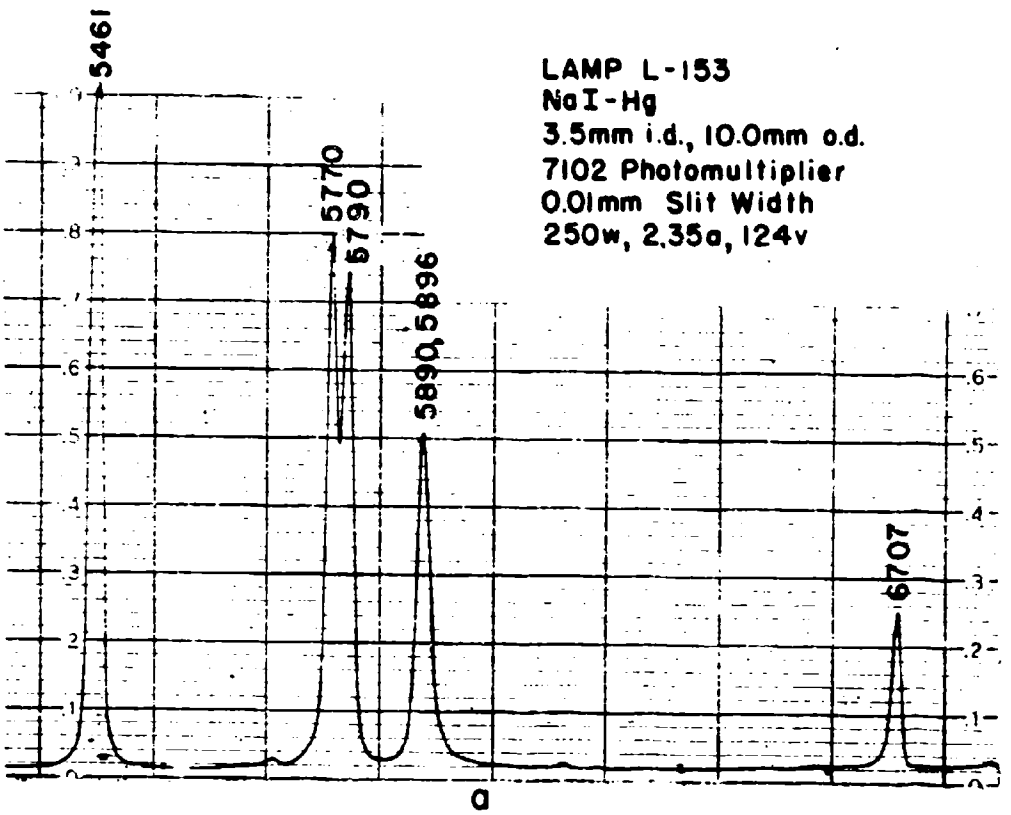
LAMP L-153
NaI-Hg
3.5mm i.d., 10.0mm o.d.
7102 Photomultiplier
0.01mm Slit Width
250w, 2.35a, 124v
5461
5770
5790
5890
5896
6707
a
LAMP L-153
NaI-Hg
3.5mm i.d., 10.0mm o.d.
7102 Photomultiplier
0.01mm Slit Width
400w, 4.25a, 104v
5461
5770
5790
5890
5896
6707
b

Figure 60

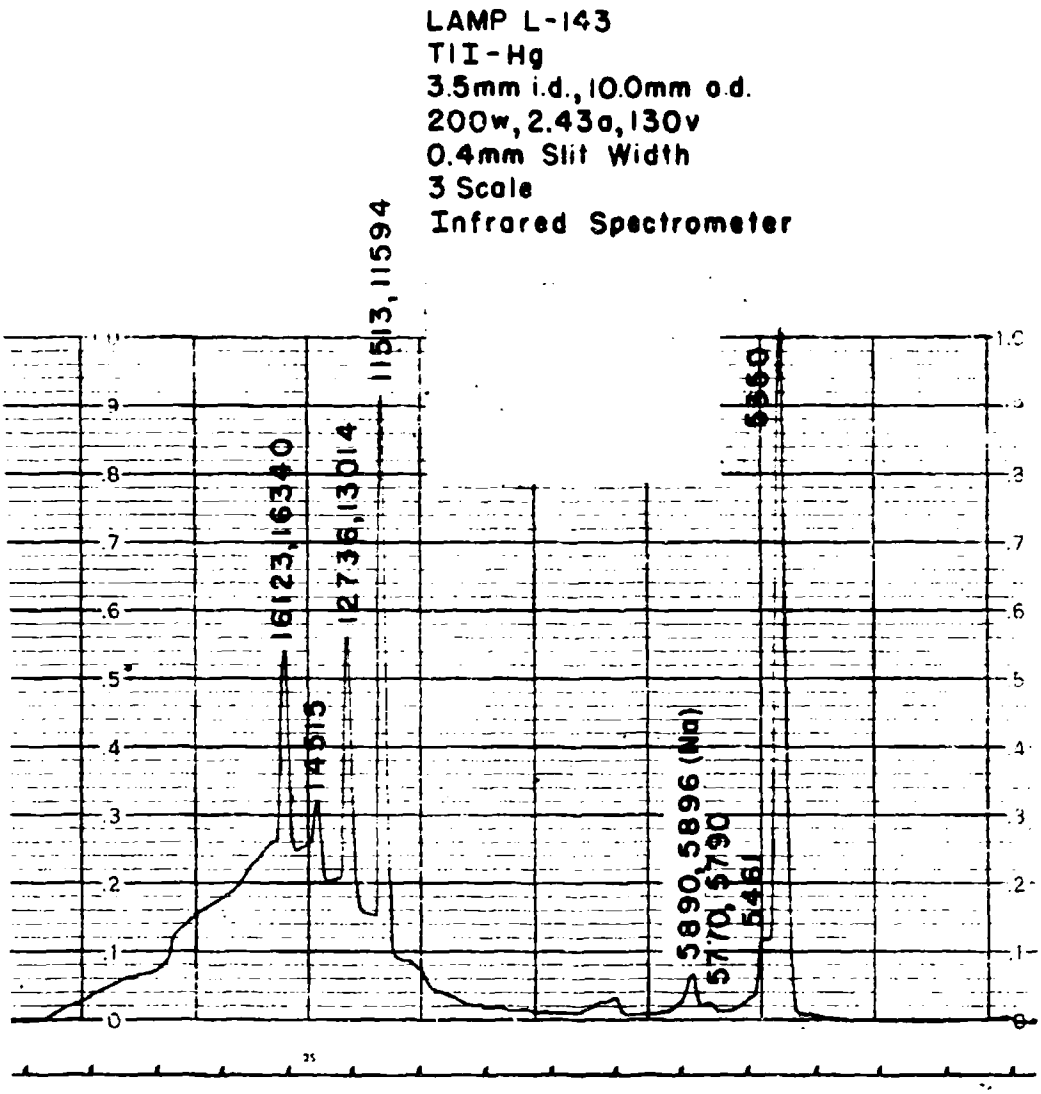
LAMP L-143
TII-Hg
3.5mm i.d., 10.0mm o.d.
200w, 2.43a, 130v
0.4mm Slit Width
3 Scale
Infrared Spectrometer
11513, 11594
16123, 16340
14515
12736, 13014
5890, 5896 (Na)
5770, 5790
5461
4360

Figure 61

LAMP L-145
TII - Hg
3.5mm i.d., 10.0mm o.d.

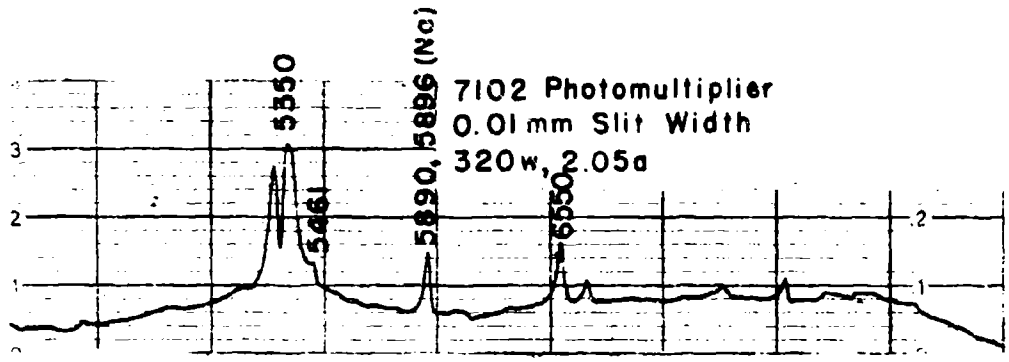

a

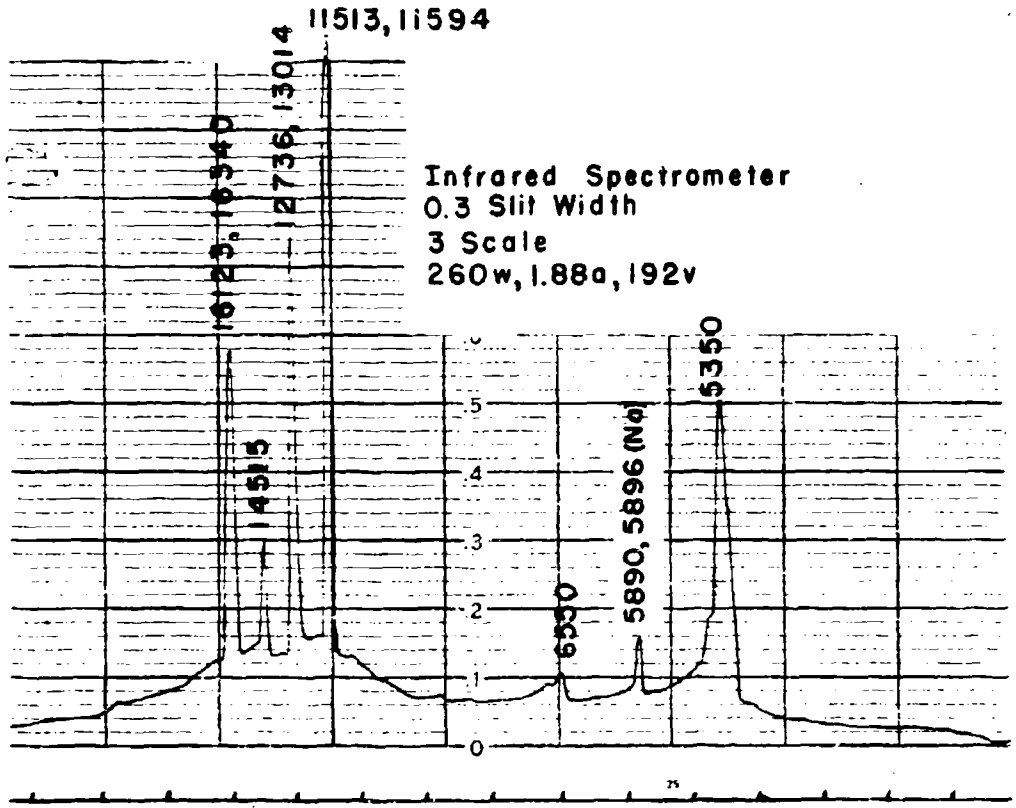

b

Figure 62

LAMP L-145
TlI - Hg
3.5mm i.d., 10.0mm o.d.
0.01 Slit Width
7102 Photomultiplier

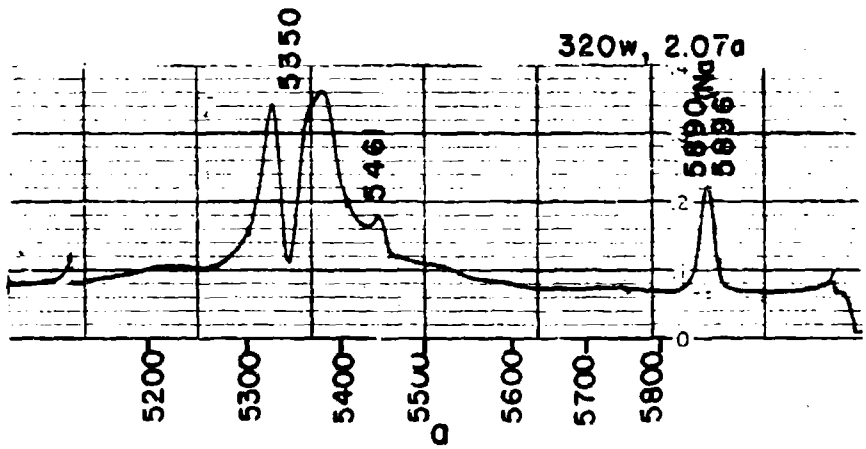

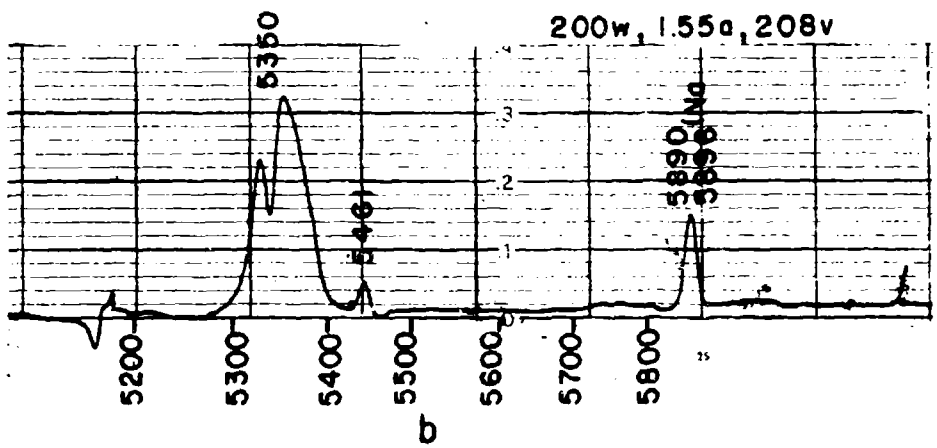

Figure 63

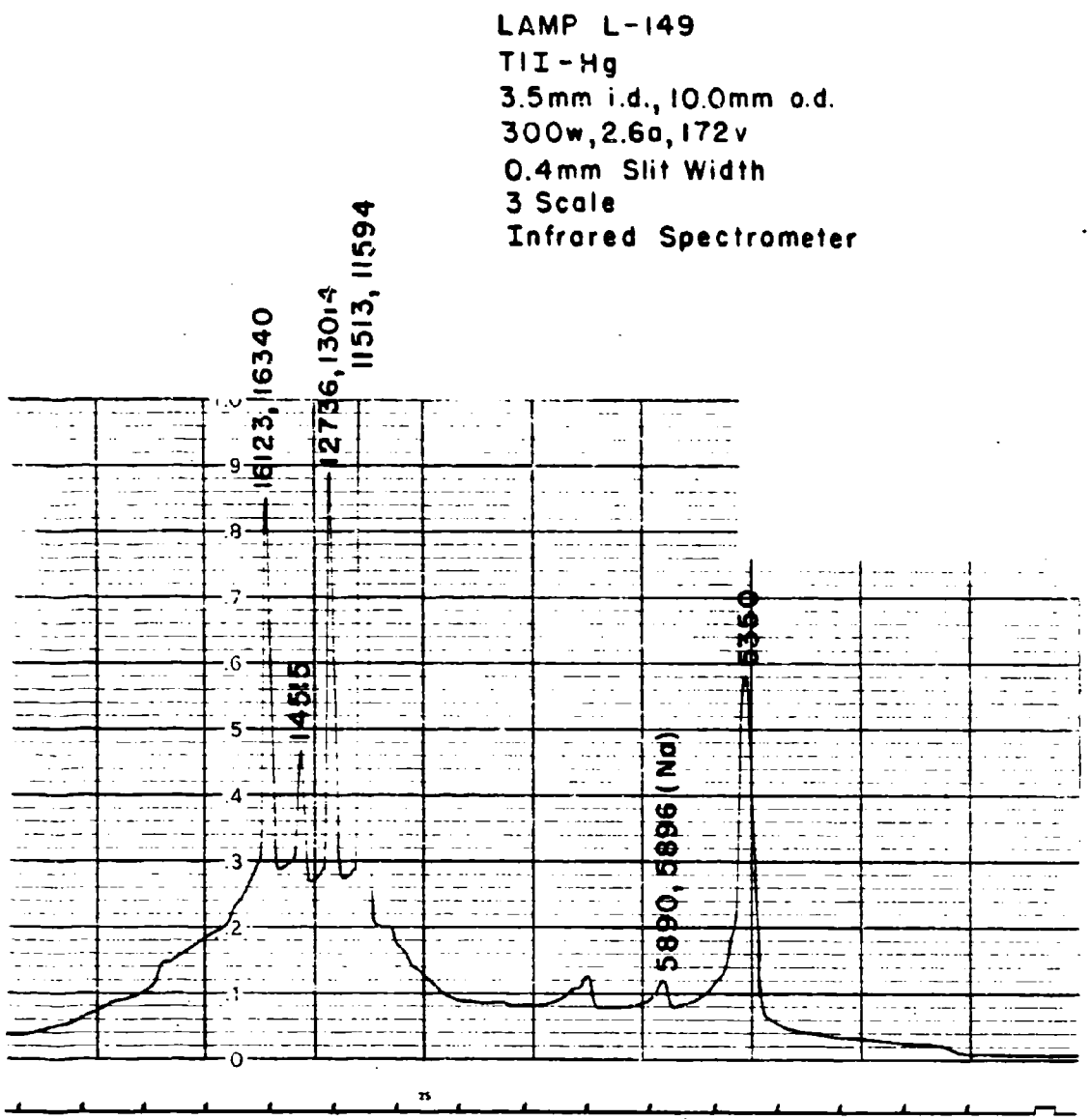
LAMP L-149
TII-Hg
3.5mm i.d., 10.0mm o.d.
300w, 2.6a, 172v
0.4mm Slit Width
3 Scale
Infrared Spectrometer
18123, 16340
12736, 13014
11513, 11594
14515
5350
5890, 5896 (Na)
9
8
7
6
5
4
3
2
1
0

Figure 64

LAMP L-149
TlI-Hg
3.5mm i.d., 10mm o.d.
7102 Photomultiplier

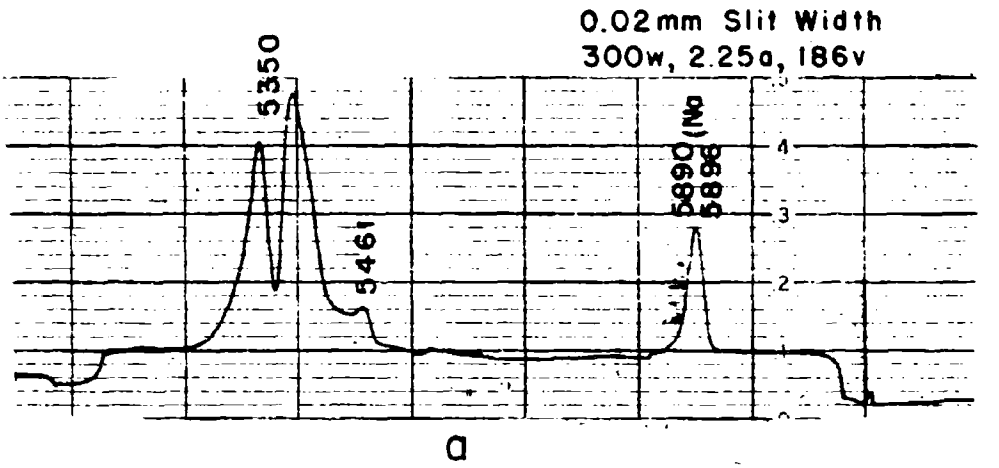

a

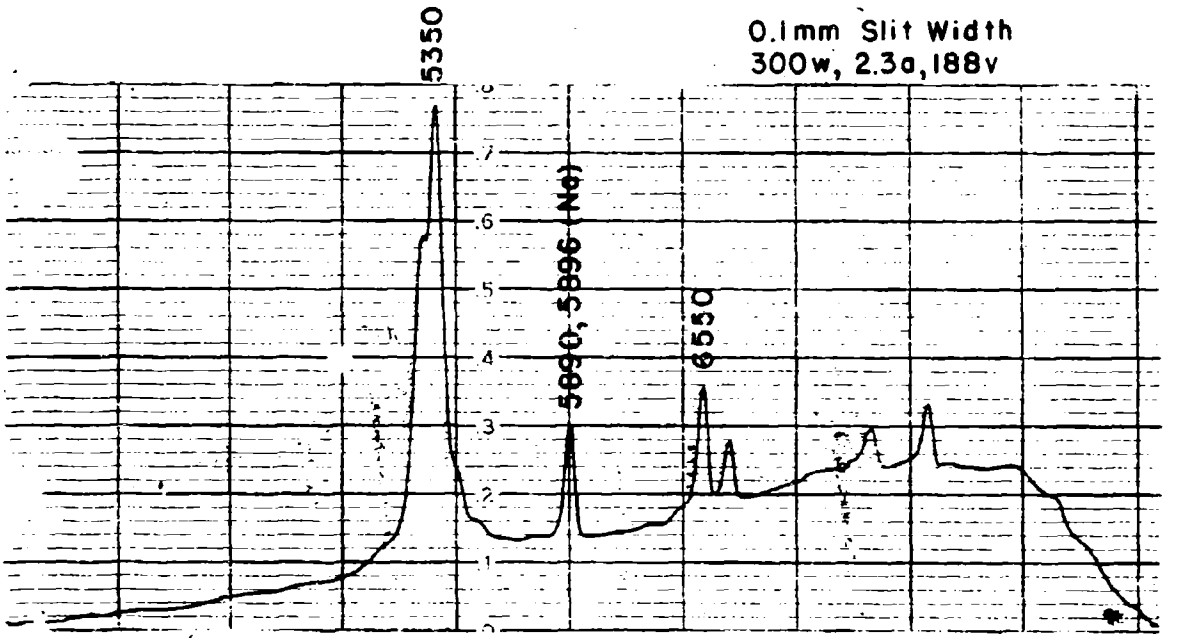

b

Figure 65

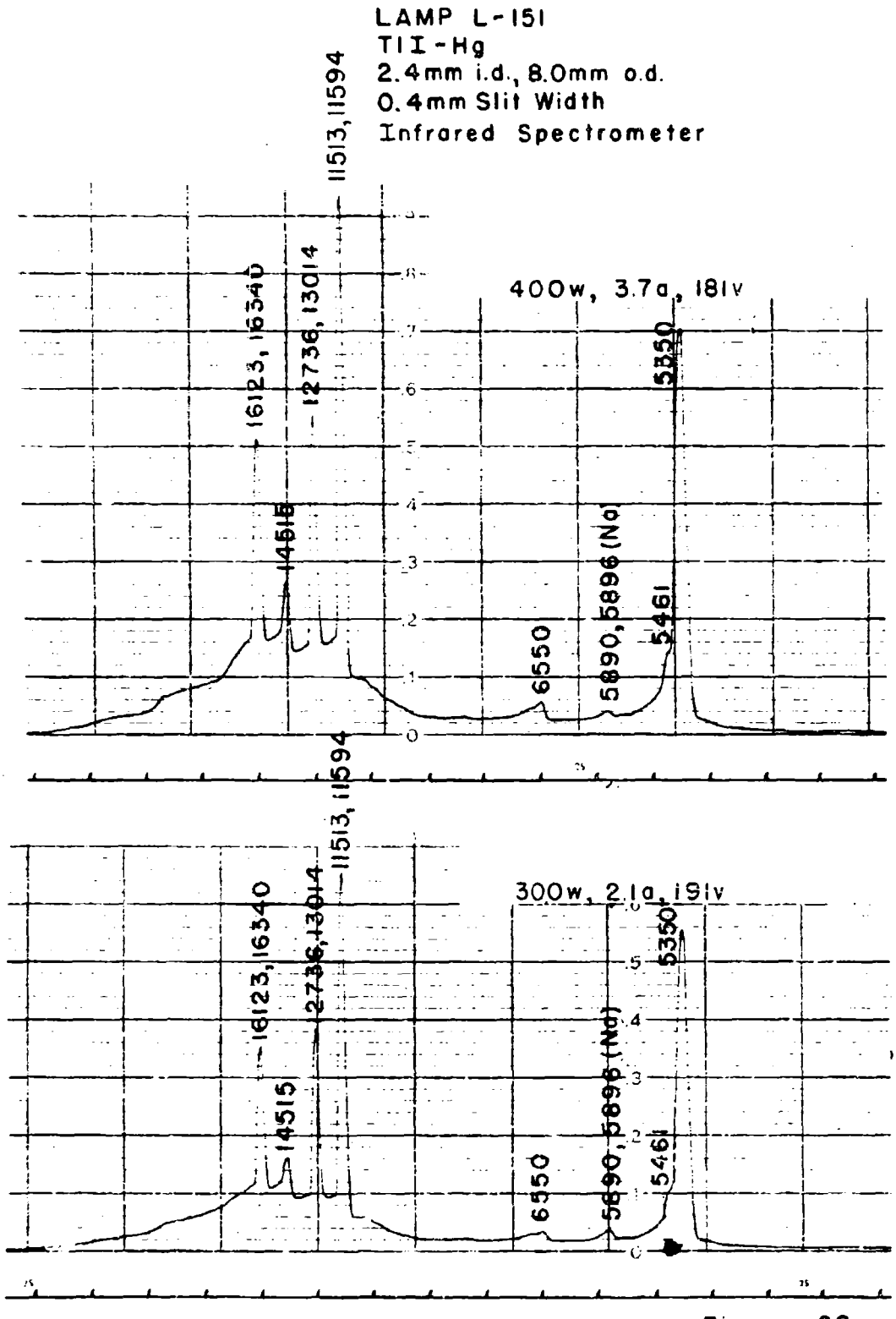
LAMP L-151
TII-Hg
2.4mm i.d., 8.0mm o.d.
0.4mm Slit Width
Infrared Spectrometer
400w, 3.7a, 181v
11513, 11594
16123, 16340
12736, 13014
14515
6550
5890, 5896 (Na)
5461
5350
300w, 2.1a, 191v

Figure 66

LAMP L-151
TlI-Hg
2.4mm i.d., 8.0mm o.d.
0.1mm Slit Width
7102 Photomultiplier

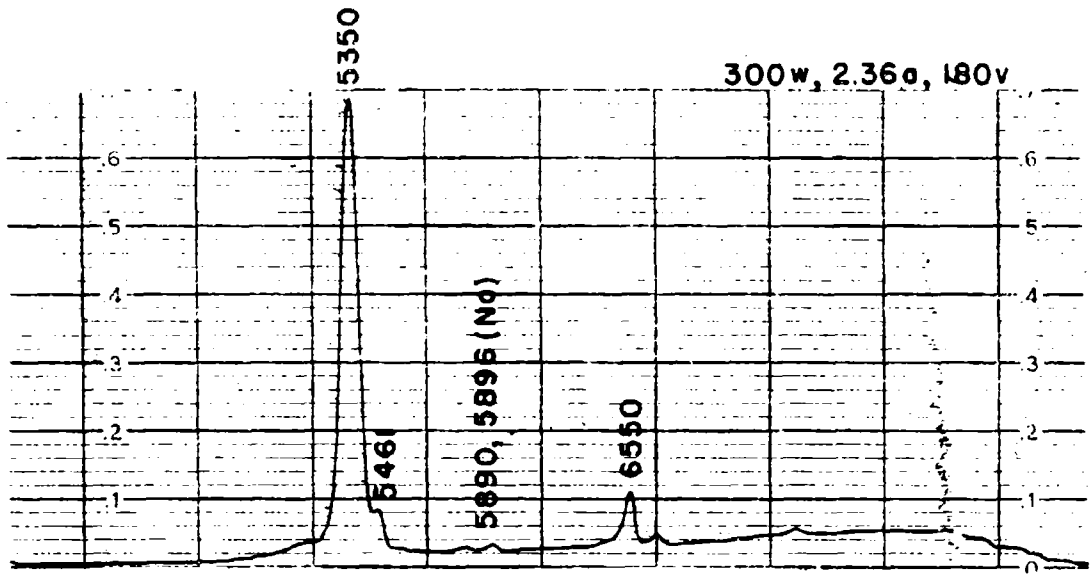

a

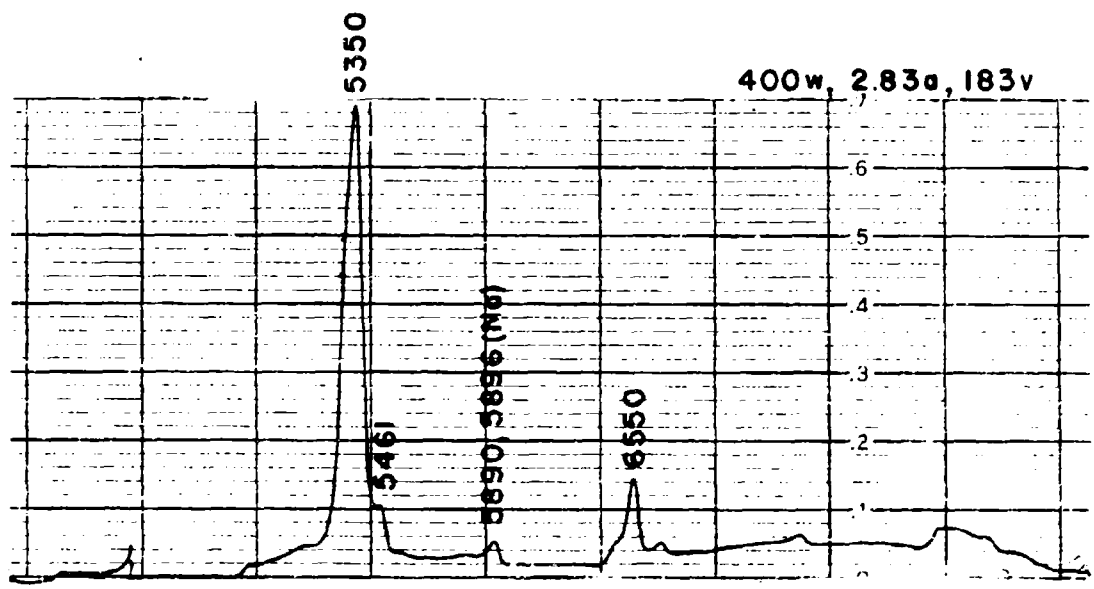

b

Figure 67

LAMP L-151
TlI-Hg
2.4mm i.d., 8.0mm
0.02mm Slit Width
7102 Photomultiplier

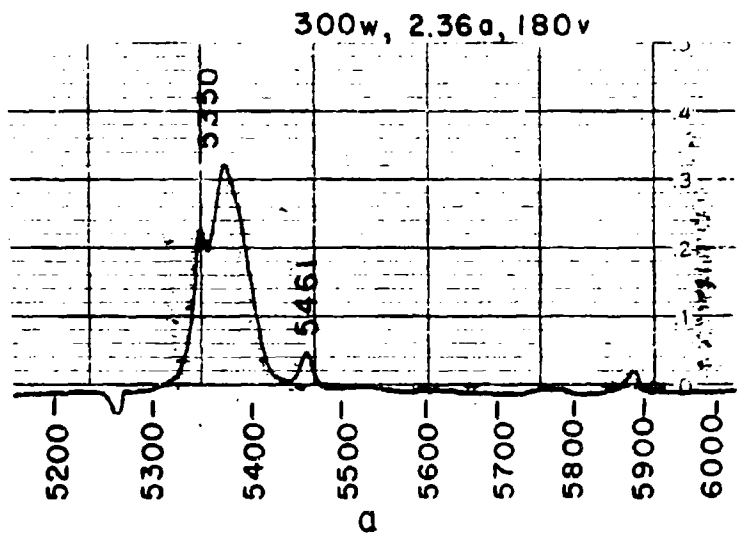

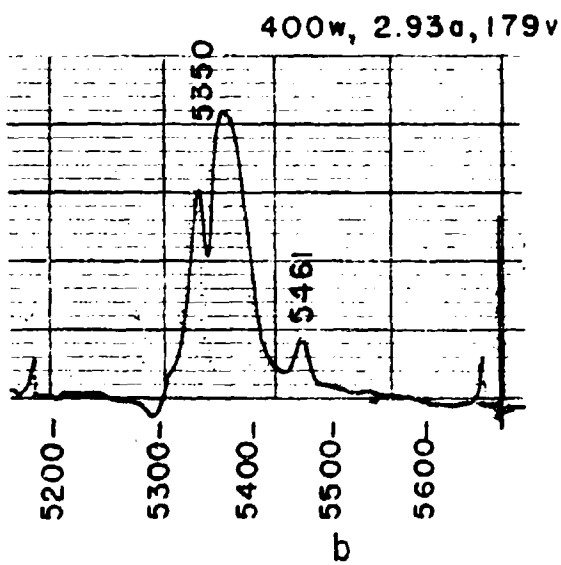

Figure 68

LAMP L-146
Hg
3.5mm i.d., 10.0mm o.d.
300w, 2a, 208v
Infrared Spectrometer

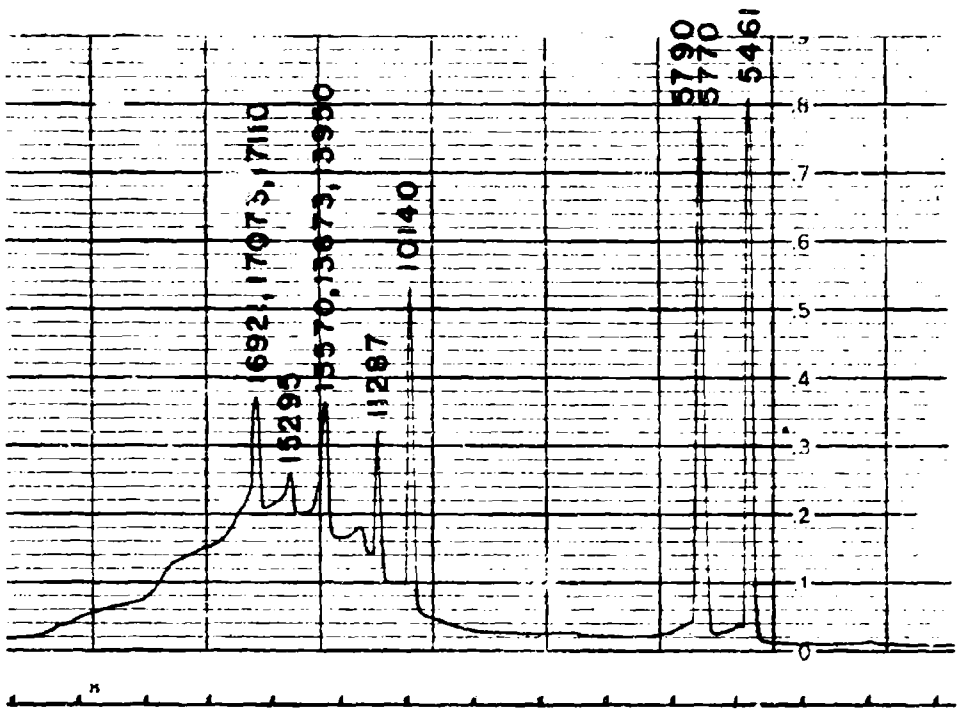

Figure 69

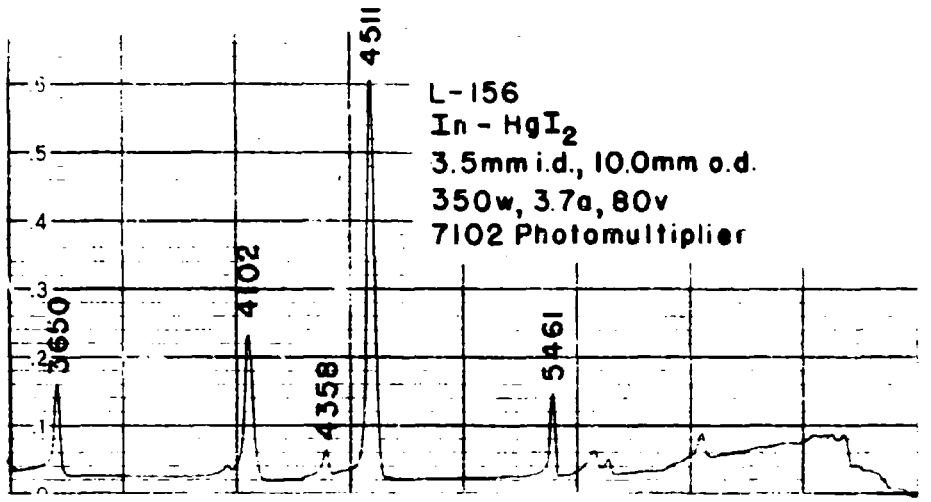
L-156
In - HgI2
3.5mm i.d., 10.0mm o.d.
350w, 3.7a, 80v
7102 Photomultiplier
4511
4102
3650
4358
5461
a

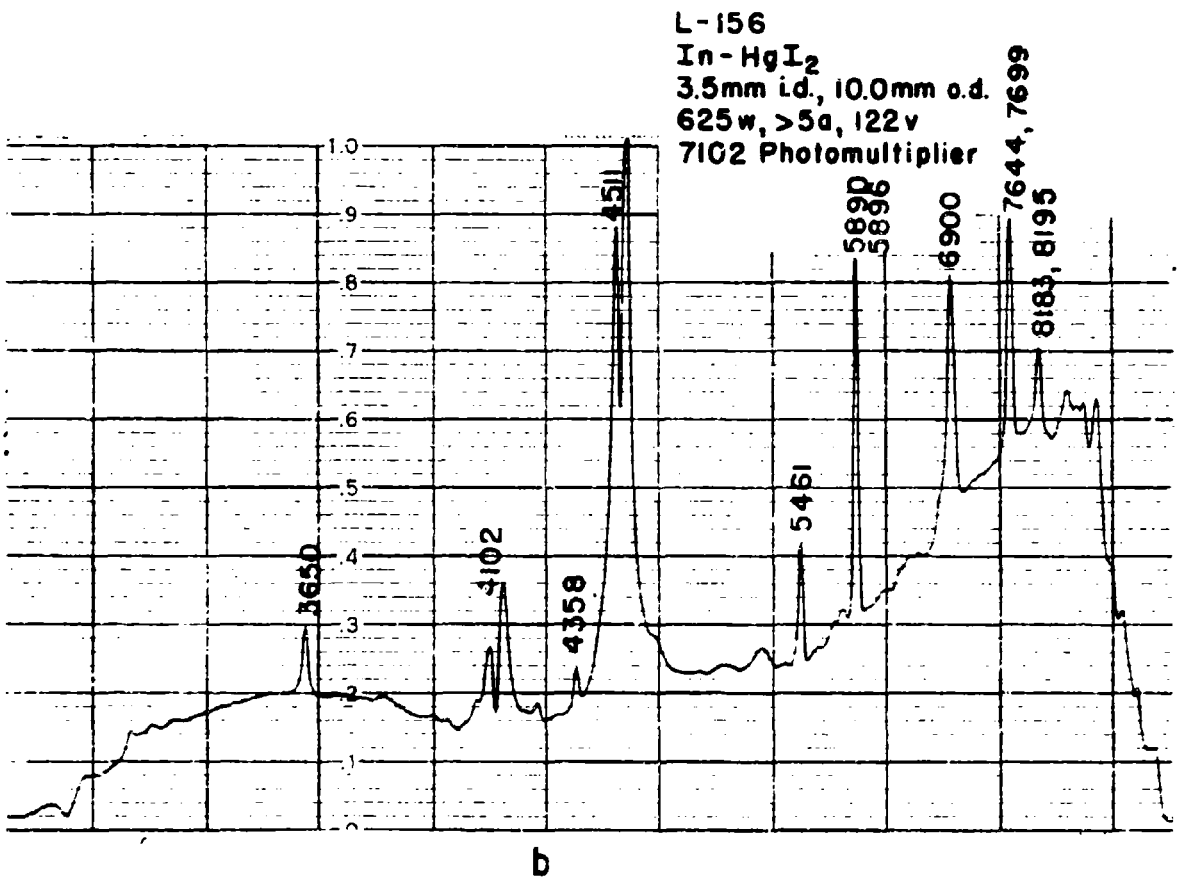
L-156
In - HgI2
3.5mm i.d., 10.0mm o.d.
625w, >5a, 122v
7102 Photomultiplier
4511
5890
5896
6900
7644, 7699
8183, 8195
5461
4102
3650
4358
b

Figure 70

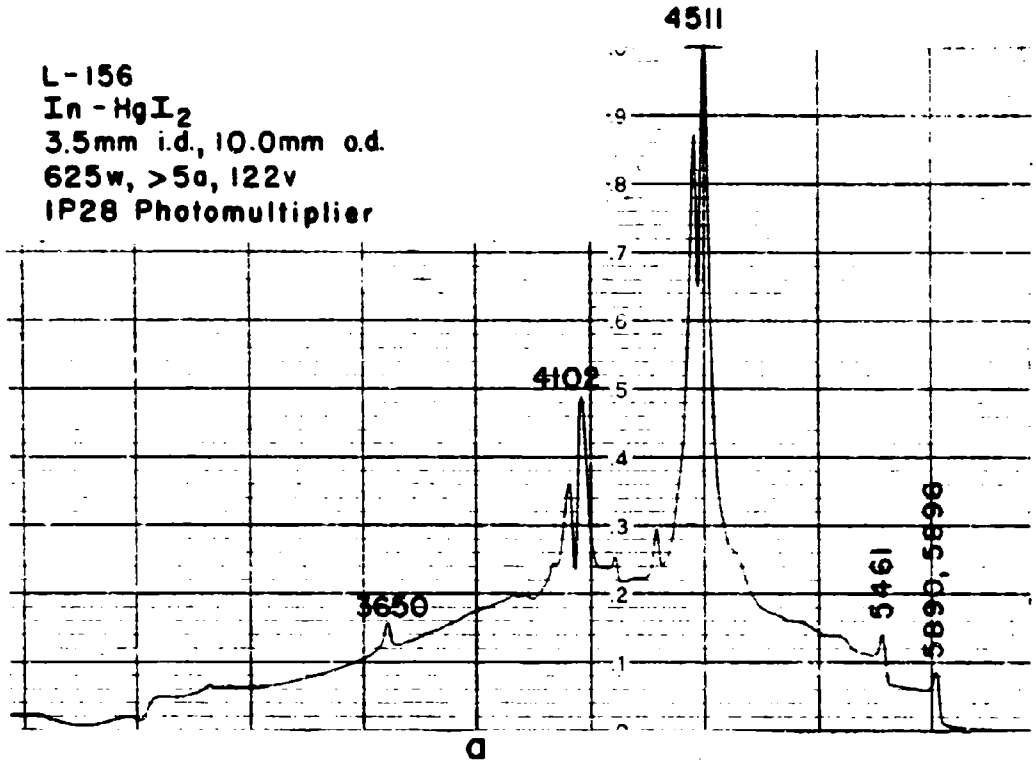
L-156
In - HgI_2
3.5mm i.d., 10.0mm o.d.
625w, >5a, 122v
IP28 Photomultiplier
4511
4102
3650
5461
5890, 5896
.9
.8
.7
.6
.5
.4
.3
.2
.1

a

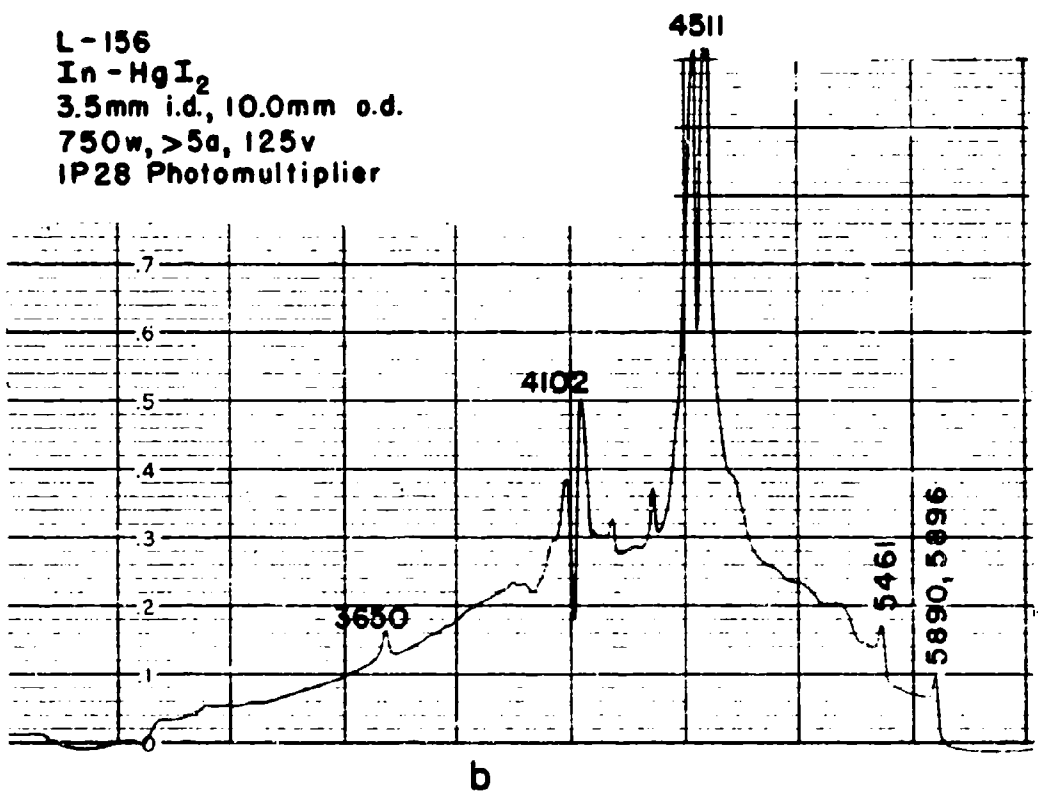
L-156
In - HgI_2
3.5mm i.d., 10.0mm o.d.
750w, >5a, 125v
IP28 Photomultiplier
4511
4102
3650
5461
5890, 5896
.7
.6
.5
.4
.3
.2
.1
0

b

Figure 71

L-158
Ga - HgI_2
3.5mm i.d., 10.0mm o.d.
345w, 6a, 64v
7102 Photomultiplier

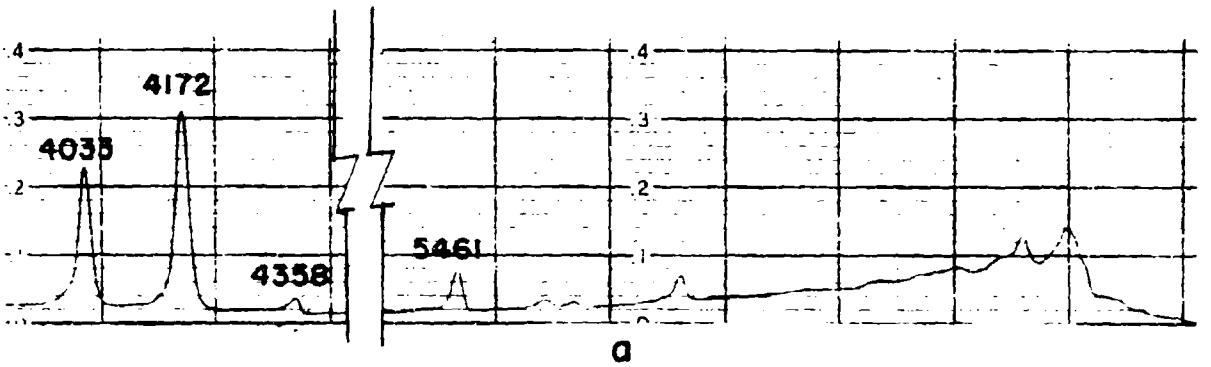

a

L-158
Ga - HgI_2
3.5mm i.d., 10.0mm o.d.
345w, 6a, 64v
IP28 Photomultiplier

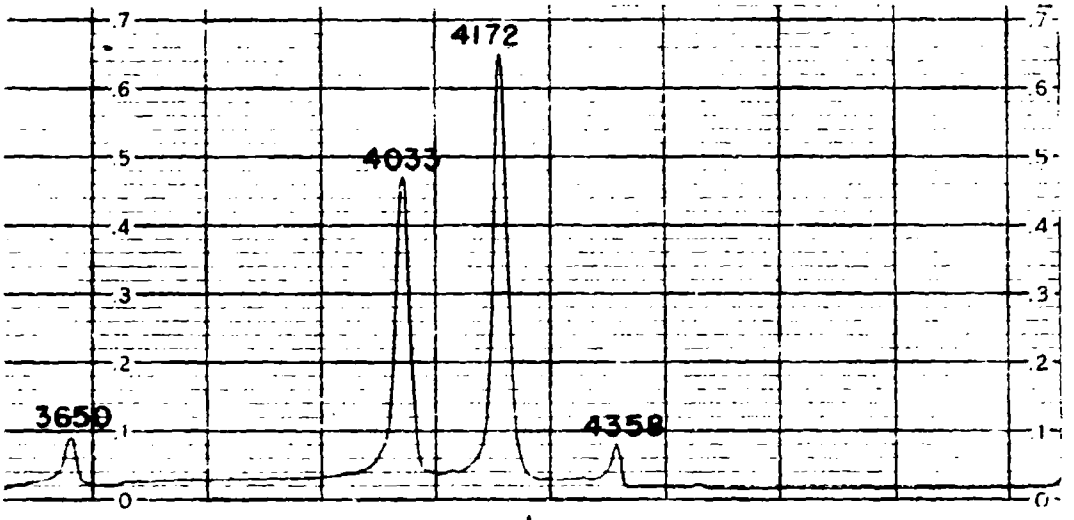

b

Figure 72

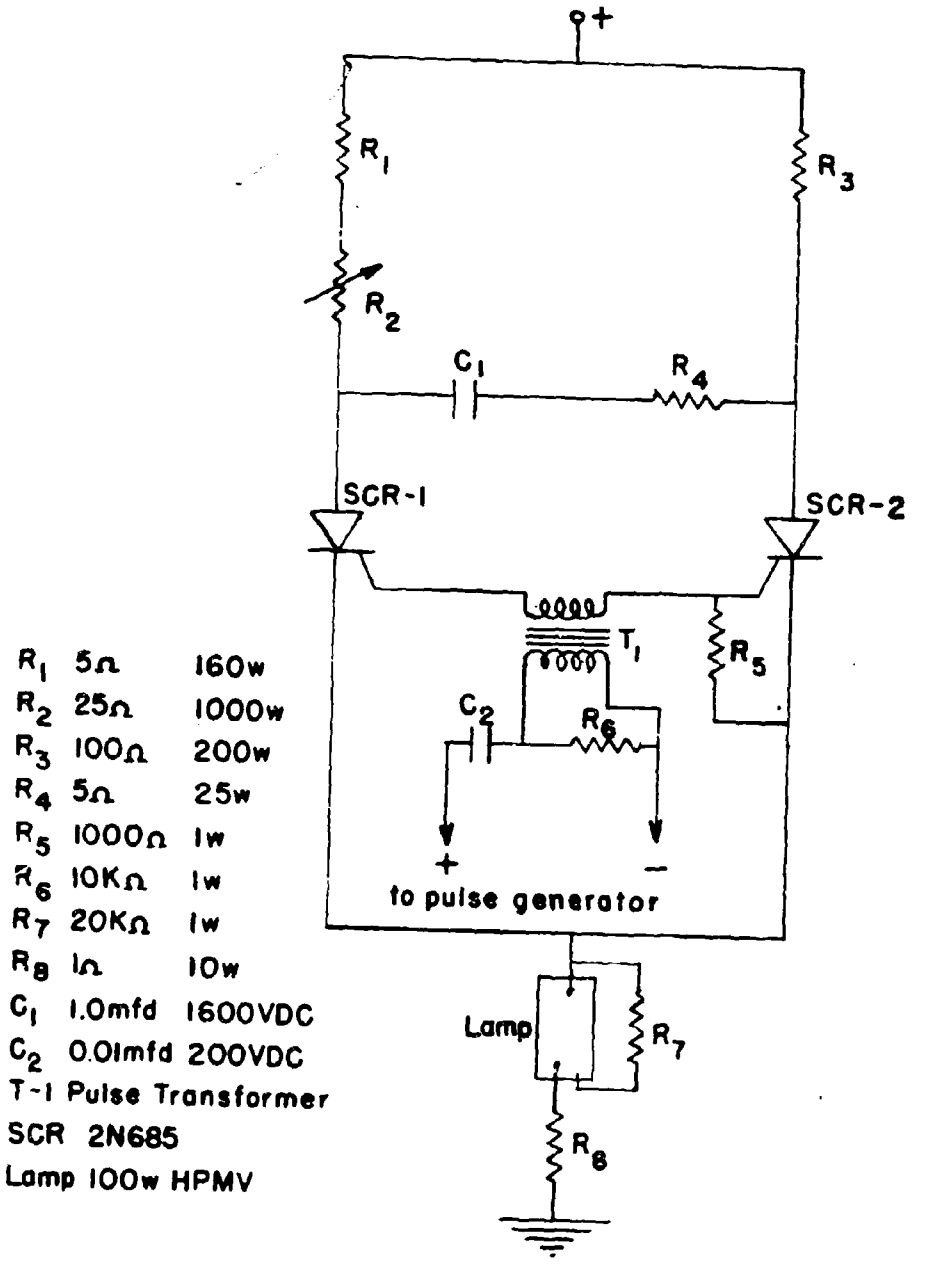

R_1	5Ω	160w
R_2	25Ω	1000w
R_3	100Ω	200w
R_4	5Ω	25w
R_5	1000Ω	1w
R_6	10KΩ	1w
R_7	20KΩ	1w
R_8	1Ω	10w
C_1	1.0mfd	1600VDC
C_2	0.01mfd	200VDC

T-1 Pulse Transformer
SCR 2N685
Lamp 100w HPMV

PULSE CIRCUIT

Figure 73

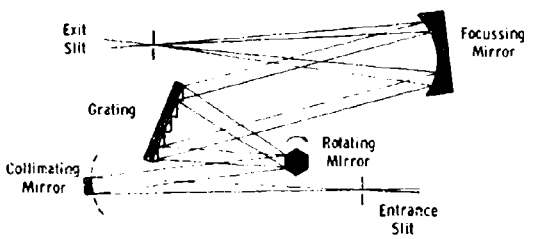

Optical arrangement of ultra-rapid scanning monochromator

Figure 74

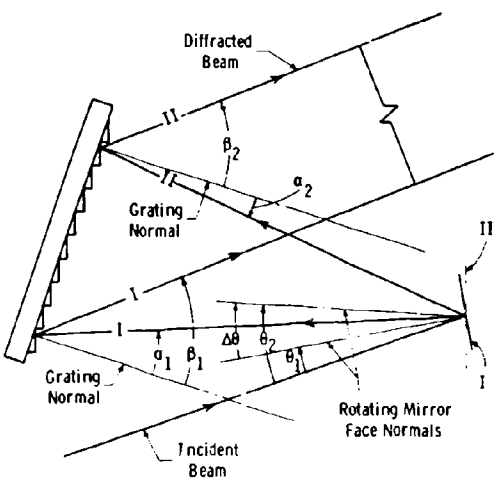

Arrangement of ultra-rapid scanning monochromator showing geometrical factors governing spectral range, and speed

Figure 75

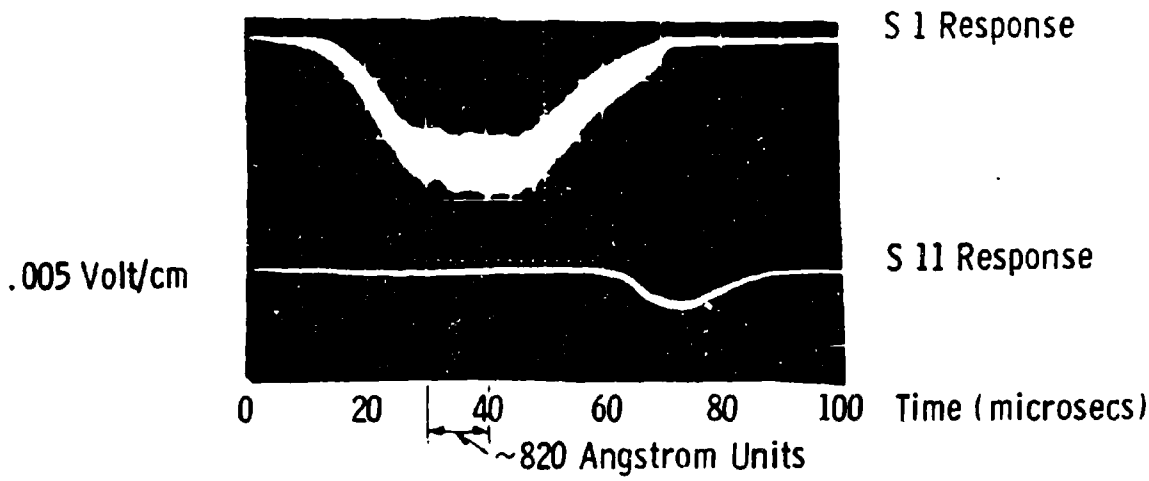

Fig. 76 – Spectral radiance of calibrated tungsten ribbon-filament standard lamp

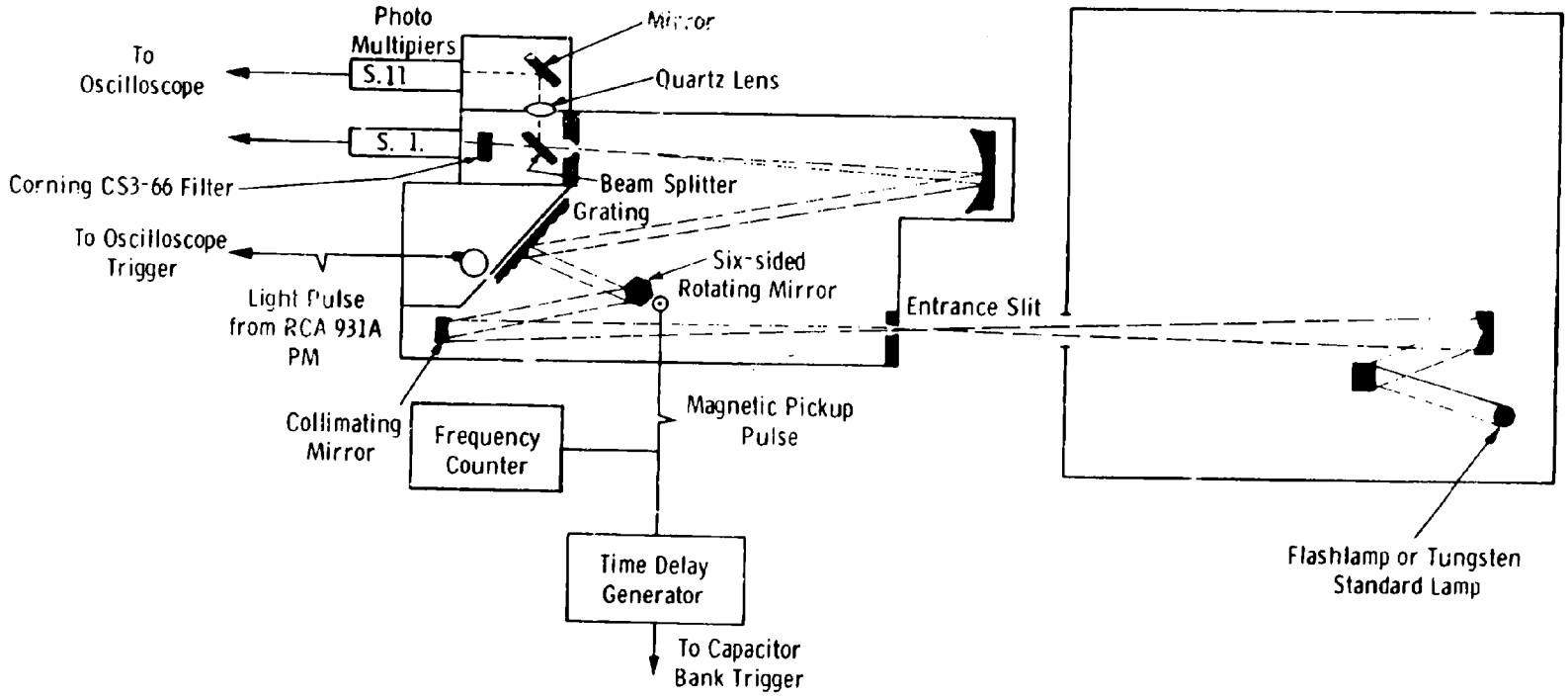

Fig. 77 – Arrangement of rapid scanning spectrometer for pulsed lamp studies

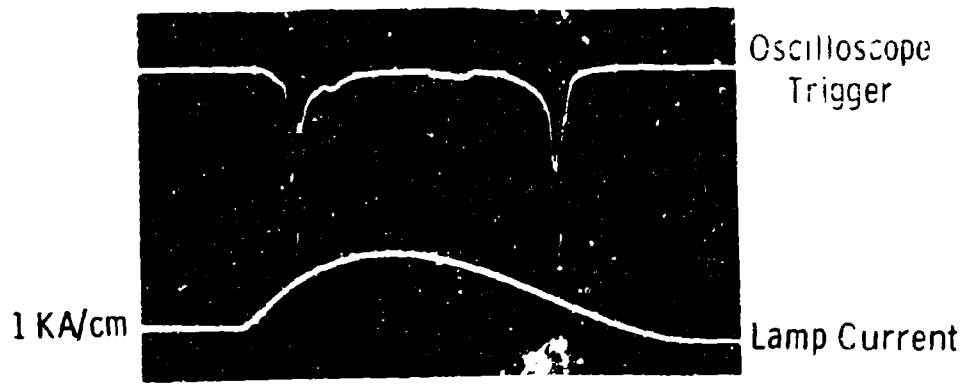

(a)

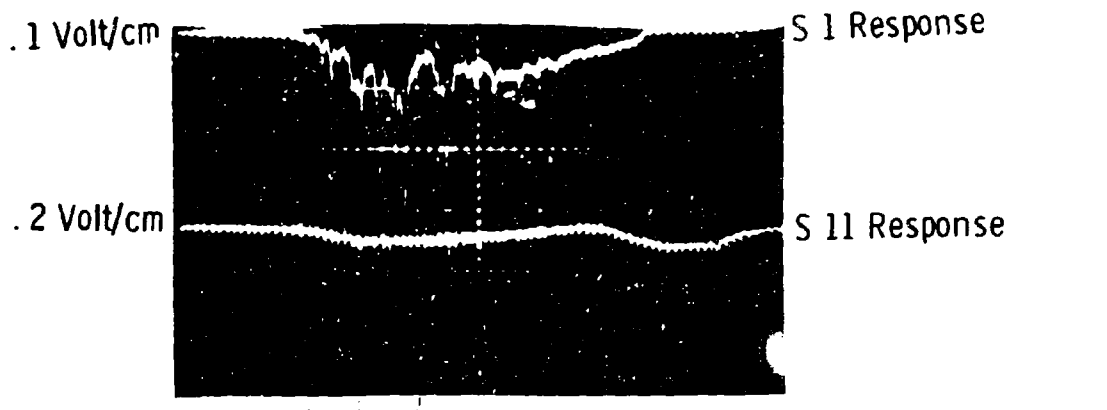

(b)

Fig. 78 –Xenon flashlamp

Energy input 200 joules (1KV, 400μf, 100μh)

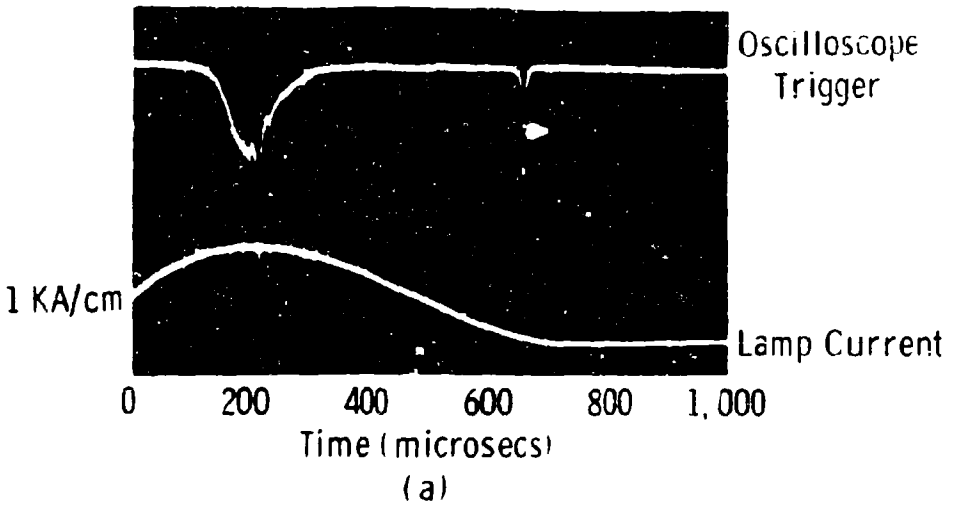

(a)

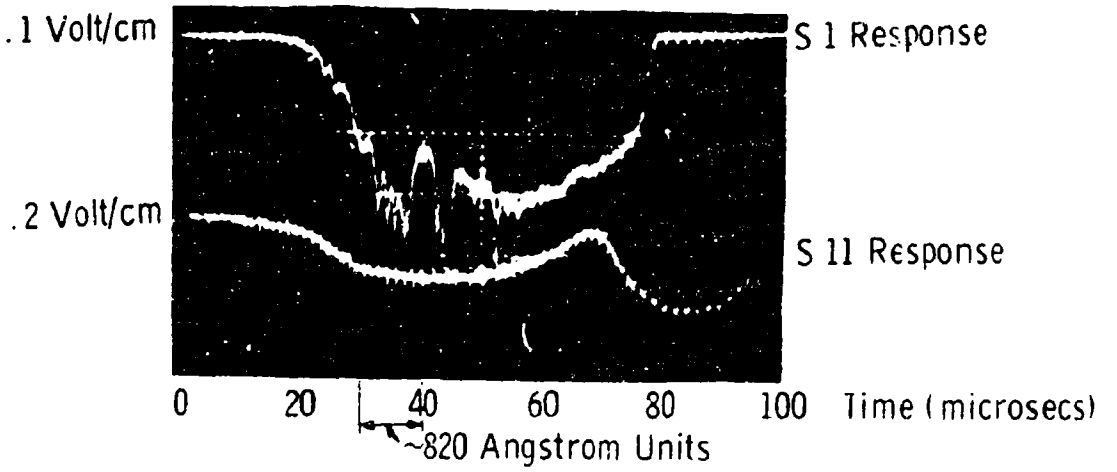

(b)

Fig. 79—Xenon flashlamp

Energy input 200 joules (1KV, 400uf, 100μh)

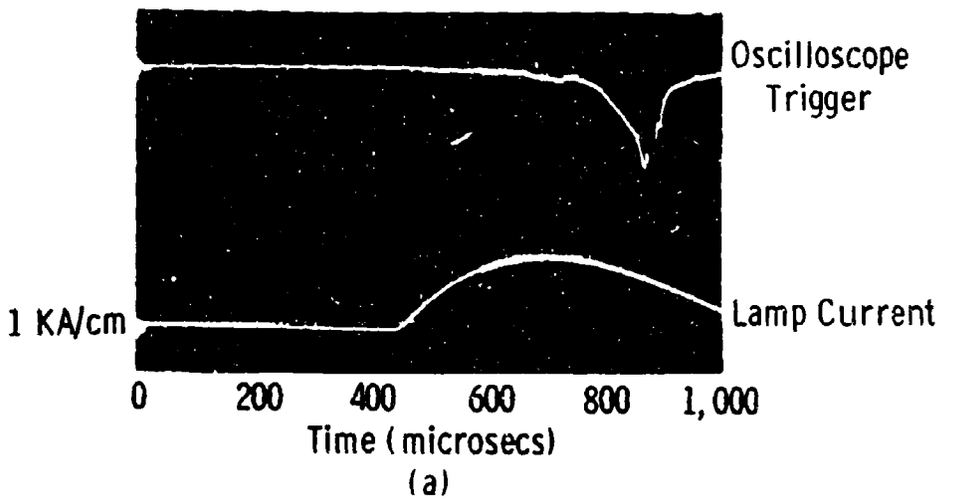

(a)

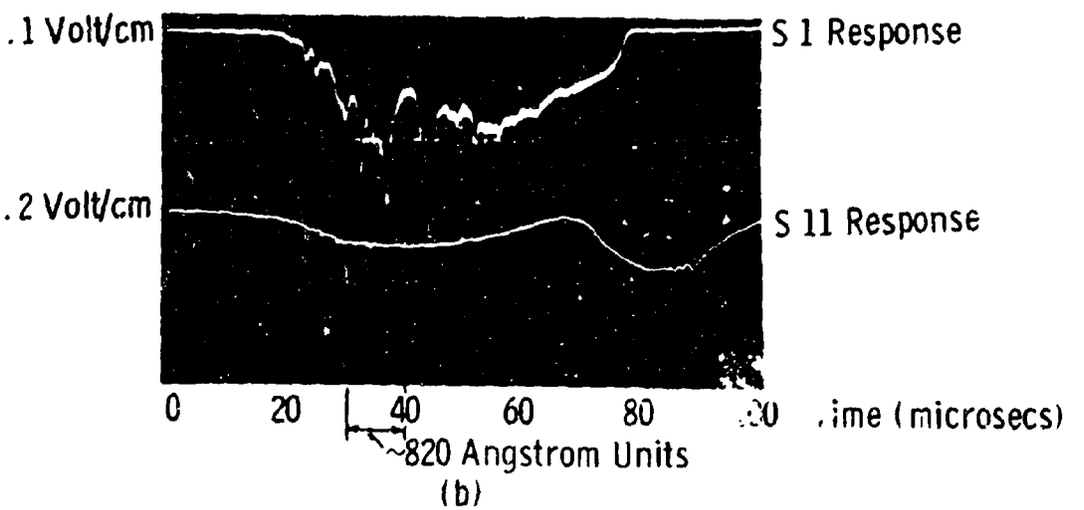

(b)

Fig. 80—Xenon flashlamp

Energy input 200 joules (1KV, 400μf, 100μ h)

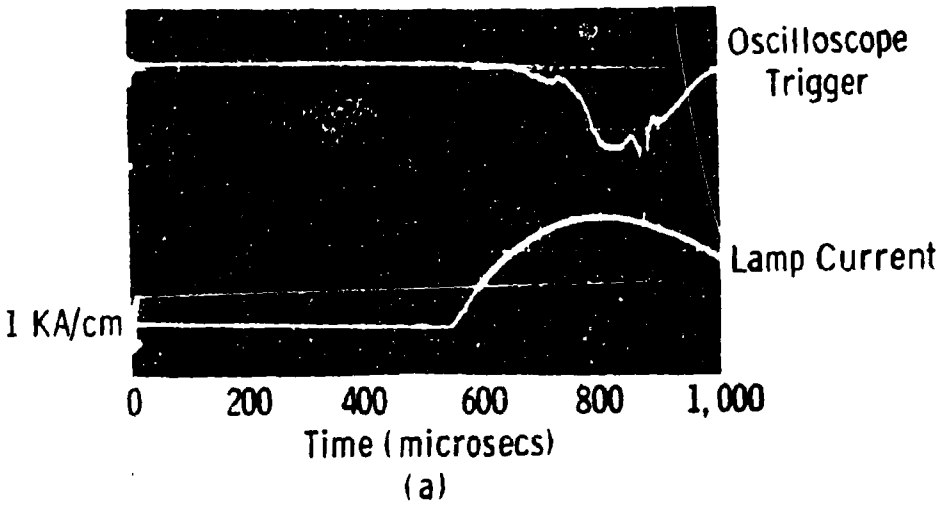

(a)

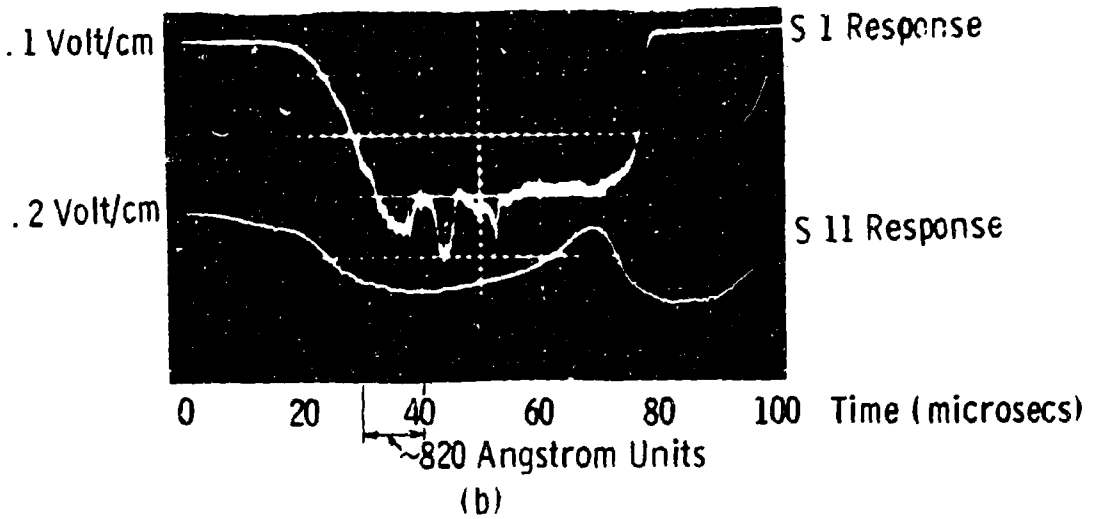

(b)

Fig. 81—Xenon flashlamp
Energy input 400 joules (1.4KV, 400μf, 100 μh)

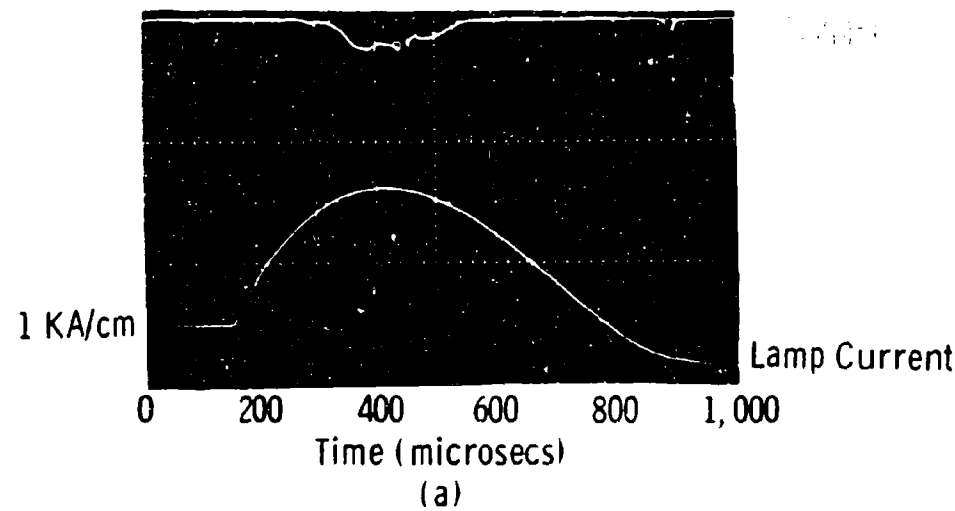

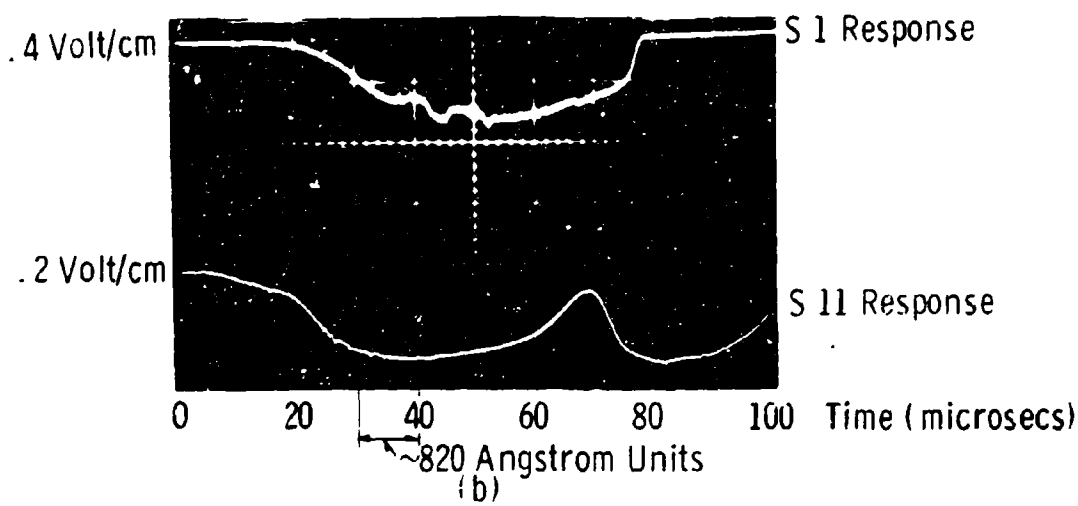

Fig. 82—Xenon flashlamp

Energy input 600 joules (1.7KV, 400μf, 100μh)

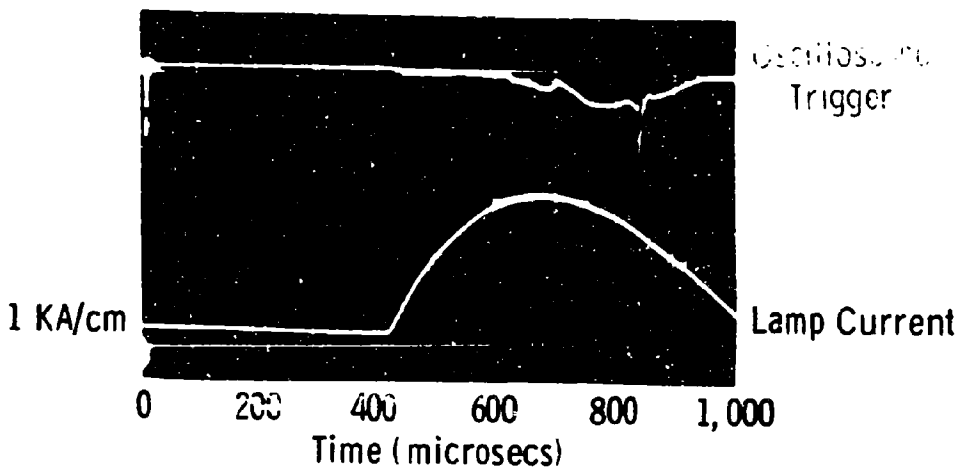

(a)

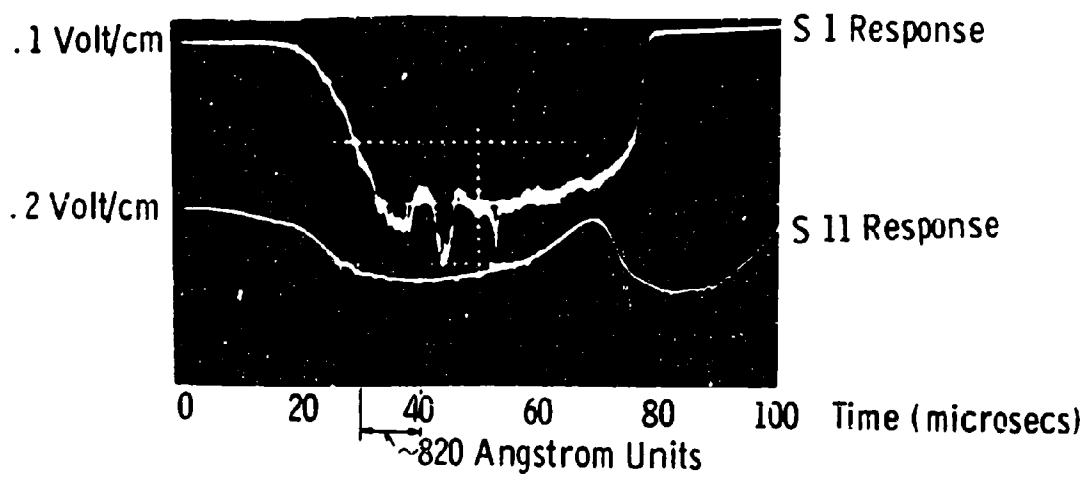

(b)

Fig. 83–Xenon flashlamp

Energy input 600 joules (1.73KV, 400μf, 100μh)

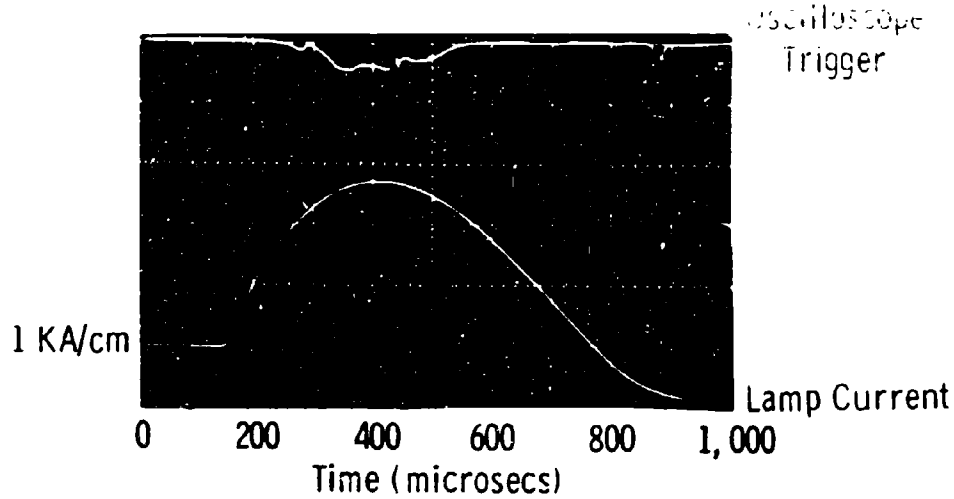

(a)

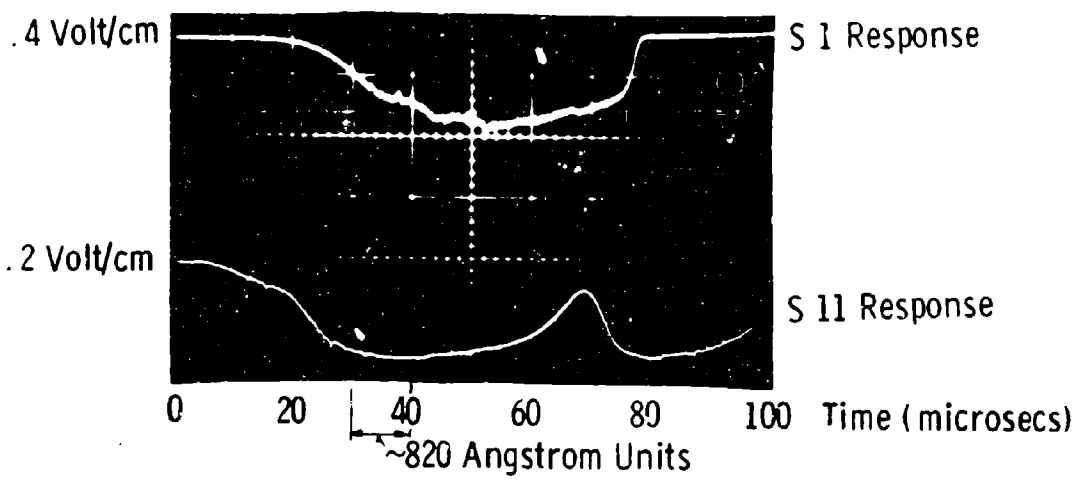

(b)

Fig. 84—Xenon flashlamp

Energy input 800 joules (2 KV, 400μf, 100μh)

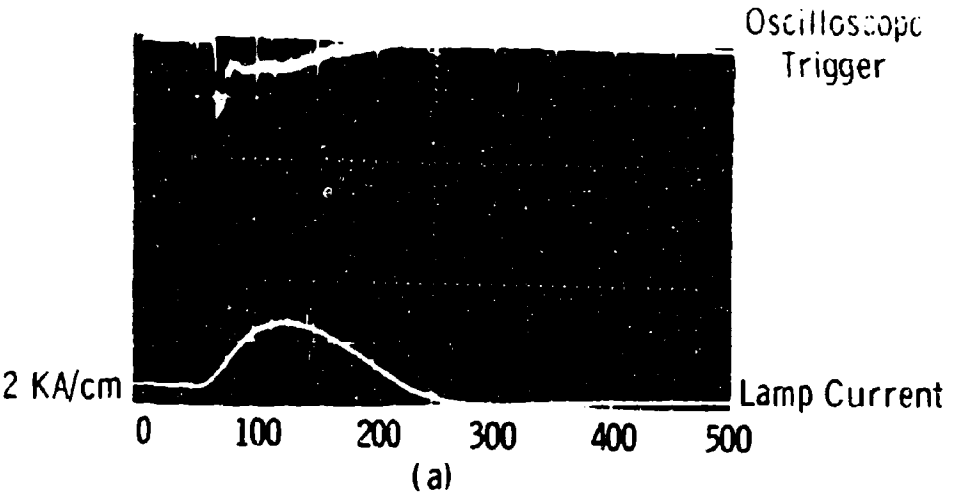

(a)

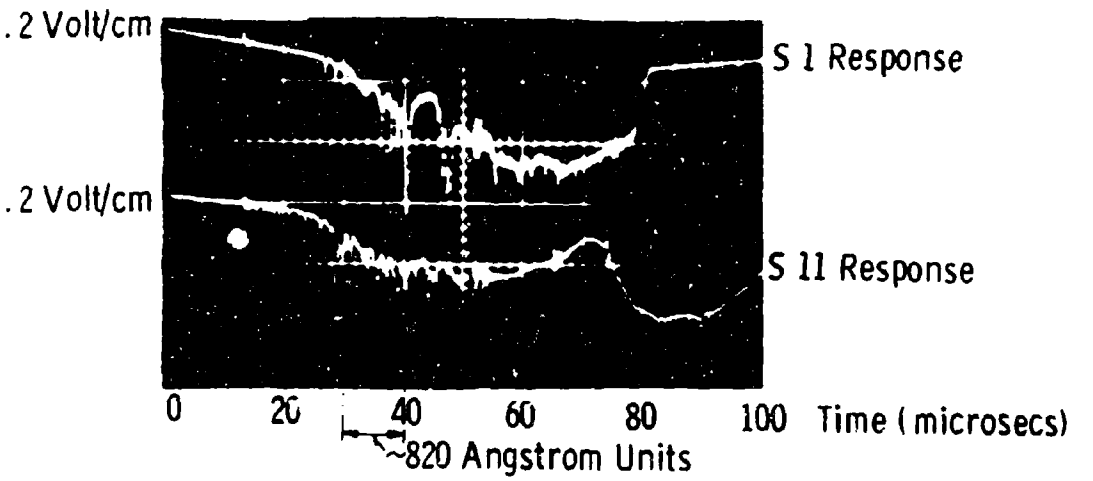

(b)

Fig. 85—Xenon flashlamp

Energy input 100 joules (1KV, 200μf, 10μh)

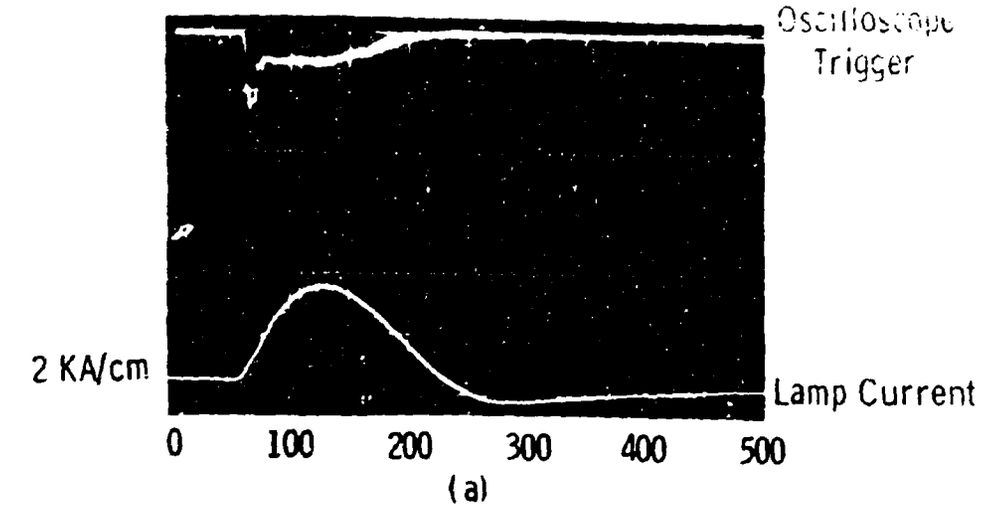

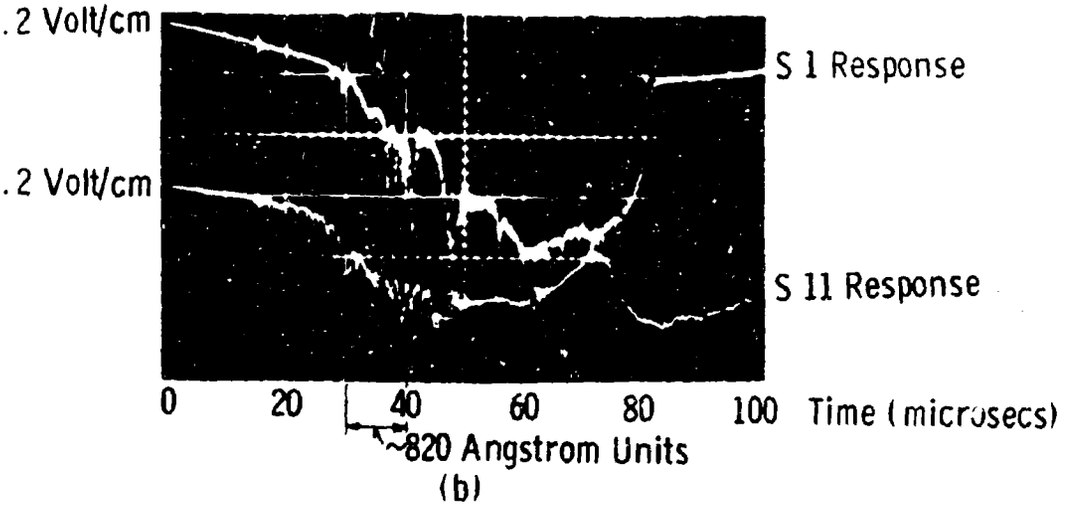

Fig. 86—Xenon flashlamp

Energy input 200 joules (1.4KV, 200μf, 10μh)

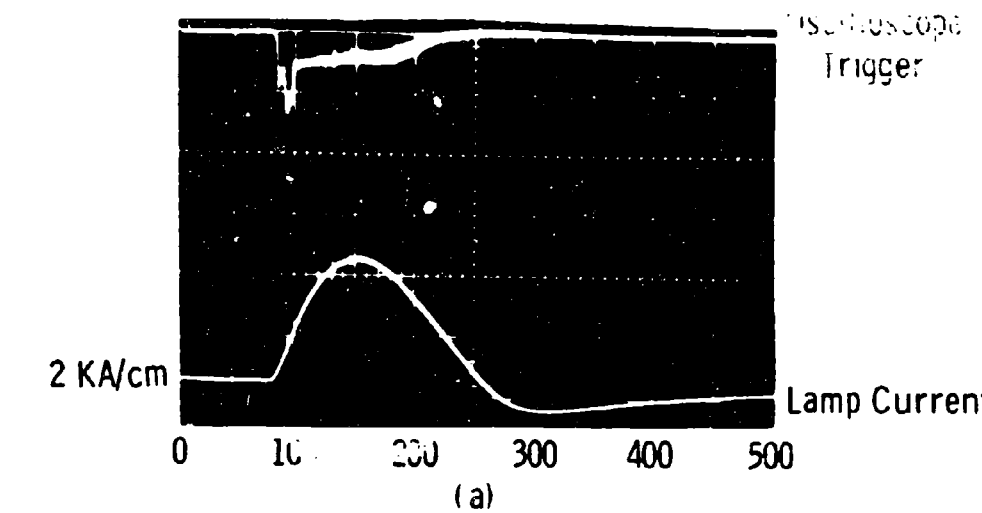

(a)

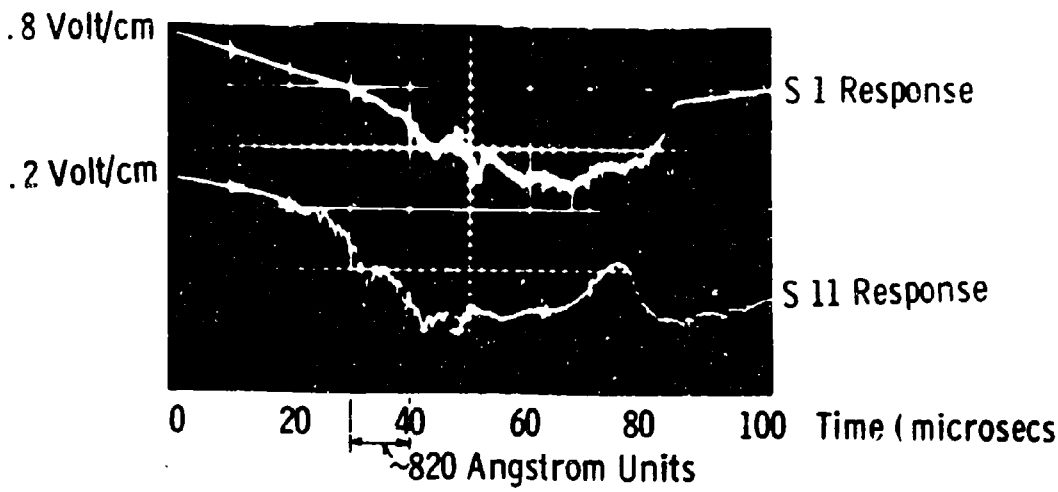

(b)

Fig. 87 –Xenon flashlamp

Energy input 300 joules (1.7KV, 200μf, 10μh)

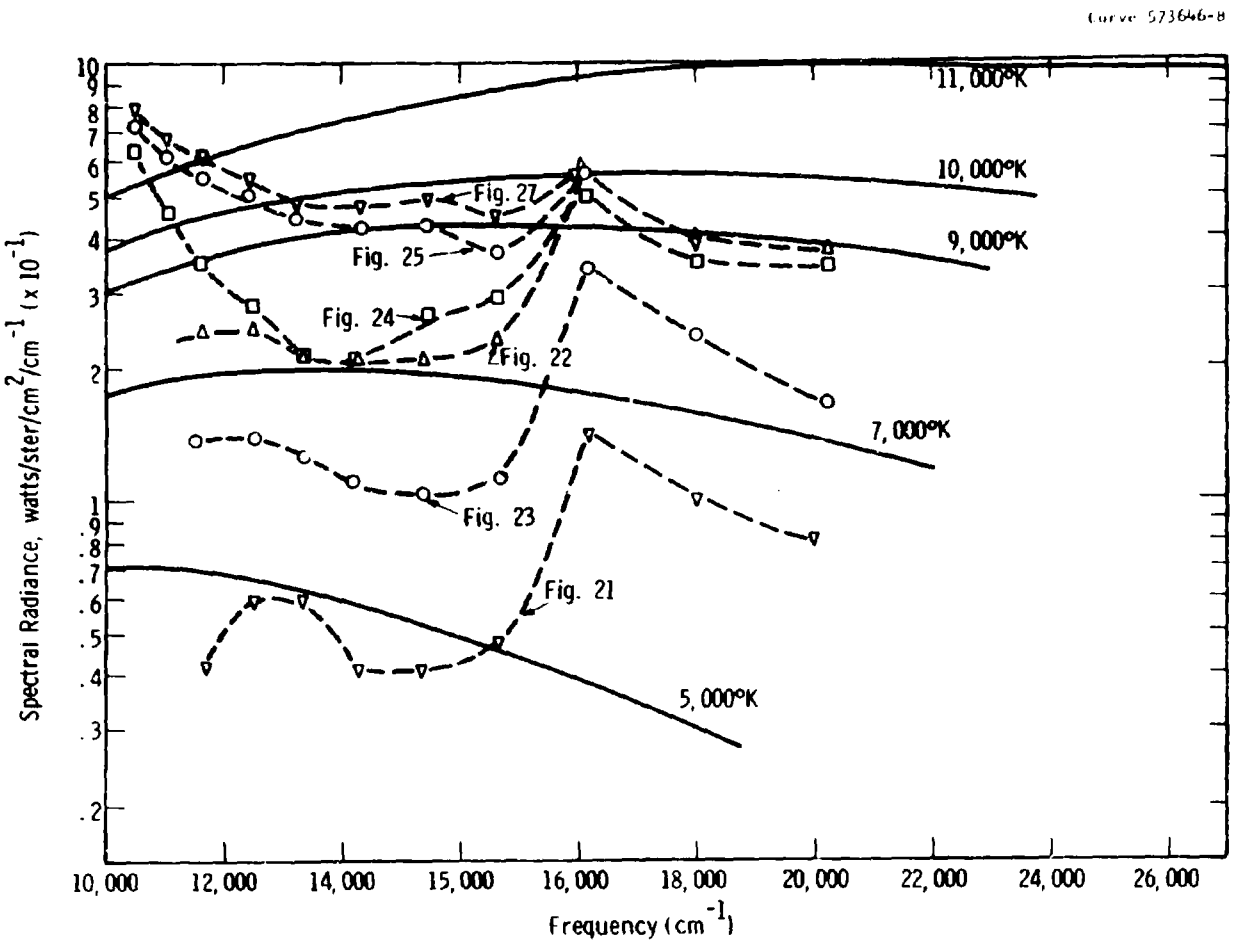

Fig. 88—Comparison of spectral radiances of xenon flashlamp with spectral radiance of a blackbody at varying temperatures

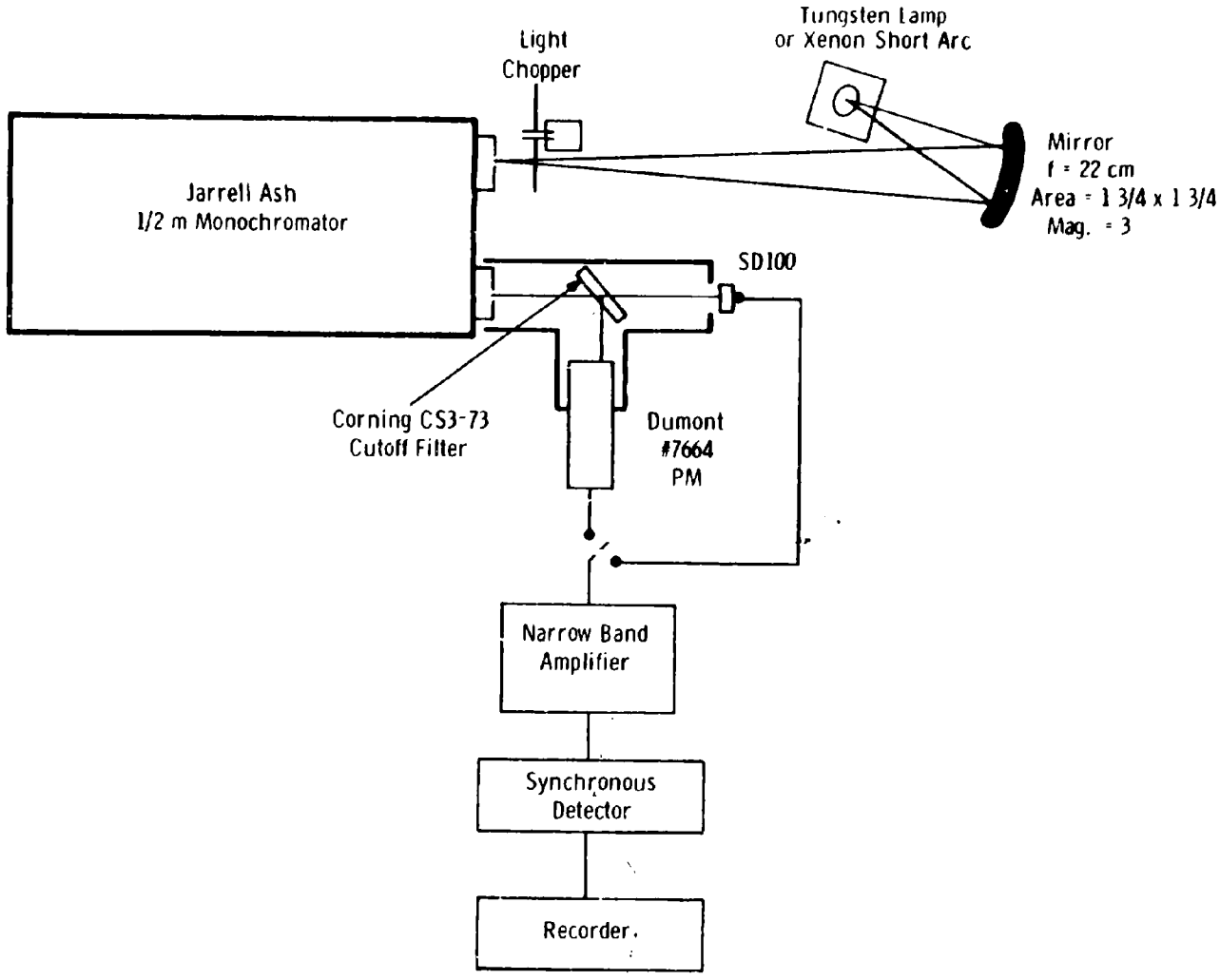

Fig. 89 – Arrangement of high resolution scanning spectrometer

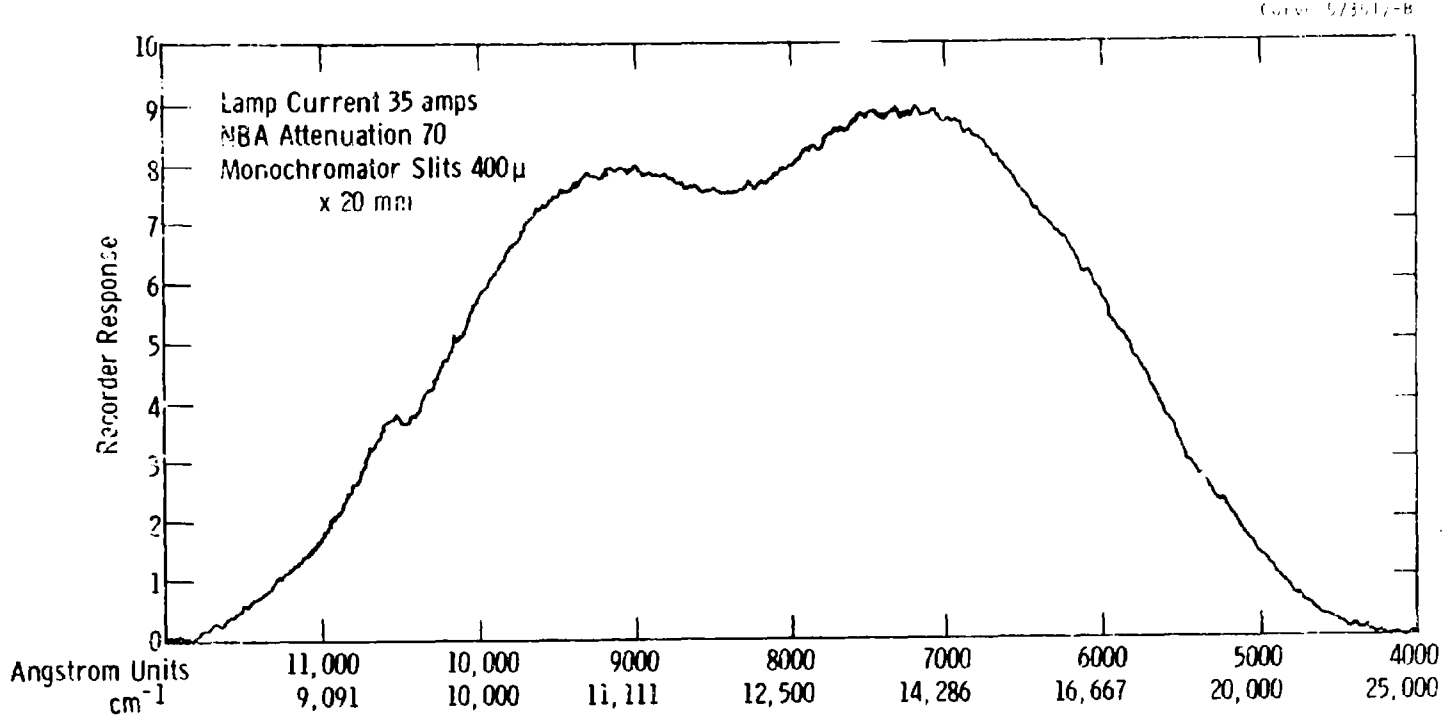

Fig. 90 - Spectral radiance of standard tungsten lamp measured with SD100 photodiode

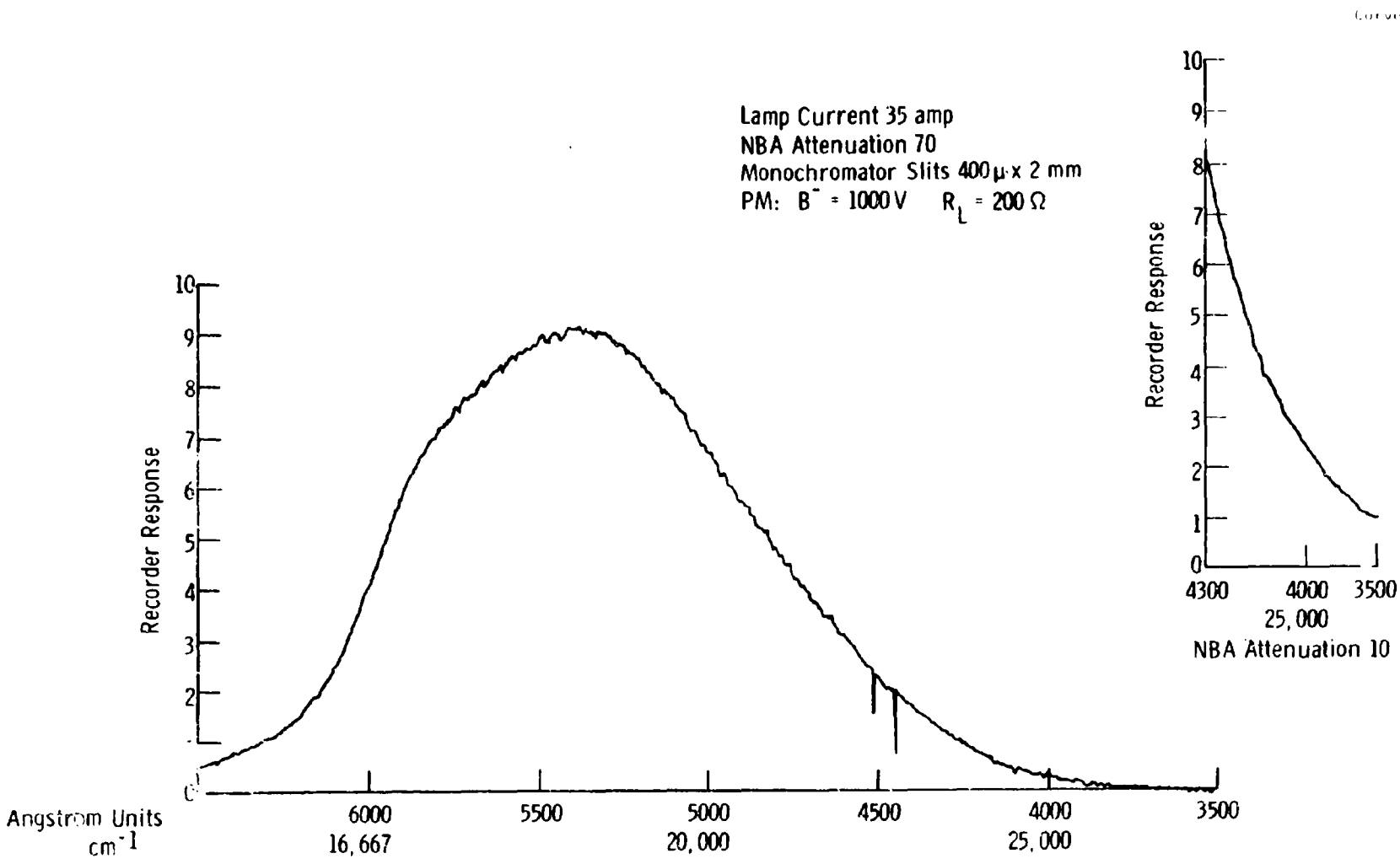

Fig. 91—Spectral radiance of standard tungsten lamp measured with S13 response photomultiplier

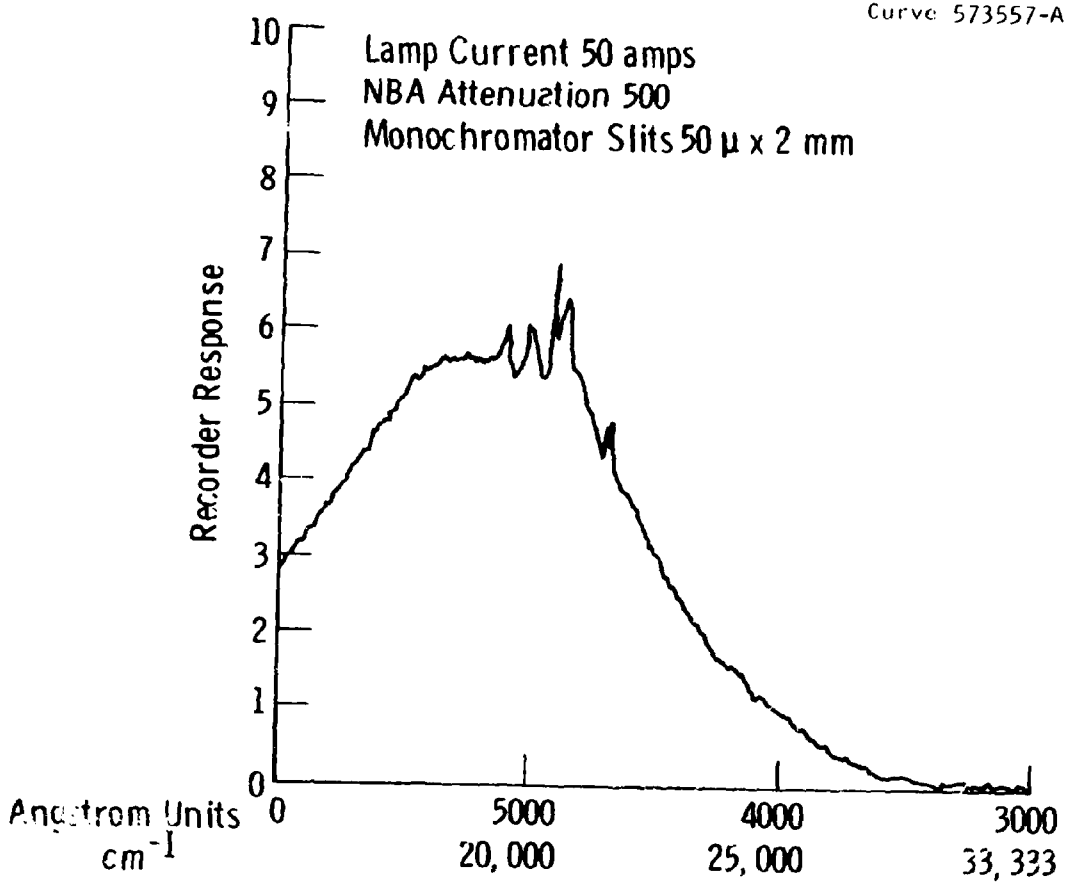

Fig. 92—Spectrum of xenon short arc measured with S13 response photomultiplier

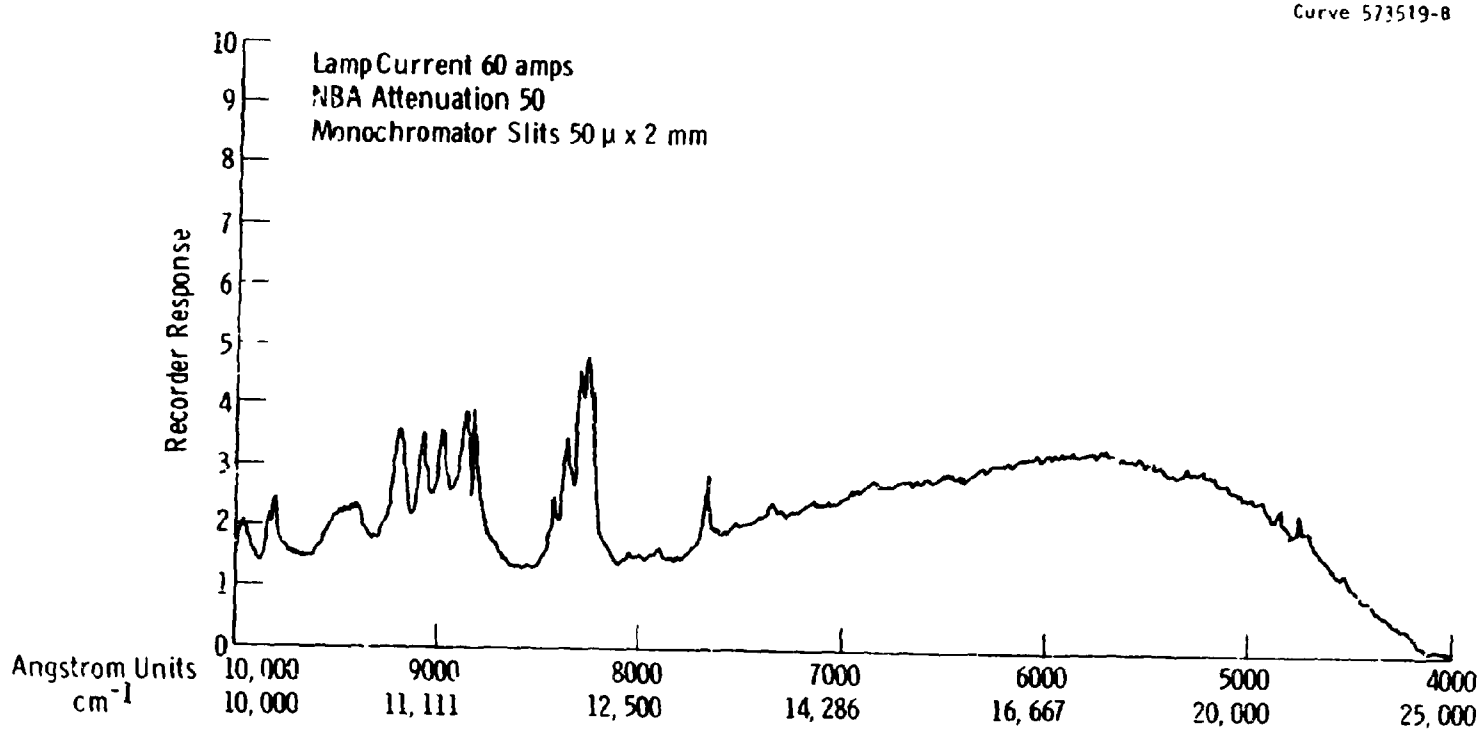

Fig. 93—Spectrum of xenon short arc measured with SD100 hpotodiode

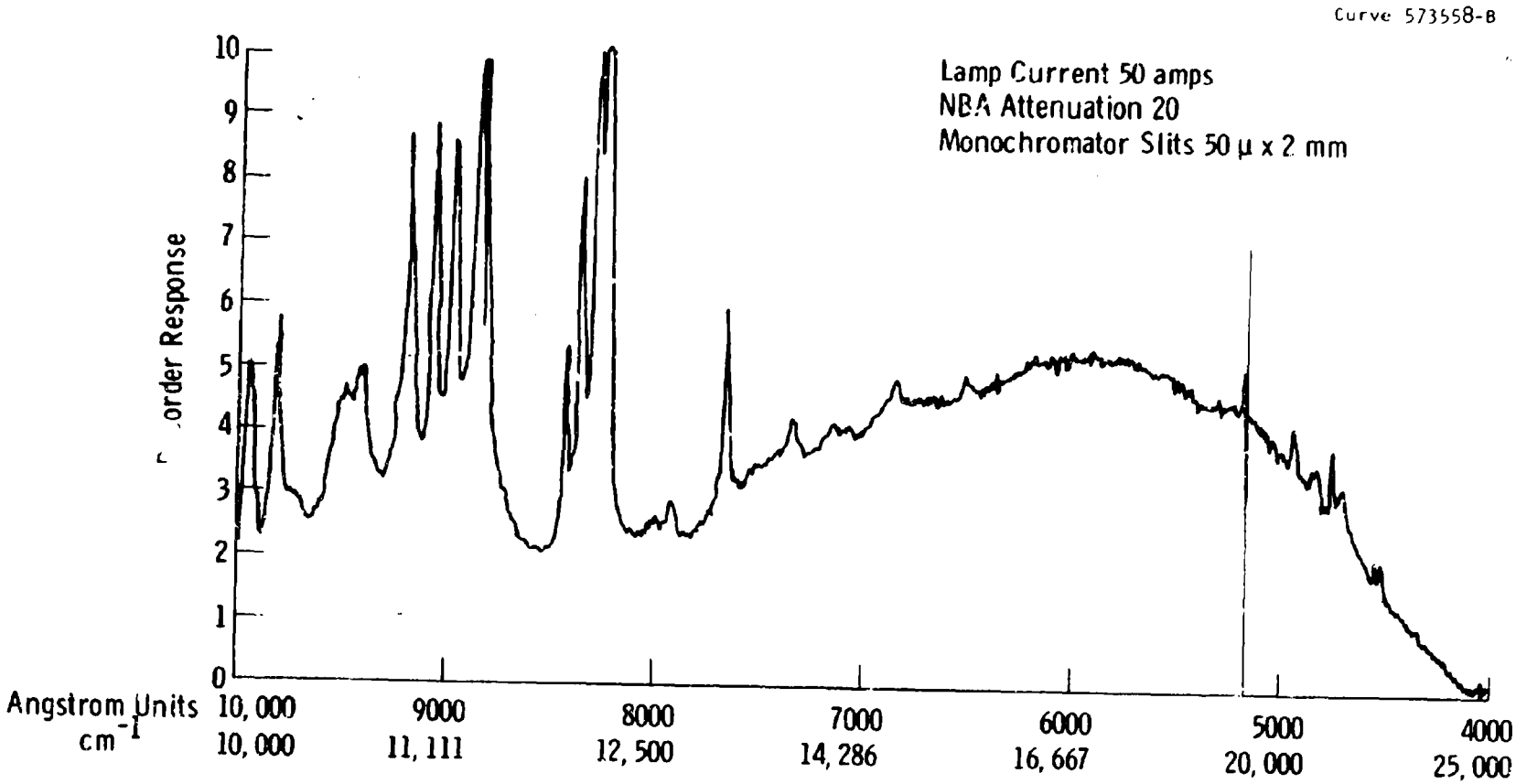

Fig. 94—Spectrum of xenon short arc measured with SD100 hpotodiode

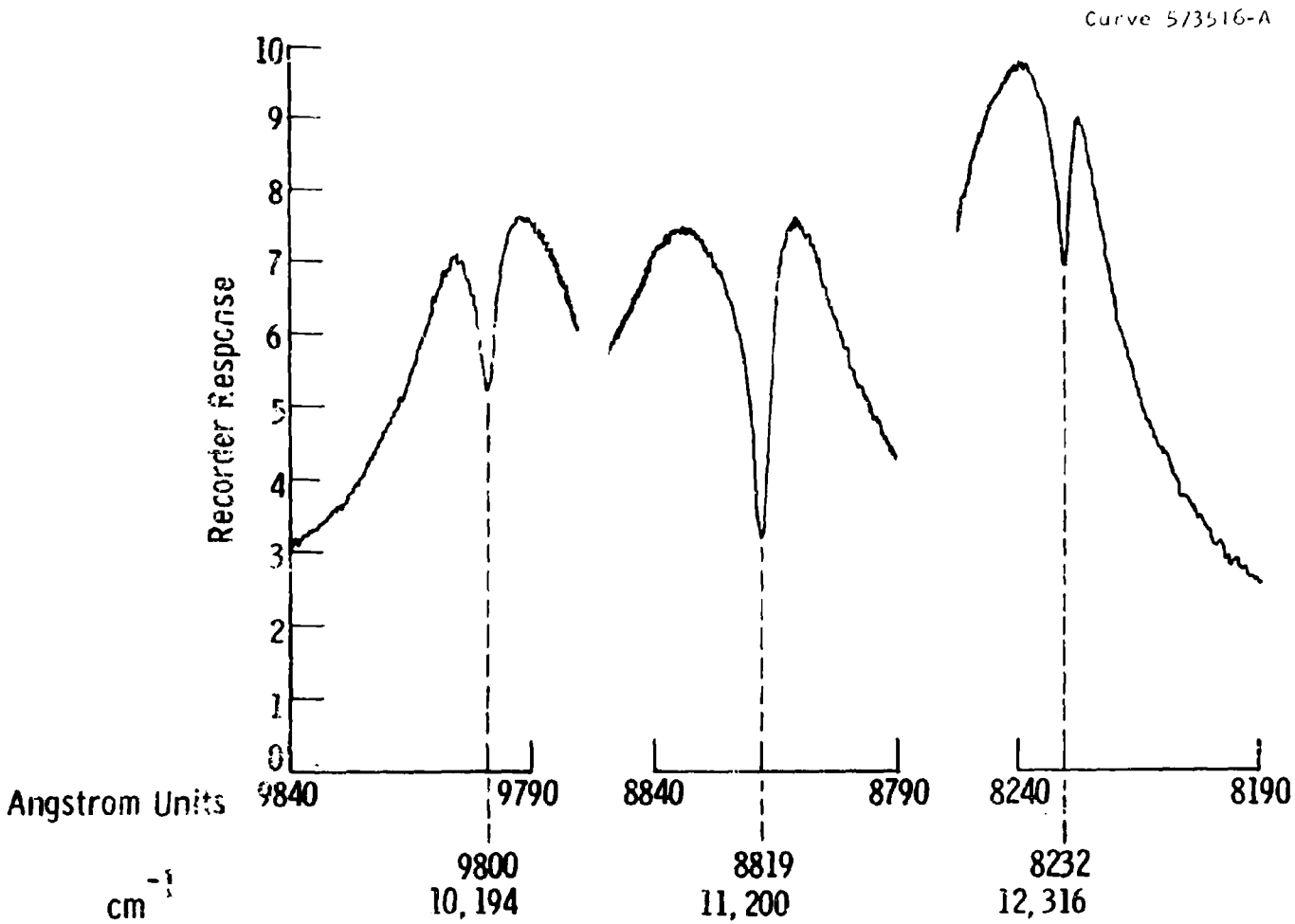

Fig. 95 – Portions of expanded spectrum of xenon short arc measured with SD100 photodiode

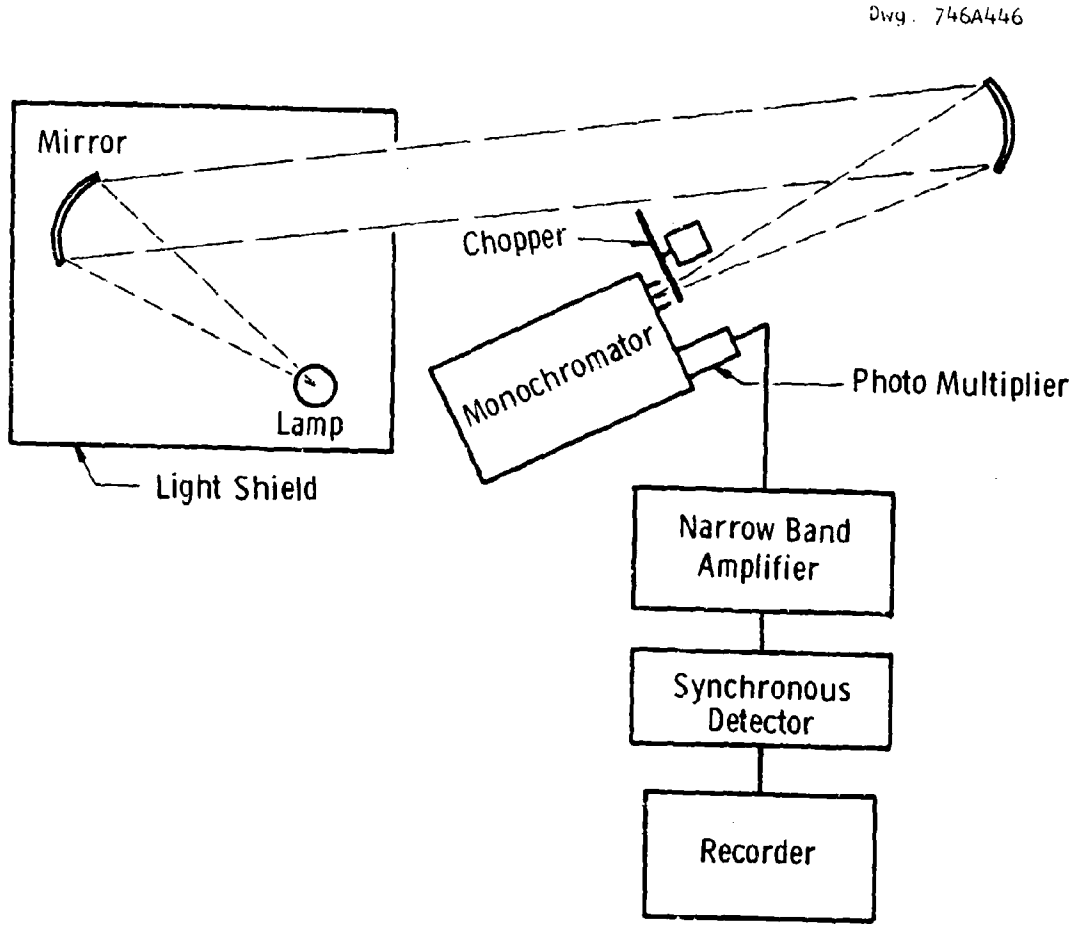

Fig. 96—Arrangement used for taking high resolution spectra

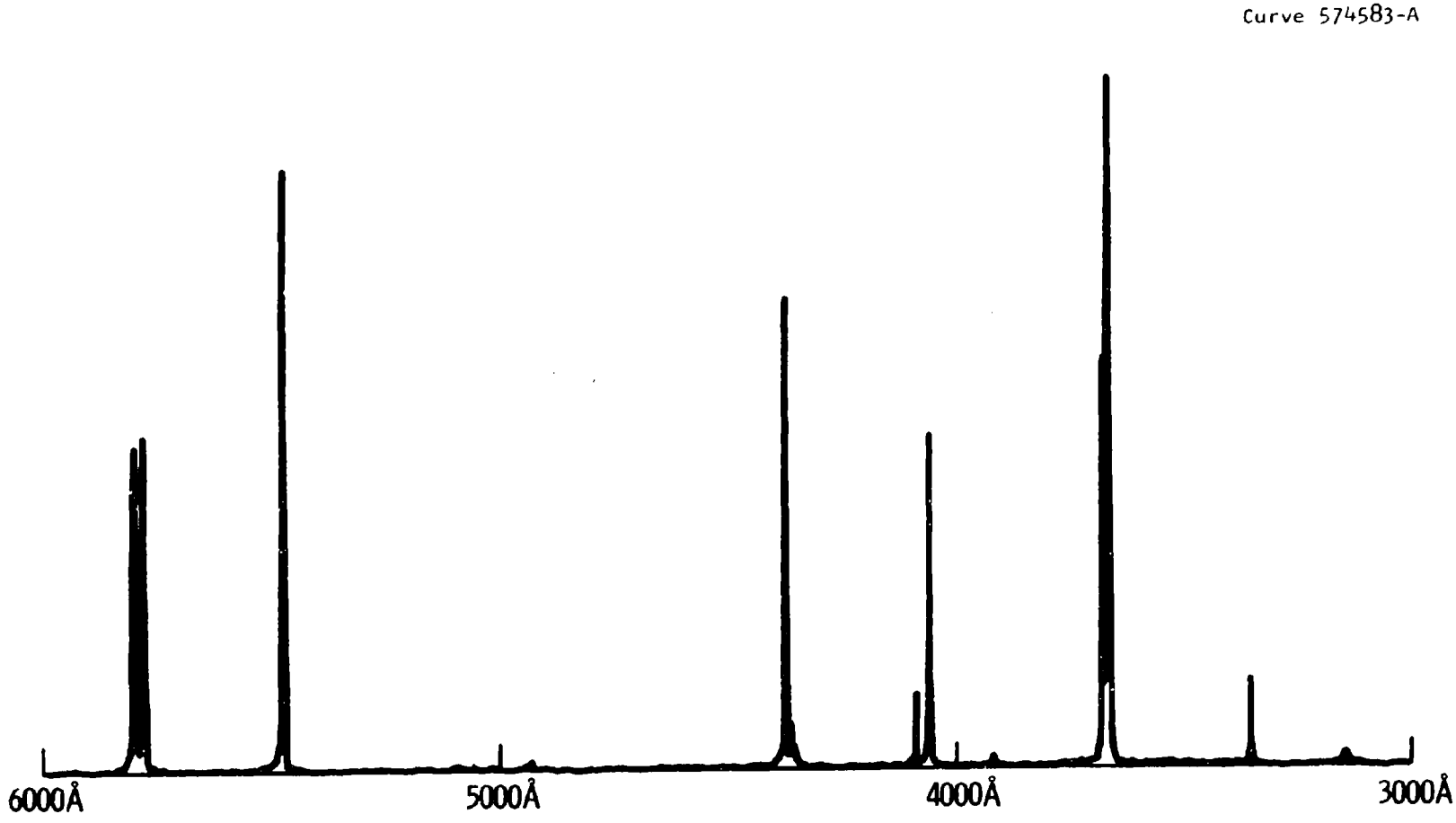

Fig. 97 – Spectrum of the standard mercury lamp

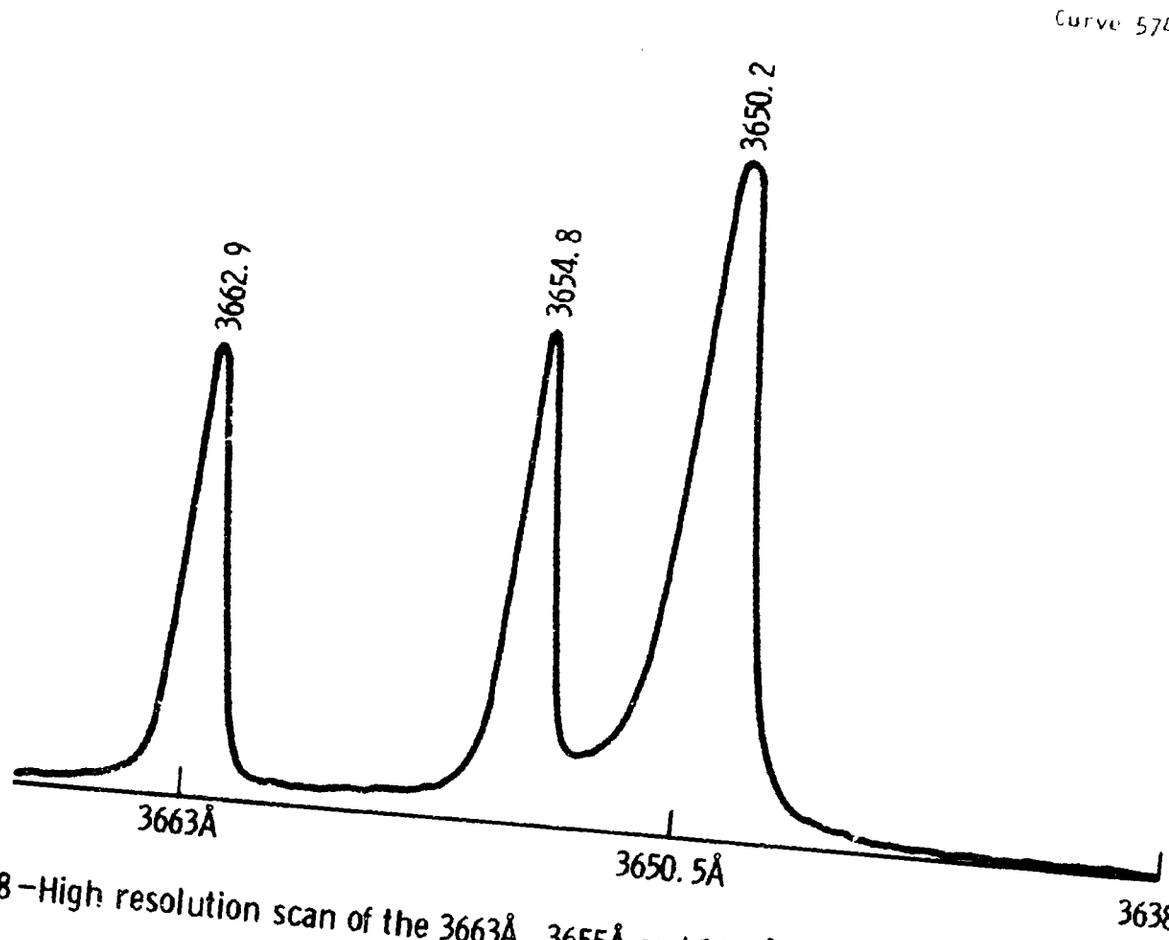

Fig. 98 – High resolution scan of the 3663Å, 3655Å and 3650Å lines in a standard mercury lamp

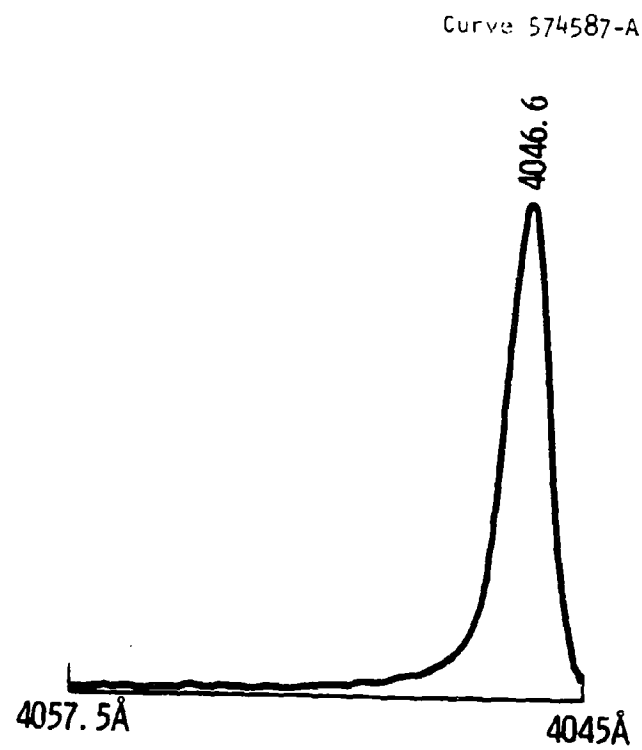

Fig.99 –High resolution scan of 4047Å line in the mercury standard lamp

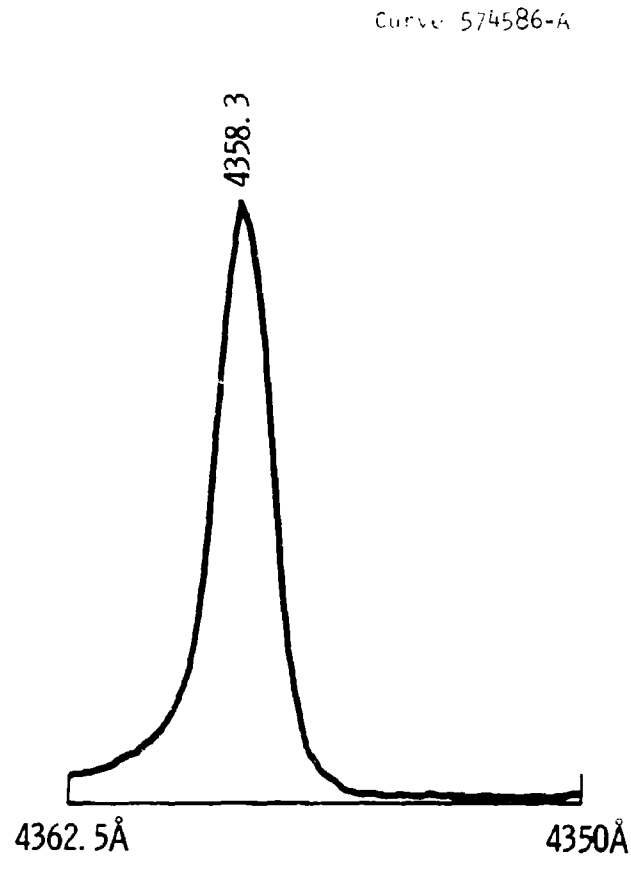

Fig. 100–High resolution scan of 4358Å Hg line in the mercury standard lamp

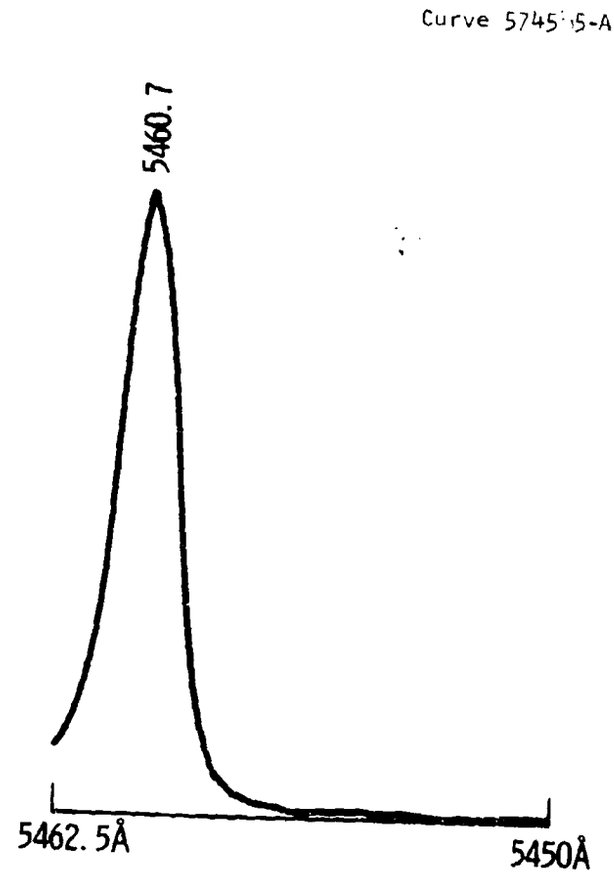

Fig. 101—High resolution scan of 5461Å Hg line in the mercury standard lamp

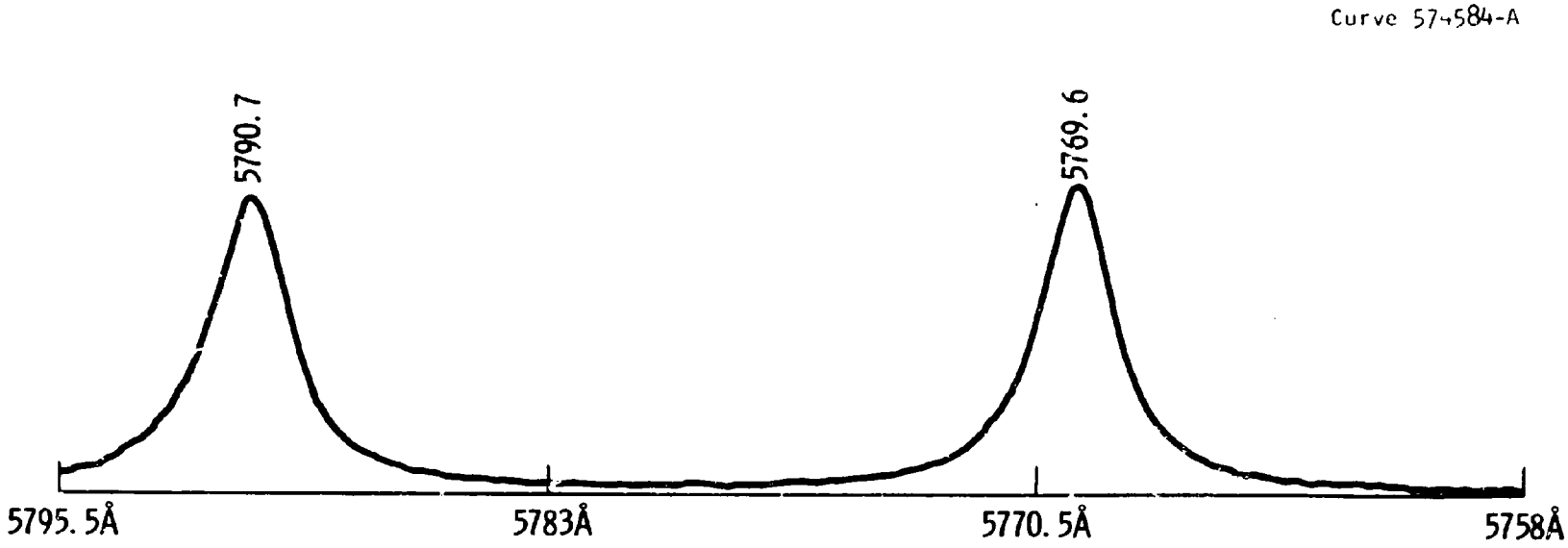

Fig. 102–High resolution scan of 5770Å - 5791Å Hg doublet in the mercury standard lamp

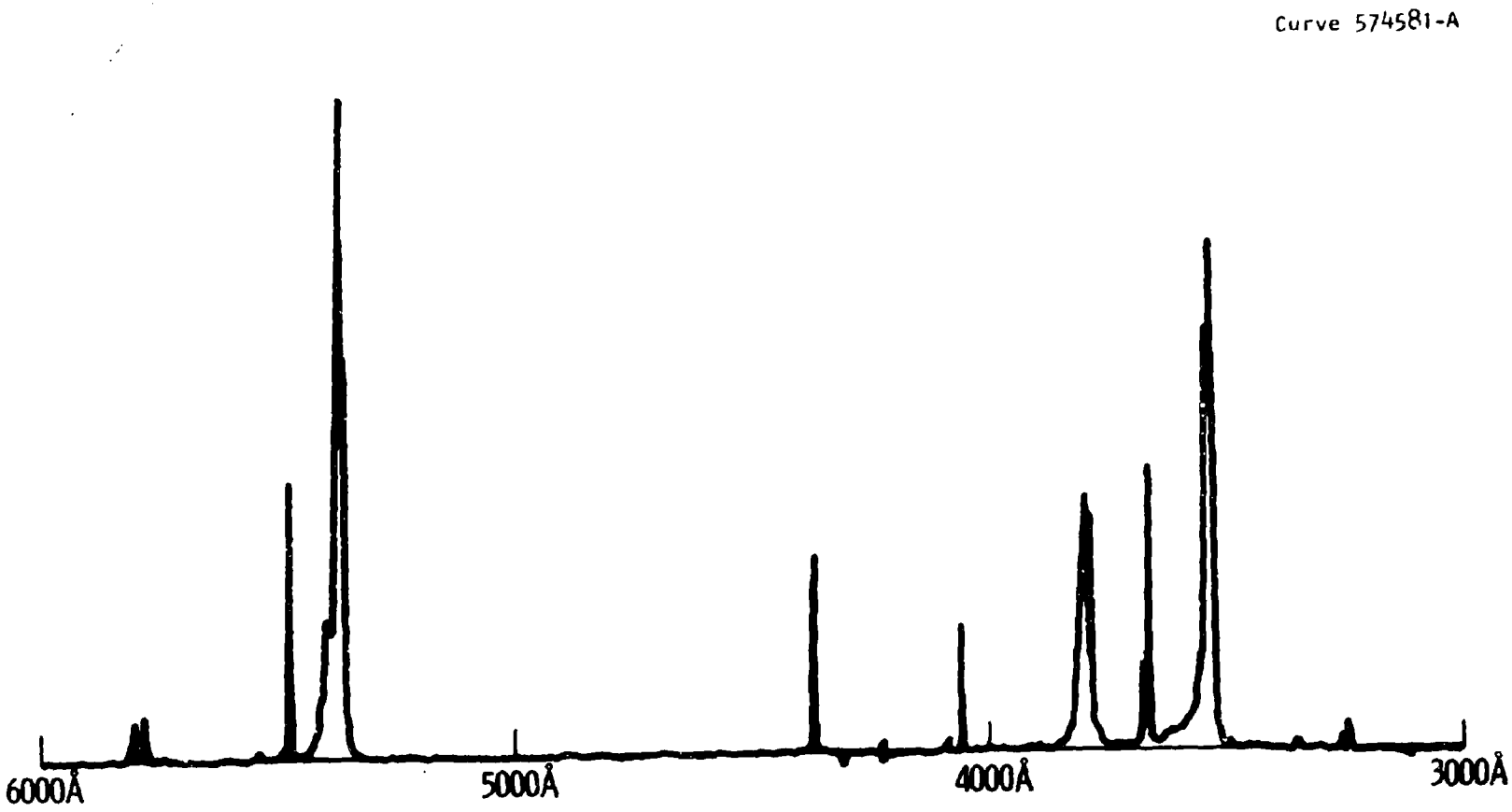

Fig.103-Spectrum of the TII lamp

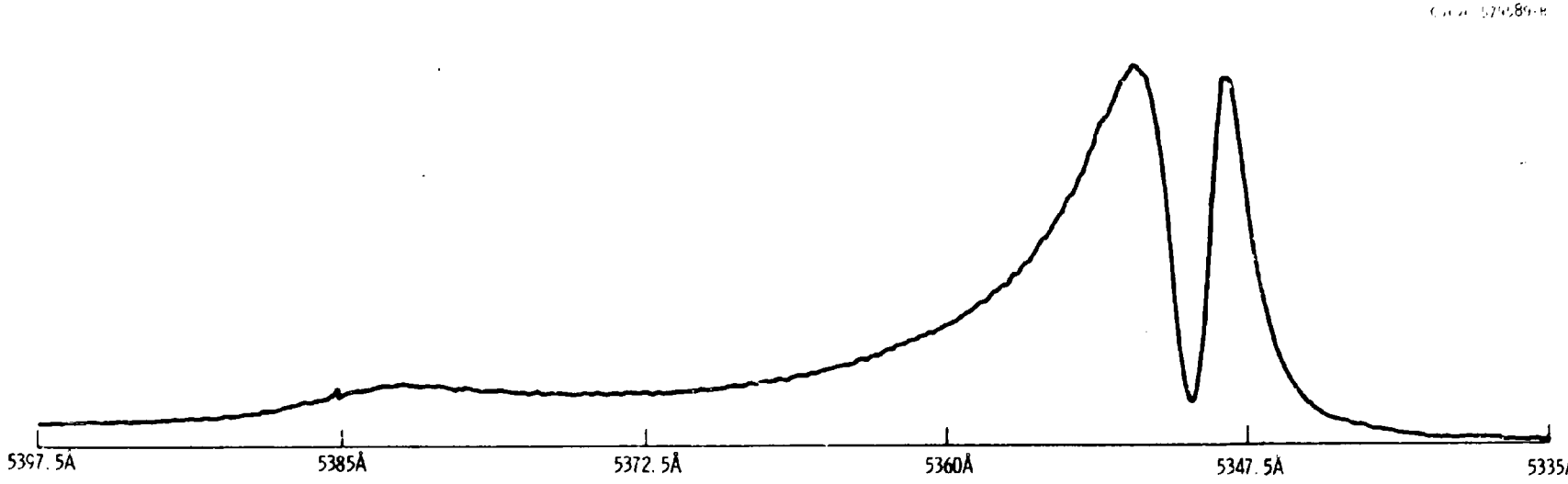

Fig. 104–High resolution scan of the TI lines at 5350Å in the TII lamp

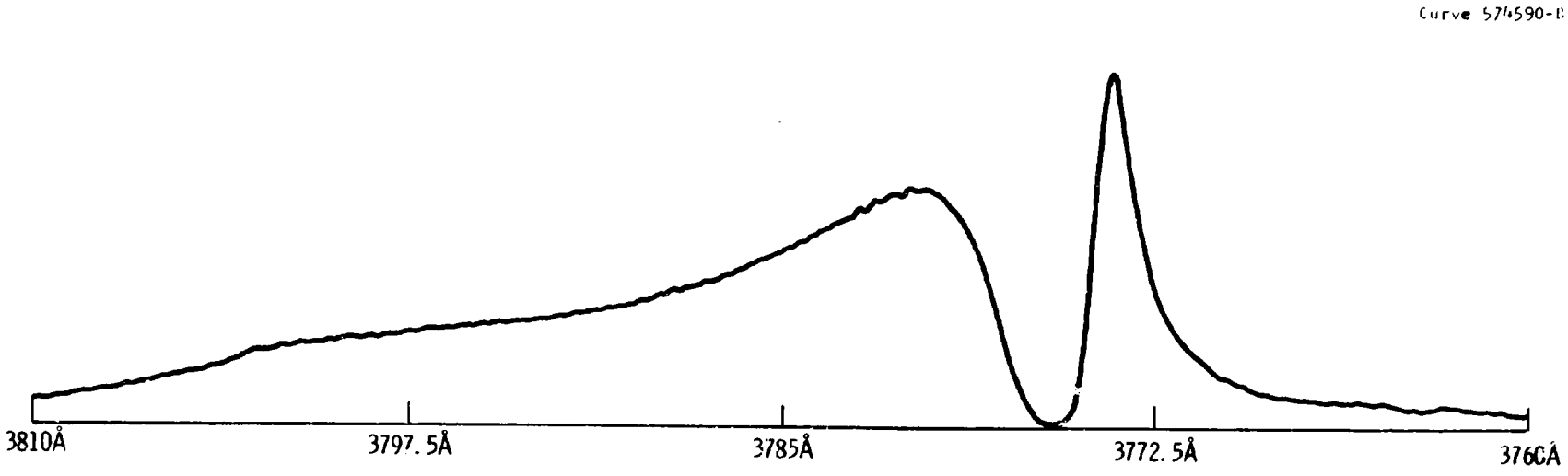

Fig. 105—High resolution scan of the TI lines at 3775Å in the TII lamp

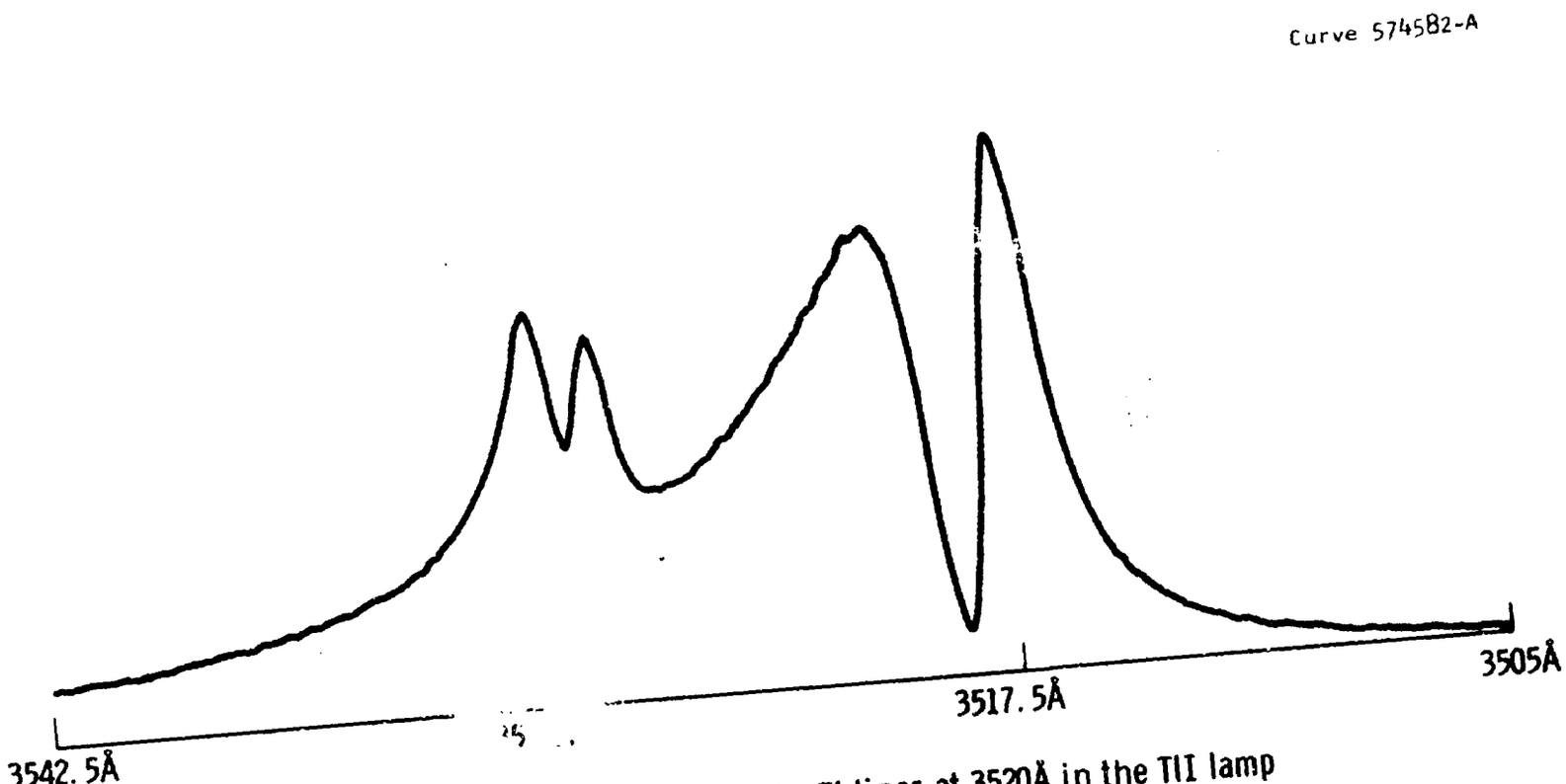

Fig.106—High resolution scan of the TI lines at 3520Å in the TII lamp

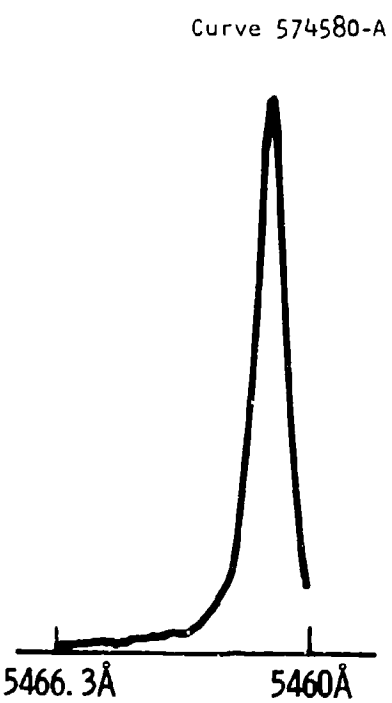

Fig. 107—High resolution scan of 5461Å Hg line in the TII lamp

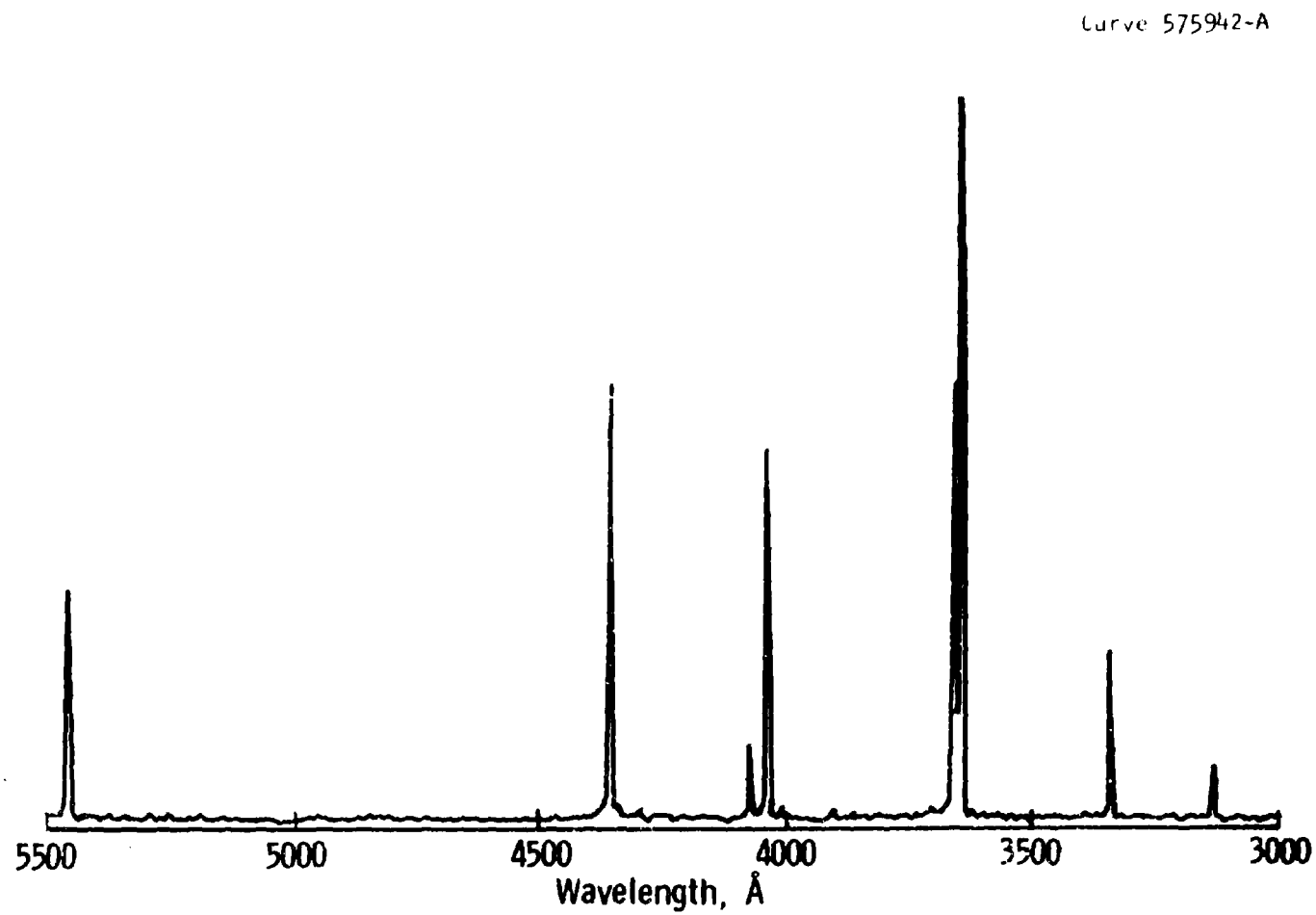

Fig. 108—Spectra of CsI additive lamp #L79A at 600 watts input

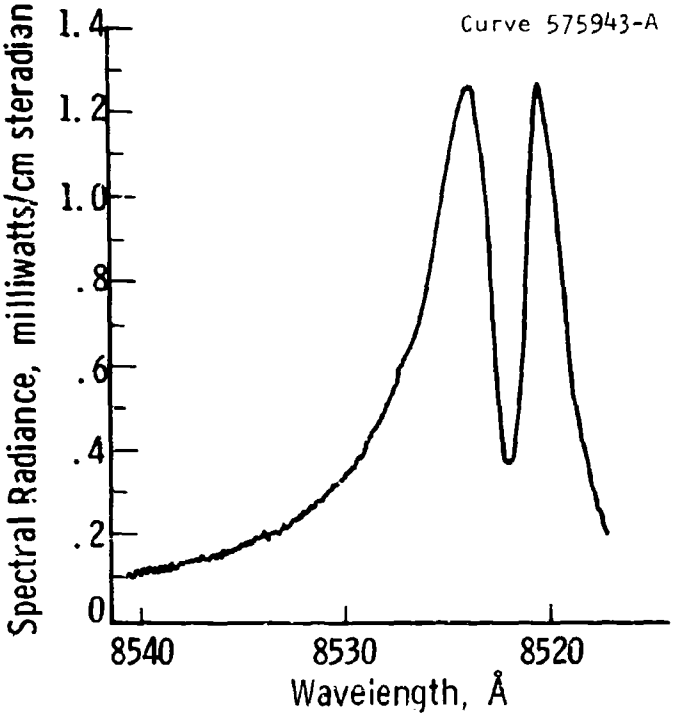

Fig. 109—High resolution scan of the 8512 Å Cs line at 600 watts

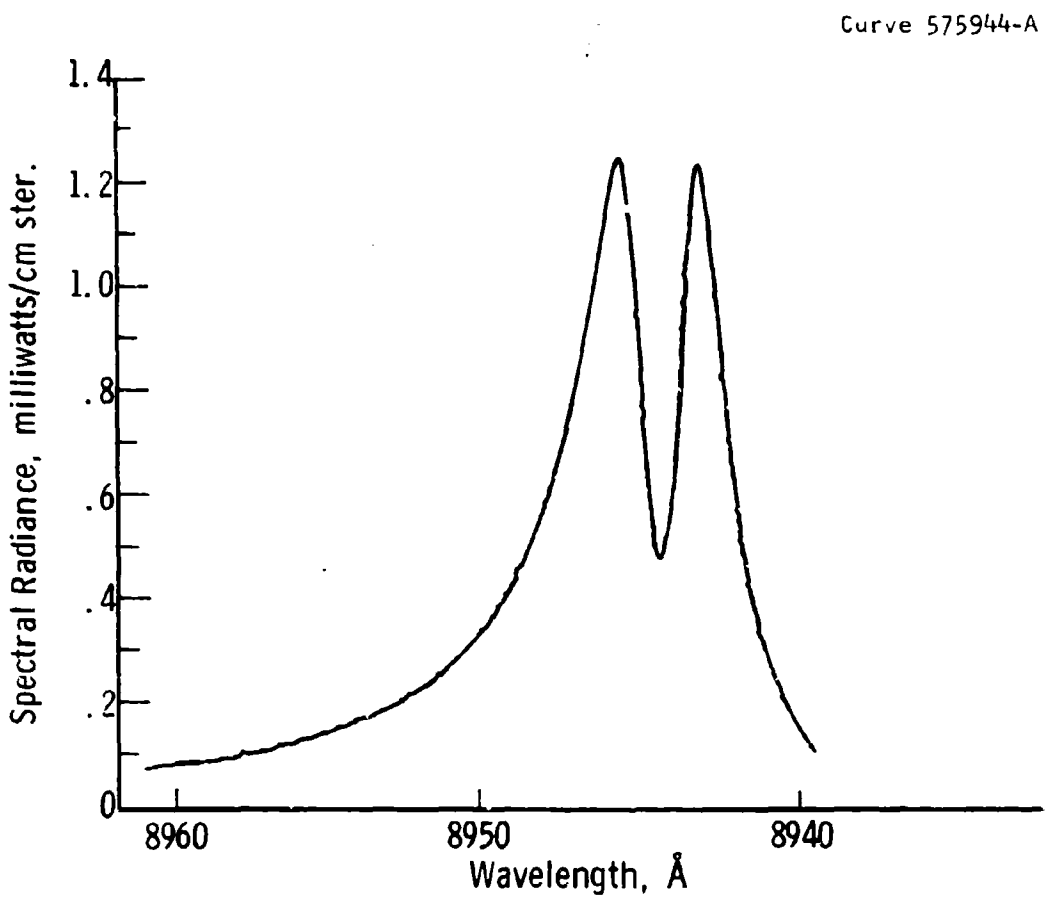

Fig. 110—High resolution scan of the 8944 Å Cs line at 600 watts

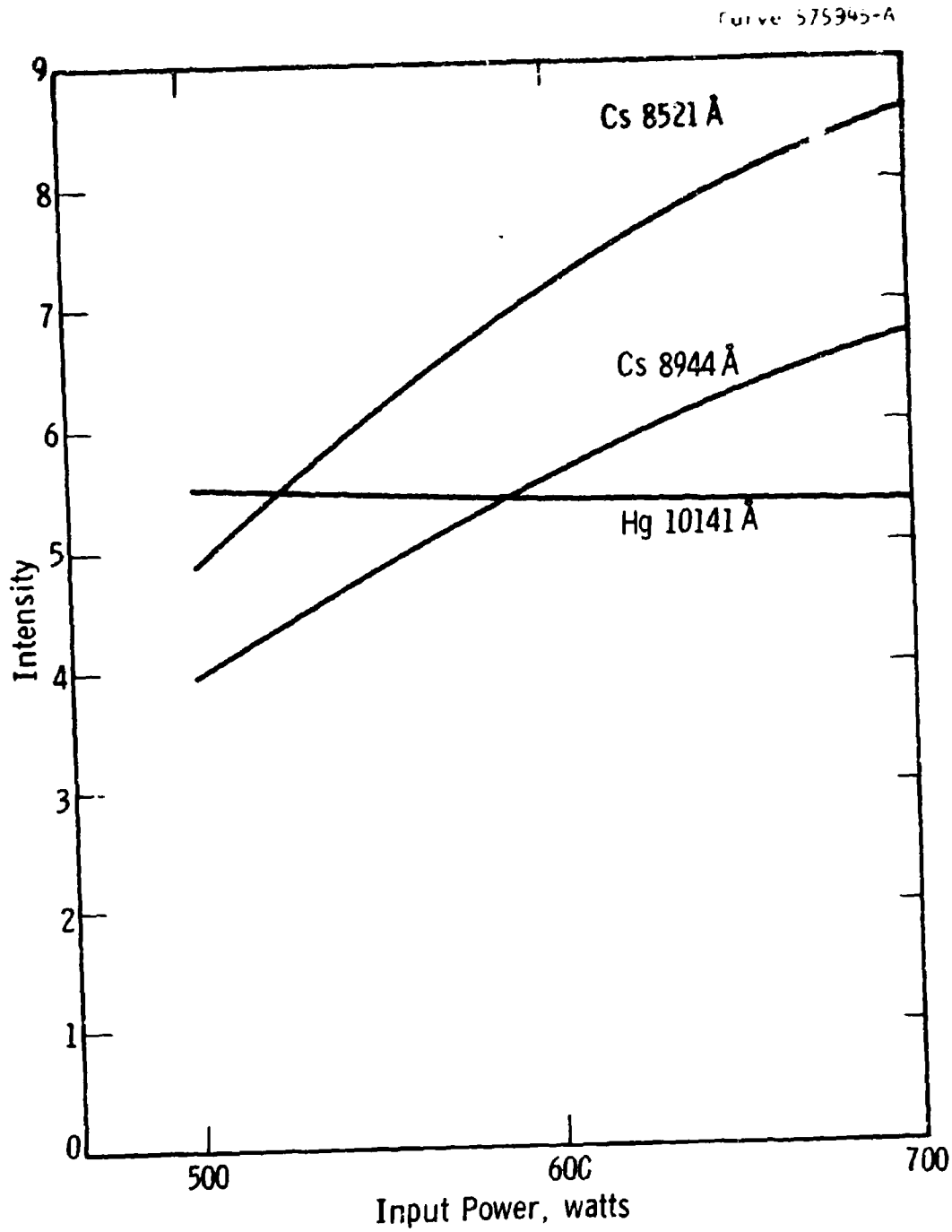

Fig. 111—Peak intensity vs power input for the 8512 Å and 8944 Å Cs lines and the 10, 139 Å Hg line

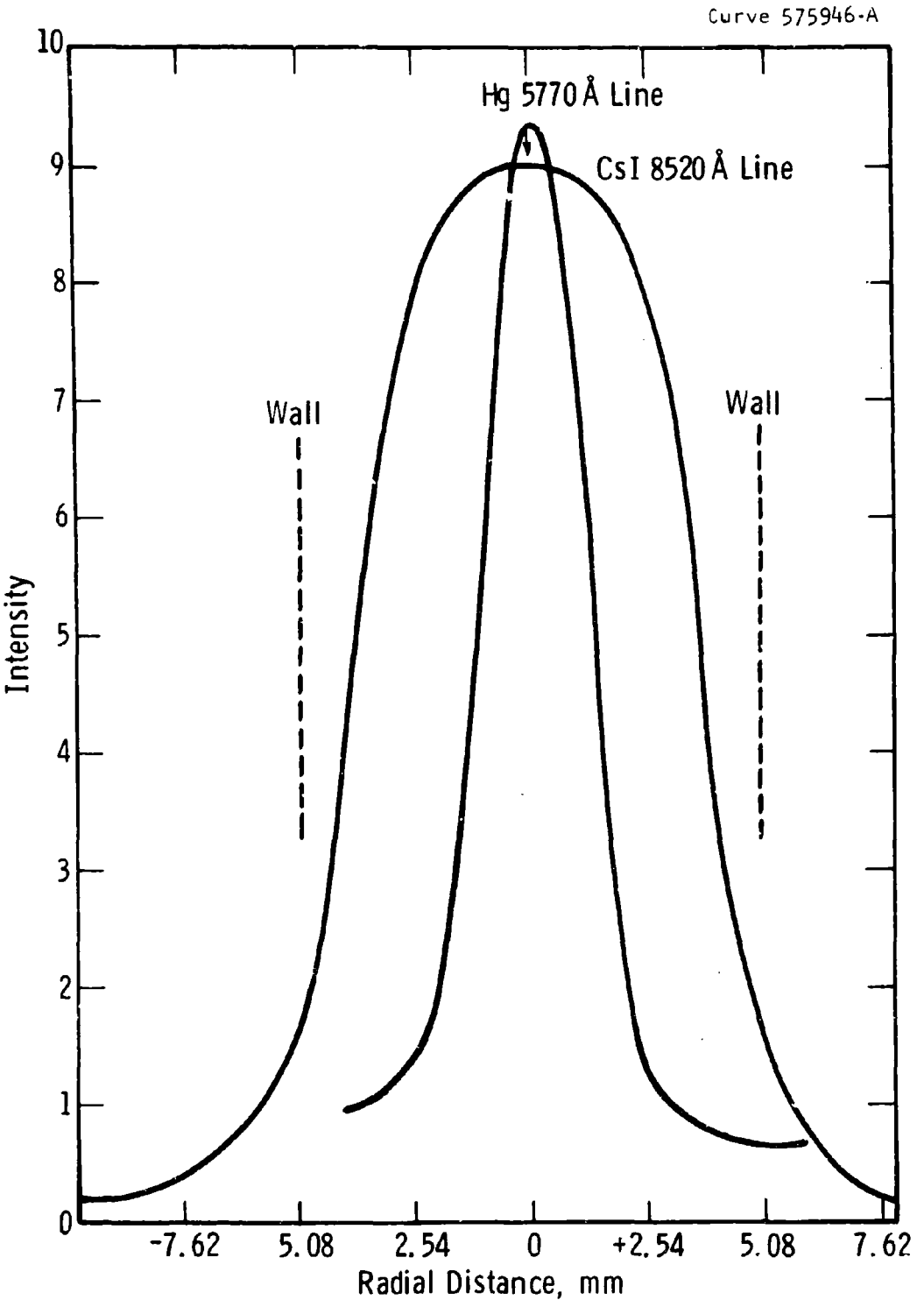

Fig. 112—Radial scan of the 8521 Å Cs line and the 5770 Å Hg line

Curve 575947-A

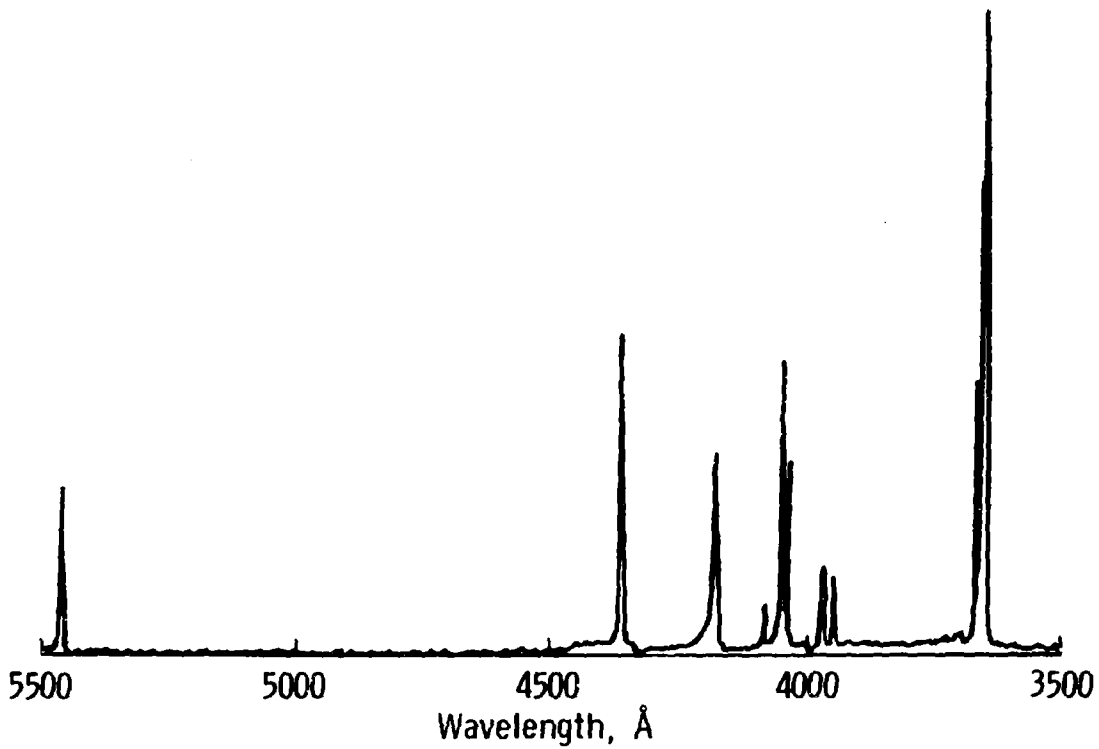

Fig. 113—Spectra of GaI additive lamp #L110 at 400 watts

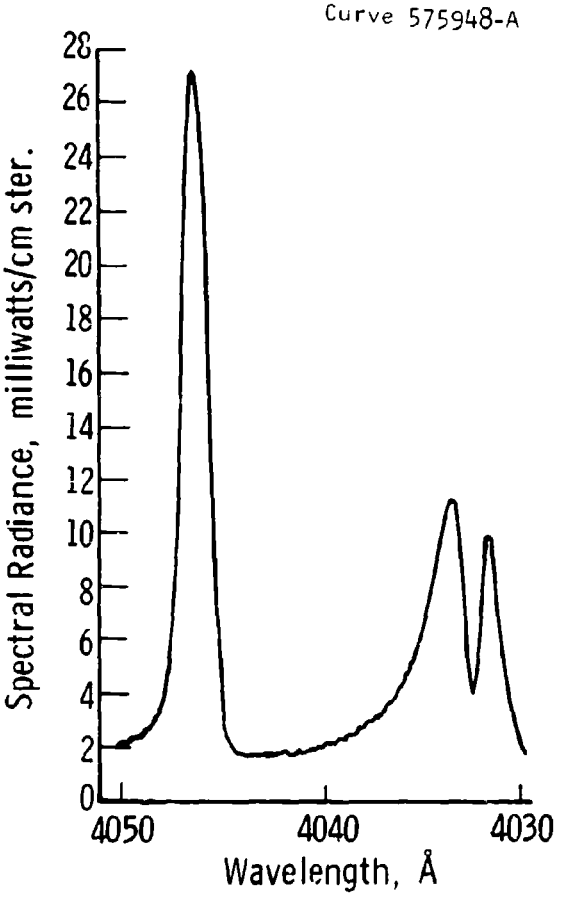

Fig. 114 High resolution scan of the 4033 Å Ga line and the 4047 Å Hg line at 400 watts

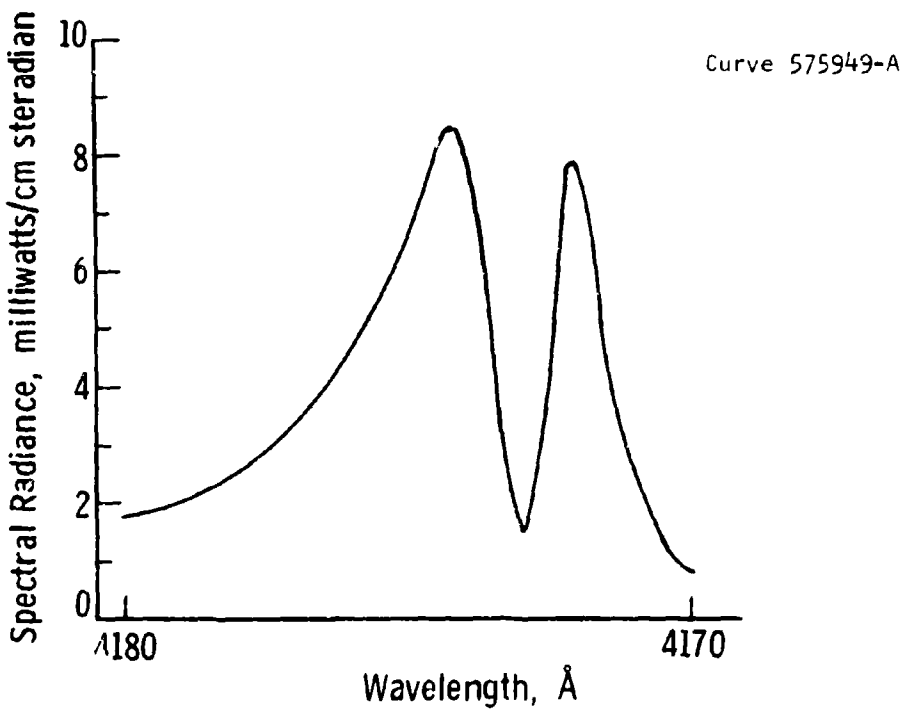

Fig. 115—High resolution scan of the 4172 Å Ga line at 400 watts

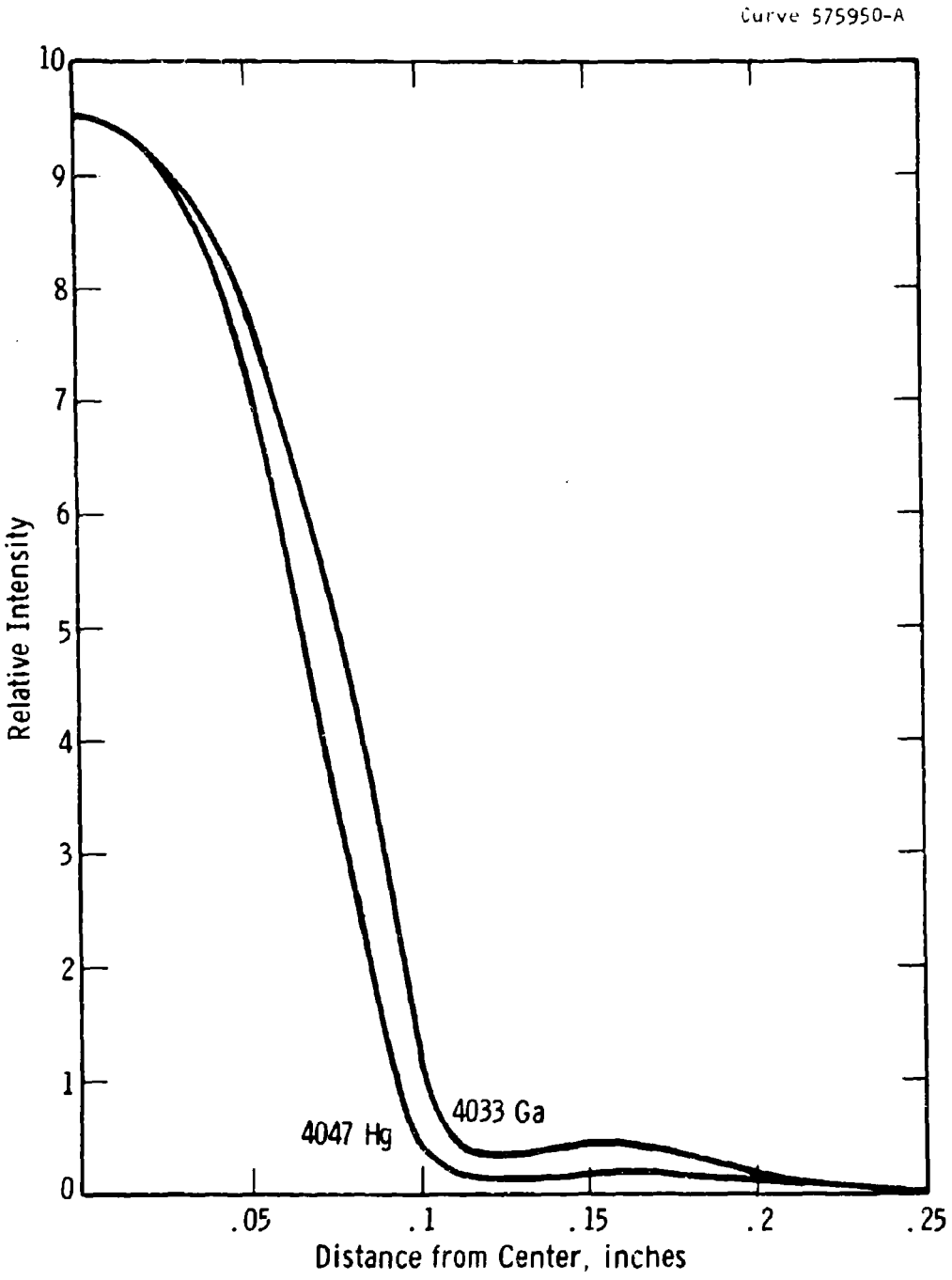

Fig; 116-Radial scans of the 4033 Å Ga resonance line and the 4047 Å Hg line

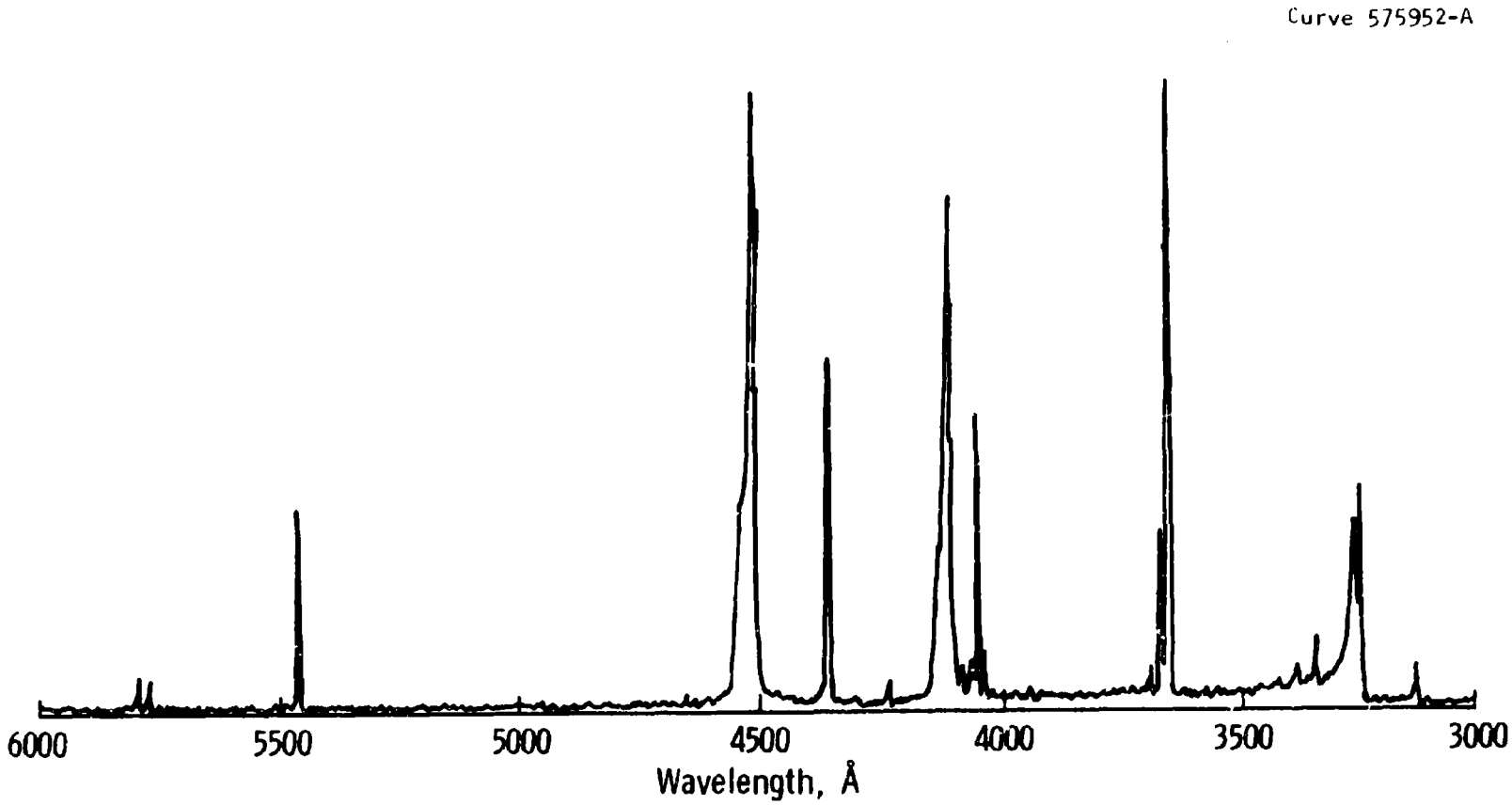

Fig. 117—Spectra of InI additive lamp #L106 at 450 watts

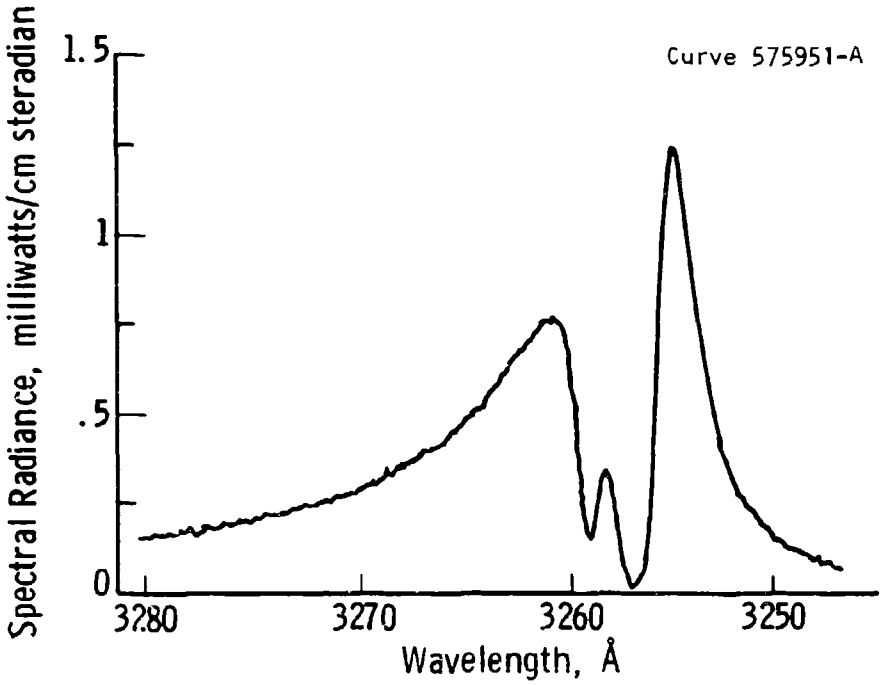

Fig. 118—High resolution scan of the 3256 Å In line at 450 watts

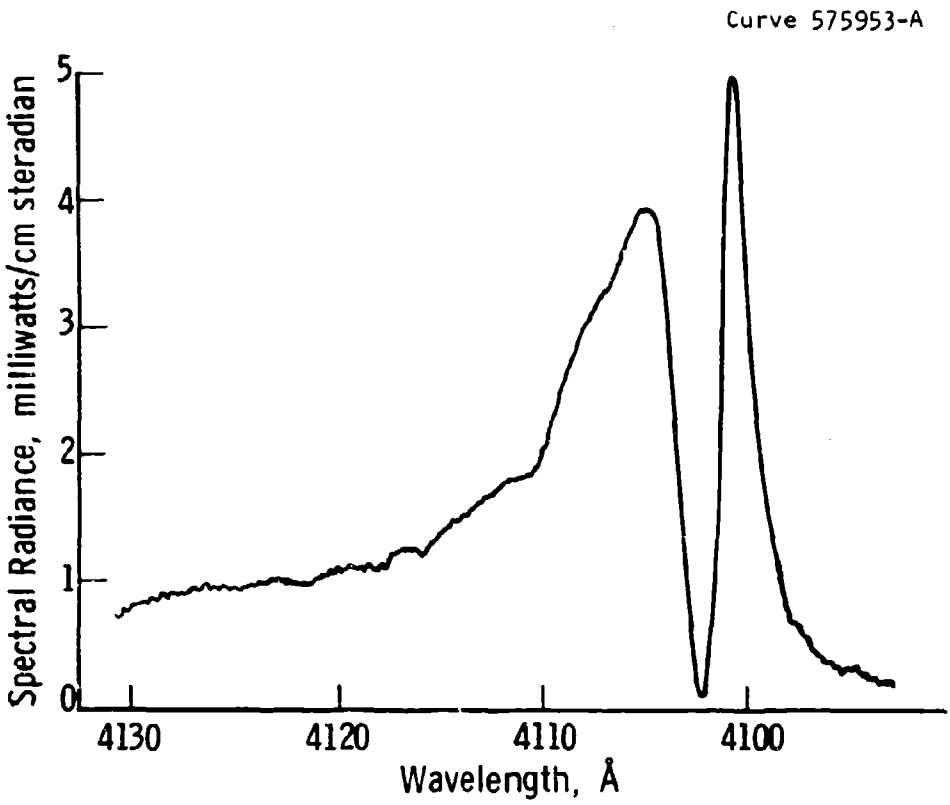

Fig.119—High resolution scan of the 4102 Å In line at 450 watts

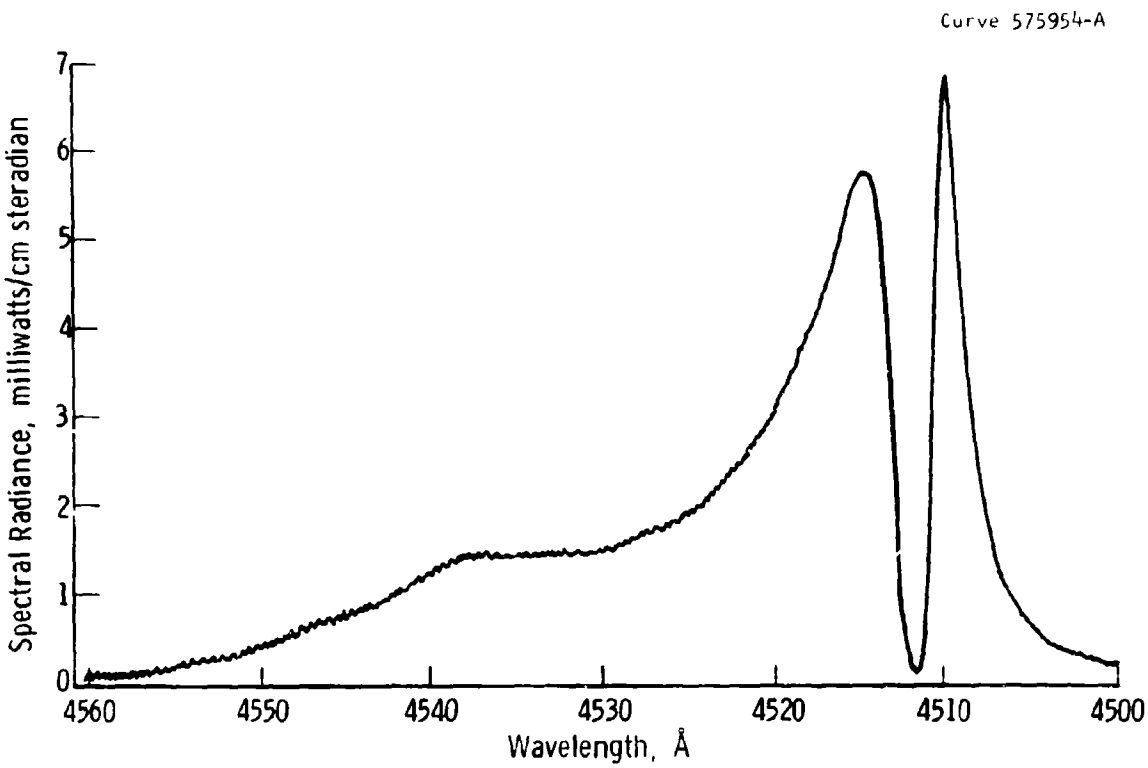

Fig. 120—High resolution scan of the 4511 Å In line at 450 watts

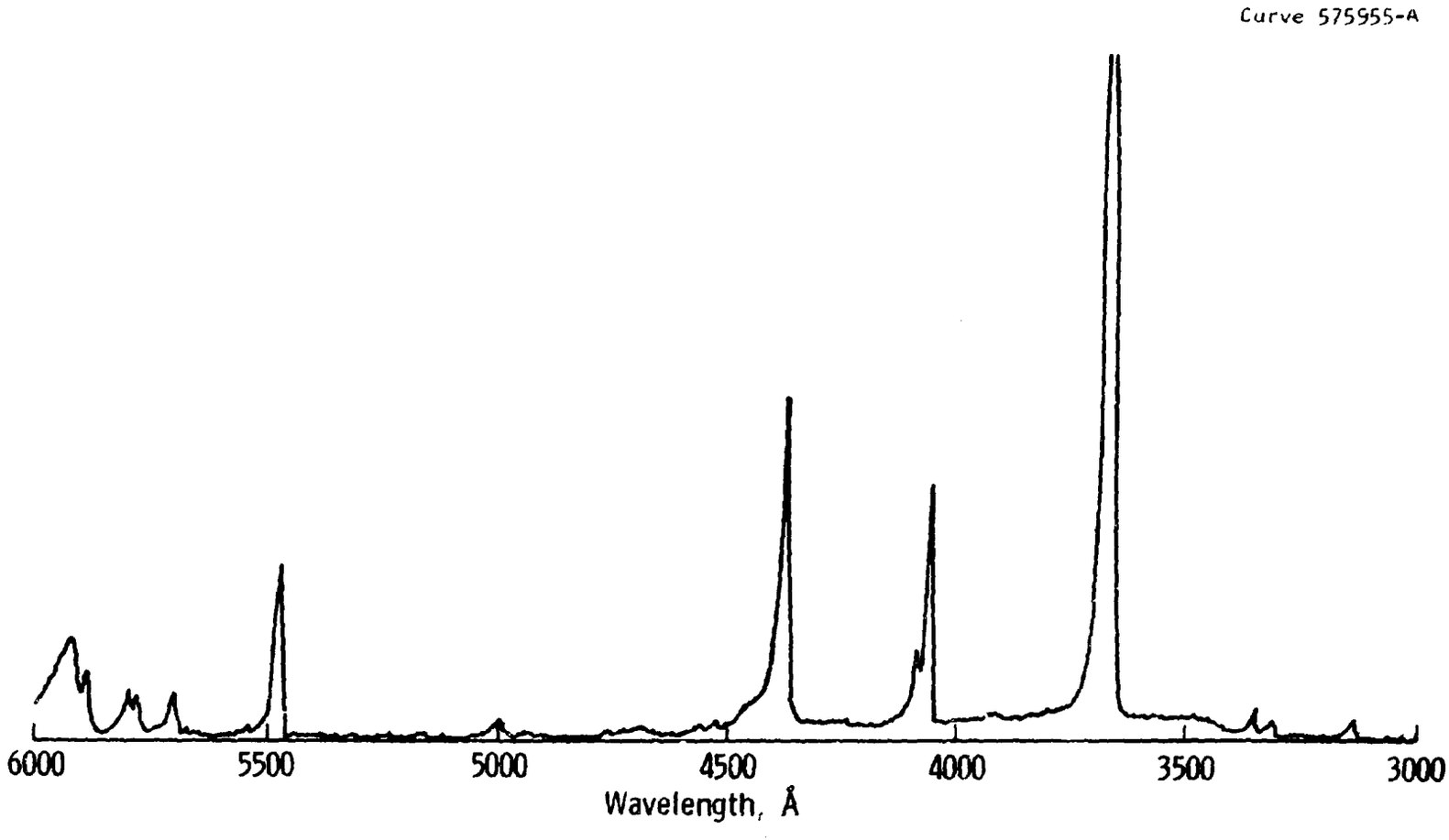

Fig.121—Spectra of NaI additive lamp [illegible]3 at 290 watts

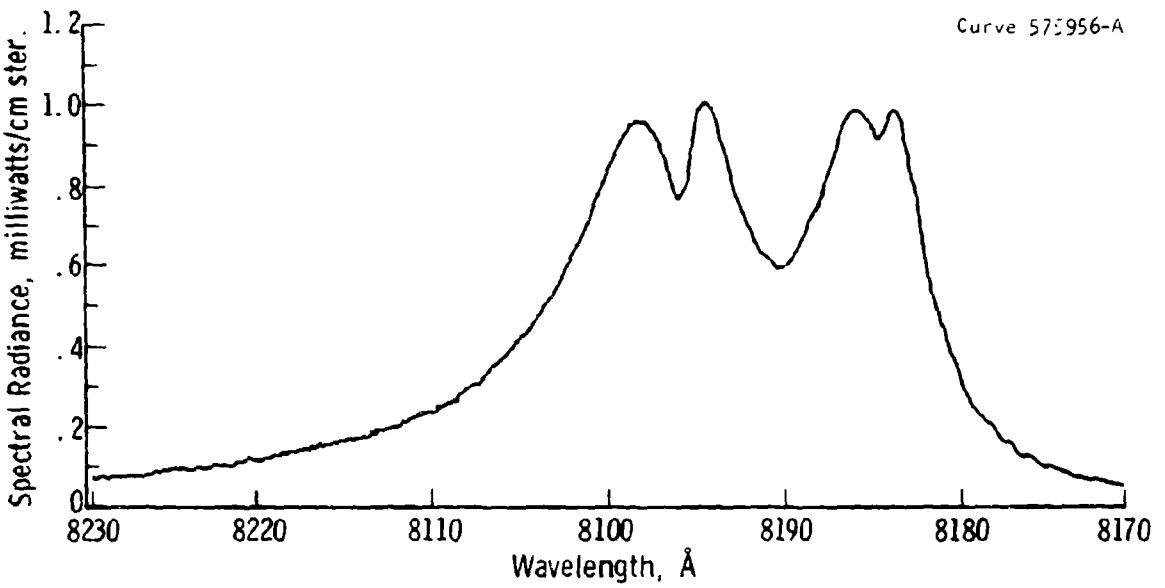

Fig. 122—High resolution scan of the 8183 Å and 8195 Å lines of Na at 290 watts

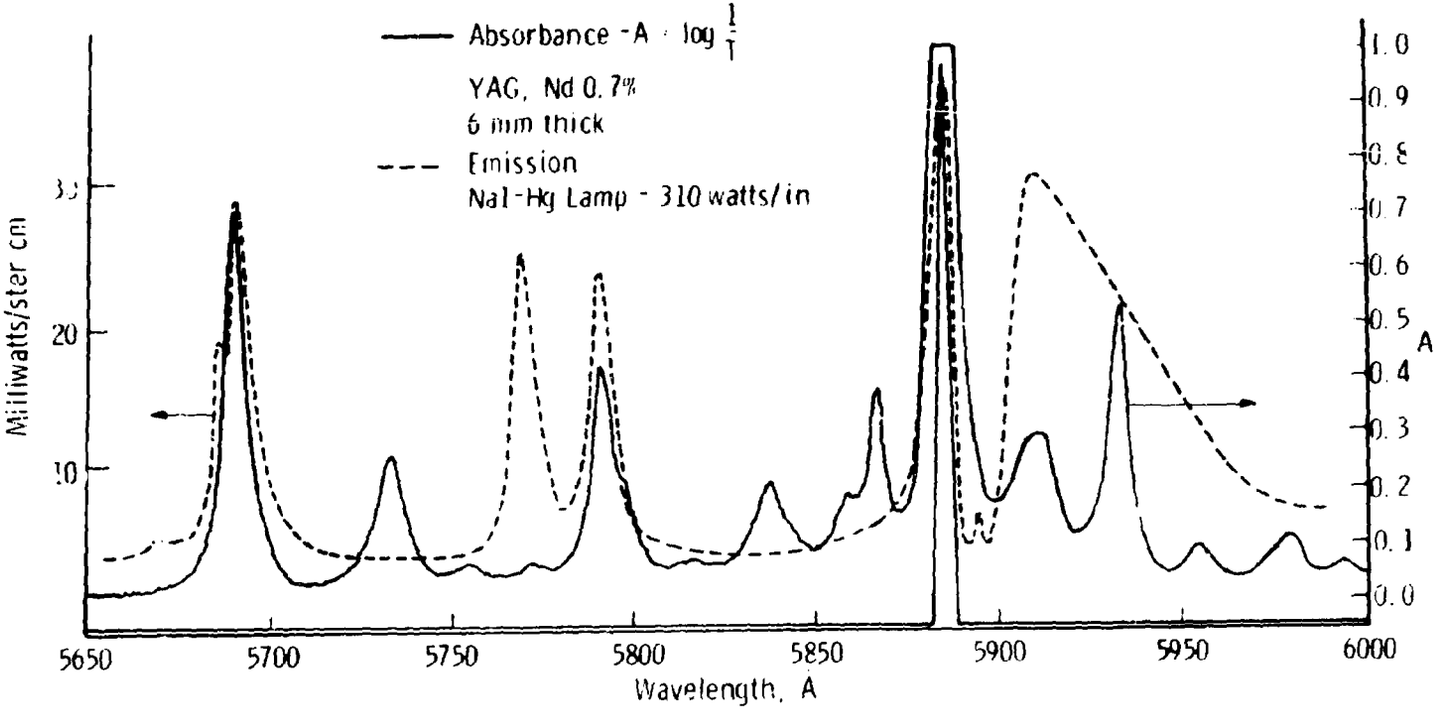

Fig. 123— High resolution scan from 5650 A to 6000 A of the NaI additive lamp (3.5 x 10 mm) with the absorbance spectrum of Nd^{3+} in YAG

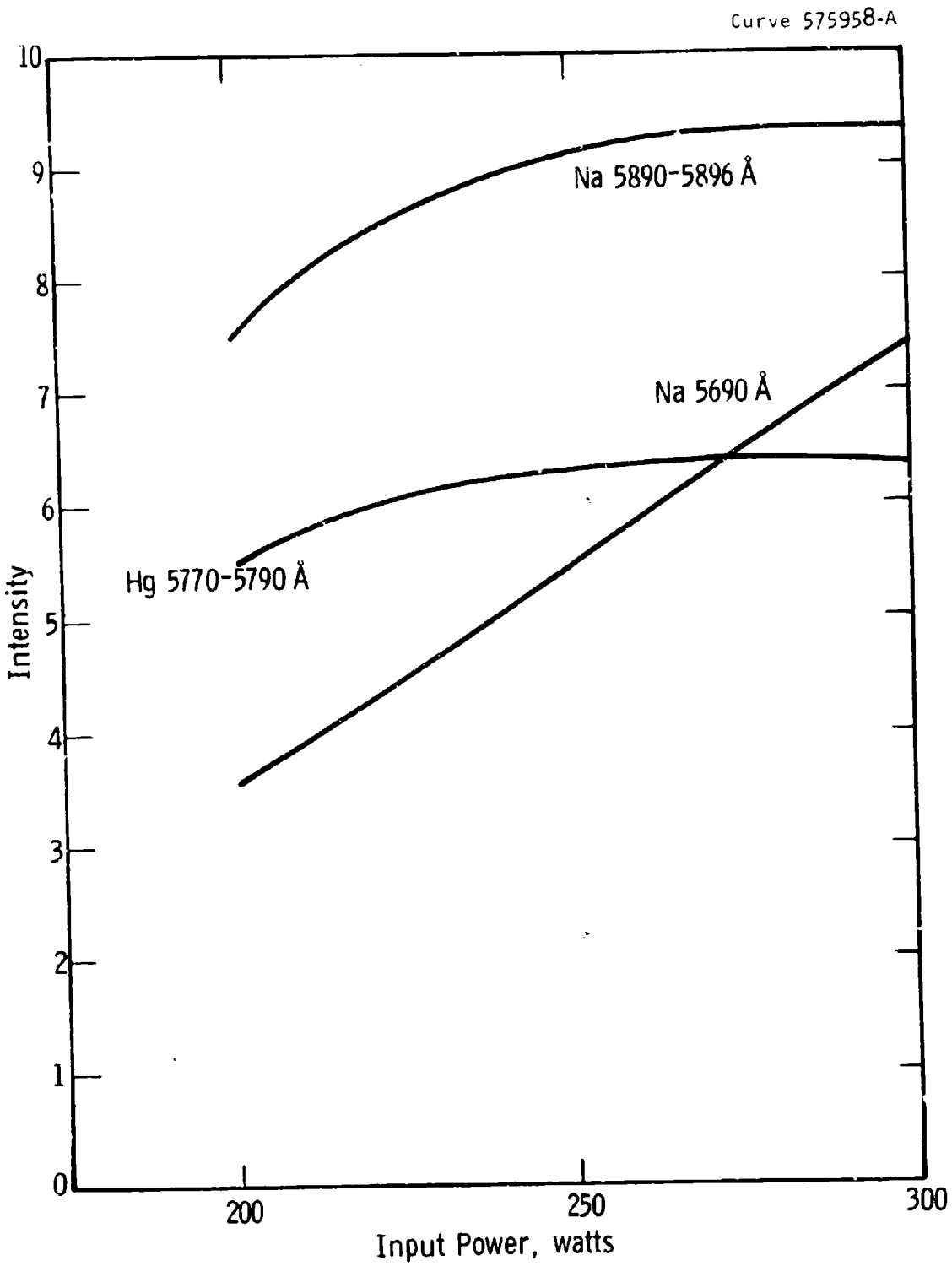

Fig. 124—Peak intensity vs power input of the 5690 Å line and the 6890-5896 Å doublet of Na and the 5770 Å Hg line

Appendix A

Table of Temperatures Required
for 1 Torr and 760 Torr of Various
Metallic Additives

Energy Level Diagrams for
Various Metallic Additives

Temperature Required for 1 Torr and 760 Torr for Various Metal Iodides

Iodide	1 Torr	760 Torr
GaI_3	~140°C	346°C
HgI_2	157.5	354
InI_3	-	500
CaI_2	-	718
TlI	438	823
PoI_2	479	872
LiI	723	1171
CsI	738	1280
KI	745	1324
NaI	767	1304

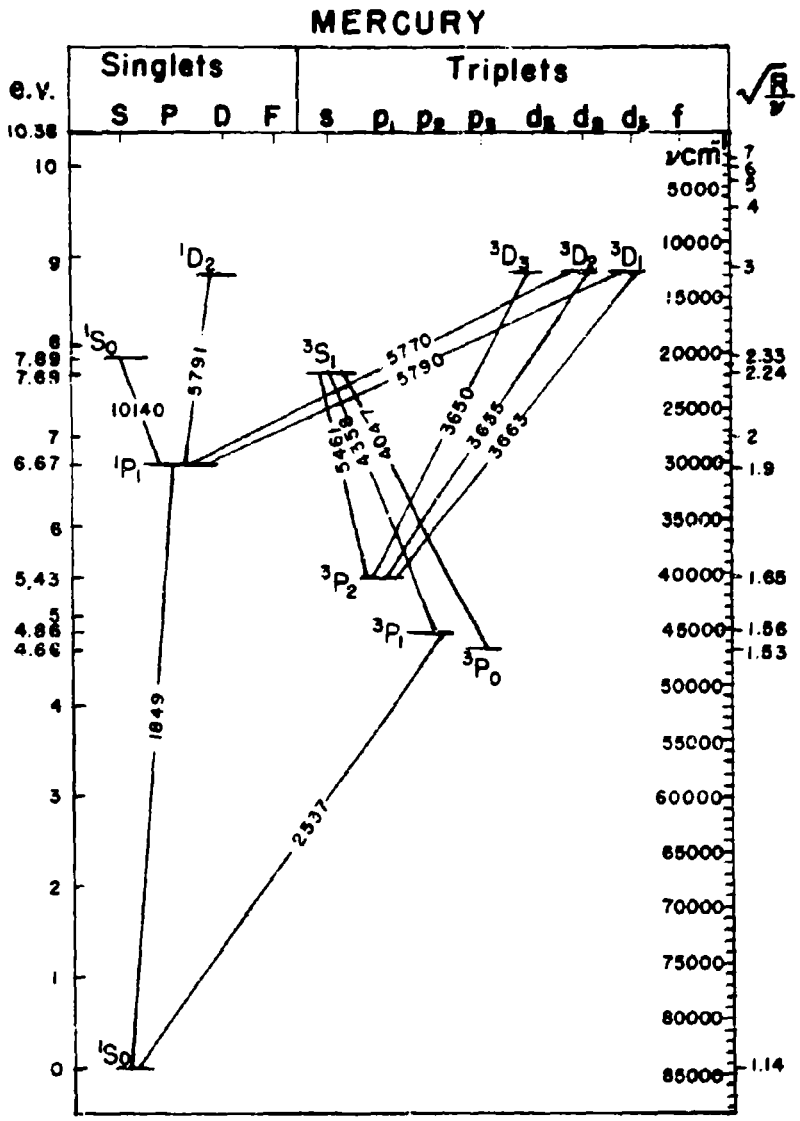

ENERGY LEVEL DIAGRAM

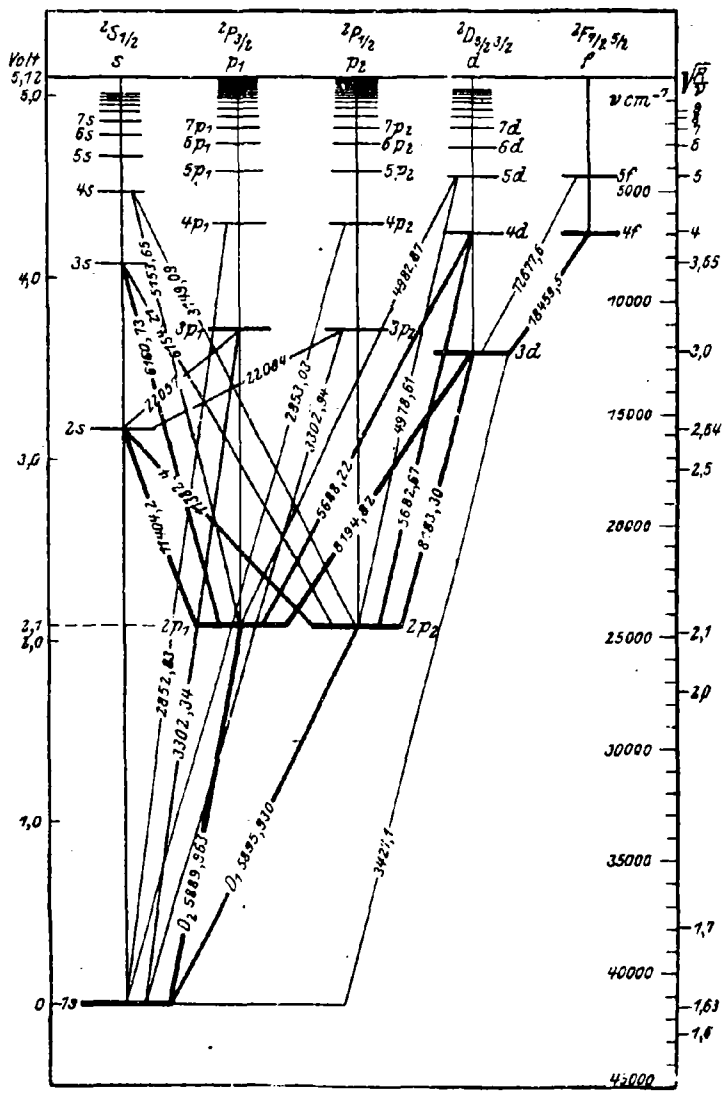

Fig. 18, II, Text S. 63 Niveauschema des Natrium I.

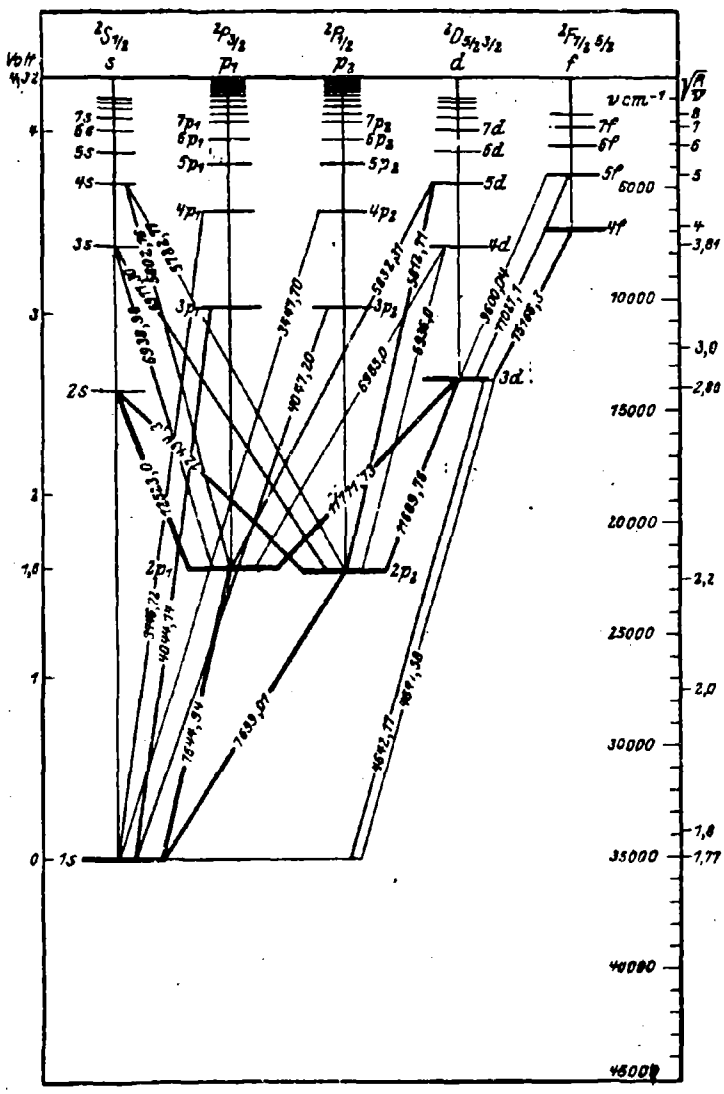

Fig. 25, II, Text S. 84. Niveauschema des Kalium I.

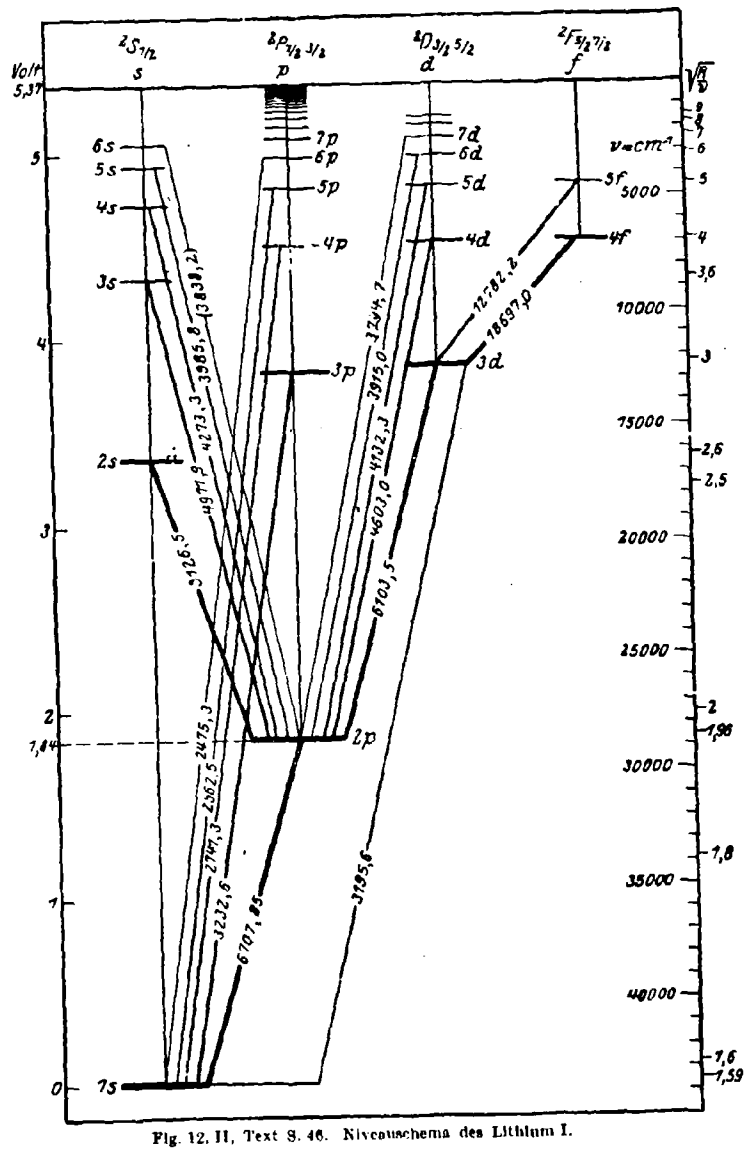

Fig. 12. II, Text S. 46. Niveauschema des Lithium I.

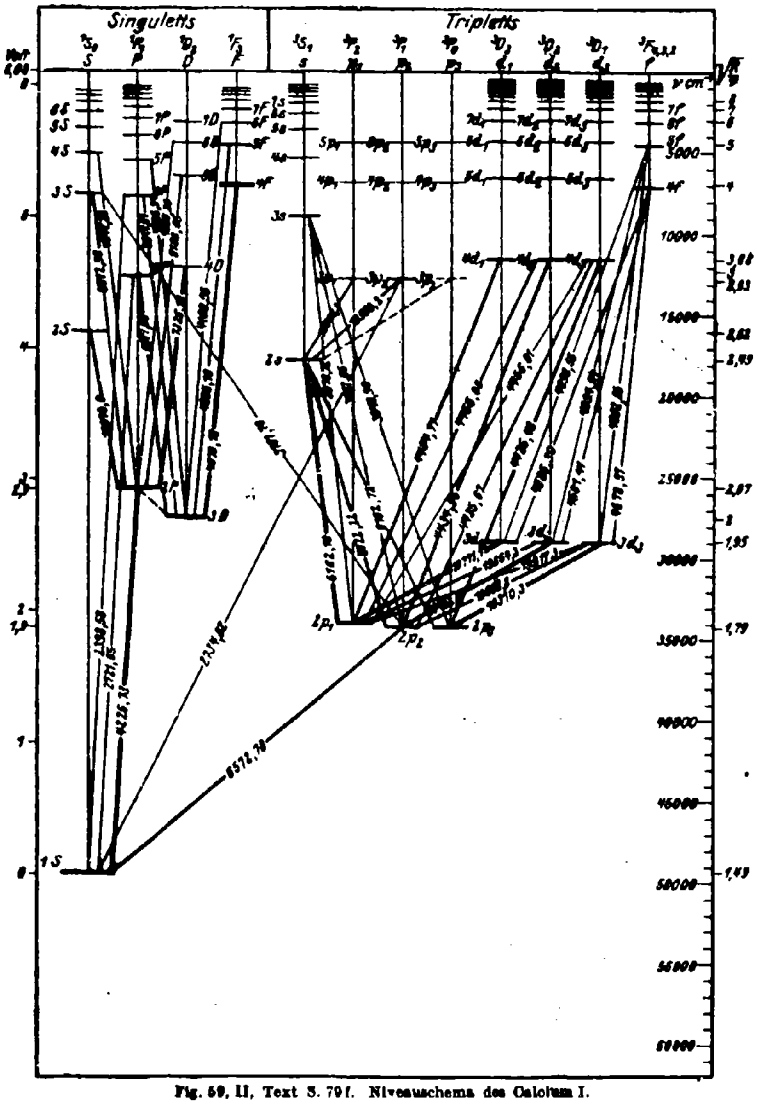

Fig. 59, II, Text S. 79 f. Niveauschema des Calcium I.

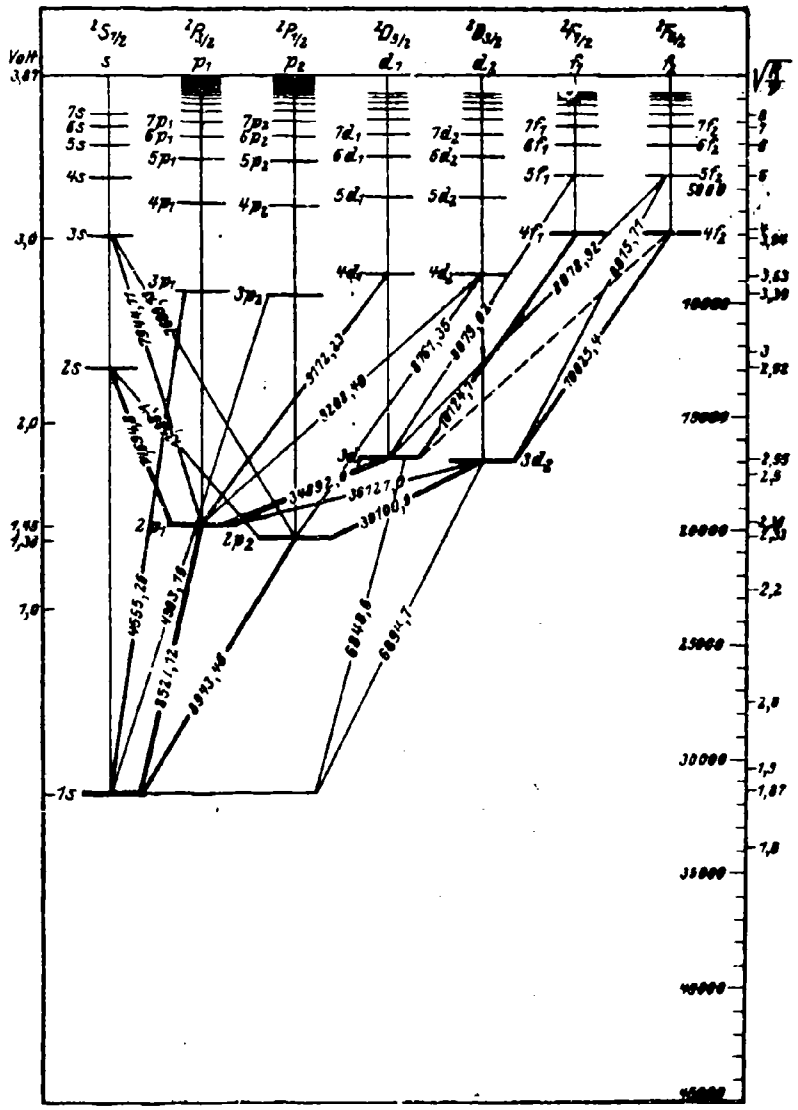

Fig. 36. II, Text S. 60. Niveauschema des Caesium I.

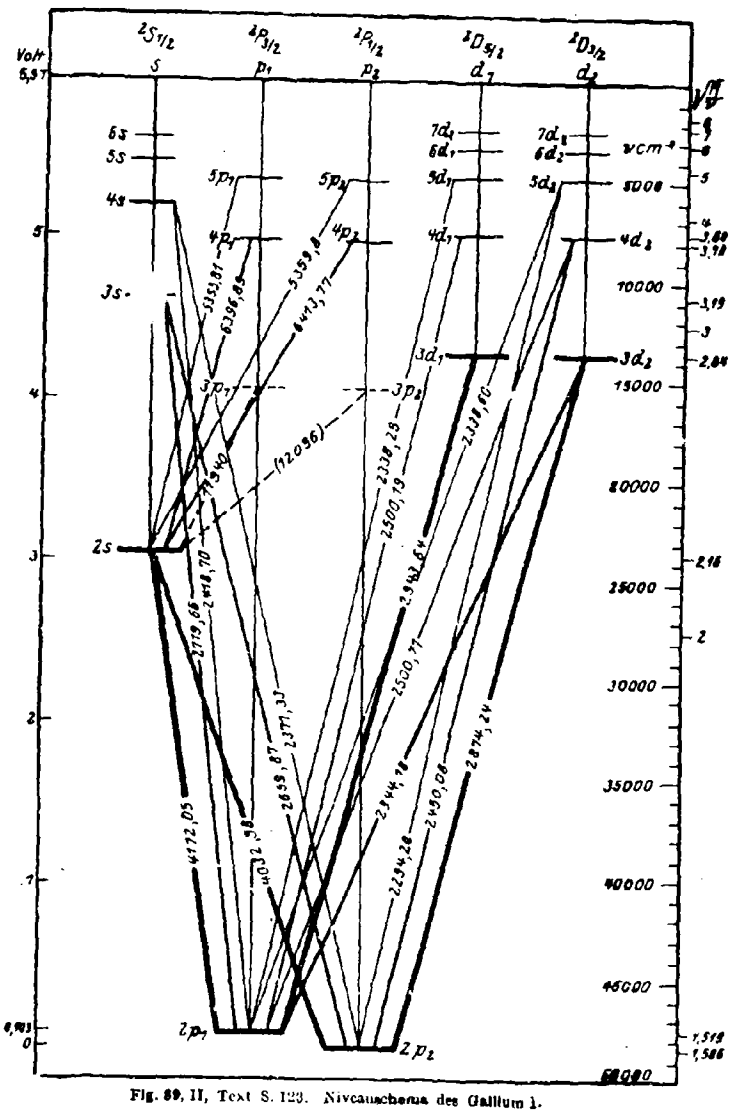

Fig. 89, II, Text S. 123. Niveauschema des Gallium I.

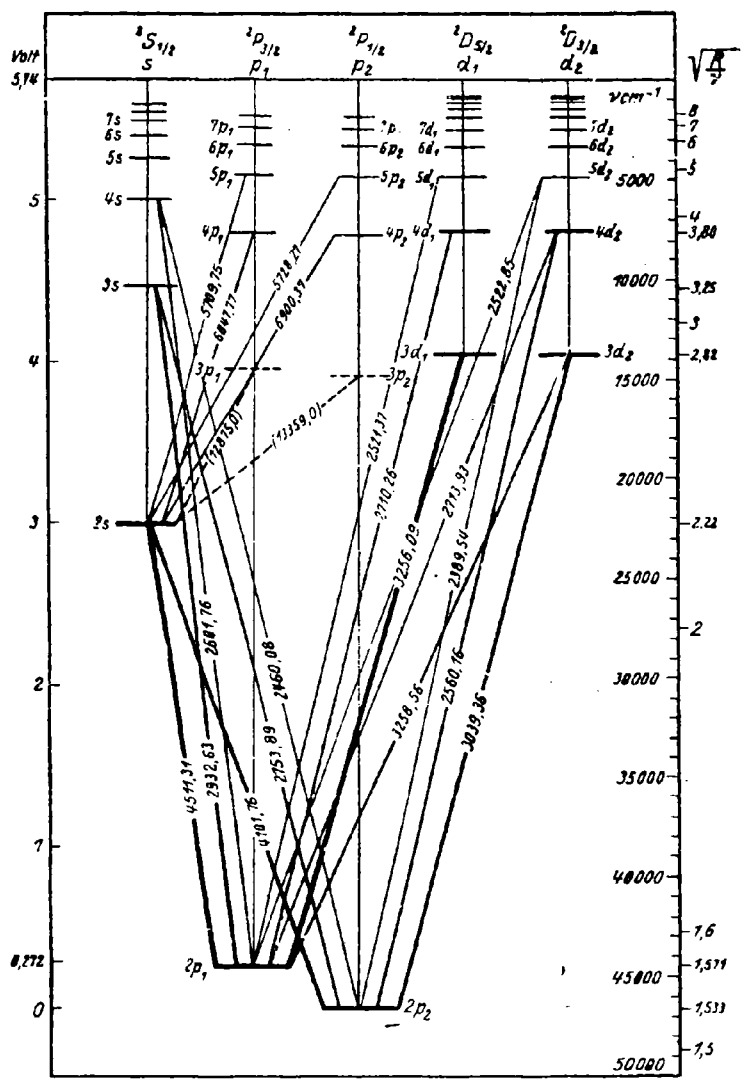

Fig. 92, II, Text S. 123. Niveauschema des Indium I.

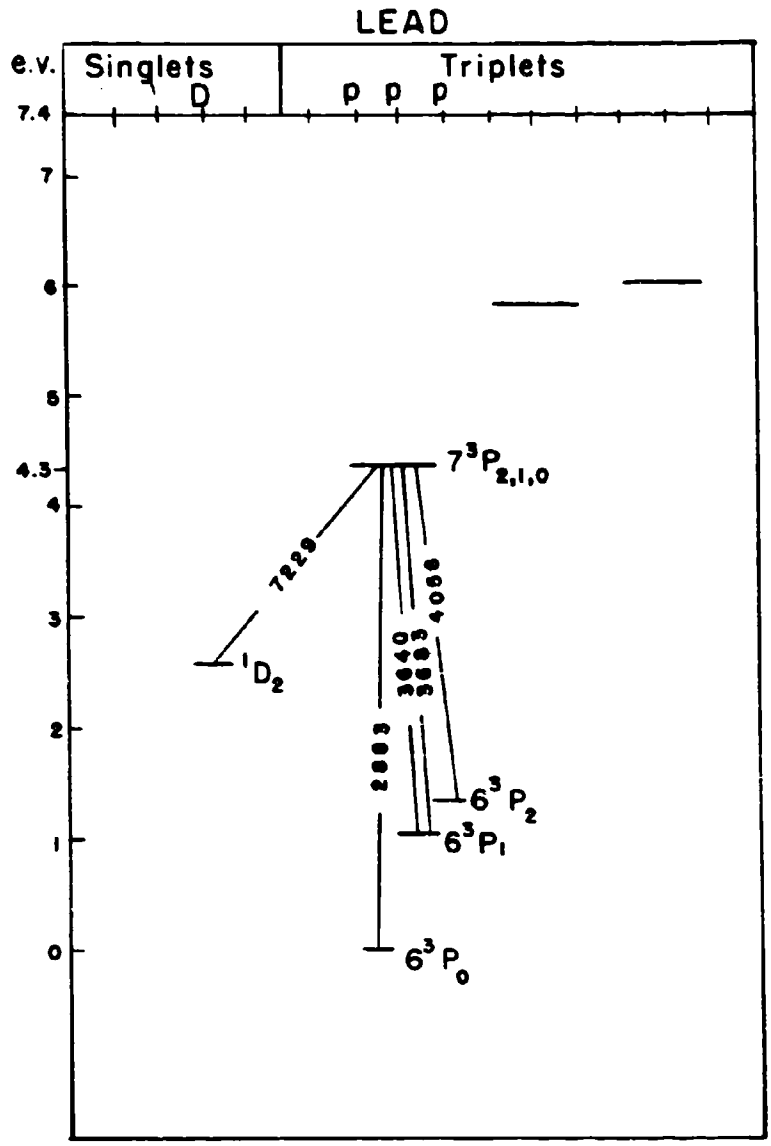

ENERGY LEVEL DIAGRAM

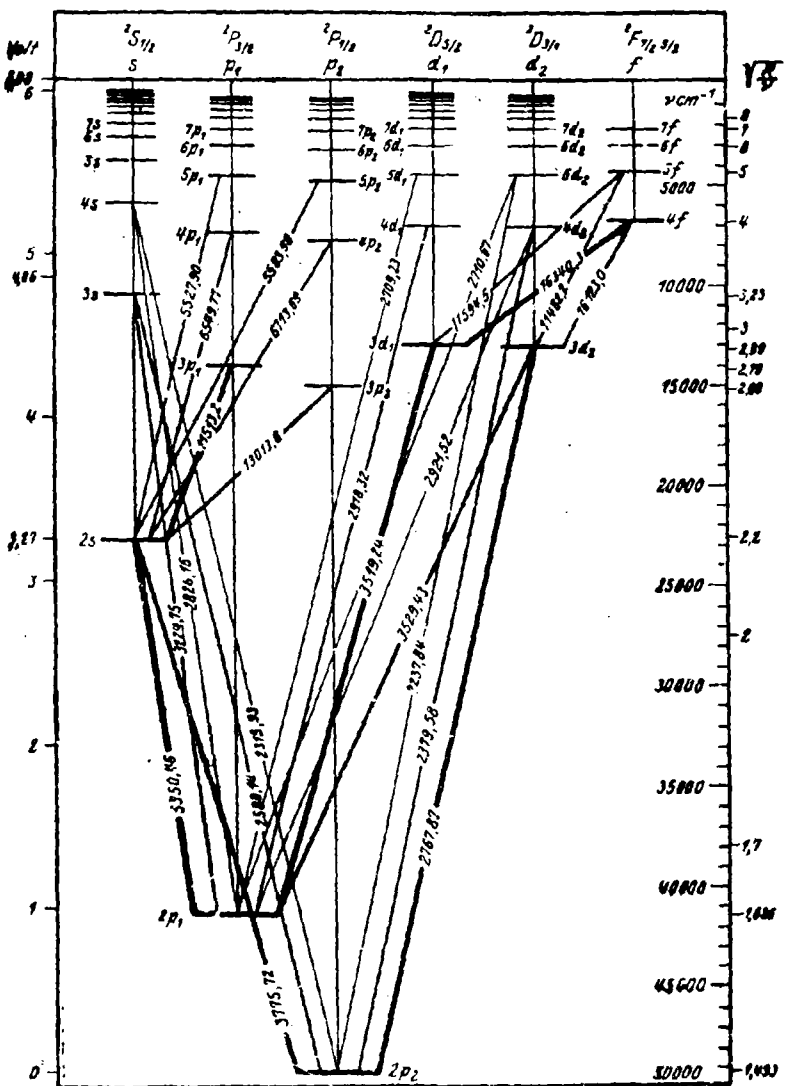

Fig. 95, II. Text S. 128. Niveauschema des Thallium I.

Appendix B

Transmission Curves for Filters Used in These Measurements

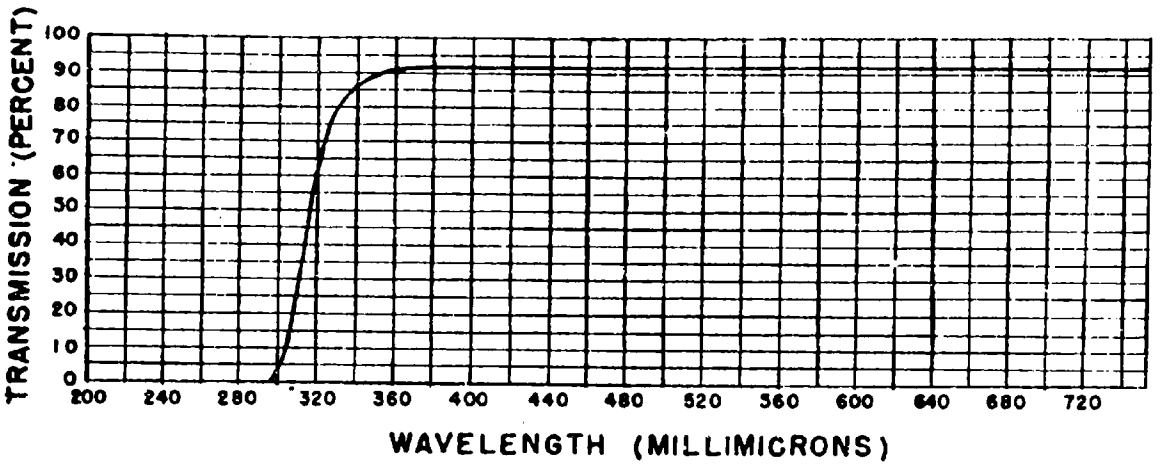

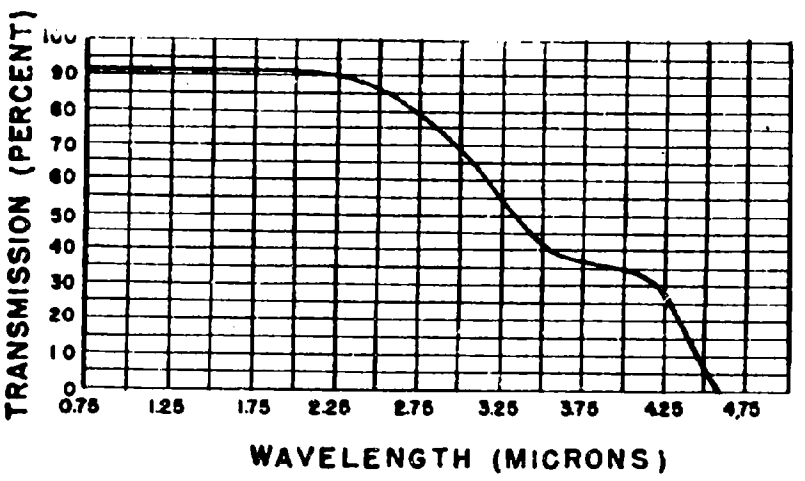

CORNING 0160 FILTER

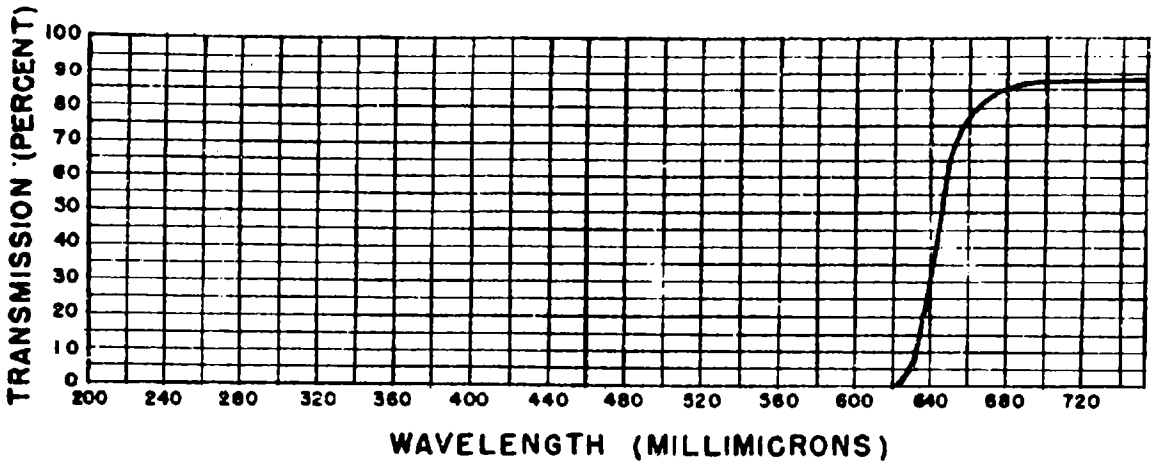

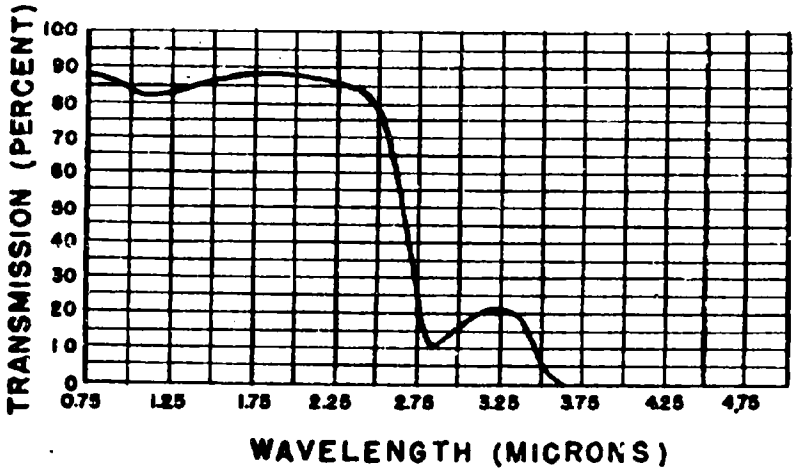

CORNING 2403 FILTER

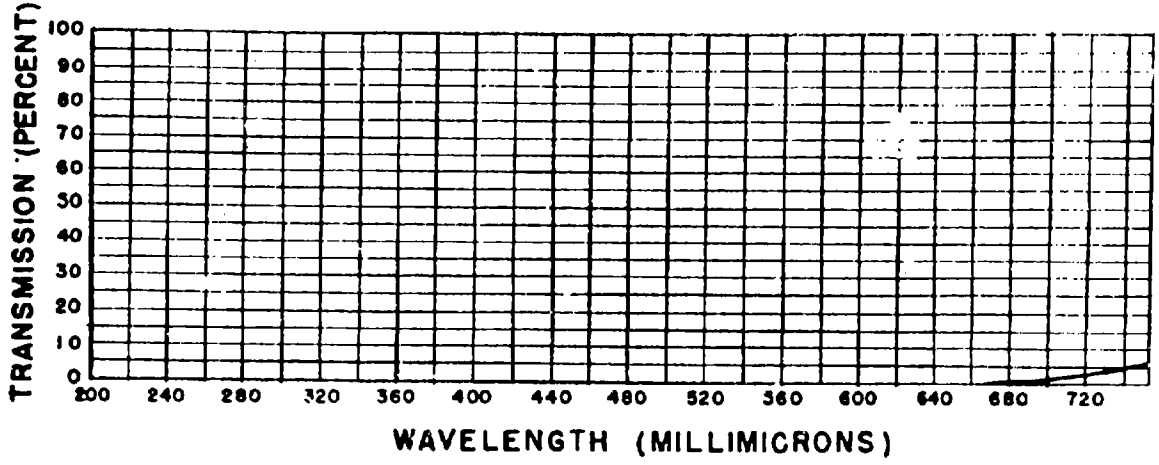

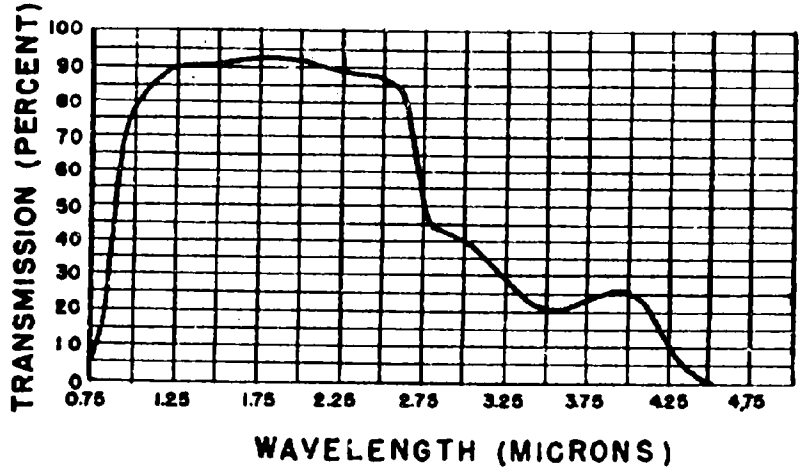

CORNI. 3 2550 FILTER

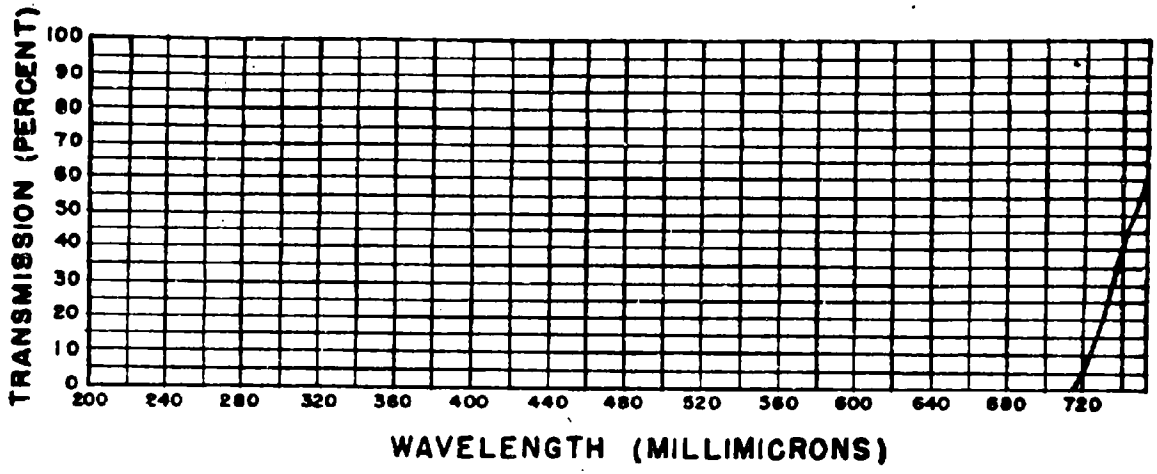

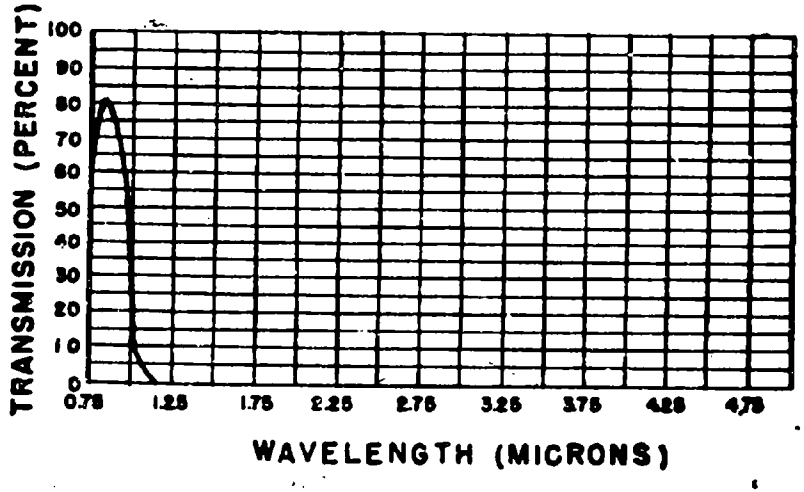

CORNING 2600 FILTER

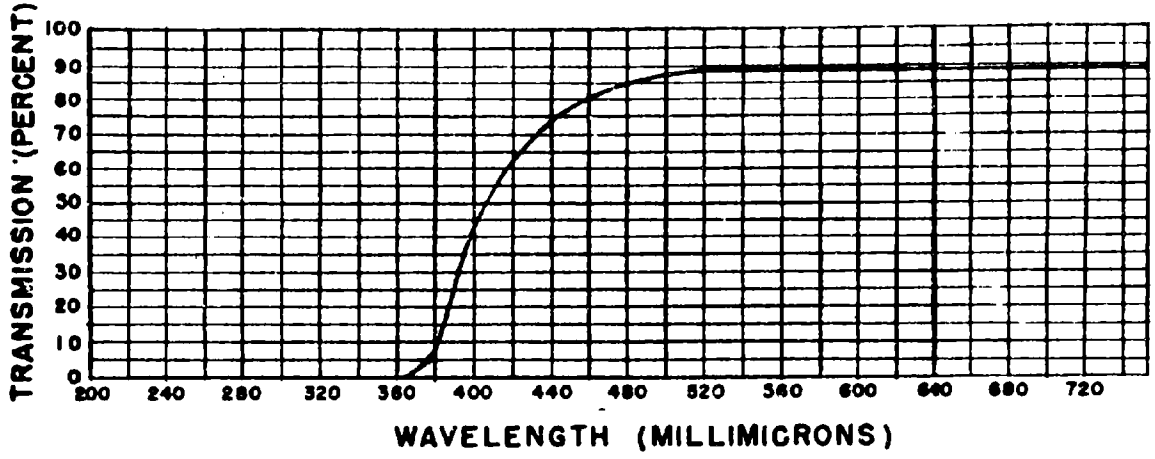

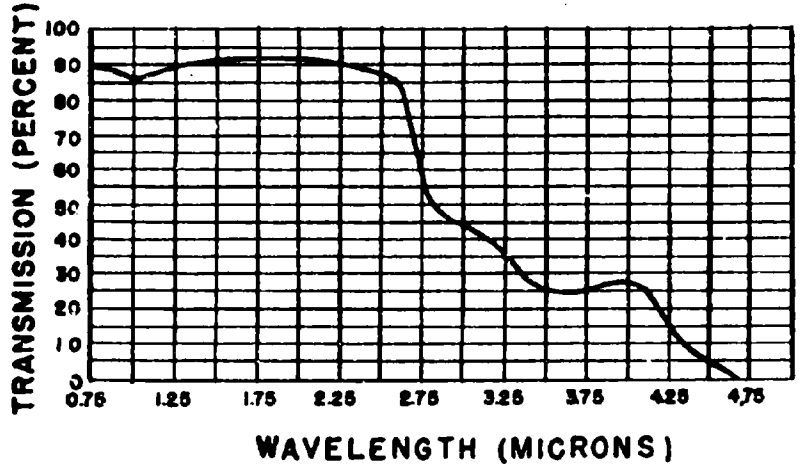

CORNING 3060 FILTER

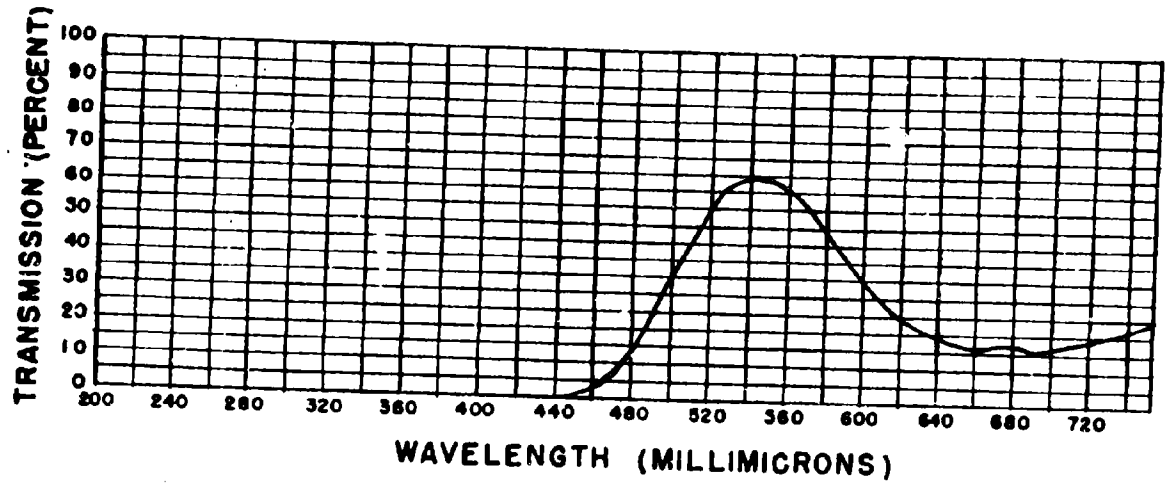

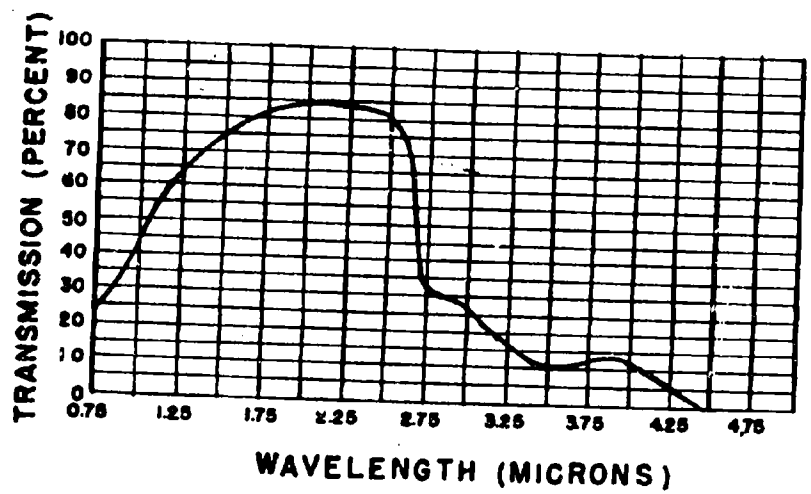

CORNING 4015 FILTER

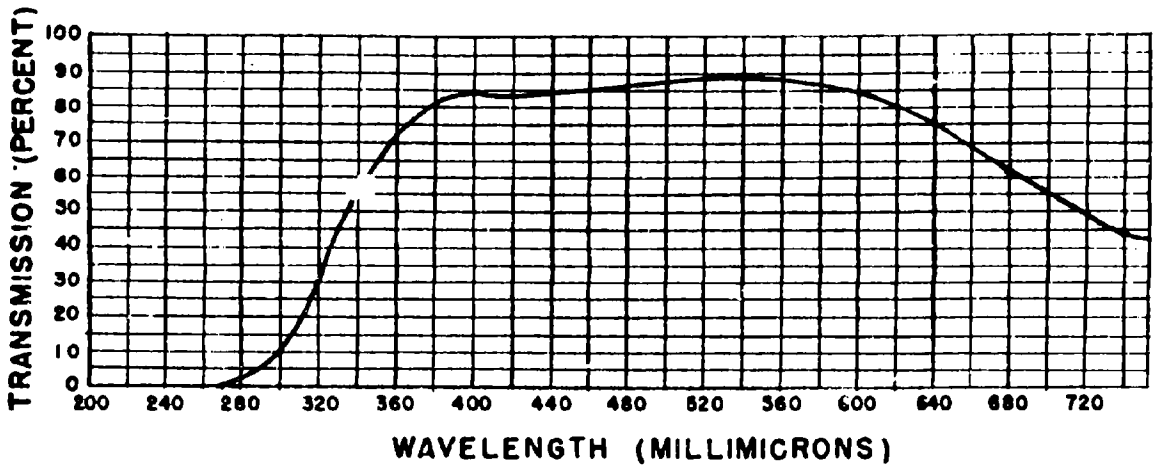

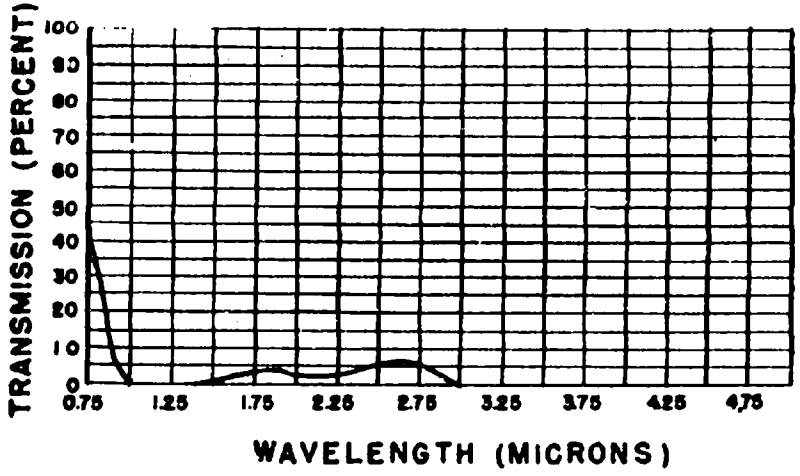

CORNING 4600 FILTER

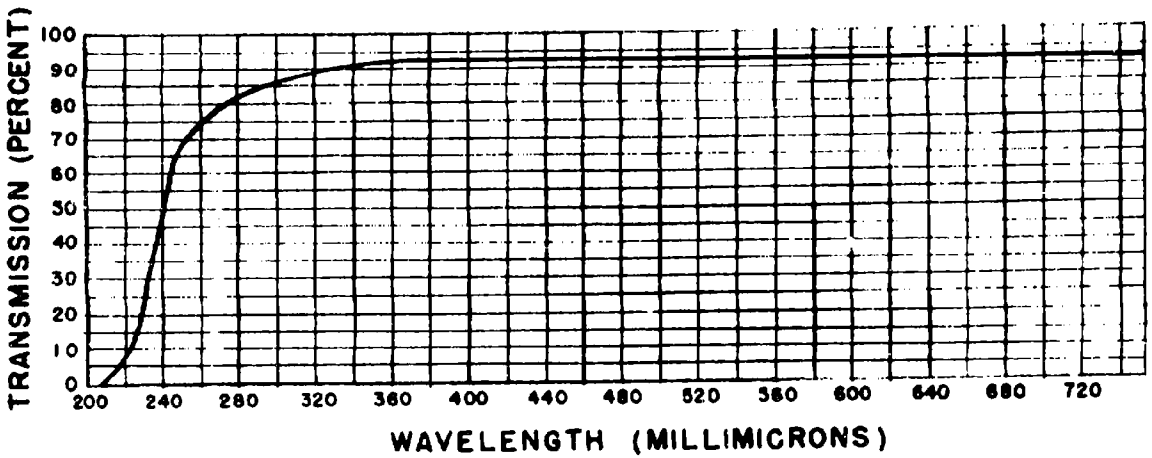

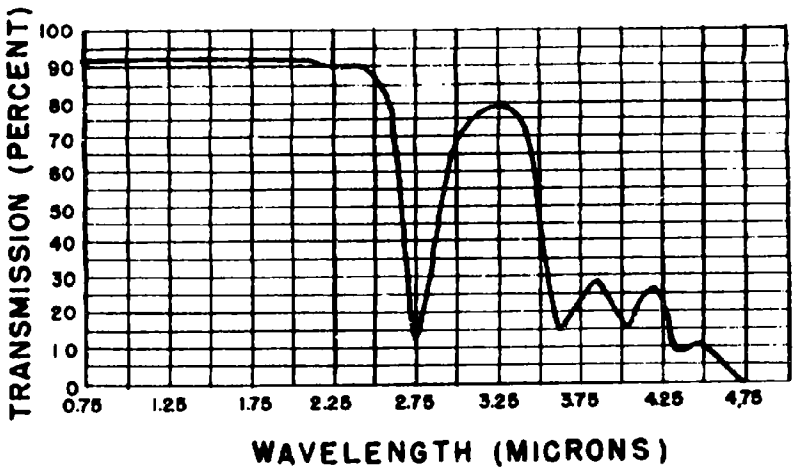

CORNING 7910 FILTER

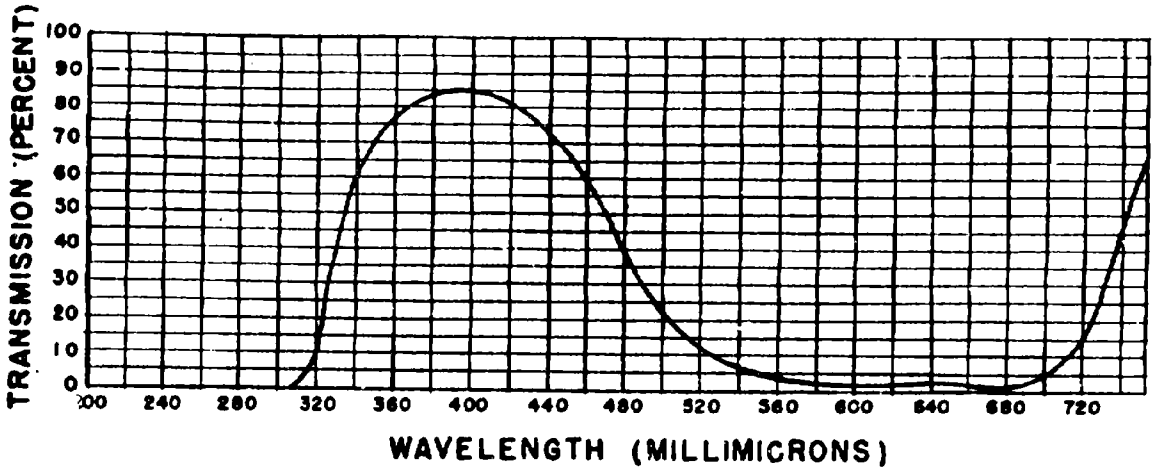

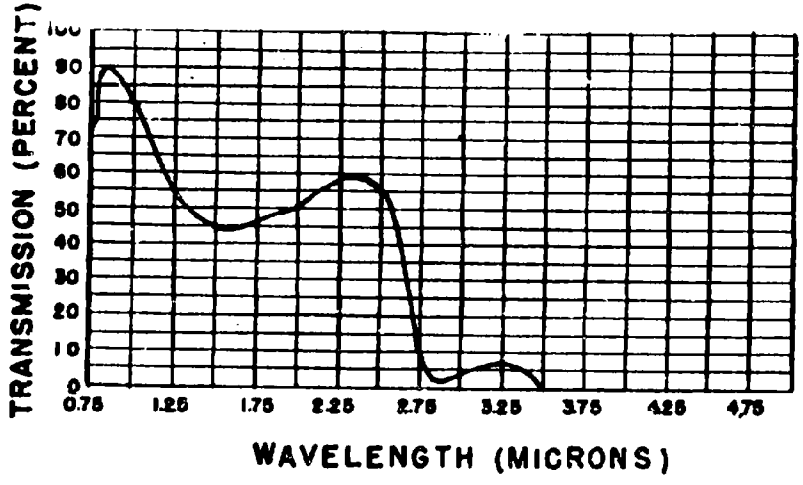

CORNING 5330 FILTER

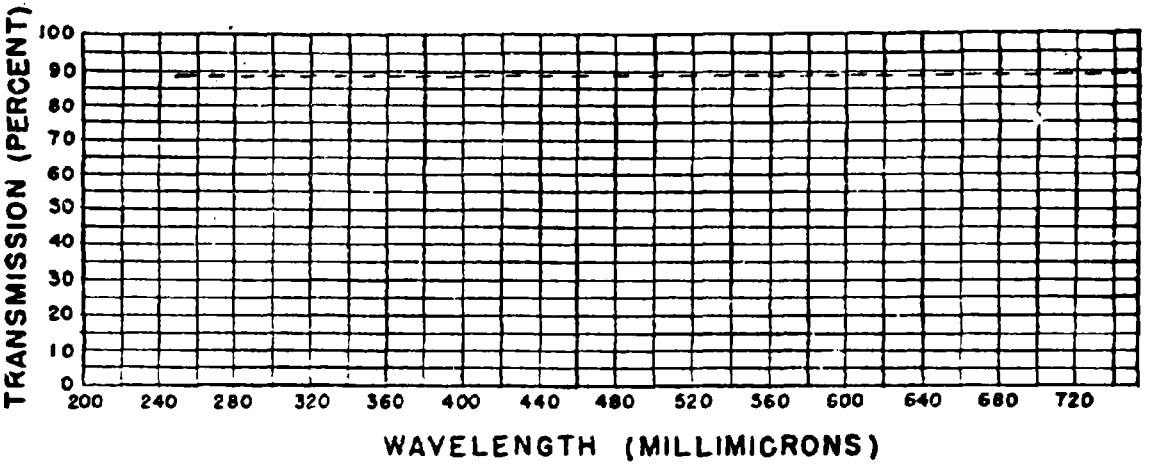

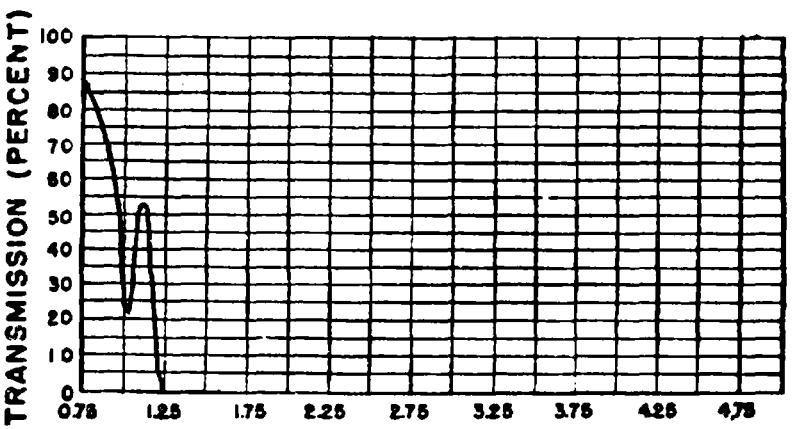

DISTILLED WATER FILTER

Appendix C

"A Wide Spectral Range Ultra-Rapid Scan Spectrometer"
reprinted from Applied Optics 5, 241 (1966).
Reproduced by permission of the copyright owner.

Reprinted from APPLIED OPTICS, Vol. 5, page 241, February 1966
Copyright 1966 by the Optical Society of America and reprinted by permission of the copyright owner

A Wide Spectral Range Ultra-Rapid Scan Spectrometer

Charles H. Church and Leonard Gampel

A grating spectrometer has been designed and built which allows extremely rapid scanning rates (over 200 Å/μsec) over a wide spectral range (4000–11,000 Å) in one order with a theoretical resolving power of ~6000. The basic principles of the instrument are described together with some spectra (taken at speeds of ~90 Å/μsec) illustrating its capabilities.

For many problems in spectroscopy, such as the study of pulsed arc discharges and photo flash reactions, it is useful to be able to scan rapidly at moderate resolution over a fairly wide spectral range. Recently, Hill and Beckner[1] discussed a spectrometer which could scan over a limited spectral range (on the order of 200 Å, depending upon the width of the mirror) at rates varying between 10 Å/μsec and 200 Å/μsec. In another publication, Niesel *et al.*[2] describe a spectrometer system that includes a monochromator that is capable of scanning over a wider spectral range (typically 3500–7000 Å), but at rates of the order of 0.3 Å/μsec.

In the instrument to be described, we have taken the approach of Niesel *et al.*, but have used a rotating mirror which is capable of much higher speed together with a modified Czerny-Turner monochromator layout arrangement rather than the Pfund mounting of Niesel *et al.* The optical system used in the system to be described is much simpler to construct than the Pfund, and it allows the use of longer slits for a significant gain in the light intensity, i.e., radiance, passing through the instrument.

Principle

The optical arrangement of the basic rapid scan monochromator is shown in Fig. 1 and in detail in Fig. 2.

The rotating mirror reflects the collimated beam onto the grating varying the angle of incidence (α). The angle of incidence α and of diffraction β are measured from the grating normal and are considered positive when they are measured in the same direction. The geometrical relationship between the exit slit, the focusing mirror, and the grating define the angle of diffraction (β), which is the same for all of these angles of incidence. Additional exit slits in the focal plane of the focusing mirror would define other angles of diffraction. The projected width of the rotating plane mirror which is the width of the collimating mirror times the cosine of the angle determines the effective width of the grating, and thus the aperture, and the theoretical resolving power of the instrument. The actual width of the ruled portion of the grating subtending the rotating mirror together with the distance of the grating from this mirror determine the spectral range of the instrument for a particular grating. These parameters, in the instrument under discussion, have been designed to give a spectral range that will require only one separation of overlapping orders.

Figure 2 illustrates the above principles. In order for rays I and II to be brought to the same focal point at the exit slit:

$$\beta = \beta_1 = \beta_2.$$

The grating equation is then written for the two cases as

$$m\lambda_1 = d(\sin\alpha_1 + \sin\beta), \tag{1a}$$

$$m\lambda_2 = d(\sin\alpha_2 + \sin\beta). \tag{1b}$$

Subtracting Eq. (1b) from Eq. (1a) we obtain

$$m\Delta\lambda = m(\lambda_2 - \lambda_1) = d(\sin\alpha_2 - \sin\alpha_1) \tag{2a}$$

$$= 2d\cos\left(\frac{\alpha_2 + \alpha_1}{2}\right)\sin\left(\frac{\alpha_2 - \alpha_1}{2}\right). \tag{2b}$$

Equation (2a) indicates the factors which govern the spectral range, $\lambda_2 - \lambda_1$, of the instrument. It can also

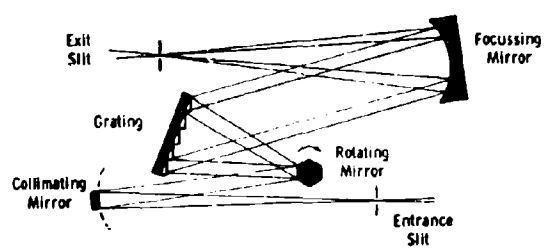

Fig. 1. Optical arrangement of ultra-rapid scanning monochromator.

Both authors were with Westinghouse Research Laboratories, Pittsburgh, Pennsylvania. The present address of L. Gampel is Electro-Optical Systems, Inc., Pasadena, Calif.

Received 4 June 1965.

be shown from simple geometrical considerations that, for an angular rotation θ,

$$2(\theta_2 - \theta_1) = 2\Delta\theta = (\alpha_2 - \alpha_1) = \Delta\alpha. \quad (3)$$

Now for the maximum light intensity to be diffracted into the first order ($m = 1$), the grating should be used at angles near to the blaze angle. A possible choice, though not necessarily optimum, is to have α_1 and α_2 on either side of the blaze angle (θ_B) such that

$$\frac{\alpha_2 + \alpha_1}{2} = \theta_B. \quad (4)$$

Combining Eqs. (2), (3), and (4) we obtain for first order:

$$\Delta\lambda = 2d\cos\theta_B \sin\Delta\theta,$$

and for small angular displacements $\Delta\theta \ll 1$ in a short time interval $\Delta t \ll 1$, we can write $\Delta\lambda/\Delta t = 2d\cos\theta_B\ (\Delta\theta/\Delta t) = 2d\ \omega\cos\theta_B$, where ω is the angular speed of the mirror in rad/sec.

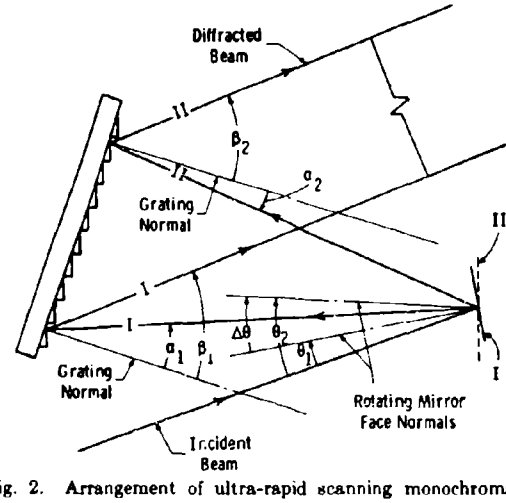

Fig. 2. Arrangement of ultra-rapid scanning monochromator showing geometrical factors governing spectral range and speed.

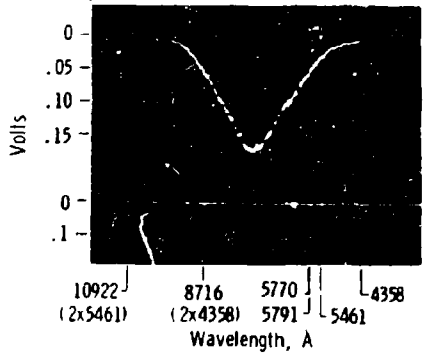

Fig. 3. Upper trace: spectrum from a tungsten standard lamp. Lower trace: spectrum from the mercury lamp. Both traces recorded simultaneously at sweep rates of 10 μsec/cm and a scanning speed of 93 Å/μsec.

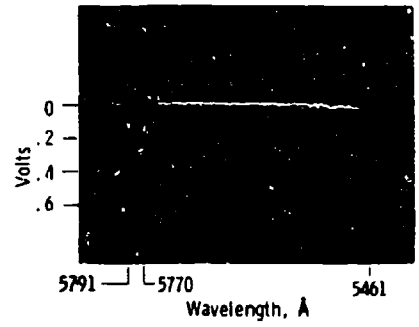

Fig. 4. Expanded trace of part of the spectrum from the mercury lamp at a sweep rate of 1/3 μsec/cm and a scanning speed of ~93 Å/μsec.

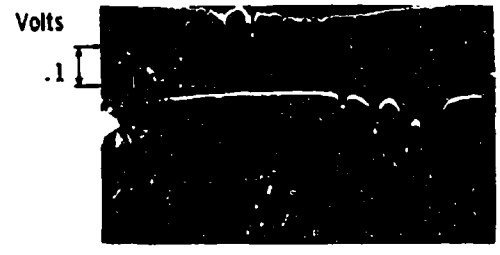

Fig. 5. Spectrum from the xenon short-arc lamp at a scanning speed of 80 Å/μsec. Upper trace: sweep rate 10 μsec/cm. Lower trace: sweep rate 1 μsec/cm.

Experimental Arrangement

Monochromator

Two 0.5-m focal length spherical mirrors were used in the Czerny-Turner arrangement of Fig. 1. The aperture of the collimating mirror was such as to just fill one of the faces of the rotating plane mirror; the focusing mirror was wide enough to receive the diffracted beam from both ends of the width of the grating. The entrance and exit slits were straight slits approximately 2 cm long.

The rotating plane mirror presently being used is the six-sided turbine-driven mirror of the AVCO-MC300-2 streak camera, mounted with the mirror axis vertical.* The mirror faces were about 1.2 cm wide and 9 cm long for an effective area of 10.8 cm² for use in aperture or f-number calculation. The diffraction grating has a 102 mm × 102 mm ruled area, ruled with 600 lines/mm, and with a blaze angle of about 8°. The width of the mirror face of 1.2 cm gives an approximate theoretical resolving power in first order of 7200 for $\theta \approx 0°$.

* The manufacturers recommended limiting the speed of the mirror to about 1500 cps when the camera is mounted vertically; a 9.5-mm thick steel housing was built to contain the mirror fragments in the advent of a mirror explosion at these high rotational speeds.

If we refer to Fig. 1, it can be seen that the angle at which the beam is incident upon the exit slit varies with the illumination of the grating by the rotating mirror. The detector optics and the area of the radiation detector must be designed to include this range of angles. Effectively, this usually results in the detector optics being designed as though the entire focusing mirror were being illuminated as would occur in the more usual instrument with this size grating. This variation in exit angle, which corresponds to variation in wavelength, permits filters to be positioned so as to remove overlapping orders occurring in the same spatial portion of the sweep, while allowing the shorter wavelengths to be incident upon the detector in first order. In the instrument being described, which is intended to sweep from 4000 A to 1100 A in first order, a Corning CS2-63 filter, which passed wavelengths longer than ~6000 Å, was inserted in the longer-wavelength position of the exit beam just beyond the exit slit to remove the shorter wavelength second order from the longer wavelength first order. The partial insertion of the filter permitted the first order at the shorter wavelength region (~4000 A) to be detected by the same photodetector.

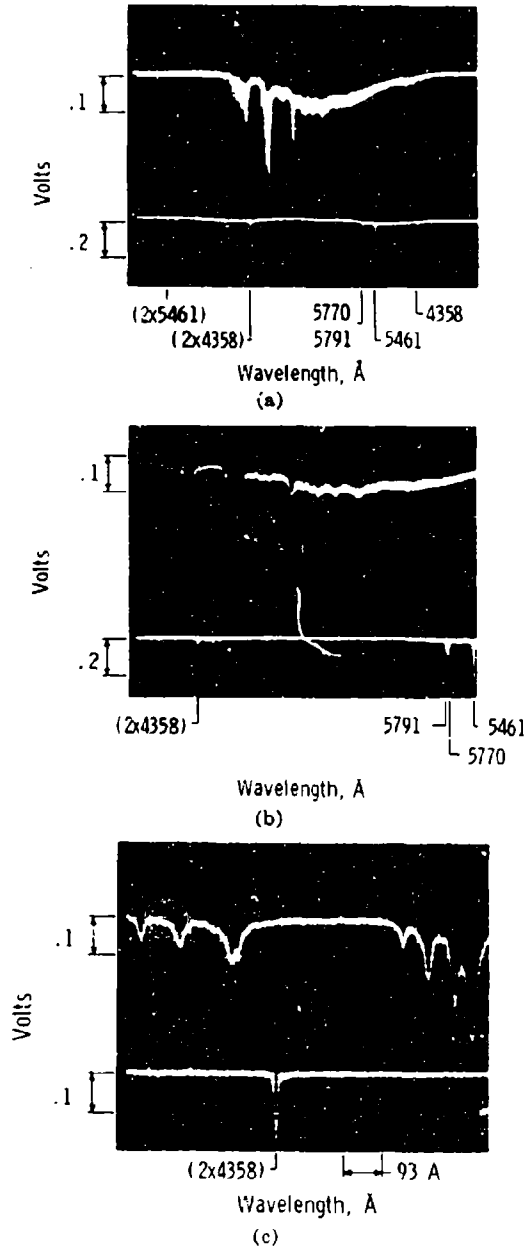

Fig. 6. Spectra from the xenon lamp and the mercury lamp recorded simultaneously at a scanning speed of 93 Å/μsec. Sweep rate: (a) 10 μsec/cm; (b) 5 μsec/cm; (c) 1 μsec/cm.

Wavelength Calibration

Wavelength calibration was effected by using the advantage offered by the long slits. A low-pressure mercury lamp was imaged on the upper 20% of the entrance slit along the same path as the light from the principal source. The radiance from the mercury source and the radiance from the source being measured traversed the instrument together and were separable at the exit slit by virtue of the stigmatic character of the optical system.

The principal source radiation was detected by a Dumont 6911 photomultiplier (which has an S1 response) using the spatial filter arrangement described above. The light from the mercury lamp passed through a Corning CS3-73 filter, which blocked the mercury lines below 4300 Å and their second- and third-order components, and was detected by a Dumont 7664 photomultiplier which has an S13 response.* (See Figs. 5 and 6.)

The signals from the two photomultipliers can then be displayed separately using a Tektronix 555 dual-beam oscilloscope and the same time base generator. The mercury spectral lines on one of the oscilloscope traces are then used as wavelength markers for the spectral display on the other oscilloscope trace. Varying the sweep rate of the oscilloscope varied the fraction of the spectral range displayed.

In the present work, the oscilloscope display was triggered with a pulse generated by an RCA 931A photomultiplier mounted at one side of the grating so that it detected the sweeping light beam from the rotating mirror before the light was incident on the grating. The trigger pulse was put through the variable time delay generator on the oscilloscope so that different portions of the spectrum could be displayed (see Fig. 4).

Intensity Calibration

Figure 3 shows the spectrum of a tungsten ribbon-

* This particular photomultiplier was not necessary but was readily available. A Dumont 6292 photomultiplier with an S11 response is now being used.

filament lamp,* operated at 35 A with the spectrometer slits opened to 1.0 mm, on the upper trace and the mercury spectrum on the lower trace. The trace, together with the wavelength markers, allows a calibration of the spectrometer from the known absolute spectral radiance of the source.

Results

Figure 4 shows, clearly resolved, the yellow doublet of mercury occurring at 5770 Å and 5790 Å, and the green line at 5461 Å. The actual slit-widths were 0.20 mm, and the mirror was rotating at 441 rps which gives a scanning speed of about 93 Å/μsec. The source was an Osram mercury lamp (Ealing catalog No. 26-226) operated at 1.2 A and 50 V; the detector was the Dumont 7664 photomultiplier operated at 1400 V with an anode resistor of 50 Ω matching the line impedance.

Figure 5 indicates the versatility of the electronic arrangement: the signal from the Dumont 6911 photomultiplier was put into both channels of the dual-beam oscilloscope; the upper trace is the spectrum from ~4300 Å to ~10,000 Å of an Osram XBO-1600 xenon lamp operated at 55 A and 22 V. The actual slit-width was 0.20 mm, the mirror speed was 375 rps and the oscilloscope sweep rate was 10 μsec/cm. The lower trace is an expansion, at a sweep rate at 1 μsec/cm. of part of the upper trace using the variable time delay generator.

Figures 6(a), 6(b), and 6(c) show the spectrum from the xenon lamp on the upper traces and the mercury lines on the lower traces, and allow identification of the xenon lines to within 5 Å. The actual slit-width was 0.2 mm, the mirror speed was 441 rps, and the sweep rates were as shown.

In Figs. 4–6, the Dumont 6911 photomultiplier was operated at 1400 V with an anode resistor of 180 Ω.

* GE type 30A/T24/17 lamp with a tungsten ribbon filament calibrated from a similar type secondary standard of spectral radiance calibrated by the Eppley Laboratory, Inc., Newport, Rhode Island.

Discussion

While the rate at which a spectrum could be scanned depends on the frequency response of the photodetector used together with that of the oscilloscope, the limiting wavelength resolution depends on both the effective resolving power of the monochromator and the frequency response of the photodetector and oscilloscope.

To utilize the full resolving power and scanning rate capabilities of this instrument, the frequency response of the measuring electronics must be high. For a mirror speed of 500 rps, the instrument will scan over the 7,000 Å in about 75 μsec, which, for a wavelength resolution of 3 Å, would require a response time of less than 30 nsec, that is, a frequency response of 12 sec. At such bandwidths the photon shot noise in the light beam may govern the signal-to-noise ratio for the low signals such as that provided by the tungsten lamp. To increase the signal-to-noise ratio for the calibration measurements, the slits may be opened. As the spectrum is a continuum, the requirements on the spectral resolution would be less stringent.

This rapid scanning spectrometer is being used in the study of pulsed arc discharges, in which there is a mixture of line and continuum radiation. These discharges last about a millisecond or more. The wide spectral range allows display of the continuum while the high spectral resolution reduces instrument line broadening (and therefore smearing of the line). The high spectral resolution can be used to study line contours in the discharge. The results of this work will be described in future publications.

This work was partially supported by the U.S. Army Electronics Laboratories, U.S. Electronics Command and by Project DEFENDER, which is under the joint sponsorship of the Advanced Research Projects Agency, the Office of Naval Research, and the Department of Defense.

References

1. R. A. Hill and E. H. Beckner, Appl. Opt. **3**, 929 (1964).
2. W. Niesel, D. W. Lübbers, D. Schneewolf, J. Richter, and W. Bottcher, Rev. Sci. Instr. **35**, 578 (1964).

Appendix D

"High Efficiency NaI Pumping of a
Continuous YAG:Nd^{3+}, cr^{3+} Laser"

A paper presented at the 4th
International Quantum Electronics Conference
(April 1966)

High Efficiency NaI Pumping of a Continuous YAG:Nd^{3+}:Cr^{3+} Laser*

by

R. G. Schlecht and C. H. Church

Westinghouse Research Laboratories
Pittsburgh, Pennsylvania 15235

Daniel A. Larson

Lamp Division, Westinghouse Electric Corp.
Bloomfield, New Jersey

Of the continuous solid state laser materials presently available the Nd^{3+} doped Yttrium Aluminum Garnet (YAG) laser[1] has one of the lowest thresholds and has attained the highest continuous power output. However due to the narrow absorption bands of the Nd^{3+} ion in YAG the overall efficiency of these lasers has been quite low. The efficiency has been improved by double-doping the YAG crystal with both Nd^{3+} and Cr^{3+}.[2] The Cr ion in YAG has two broad absorption bands at 4300Å and 6000Å. Energy absorbed by the Cr^{3+} is then transferred to the Nd^{3+} and in this way the efficiency of the YAG laser can be increased. We have attempted to further increase the efficiency of YAG by using a selective pumping source. The sources which we have investigated are the metallic iodides in a mercury arc.[3] These sources, generally speaking, are broad line emitters.

Spectra have been taken of several of the metallic iodides in a mercury arc. Due to the close match of the sodium D lines to the major

* This work was partially supported by the United States Army Electronics Laboratories U. S. Army Electronics Command on Contract DA-28-043-AMC-00292(E).

absorption band of Nd^{3+} in YAG we felt this to be the most promising. Whereas a sodium metal lamp has the disadvantage of the sodium reacting with the quartz envelope the NaI lamp is superior in this regard. In this lamp the NaI is vaporized from the wall, is dissociated and excited in the arc and then upon diffusing toward the wall recombines with the iodine and is deposited on the cooler wall again as NaI, the iodide not reacting with the wall.

A NaI + Hg capillary lamp was constructed and absolute intensity measurements were made. The results in the 5650-6000Å region of interest are shown in Figure 1. Overlaying the lamp emission is the absorption spectrum of Nd^{3+} in YAG. The bottom trace is the second decade of the absorption spectrum. Therefore, the absorption peak at 5886Å has a value of 2 for the absorbance and a width of 7Å. One can readily see that several of the absorption peaks of Nd^{3+} in YAG show a good spectral match with the emission of this lamp. The position and intensity of the peak can be controlled by varying the amount of sodium in the arc and by the loading of the arc. As the arc is hit harder the self-absorption of the resonance radiation becomes broadened and the intensity of the wings of the lines increases. The value of the peak radiance at approximately 5886Å of 30 milliwatts/ster cm can be compared to the radiance of the usual tungsten lamp at this wavelength of approximately 1.8 milliwatts/ster cm.

The lamps used for laser pumping were constructed of 3.5 x 10 mm quartz tubing with molybdenum ribbon seals. The electrode spacing used was from 20 to 50 mm.

The cavity used in the laser pumping experiments was a 38 mm pyrex cylinder 1 1/2 inches long. The cylinder had an aluminum reflective

coating on the inside surface. The laser rod and lamp were fixed in position with as tight a coupling as possible and the cylinder was adjusted about the lamp and rod. The laser rod was a 3 x 30 mm doubly doped YAG:Nd^{3+}:Cr^{3+} rod with confocal dielectric resonators of greater than 99.5% reflectivity. With this cavity and rod a pulse threshold of 0.4 joules was obtained with a PEK XE 2-1 flashlamp and a 5 μf power supply.

The continuous pumping of the YAG laser with the NaI lamp was compared to pumping the rod with a 500 T3Q/CL 500 watt tungsten iodine lamp. This lamp has a filament diameter of about 1.5 mm 0.06 inches and therefore has much better coupling efficiency to the small diameter laser rod than the thick-walled NaI lamp. The NaI lamp was also hand-made and therefore had very poor optical quality. A threshold of approximately 465 watts and a slope efficiency of approximately 0.22% were obtained with the tungsten iodine lamp while a threshold of approximately 310 watts and a slope efficiency of approximately 0.33% were obtained with the NaI pump source. These results were obtained without maximizing the NaI content. It is felt that with further improvement in the optical quality of the lamp envelope, by using larger diameter laser rods and by maximizing the NaI content a significant improvement over tungsten pumping can be achieved.

References

1. J. E. Geusic, H. M. Marcos and L. G. VanUitert, Appl. Phys. Letters 4, 182 (1964).

2. D. A. Larson, H. D. Fraser, W. V. Cushing and M. C. Unglert, Illum. Eng. 58, 434 (1963).

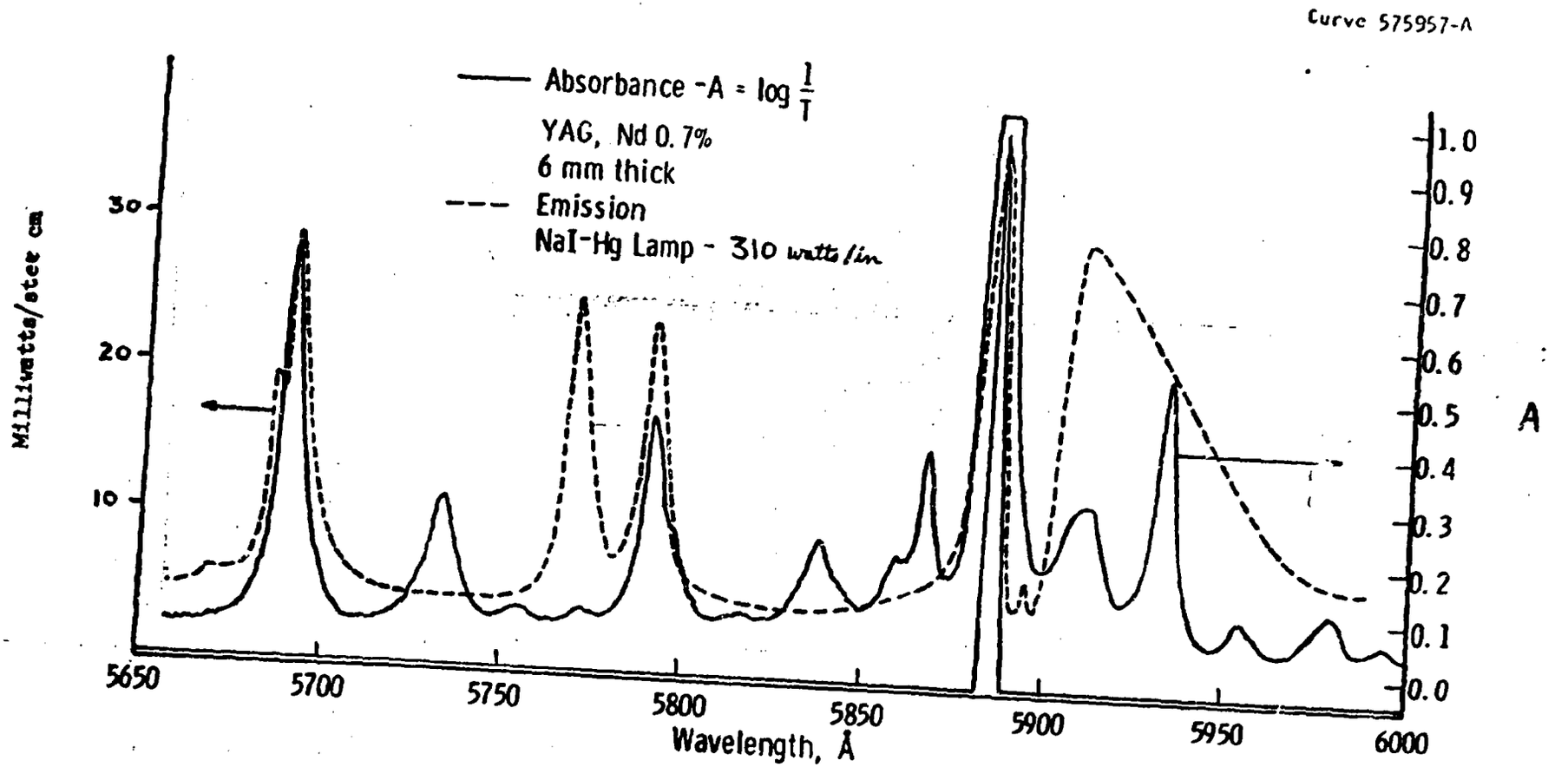

Fig. 1 —High resolution scan from 5650 Å to 6000 Å of the NaI additive lamp (3.5×10 mm) with the absorbance spectrum of Nd^{3+} in YAG

SUPPLEMENTARY

INFORMATION

AD-482130

ERRATA SHEET
(June 1, 1966)

This is a corrected figure for the report "Optical Pumps for Lasers" on contract DA28-043-AMC-00292(E), dated 1 July 1964 - 25 February 1966.

Westinghouse Research Laboratories
PITTSBURGH, PENNSYLVANIA 15235

RM 3503

Curve 577709-B

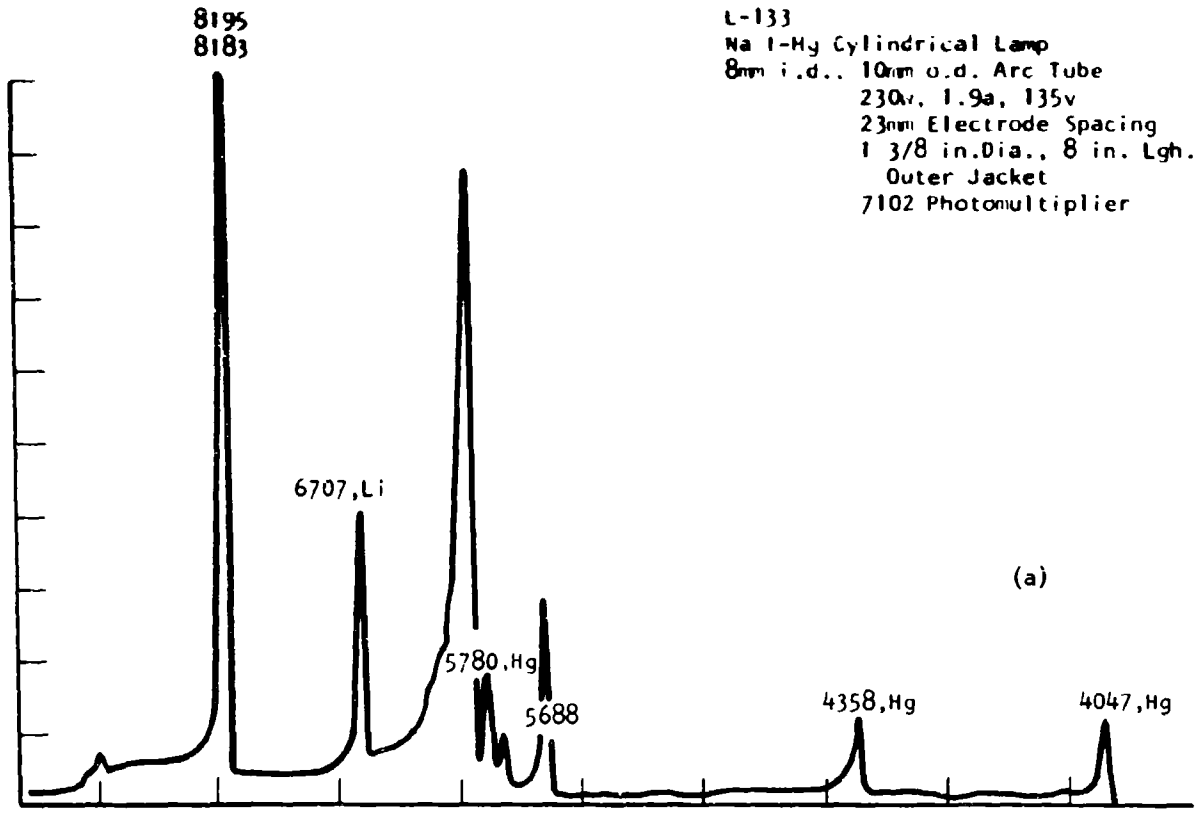

L-133
Na I-Hg Cylindrical Lamp
8mm i.d., 10mm o.d. Arc Tube
230w, 1.9a, 135v
23mm Electrode Spacing
1 3/8 in.Dia., 8 in. Lgh.
Outer Jacket
7102 Photomultiplier

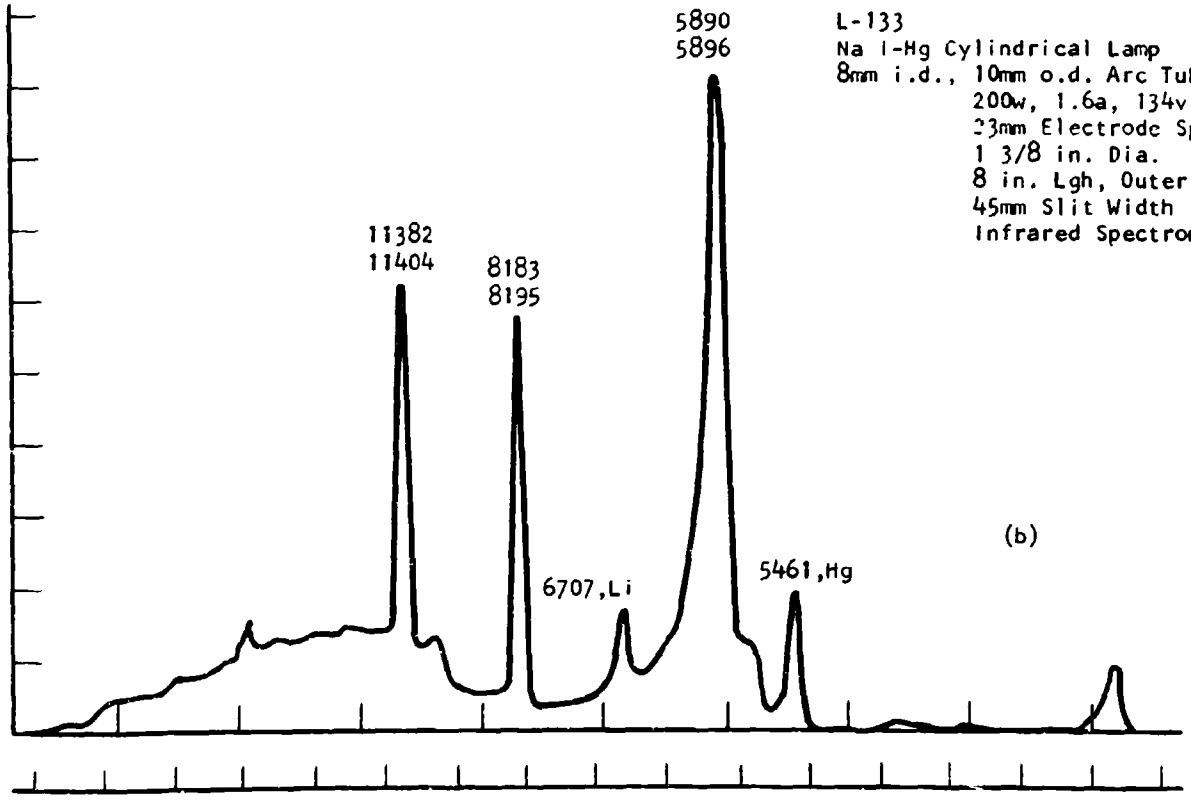

L-133
Na I-Hg Cylindrical Lamp
8mm i.d., 10mm o.d. Arc Tube
200w, 1.6a, 134v
23mm Electrode Spacing
1 3/8 in. Dia.
8 in. Lgh, Outer Jacket
45mm Slit Width
Infrared Spectrometer

Fig. 44